

# IKBFU

IMMANUEL KANT  
BALTIC FEDERAL  
UNIVERSITY



Smart Materials &  
Biomedical Applications  
IKBFU Research and Education Center



# IBSCM 2025

VI International Baltic  
Conference on Magnetism

## Книга тезисов

2025

17-21 августа 2025  
Калининград, Россия

## CONTENTS

<b>Plenary lectures .....</b>	<b>3</b>
<b>Invited talks .....</b>	<b>12</b>
<b>Oral talks .....</b>	<b>35</b>
<b>Poster presentations .....</b>	<b>122</b>
<b>Author index .....</b>	<b>198</b>

# Plenary lectures

# Modern Applications of Magnetic Materials: Trends and Challenges

A. Tishin<sup>a,b,c\*</sup>

<sup>a</sup> Lomonosov Moscow State University, 119991, Leninskie gory 1, Moscow, Russia

<sup>b</sup> AMT&C Group, 108840, Moscow, Troitsk, Promyshlennaya, str., 4, building 1

<sup>c</sup> Moscow Institute of Physics and Technology, 141701, Institutskiy per. 9, Dolgoprudny, Mosc. Reg., Russia

\*tishin@amtc.org

The first pulses of wide investigation into the magnetocaloric effect (MCE) were triggered by the discovery of a large MCE during first-order magnetic phase transitions in the compound  $\text{NdMn}_2\text{Si}_2$  in 1987 [1], alloy  $\text{Fe}_{0.49}\text{Rh}_{0.51}$  in 1990 [2], and compound  $\text{Gd}_5(\text{Si}_2\text{Ge}_2)$  in 1997 [3]. The work [4] suggested using the MCE for magnetic hyperthermia within the field generated by MRI sources and for drug delivery [5]. Work [5] has paved the way to initiate phase transitions in non-magnetic materials—such as thermoresponsive polymers like PNIPAM—by applying the magnetic field.

Unlike the MCE, which has known limiting specific values at the level of about 18K/T, the limiting dimensions of long-wave antennas and methods for reducing them have not yet been determined. Mechanisms to ensure wave compression at resonance within the required frequency range (not in the eigenmodes of the emitter) are proposed in work [7] to downsize electrically large antennas by orders of magnitude, utilizing textured composite encapsulation comprising dielectrics, magnetic, and conductive materials. The idea of using material parameters to reduce the physical size of the resonant antenna is unrelated to the concept of making the radiation mode depend on the shape of the dielectric antenna. In an ideally encapsulated emitter, the eigenmodes of radiation are suppressed through the composition and texture of the encapsulation and by matching the wave impedance.

Increasing the (BH)<sub>max</sub> value of permanent magnets (PM) by nearly 100 times over the century has broadened their applications in medicine [8] and electromobility. The work presents application examples [9] and reviews the current state of PM synchronous motors (PMSM). Recent progress in balancing high magnetic properties, cost, and supply chain risks is also described. Advanced use of materials with magnetic phase transformations for smart rotor applications in controllable-salient PMSM (CSPMSM) [10] and hybrid PMs was introduced [11]. Estimates [12] suggest that the maximum power density of PMSMs could reach approximately 1 MW/l, and at least an order of magnitude improvement may enhance the current level of PMSMs in mass production.

[1] S.A.Nikitin, Yu.F.Popov, R.Torchinova, A.M.Tishin, I.A.Arkharov, *Solid. State. Physics*, 29, 2, 572(1987), A.M.Tishin, Ph.D. Thesis, Moscow State Univ. (1988)

[2] S.A.Nikitin, G. Mylikgulyev, A.M.Tishin et al, *Phys. Lett. A*, 148, 6-7, 363 (1990).

[3] V.K.Pecharsky and K.A.Gschneidner, Jr, *PRL*, 78,23,4494 (1997)

[4] A.M.Tishin, Patent EP 1 897 590 B1, date of pub. 09.11.2016

[5] A.M.Tishin, Yu.A.Rochev, A.V.Gorelov, and US 9,017,713 B2, date of pat.: Apr. 28, 2015

[7] A.M.Tishin, S.V.Halilov, US 2016/0013547 A1, pub. date: Jan. 14, 2016

[8] *Magnetic materials and technologies for medical applications*, Ed. by Alexander M.Tishin, Elsevier, ISBN 978-0-12-822532-5, 638 p., 2022

[9] L.V.Dolgov, A.N.Doroshenko, A.M.Tishin, US 10,131,218 B2, date of patent: Nov.20, 2018

[10] A.M.Tishin, Patent application № 2025121629, date of application 05.08.2025

[11] A.M.Tishin, patent RU2827925 date of pub 04.10.2024

[12] <https://www.linkedin.com/pulse/what-pinnacle-power-density-future-alexander-tishinvcvze/?trackingId=zeWVmTHuNFQ3pbnIdViFgw%3D%3D>

# Magnetic Nanocomposites “Ferromagnetic Metal-Insulator”

A. Granovsky<sup>a,b,c\*</sup>

<sup>a</sup> Lomonosov Moscow State University, 119991, Leninskie gory 1, Moscow, Russia

<sup>b</sup> Samarkand State University, 140104, University blv. 15, Samarkand, Uzbekistan

<sup>c</sup> Institute for Theoretical and Applied Electrodynamics of Russian Academy of Sciences, 125412, Izhorskaya 13, Moscow, Russia

\* granov@magn.ru

The continuous interest in recent years in magnetic nanocomposites of the “ferromagnetic metal-dielectric” type is associated both with the variety of their properties that are promising for practical applications, and with the fact that they can be considered as a convenient platform for studying the properties of disordered systems and interactions in a system of magnetic nanoparticles [1-5]. Depending on the volume fraction of magnetic nanoparticles embedded in dielectric matrix, their size and shape nanocomposites can be in superparamagnetic, superspin-glass, superferromagnetic and ferromagnetic states or a mixture of them. Recently, it has been understood that the metal-insulator transition does not occur at the same concentration as the infinite cluster of direct contact granules is formed. The later concentration is called as the percolation threshold  $x_{\text{per}}$ , but it does not coincide with the critical concentration for the metal-insulator transition  $x_{\text{MI}}$  and also with concentration  $x_{\text{FM}}$  of long-range ferromagnetic order appearance.

I present recent results on structural, magnetic, magnetotransport, magneto-optical properties of magnetic nanocomposites focusing on peculiarities of electrical resistivity, anomalous Hall effect, magnetoresistance, transverse Kerr effect for compositions close to the percolation threshold.

[1] I.S. Beloborodov et al., Rev. Mod. Phys. 79, 416 (2007)

[2] S.N. Nikolaev et al., UFN 195, N 5 (2025)

[3] S.N. Nikolaev et al., JETP Letters 118, 58 (2023)

[4] E.A. Ganshina et al., JETP 137, 572 (2023)

[5] M.N. Martyshov et al., Phys. Rev. Appl. 14, 034016 (2020)

## **Reviewing recent R&D in magneto optic applications**

A. Baryshev<sup>a,\*</sup>, M. Dokukin<sup>a</sup>, D. Kulikova<sup>a</sup>, E. Sgibnev<sup>a</sup>, A. Shelaev<sup>a</sup>, P. Tananaev<sup>a</sup>

<sup>a</sup> Dukhov Automatics Research Institute (VNIIA), 127055 Moscow, Russia

\*baryshev@vniia.ru

Following the example of a work entitled 'Research activities on magneto optical devices in Japan' by Tsushima & Koshizuka (1987), a review of the key published achievements in magneto optical materials, technologies of their fabrication, and applications over a five-year period will be presented. The report will concentrate on the development of magneto optical glasses, various rare-earth garnets and garnet ceramics, as well as magneto optical nanoparticles and nanostructures. A review of the challenges associated with the developing of fiber optical isolators and photonic integrated circuits, as well as bio- and other sensing problems will be presented. Finally, the magneto optical methods will be appraised in terms of their practical applications.

# Spintronics Beyond MRAM: From Data Storage to Computations

V. Yurlov, P. Skirdkov, G. Kichin, K. Zvezdin \*

New Spintronic Technologies, 121205, Bolshoy blv. 30, Moscow, Russia

\*k.zvezdin@nst.tech

Spintronics has long been associated with magnetic data storage, from hard drives to the commercial deployment of magnetic tunnel junction (MTJ)-based MRAM. However, as CMOS technologies approach fundamental limits in power and scaling, spintronics reveals its broader promise — not only as a memory platform but as a foundation for radically new approaches to computation. This talk traces the evolution of spintronic technologies from non-volatile storage toward their transformative roles in logic, probabilistic computing, and in-memory processing.

We begin by revisiting the physical foundations, spin-transfer torque, spin-orbit coupling, and thermal stochasticity, which, beyond enabling MRAM, now serve as building blocks for spin-based computing. A key highlight is the progress in stochastic MTJs (p-bits), which exploit intrinsic thermal noise for hardware implementations of probabilistic models such as Ising machines and Boltzmann samplers. These developments not only open new paths for combinatorial optimization and inference but also suggest long-term potential as scalable platforms for quantum-inspired computing.

The second focus is spintronic rectification and high-frequency signal processing. I will present our recent results demonstrating broadband spin-torque rectification in MTJs, arising from inhomogeneous magnetization dynamics. Unlike conventional diode effects reliant on resonance tuning, this mechanism supports wideband GHz-range detection in a field-free configuration, paving the way for compact spintronic RF front-ends and neuromorphic sensory circuits.

Finally, I will explore the application of spintronic devices in analog computing arrays for AI inference. Leveraging the non-volatility and current-mode behavior of SOT-MRAM crossbars, we demonstrate analog vector-matrix multiplication (VMM) directly in memory, achieving significant energy savings. Our methodology adapts pre-trained AI models through quantization and weight mapping, eliminating the need for retraining and ensuring robustness to device-level variability.

Altogether, this talk envisions a future where spintronics transitions from a supporting role in memory technology to a central enabler of physics-driven computation. It calls for a redefinition of computational architecture, integrating device physics, circuit design, and algorithmic adaptation, where non-volatility, stochastic behavior, and spin dynamics become active computational resources.

- [1] S.I. Kiselev et al. // Nature. 2003. V. 425. P. 380-383
- [2] A. Tulapurkar et al. // Nature. 2005. V. 438. P. 339
- [3] A.G. Buzdakov, K.A.Zvezdin et al. // Phys. Rev. Appl. 2021. V. 15. P. 054047
- [4] P.N. Skirdkov, K.A.Zvezdin // Annalen der Physik. 2020. V. 532. P. 1900460

# **Mathematical Modelling of the Magnetoelectric Effect in Polymer Composites on the Base of PVDF**

Yu. Raikher<sup>\*</sup>, O. Stolbov

Institute of Continuous Media Mechanics, Russian Academy of Sciences, Ural Branch,  
614018, Korolyova 1, Perm, Russia

<sup>\*</sup>raikher@icmm.ru

PVDF (polyvinylidene fluoride) is nowadays the most widely used piezoelectric polymer, very appropriate for producing magnetoelectric materials (multiferroics) of the 0–3 morphology. This implies that the PVDF matrix is filled with fine powder of a ferro- or ferrimagnet. Most often, for this solid phase cobalt ferrite (CFO) is taken due to its outstandingly high among other ferrites magnetostriction constant. The greater this parameter the more efficiently the composite (usually, it is a film) performs the magnetic-to-electric conversion. Indeed, the applied field via the magnetostriction effect changes the shape of the ferrite particles, and these deformations induce mechanical stresses inside the matrix. The latter, being a piezoelectric, polarizes in response to the stresses and, thus, becomes a source of electric voltage.

Certainly, the polymer multiferroics of that kind cannot rival in their output power with the schemes which use solid ferromagnets and piezocrystals in the form of compacted powders or direct juxtapositions: e.g., the plates of both phases stuck together. However, the unbeatable advantages of polymer composites are their mechanical flexibility and biocompatibility. Because of that, they are appropriate for a great many of biomedical applications where magnetoelectric conversion units are (or yet might be) useful. These elements do not require high voltages and less so currents whereas a miniature size is highly desirable. No surprise that in recent years the number of papers on magnetoelectric stimulation of neural and brain activities or stem cell accommodation on the scaffolds just enhances.

A specific feature of the CFO particles is their high magnetic anisotropy. This implies that upon a field is applied, along with magnetostriction, the particle experiences a mechanical torque resulting from non-collinearity of its magnetic moment and the field. Inside the piezoelectric matrix this torque as itself produces mechanical stresses and by that yields an independent and also ever existing contribution to the magnetoelectric effect. This means that in the composites with low-magnetostrictive fillers this alternative route to electric response might become the major one.

The talk discusses relative contributions from the two sources of the magnetoelectric effect in composites with PVDF as a matrix. The systems in question are considered in the framework of mesoscopic approach. This is done mainly by way of computer simulations since in this case one has to deal with essentially multiparticle assemblies whose entities are coupled by magnetostatic and elastic interactions. Both of them are long-range and, thus, are quite poorly prone to analytical studies. The results presented demonstrate the effect of the magnetic particle shape (quasi-spherical CFOs vs barium hexaferrite platelets [1,2] and the orientations of the field and matrix poling directions on the voltage generated by the model filaments and monolayer films.

[1] O. Stolbov, Yu. Raikher, *Nanomaterials* 15, 438 (2025)

[2] O. Stolbov, Yu. Raikher, *Advanced Theory and Simulations* 8, 2401318 (2025)



## A first MEG-feasible fluxgate magnetometer

P. Vetoshko<sup>a,b\*</sup>, A. Kuzmichev<sup>b</sup>, E. Pavluk<sup>a</sup>, M. Ostras<sup>b</sup>, V. Belotelov<sup>b,c</sup>

<sup>a</sup> V.I. Vernadsky Crimean Federal University, 295007, Simferopol Russia

<sup>b</sup> Russian Quantum Center, 121205, Moscow Russia

<sup>c</sup> Lomonosov Moscow State University, 119991, Leninskie gory 1, Moscow, Russia

\*pvetoshko@mail.ru

This work introduces a novel solid-state MEG-compatible sensor based on a yttrium-iron garnet magnetometer (YIGM) operating at room temperature via the fluxgate principle [1]. The technology combines a solid-state design with a wide dynamic range. Theoretical sensitivity below 1 fT/ $\sqrt{\text{Hz}}$  and experimentally achieved 35 fT/ $\sqrt{\text{Hz}}$  (with potential tenfold improvement), coupled with compactness, position YIGM as a promising solution for multichannel MEG systems.

Experimental validation includes human alpha rhythm detection using YIGM and comparative noise analysis with an OP-MEG system [2], selected for comparable scalp–sensor distances. Results confirm YIGM’s compliance with biomagnetic measurement standards, including magnetocardiography (MCG) and magnetic nanoparticle detection.

The study outlines applications beyond laboratory settings: low-field NMR spectroscopy, multimodal neuroimaging platforms, and overcoming OPM/SQUID limitations. YIGM adaptation could enable a new generation of affordable, robust, and portable systems, redefining functional diagnostics. In the end we will discuss the operating principle, characteristics and examples of practical application of magnetometers based on coherent rotation of magnetization in single-crystal films of ferrite garnets. The applicability of this type of magnetometers for recording magnetoencephalograms and other biomagnetic measurements, such as magnetocardiography, low-field nuclear magnetic resonance and registration of magnetic nanoparticles, will be presented.

[1] Vetoshko, P., Gusev, N., Chepurnova, D., Samoilova, E., Syvorotka, I., Syvorotka, I., Belotelov, V. (2016a). Flux-gate magnetic field sensor based on yttrium iron garnet films for magnetocardiography investigations. *Technical Physics Letters*, 42(8), 860–864

[2] Koshev, N., Butorina, A., Skidchenko, E., Kuzmichev, A., Ossadtchi, A., Ostras, M., Fedorov, M., & Vetoshko, P. (2021). Evolution of MEG: A first MEG-feasible fluxgate magnetometer. *Human Brain Mapping*, 1–13. <https://doi.org/10.1002/hbm.25582>

# From nano-to-micro magnetoplasmonic hybrids for combined therapies: design, magnetic and optical properties

L. Panina<sup>a\*</sup>, A. Anikin<sup>b</sup>, V. Salnikov<sup>b</sup>, A. Omelyanchik<sup>b</sup>, A. Motorzhina<sup>b</sup>, S. Pshenichnikov<sup>b</sup>,

K. Levada<sup>b</sup>, V. Belyaev<sup>b</sup>

<sup>a</sup> National University of Science and Technology «MISIS», 119049, Leninskiy av. 4, Moscow, Russia

<sup>b</sup> Immanuel Kant Baltic Federal University, 236004, Nevskogo 14, Kaliningrad, Russia

\*drlpanina@gmail.com

The utilisation of nanomaterials has the potential to enhance the efficacy of cancer treatment methodologies. In order to enhance efficiency, a number of therapeutic mechanisms have been contemplated, with a focus on hybrid particle architectures. The combination of magnetic and plasmonic properties has potential for use in therapy involving magnetic hyperthermia and photothermia. Furthermore, the magnetomechanical effect can be employed for the point-by-point destruction of pathological cells.

In the context of such applications, the utilisation of nano- and mesoscale particles of diverse geometric forms (e.g. rods, stars, tubes and discs) and designs, alternating between ferromagnetic and plasmonic materials (e.g. core/shell, layered), is proposed.

Combining plasmonic and ferromagnetic (or ferrite) components results in an increased extinction cross section at plasmon resonance. Using as a core transition metals contributes to an increase in saturation magnetization and a high aspect ratio also provides higher magnetic anisotropy. The interplay of these factors culminates in elevated levels of heat dissipation during instances of magnetic hyperthermia and photothermia. Furthermore, ferromagnetic particles with anisotropic shape have the capacity to transmit mechanical force to a cell when an alternating magnetic field is applied. The present paper presents a comparative analysis of the optical, magnetic and photothermal properties of several types of hybrid particles.

The optical density could be tuned to produce an absorption peak at the NIR region by changing the particle shape and coating material. For example, covering the gold nanoparticles with thin magnetic shells shifts the absorption peak to the red region. Alternatively, magnetic particles of an anisotropic shape (discs, rods, tubes) covered with plasmonic metal also demonstrate enhanced red shift of plasmon resonance. Such particles with ferromagnetic core and gold shell can be nontoxic and can give access to combined magnetic hyperthermia, magnetomechanical and photothermal therapies.

This research was funded by RSF, grant number 21-72-20158-II.

# Biomedical applications of piezoelectric and magnetoelectric materials

R. Surmenev\*, M. Surmeneva, L. Shlapakova, A. Fetisova, P. Chernozem, R. Chernozem

National Research Tomsk Polytechnic University, 634050, Lenina street 30, Tomsk, Russia

\* rsurmenev@mail.ru; surmenev@tpu.ru

The lecture will be devoted to an overview of various types of piezoelectric and magnetoelectric materials in the form of nanoparticles and scaffolds for targeted drug delivery, stimulation of cellular activity (proliferation, differentiation, etc.), as well as for regeneration of tissues [1-4]. Piezoelectric and magnetoelectric materials are being studied for tissue engineering such as bone, peripheral nerves, muscles and others. The key advantages of these materials are their capability of non-invasive electrical stimulation and/or targeted drugs delivery/release, when exposed to an external physical stimuli (e.g. ultrasound, magnetic fields in modes safe for biological tissues) [5, 6].

Currently, large-scale interdisciplinary studies are being conducted around the world on the possibilities of using electroactive nanomaterials to treat various topical diseases, such as oncology, neurodegenerative diseases, which in some cases are not amenable to treatment by traditional methods.

The work is supported by the Russian Science Foundation (No. 25-13-20055) and TPU development program Priority 2030. The authors are thankful to Dr. A.L. Kholkin, Mrs Yu.R. Mukhortova for fruitful discussions.

- [1] Bin Firoz, A., V. Rybakov, A.A. Fetisova, L.E. Shlapakova, I.O. Pariy, N. Toropkov, A.S. Lozhko-moev, Y.R. Mukhortova, A.L. Kholkin, M.A. Surmeneva, R.A. Surmenev, 3D-Printed biodegradable composite poly(lactic acid)-based scaffolds with a shape memory effect for bone tissue engineering. *Advanced Composites and Hybrid Materials*, 2025. 8: p. article number 95
- [2] Chernozem, R.V., A.O. Urakova, P.V. Chernozem, D.A. Koptsev, Y.R. Mukhortova, I.Yu. Grubova, D.V. Wagner, E.Yu. Gerasimov, M.A. Surmeneva, A.L. Kholkin, R.A. Surmenev, Novel Biocompatible Magnetoelectric MnFe<sub>2</sub>O<sub>4</sub> Core@BCZT Shell Nano-Hetero-Structures with Efficient Catalytic Performance. *Small*, 2023: p. 2302808
- [3] Kopyl, S., R. Surmenev, M. Surmeneva, Y. Fetisov, A. Kholkin, Magnetoelectric effect: principles and applications in biology and medicine – a review. *Materials Today Bio*, 2021. 12: p. 100149
- [4] Shlapakova, L.E., M.A. Surmeneva, A.L. Kholkin, R.A. Surmenev, Revealing an important role of piezoelectric polymers in nervous-tissue regeneration: A review. *Materials Today Bio*, 2024. 25: p. 100950
- [5] Chernozem, P.V., A.V. Romashchenko, O.I. Solovieva, A.Zh. Ibraeva, G. Nosov, D.A. Koptsev, S.A. Lisitsyn, M.A. Surmeneva, D.V. Wagner, E.Yu. Gerasimov, S.O. Kazantsev, A.S. Lozhkomoev, G.B. Sukhorukov, R.A. Surmenev, R.V. Chernozem, The Effect of Various Surface Functionalizations of Core-Shell Nanoactuators on Magnetolectrically Driven Cell Growth. *ACS Appl. Mater. Interfaces*, 2025. 17: p. 21614–21629
- [6] Sharapova, M.B., D.S. Zuev, E.K. Silvanovich, A.Zh. Ibraeva, K.N. Morozova, E.V. Kiseleva, P.V. Chernozem, A.O. Urakova, D.V. Wagner, E.Yu. Gerasimov, O.B. Shevelev, B.G. Sukhov, M.A. Surmeneva, R.A. Surmenev, E.L. Zavjalov, R.V. Chernozem, A.V. Romashchenko, Nose-to-Glioblastoma Axonal Transport of Manganese Ferrite Nanoparticles under the Influence of Olfactory Stimulation. *ACS Appl. Nano Mater.*, 2025. 8(14): p. 6930–6942

# Invited talks

# Ultrafast excitation of propagating exchange spin waves by nanophotonic structures

V. Belotelov<sup>a,b\*</sup>

<sup>a</sup> Lomonosov Moscow State University, Moscow, Russia

<sup>b</sup> Russian Quantum Center, Moscow, Russia

\*belotelov@physics.msu.ru

All-dielectric nanostructures are very promising for efficient spin control in magnetic materials using femtosecond laser pulses. Such structures with specially selected parameters allow obtaining various optical resonances in a magnet (optical waveguide modes, Mie mode, Fabry-Perot resonance) and, thus, properly distributing the optical spin angular momentum (effective magnetic field of the inverse magneto-optical Faraday and Cotton-Mouton effects) in a magnetic material, which ultimately leads to the excitation of various spin modes with high amplitude [1-4].

In particular, in magnetophotonic crystals and nanostructured magnetic films, excitation of standing spin waves limited in one or all three dimensions is ensured. When connecting optical Mie resonances in magnetic nanospheres or nanocylinders, it becomes possible to restructure within the local and individual effective field of the inverse Faraday effect to include standing modes of high sequences. On the other hand, by applying a non-magnetic nanograting to a magnetic film, laser pulses excite ultrashort running spin waves with a length of 100-300 nm, which significantly reduces the wavelength of light in a magnet. In this case, nanogratings play a dual role - they allow not only to excite short spin waves, but also to observe them, which is impossible for homogeneous magnetic films. With this, the use of nanogratings allows creating new optomagnetic effects, such as the rotational equatorial Kerr effect, which significantly expands the range of possibilities for controlling spins using light.

Financial support by Russian Science Foundation (project № 23-62-10024) is acknowledged.

- [1] Krichevsky D.M., Bel'kova A.V., Ozerov V.A., Sylgacheva D.A., Kalish A.N., Evstigneeva S.A., Pakhomov A.S., Mikhailova T.V., Lyashko S.D., Kudryashov A.L., Semuk E.Yu., Chernov A.I., Berzhansky, V.N., Belotelov V.I. Nanophotonics vol. 13, no. 3, 2024, pp. 299-306. (2024)
- [2] D. Ignatyeva, D. Krichevsky , D. Karki , A. Kolosvetov , P. Zimnyakova , A. Shaposhnikov , V. Berzhansky , M. Levy , A. Chernov , V. Belotelov, Physical Review Applied, 21, 034017 (2024)
- [3] D.O. Ignatyeva, C.S. Davies, D.A. Sylgacheva, A. Tsukamoto, H. Yoshikawa, P.O. Kapralov, A. Kirilyuk, V.I. Belotelov, and A.V. Kimel, Nature Communications 10(1), 4786 (2019)
- [4] A.I. Chernov, M.A. Kozhaev, D.O. Ignatyeva, E.N. Beginin, A.V. Sadovnikov, A.A. Voronov, D. Karki, M. Levy, V.I. Belotelov, Nano Lett. 20(7), 5259-5266 (2020)

# **Ferrofluid Composites: Microstructure and Properties**

A. Zakinyan \*

North-Caucasus Federal University, 355017, Pushkina 1, Stavropol, Russia

\*art.zakinyan@gmail.com

The study of heterogeneous composite materials is of widespread scientific interest due to their prevalence in nature and engineering. A central scientific problem is identifying regularities in the fundamental relationship between the macroscopic properties of these materials and their micro- or mesoscale structural state.

This study focuses on new composite soft magnetic materials with a multicomponent composition representing magnetic nanocolloids with additional microparticles, which can be solid or liquid. The microgeometry of these materials can be controlled by forming ordered clusters of particles and by deforming the interfacial boundary in a magnetic field.

We have conducted a thorough investigation of the electrical, magnetic, rheological, and thermophysical properties of these new composite materials. The study considers the processes of structure formation and the dynamics of dispersed phase particles interacting with magnetic and electric fields. Considerable attention is given to studying the microstructuring processes, microgeometry, and structural anisotropy of these materials. Additionally, we examine the correlation between these factors and the macroscopic properties of the medium [1–4].

We present the results of experimental studies and approaches to computer modeling of the phenomena under study.

This work was supported by the North-Caucasus Center for Mathematical Research under agreement No 075-02-2023-938 with the Ministry of Science and Higher Education of the Russian Federation, and also by the Ministry of Science and Higher Education of the Russian Federation, project FSRN-2023-0006.

- [1] S. Turkin, A. Zakinyan, S. Bozhenko, *Phys. Scripta* 99 (4), 045507 (2024)
- [2] S. Turkin, A. Zakinyan, S. Semyonova, S. Kunikin, *Appl. Phys. A* 130 (4), 244 (2024)
- [3] A.R. Zakinyan, A.A. Zakinyan, L.S. Mesyatseva, *Chem. Phys. Lett.* 813, 140319 (2023)
- [4] A. Zakinyan, I. Arefyev, *Colloid Polym. Sci.* 298, 1063 (2020)

# Magnetosomes in nature, biomedicine and physics

N. Usov<sup>a\*</sup>

<sup>a</sup> Pushkov Institute of Terrestrial Magnetism, Ionosphere and Radio Wave Propagation, Russian Academy of Sciences, IZMIRAN, 108480, Troitsk, Moscow, Russia

\* usov@obninsk.ru

Magnetotactic bacteria are living organisms that grow magnetite nanoparticles called magnetosomes in their body. A linear chain of uniformly magnetized magnetosomes grown inside a magnetotactic bacterium is a kind of magnetic needle that helps the bacterium navigate in the weak Earth's magnetic field in search of the best habitat. In contrast to chemically synthesized magnetite nanoparticles, magnetosomes have a perfect crystal structure, a narrow size distribution, and a high saturation magnetization close to that of bulk magnetite.

Magnetosomes are very promising for use in biomedicine, in particular, in magnetic hyperthermia for the cancer treatment. Based on the stochastic Landau-Lifshitz equation the detailed calculation of the specific absorption rate (SAR) was carried out for assemblies of magnetosome chains depending on the particle size  $D$ , the distance  $L$  between particle centers in the chain, and the angle of the applied magnetic field with respect to the chain axis [1]. For a dilute oriented chain assembly with optimally chosen  $L/D$  ratio a strong magneto- dipole interaction between the chain particles leads to almost rectangular hysteresis loop, and to a large SAR of the order of 400 – 450 W/g at moderate frequency  $f = 300$  kHz and small magnetic field amplitudes  $H_0 = 50 - 100$  Oe.

Interestingly, chains of magnetosomes are sometimes found in weakly magnetized fossil rocks and bottom sediments, the study of which provides valuable information about the geological and biological past of the Earth. The use of the stochastic Landau-Lifshitz equation enables us to calculate the ferromagnetic resonance (FMR) spectra of oriented and non oriented assemblies of linear magnetosome chains depending on the particle diameter, the number of particles in a chain, the distance between the centers of neighboring particles, the mutual orientation of the cubic axes of particle anisotropy, and the value of the magnetic damping constant [2]. The FMR spectra of non oriented assemblies of magnetosome chains are compared with that of random clusters of interacting spherical magnetite nanoparticles. The shape of FMR spectra of both assemblies is shown to differ appreciably even at sufficiently large values of filling density of random clusters.

To further characterize the magnetic properties of magnetosome chains a detailed comparison of the quasi-static hysteresis loops of assemblies of single and double magnetosome chains, as well as assemblies of flux-close magnetosome rings is carried out using numerical simulation [3]. It is shown that the hysteresis loops of the studied assemblies differ significantly from each other and from the hysteresis loop of a random assembly of non-interacting spherical magnetite nanoparticles. Therefore, in addition to FMR spectra, the presence of biogenic magnetite in natural samples of weakly magnetized ancient rocks can be detected also from the quasi-static hysteresis loop measurement.

[1] N. A. Usov, E. M. Gubanova. *Nanomaterials* 10, 1320 (2020)

[2] E. M. Gubanova, N. A. Usov. *Beilstein J. Nanotechnol.* 15, 157 (2024)

[3] N. A. Usov. *J. Supercond. Novel Magnetism* 38, 96 (2025)

## High performance polymer materials for additive technologies

A. Zhansitov, K. Shakhmurzova, Zh. Kurdanova, A. Slonov, I. Musov, A. Baykaziev, S. Khashirova

Kabardino-Balkarian State University named after H.M. Berbekov, Nalchik, 360004, Chernyshevsky 173,

Nalchik, Russia

\*azamat-z@mail.ru

In modern industry, there is a growing interest in the use of additive technologies for the production of functional parts from highly heat-resistant polymers. Of particular interest are polyether ketones (PEK), which, due to their unique properties, are used in the aerospace, automotive and medical industries. Fused deposition modeling (FDM) technology is one of the most accessible methods of 3D printing of thermoplastics, but when working with polyether ketones, a number of specific problems arise due to their semi-crystalline nature.

Uneven crystallization of the material during the printing process leads to the occurrence of internal stresses and deformations of products, and high melting temperatures require the use of specialized equipment. Also, high crystallinity negatively affects interlayer adhesion, which reduces the strength characteristics of finished products. In this regard, an extremely important task is to identify the key structure-forming factors that determine the formation of PEK with an optimized macromolecular architecture, which helps to reduce the degree of crystallinity and melting temperature, which are favorable for additive manufacturing using 3D printing. The report presents the results of a comprehensive analysis of the relationship between the synthesis conditions and the composition of copolyether ketones (CPEK) and their characteristics, including rheological, mechanical and thermal properties.

The key achievement was the development of an optimized method for obtaining CPEK with an improved macromolecular architecture, providing a targeted decrease in the degree of crystallinity by integrating comonomer units such as 4,4'-dihydroxydiphenyl or 4,4'-dihydroxyphthalophenone into the polyether ether ketone structure. It was experimentally established that a targeted decrease in the degree of crystallinity and melting point of CPEK by structural modification significantly improves the quality of products obtained by FDM in 3D printing.

The study was supported by the grant of the Russian Science Foundation No. 25-23-2234 dated 17.04.2025.



# Magnetoelectric Composite Materials from Bulk to MEMS

A. Turutin<sup>\*</sup>, I. Kubasov, A. Temirov, V. Kuts, A. Kislyuk, E. Bolotina, M. Malinkovich,

Yu. Parkhomenko

National University of Science and Technology “MISIS,” Leninskiy Prospekt, 4, Moscow, 119049, Russia

<sup>\*</sup>aturutin92@gmail.com

Composite magnetoelectric (ME) materials, which combine magnetostrictive (MS) and piezoelectric (PE) properties, possess a high potential for use in highly sensitive magnetic field sensors, other contactless measurement instruments, as well as in microelectronic devices. Sensitive elements based on ME composite structures show extremely high sensitivity to weak magnetic fields (detection limits approach single pT/Hz<sup>1/2</sup> at low frequencies (1–100 Hz) and tens of fT/Hz<sup>1/2</sup> at frequencies of several kHz at room temperature), sufficient to detect human cardiac magnetic fields. In the vast majority of current studies, a glue layer is used to physically bond piezoelectric and magnetostrictive layers in ME composite structures. However, this approach is technologically imperfect because the adhesive lowers the reproducibility of sensor properties, induces temperature instability, and limits the operational temperature range, making these designs unsuitable for commercial use.

Therefore, the development of technologies for fabricating ME composite materials for ultra-weak magnetic field sensors is moving toward more advanced methods of depositing functional PE and MS layers, employing more effective materials (including targeted modifications of their properties to increase sensitivity), and miniaturization with a gradual transition to microelectromechanical systems (MEMS).

The transition to thin-film ME materials requires various physical and chemical methods of depositing functional layers. Many studies focus on the fabrication of PE layers and investigating how their properties affect the ME effect. Considerably fewer studies address materials for MS layers particularly thin-film ones. While there are reports on thin films of magnetically soft amorphous alloys used in various microelectronic devices (e.g., memory), there is a lack of systematic research on utilizing such films in ME composites and on how their fabrication parameters influence ME characteristics.

This work demonstrates the transition from bulk ME structures to MEMS based on a bidomain lithium niobate (b-LN) y+128°-cut crystal and Metglas (Fe<sub>77</sub>Co<sub>4</sub>Si<sub>8</sub>B<sub>11</sub>). The Metglas deposition was conducted in a SUNPLA-40TM universal vacuum technology chamber. The operating pressure in the chamber was 0.5 Pa, and the magnetron power did not exceed 100 W. We investigated how the substrate holder temperature during deposition of the magnetostrictive layer affects the ME properties of the composite structures. We also show that post-deposition annealing can be used to control the domain structure and coercivity of thin Metglas films.

This work was supported by the Russian Science Foundation, grant no. 24-49-10017, <https://rscf.ru/project/24-49-10017/>.

# Spin-to charge conversion and Zeeman torque effect in THz spintronic structures

A. Sigov<sup>a,\*</sup>, V. Preobrazhensky<sup>a,b</sup>, M. Sapozhnikov<sup>a,c,d</sup>, A. Buryakov<sup>a</sup>, E. Mishina<sup>a</sup>

<sup>a</sup> MIREA - Russian Technological University, Moscow, Russia, 119454

<sup>b</sup> Prokhorov General Physics Institute of RAS, Moscow 119991, Russia

<sup>c</sup> Institute for Physics of Microstructures RAS, Nizhny Novgorod, 603950, Russia

<sup>d</sup> Lobachevsky State University, Nizhny Novgorod 603950, Russia

\*sigov@mirea.ru

Terahertz (THz) spintronics is an emerging field that exploits ultrafast spin dynamics and spin-orbit interactions to bridge the realms of magnetism and THz photonics [1]. A cornerstone of this approach is efficient spin-charge conversion, whereby a spin current is transformed into a transverse charge current via fundamental spin-orbit coupling mechanisms such as the inverse spin Hall effect in heavy metals, the Rashba-Edelstein effect at spin-split interfaces, and the anomalous Hall effect in magnetic conductors [2]. Complementarily, the Zeeman torque effect, in which the magnetic field component of a THz pulse directly exerts a torque on a material's magnetization, provides a direct means to drive and probe ultrafast spin precession, offering a potent mechanism for THz field detection and control of spin states on sub-picosecond timescales [3].

Against this background, our work presents new strategies for harnessing spin reorientation and magnetoelectric coupling effects in TbCo<sub>2</sub>/FeCo and Co/Pt-based systems to achieve fully controllable THz emission and detection. Our results demonstrated that femtosecond laser excitation of spintronic structures based on TbCo<sub>2</sub>/FeCo generates linearly polarized THz pulses. Due to spin-reorientation transitions, we achieved continuous polarization rotation of the THz emission by  $\pm 180^\circ$ , controlled solely by the magnitude of the applied magnetic field. In Co/Pt-based structures, we showed that introducing uniaxial magnetic anisotropy and rotating magnetization within the film plane enables full 360° control of the THz polarization, with a linear increase in output energy (up to 160 nJ/cm<sup>2</sup> at an optical pump fluence of 4 mJ/cm<sup>2</sup>). Modeling of optical absorption optimization through integration of Bragg reflectors [SiO<sub>2</sub>/TiO<sub>2</sub>]<sub>N</sub> revealed that the absorbed energy in the ferromagnetic layer can be increased more than ninefold (from 4.3% to 39%). To control the THz emission amplitude, we implemented a spin-valve structure, where interference between signals from layers with different coercivities enables modulation of the output. In micropatterned Co/Pt gratings, we achieved more than 20-fold suppression of THz emission when magnetized along the stripes compared to perpendicular magnetization. This opens promising opportunities for multi-state logic elements operating in the THz range.

For THz detection, we demonstrated the application of the Zeeman-torque effect method in thin Co and Co/Pt films. These detectors exhibit a wide bandwidth (up to 14 THz) and a simple transfer function of  $1/i\omega$ , significantly outperforming standard electro-optic sampling systems. The presented results form a foundation for the development of compact, tunable, and multifunctional THz devices of the next generation.

The work was supported by the Russian Science Foundation under Grant No. 23-19-00849 (<https://rscf.ru/en/project/23-19-00849/>).

[1] A. Leitenstorfer, J. Phys. D: Appl. Phys., 56, 223001 (2023)

[2] Yang, Y., Photonics, 11, 8, (2024)

[3] Chekhov A.L. Phys. Rev. Applied, 20, 3, 034037 (2023)

## Methods of Bioprinting

Y. Hesuari

3D Bioprinting Solutions, Moscow, Russia

\*usefhesuani@yandex.ru

Bioprinting is a promising technology for the layered formation of living tissue structures using "bioinks" — mostly hydrogels containing cells and biologically active substances. The relevance of bioprinting methods is due to their potential in regenerative medicine, pharmaceuticals, and tissue engineering.

Modern bioprinting encompasses several core techniques: inkjet, extrusion, laser-assisted, and stereolithography-based bioprinting [1-3]. Each method offers distinct advantages and limitations regarding resolution, cell viability, material compatibility, and application scope [4]. Inkjet bioprinting utilizes thermal or piezoelectric actuators to deposit micro-droplets of bioink onto substrates in a non-contact manner, similar to conventional inkjet printing and has several advantages as high speed, cost-effectiveness, and suitability for large-scale production; it also maintains high cell viability (>85%). Extrusion-based bioprinting involves the continuous deposition of bioinks through a nozzle using pneumatic, plunger, or screw-based systems [5]. The advantages of this method are capability of printing high cell densities and a wide range of materials, with high viscosity and as a result, the printing of large structures in the range of tens of centimeters [6]. Laser-assisted bioprinting employs pulsed lasers to propel cell-laden bioink from a donor ribbon onto a substrate, achieving precise cell placement and has high resolution (10–50  $\mu\text{m}$ ), high speed, no nozzle clogging [4]. Stereolithography (SLA) and Digital Light Processing (DLP). These methods of bioprinting technology utilizes light (UV, visible, etc.) to polymerize photoreactive bioinks layer-by-layer, enabling the fabrication of complex structures with high resolution. The advantages of these methods are high speed and accuracy, good mechanical properties and cell adhesion [3].

Although most bioprinters use the above bioprinting methods, new methods continue to be developed. For example, in situ bioprinting, is one of the most promising techniques. This method involves direct deposition of bioinks (cells, biomaterials, etc.) onto wound sites or damaged tissues during surgery, bypassing traditional scaffold implantation [7,8] and offers personalized tissue repair by tailoring constructs to individual anatomical defects using scanning and real-time 3D imaging, enhancing integration with native tissues [9]. Other methods such as high-throughput bioprinting using tissue spheroids enables rapid fabrication of functional tissues with high cell density, significantly accelerating tissue engineering processes [10].

Bioprinting technology seems to be pivotal for tissue engineering, regenerative medicine, drug screening, and disease modeling [11] and ongoing research focuses on increasing resolution, cell viability, and scalability, as well as developing patient-specific and functional organ models [12].

- [1] D. Tousoulis et al., *Acta Cardiol Sin.* 35(3): 284–289 (2019)
- [2] O. Emmanuella et al., *JSM Regen Med Bio Eng* 7(1): 1023 (2025)
- [3] Z. Wang et al., *Int J Mol Sci.* 24(7): 6357 (2023)
- [4] Sh. Zaghi, *Biomed Engand Comput Biology* 15: 1-12 (2024)
- [5] J. Malda et al., *Nat Rev Methods Primers* 1: 75 (2021)
- [6] R. Dokmeci et al., *Biomater Sci.* 6(5): 915–946 (2018)
- [7] N. Dubey et al., *ACS Applied Bio Materials* 7(12): 7987–8007 (2024)
- [8] Y. He et al., *Nat Commun* 13, 3597 (2022)
- [9] E. Alarcon et al., *Front Bioeng. Biotechnol* 10: 1-12 (2022)
- [10] N. Celik et al., *Nat Commun* 15: 1-21 (2024)
- [11] U. Piotrowska et al., *Int J Pharm* 25:644 (2023)
- [12] S. Wu et al., *Front Bioeng. Biotechnol* 11: 1-20 (2023)

## Bioprinting with collagen: state of art

E. Osidak<sup>a,b\*</sup>

<sup>a</sup> Imtek Ltd., Akademika Chazova st., 15A, Moscow, Russia.

<sup>b</sup> Dmitry Rogachev National Medical Research Center of Paediatric Haematology, Oncology and

Immunology, Moscow, Russia

\*egorosidak@gmail.com

Collagen, the predominant extracellular matrix (ECM) protein, is a cornerstone material in tissue engineering (TE) and regenerative medicine. Biomaterials fabricated from collagen serve as ideal three-dimensional (3D) substrates for cell culture and promising scaffolds for artificial tissue creation. A critical challenge lies in simulating the physical and morphological properties of native tissues requiring restoration or replacement. Modern additive manufacturing, particularly 3D bioprinting, emerges as a powerful solution. This abstract synthesizes the current state of collagen-based bioprinting, highlighting its advances, applications, challenges, and future prospects.

Collagen-based bioprinting leverages advanced additive technologies, primarily syringe-based deposition, to precisely pattern combinations of collagen hydrogels and cells. A key focus is developing bioinks – the support materials crucial for fabricating functional scaffolds. While composite bioinks exist, significant research targets "pure collagen" bioinks, consisting solely of collagen and cells. Preparation involves extracting collagen hydrogels, often utilizing physically crosslinked high-concentrated formulations to achieve sufficient stiffness while maintaining biocompatibility. Critical parameters influencing print fidelity and cell viability include bioink composition (e.g., collagen concentration), printing temperature, pressure, and cell density. Table 1 summarizes key parameters from recent studies utilizing pure collagen bioinks.

Table 1: Key Parameters for Bioprinting Pure Collagen Bioinks.

Parameter	Typical Range/Considerations	Impact
Collagen Conc.	High (e.g., >20-40 mg/ml)	Increases stiffness, improves shape fidelity; challenges viscosity/gelation
Gelation Method	Physical crosslinking (pH/temp) predominant	Maintains biocompatibility; may require optimization for speed
Printing Temp.	Cool (e.g., 4-10°C)	Maintains viscosity pre-deposition
Deposition Pressure	Optimized per viscosity/needle gauge	Affects cell viability, filament formation
Cell Density	Tissue-specific (High densities often used)	Critical for tissue formation; impacts bioink viscosity/printability
Post-Print Crosslink	Optional (e.g., chemical if needed for mechanics)	Can enhance mechanics but may affect biocompatibility

Collagen bioinks are highly regarded for their excellent biocompatibility, controllable printability, and efficient cell-loading capacity, making them ideal for fabricating bioinspired scaffolds. Applications are broadly categorized by target tissue:

- Soft Tissues (Skin, Cartilage, Heart, Vasculature): Successfully printed collagen scaffolds support regeneration, though demands for functional complexity (e.g., vascularization, innervation) are high.

- Hard Tissues (Bone, Skull, Teeth, Spine): Promising results are achieved, but enhancing the mechanical properties of collagen scaffolds remains a primary challenge to withstand physiological loads.

Collagen-based bioprinting represents a significant breakthrough in TE and regenerative medicine, enabling the fabrication of functional scaffolds for diverse repair scenarios. Key areas for future research include: 1) Optimizing pure collagen bioink formulations and printing strategies to overcome current limitations; 2) Enhancing the mechanical robustness of collagen constructs, especially for hard tissue applications; 3) Developing strategies to impart higher functional complexity, particularly for soft tissues; 4) Deepening the fundamental understanding of collagen assembly relevant to bioprinting. Overcoming these challenges will unlock the full potential of collagen bioprinting for creating clinically viable tissue replacements.

This work was supported by the Research Foundation Flanders (№24-15-00387, <https://rscf.ru/project/24-15-00387/>).

# Magnetization of Immobilized Multi-Core Particles Containing Few Superparamagnetic Nanogranules

A. Ivanov<sup>a,\*</sup>, A. Solovyova<sup>a</sup>, E. Grokhotova<sup>a</sup>, E. Elfimova<sup>a</sup>

<sup>a</sup> Ural Federal University named after the first President of Russia B.N. Yeltsin, 620000, Lenin Av. 51,  
Ekaterinburg, Russia

\*Alexey.Ivanov@urfu.ru

This work is devoted to the study of static magnetic properties of immobilized multi-core particles (MCPs) containing a small number of superparamagnetic nanogranules [1]. These objects model aggregates of superparamagnetic nanoparticles that are taken up by biological cells and subsequently used, for example, as magnetoactive agents for cell imaging.

In this study, we derive an analytical formula that allows us to predict the static magnetization of MCPs consisting of immobilized granules, in which the magnetic moment rotates freely through superparamagnetic fluctuations. The formula takes into account intergranule dipole–dipole interactions at the level of pair correlations, and it is suitable for determining the magnetization of MCPs with any number of granules and any structure. The theory is tested using Monte Carlo computer simulations on a series of MCP samples with 4 and 7 superparamagnetic granules with regular and arbitrary positions. The results demonstrate that the theory accurately describe the magnetization of MCPs with the intergranule dipolar coupling constant  $\lambda \leq 2$ .

It has been found that the stronger is the intergranule dipole–dipole interactions, the lower the magnetization of the MCP is. This is because dipole-dipole interactions contribute to the formation of the orientational texture of magnetic moments inside the MCP, which prevents their alignment along the field direction. In fact, the formation of an orientational texture of magnetic moments being stable to the magnetic field action is most favorable in MCPs with a regular structure. At the same time, the average magnetization of MCPs with different internal structures does not exceed the Langevin magnetization.

We propose a method for determining the magnetization of an ensemble of non-interacting immobilized MCPs with interacting granules by identifying this system with an ensemble of single-core immobilized non-interacting superparamagnetic particles, the easy magnetization axes of which are randomly oriented. For the last system we introduce the effective energy of magnetic anisotropy, the physical reason of which is the intergranule dipolar interaction inside each single MCP. For the studied MCPs with 4 and/or 7 nanogranules the effective interaction parameter is well described by the linear dependence  $\sigma \approx 2$ .

The obtained results allow us to predict the magnetic response of MCPs in biological media, for example, in biological cells, which is a theoretical basis for improving medical diagnostics and cell therapy technologies using MCPs as magnetically active agents.

The research was carried out within the financial support of the Russian Science Foundation, Grant No. 23-12-00039.

[1] A.Yu. Solovyova, E.V. Grokhotova, A.O. Ivanov, E.A. Elfimova, PCCP 27, 3442 (2025)

# Low-dimensional 2D crystals as emerging materials for electronic olfaction

V. Sysoev\*

Yuri Gagarin State Technical University of Saratov, 410054, Polytechnicheskaya 77, Saratov, Russia

\*vsysoev@sstu.ru

At present, the atmospheric gases are primarily analyzed using advanced analytical instruments like spectrometers and gas chromatographs which are capable to detect gases at trace-level concentrations down to ppb or even sub-ppb levels. However, these tools are rather bulky, expensive, and require skilled personnel to operate, limiting their employing to stationary laboratory environments. As a result, they are hard to be integrated into portable, user-friendly devices intended for on-site or personal use. For such mobile applications, chemical (nano)sensors offer a promising alternative due to their compactness and low-power demands to be still hindered by a poor selectivity. At the same time, nature offers a compelling solution to this challenge through the mammalian olfactory system, which relies on array of diverse receptors. The brain processes their collective signals enabling the identification of thousands of distinct chemical compounds, even of complex mixtures, with high reliability and selectivity. Inspired by this biological model, the technological analogs have been evolved since the 1990s to combine gas sensor arrays and pattern recognition algorithms, commonly referred to as electronic noses or electronic olfaction systems [1]. The recent progress in artificial neural networks has further boosted the development and real-world integration of these units.

To date, two major strategies have emerged in the development of electronic olfaction devices as, (i) assembling arrays composed of discrete sensors, often with differing sensing principles, to enhance a selectivity, and (ii) integrating one-type sensors within a single chip to enable miniaturization, reduce energy consumption, and ensure compatibility with state-of-art mass-scale semiconductor manufacturing [2]. Recent advances in nanotechnology have opened numerous avenues for fabricating gas-sensitive materials with low-dimensional architectures, 1D, 2D, or ordered 3D structures, just on a chip, with sub-micron or even nanometer-scale precision [3]. This approach enables fine-tuning of sensor properties in the on-chip arrays to reach a powerful selectivity, suitable for numerous applications. Importantly, to achieve optimal sensitivity, at least one structural dimension of these nanoscale materials should approach/match the Debye length at the material's surface in nanometer range. This ensures that gas-surface interactions are effectively transduced into measurable changes in electrical or optical properties, enabling reliable long-term operation [4].

Herein, we briefly discuss the fundamental principles underlying these systems and present our recent research and development efforts focused on creating on-chip multisensor arrays (Figure 1). These arrays are based on quasi-1D oxide nanowires/tubes/belts, 2D sheets of graphene and MXenes, and 3D mesoporous layers, subject of multiple functionalization strategies, including material composition tuning and control of operational parameters. Finally, we summarize challenges and perspectives for applying these on-chip multisensor systems in practice.

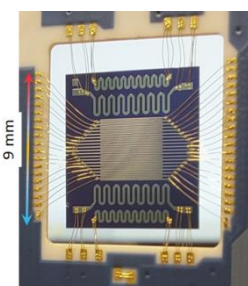


Figure 1. Photo of on-chip multi-electrode array.

- [1] F. Röck et al, Chemical Reviews 108, 705 (2008)
- [2] M. Mehdi Pour et al, Nature Communications 8, 820 (2017)
- [3] C. Wang et al, Nature Electronics 7, 157 (2024)
- [4] C. Yuan et al, Advanced Science 9 (33), 2203594 (2022)

# 2D magnetic MXenes $(M1_{1-x}M2_x)_3C_2$ ( $M1=V, Ta, Cr, Fe$ ; $M2=Cr, Mn$ ): the stability, ordering, and magnetic properties

V. Zhandun<sup>a,\*</sup>, N. Zamkova<sup>a</sup>, O. Draganyuk<sup>b</sup>

<sup>a</sup> Kirensky Institute of Physics, Federal Research Center KSC SB RAS, 660036 Krasnoyarsk, Russia

<sup>b</sup> Reshetnev Siberian State University of Science and Technology, 660037, Krasnoyarsk, Russia

\*jvc@iph.krasn.ru

Since their discovery in 2011, the MXene family of 2D materials has attracted much interest due to their unique properties, leading to practical applications. Recently, special attention has been paid to magnetic MXenes. However, despite the great diversity of the chemical composition of MXenes only a few MXenes with intrinsic magnetism have been synthesized to date. The main reason is the phase instability of both MXenes and their parent MAX phases. Here we use the DFT calculations [1] and the cluster expansion method [2] to analyze the thermodynamic stability of second-order MXenes  $(M1_{1-x}M2_x)_3C_2$  and their parent MAX phases with two transition metals. It has been shown that for compounds with  $M1 = V, Cr, Fe$  and  $M2 = Cr, Mn$  (a small difference in the atomic radii between  $M1$  and  $M2$ ), the most stable configurations are completely ordered structures at a concentration of  $x(M2)=2/3$ ,  $x(M1)=1/3$  (Fig.1a). In this case, the central layer is completely occupied by metal  $M1$ , while atoms of metal  $M2$  completely occupy the surface layer. In the case of  $M1=Hf, Ta$  and  $M2=Cr, Mn$  (large difference in atomic radii between  $M1$  and  $M2$ ) a broad minimum is observed in the concentration range of 0.5 – 0.7, due to the fact that the stability of the structure weakly depends on the specific arrangement of chromium (manganese) atoms in the surface layers. However, a tendency toward partial ordering of chromium (manganese) atoms in the outer layers with a completely ordered middle layer occupied by hafnium or tantalum atoms is observed. The magnetic and electronic structures of the studied MXenes  $(M1_{1-x}M2_x)_{n+1}C_nT$  was determined in the most stable atomic configurations and the mechanism of formation of the magnetic state is analyzed. The effect of surface functionalization with fluorine and oxygen on the properties of MXenes was also studied. At last, to analyze the possibility of MXenes experimental synthesis, a study of the stability of parent MAX phases was performed. It was found that in the dependences of the formation energy  $\Delta E(x)$  for the studied compositions  $(M1_{1-x}M2_x)_3AC_2$  with  $M1=V, Cr, Fe$ , a minimum is observed in the dependence of the formation energy on the concentration of the  $M2$  atom at a concentration of  $x \approx 2/3$  (Fig.1b).

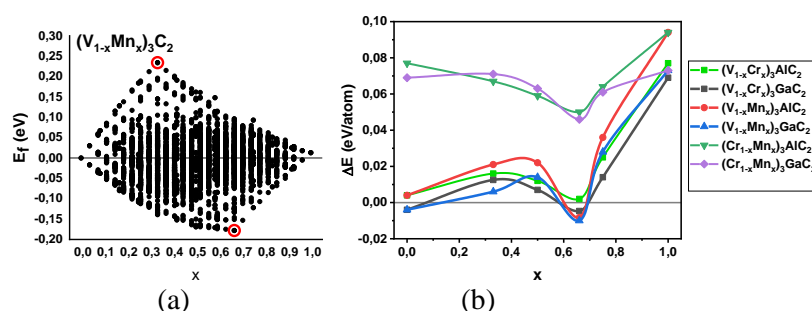


Figure 1. (a) Formation energy for different  $M2$  concentrations calculated within the cluster expansion method for  $(V_{1-x}Mn_x)_3C_2$ . The circles mark the most stable and unstable structures; (b) Dependence of the formation energy on the  $M2$  concentration of the MAX phases  $(M1_{1-x}M2_x)_3Ga(Al)C_2$ .

[1] G. Kresse, J. Furthmüller, Efficient iterative schemes for ab initio total-energy calculations using a plane-wave basis set. *Phys. Rev. B* 54, 11169 (1996)

[2] D. De Fontaine, Cluster Approach to Order-Disorder Transformations in Alloys. *Solid State Physics*, V. 33–176 (1994)

# **Defects, doping, dimensionality reduction as a way to tune the electronic, optical and magnetic properties of low-D nanomaterials. Computer Simulation and Experiment**

D. Kvashnin<sup>a,\*</sup>

<sup>a</sup> Emanuel Institute of Biochemical Physics RAS, 119334, Kosigina st. 4, Moscow, Russia

\*dgkvashnin@phystech.edu

Investigation of low-dimensional materials is quite new part of materials science which is under intensive developing. Successful synthesis of graphene lead to the opportunity to fabricate wide range of 2D materials of various compositions with huge variety of unique properties. The great interest attracts formation of novel two-dimensional materials with structure and properties having no analogues in 3D, such as silicene (twodimensional silicon), borophene (monolayer of boron atoms), CuO, Fe, FeO, CoC with unique 2D crystal structure, etc. The main feature of new class of materials is the weak atmospheric stability, which could be improved by supportive substrate, doping of embedding in stabilization matrix. Among of unique physical and chemical properties of novel low-dimensional nanostructures engineering of its properties under the influence of external conditions is still hot topic.

Fundamental knowledge of the changes of materials properties under mechanical deformation, defects of doping play an important role for future application in the key elements of novel opto- and nanoelectronic prototypes and devices. One of the most important roles in such kind of study of 2D materials in the collaboration between theory and experimental. Here the results of comprehensive investigation of low-dimensional nanomaterials will be presented. Investigation by means of the state-of-the-art quantum chemical calculations together with modern experimental equipment were performed with the aim to study the possibility of the control and engineering of its physical and chemical properties under the influence of dimension decreasing, point defects, heteroatom doping.



# **Magnetoplasmonic and terahertz photoinduced metasurfaces with anomalous dynamics of optical response**

T. Dolgova<sup>a,\*</sup>, M. Kiryanov<sup>a</sup>, I. Novikov<sup>a</sup>, V. Stadnichuk<sup>a</sup>, G. Ostanin<sup>a</sup>, D. Safiullin<sup>a</sup>, M. Inoue<sup>b</sup>, and  
A. Fedyanin<sup>a</sup>

<sup>a</sup> Faculty of Physics, Lomonosov Moscow State University, Moscow, 119991 Russia

<sup>b</sup> Department of Electrical and Electronic Information Engineering, Toyohashi University of Technology 1-1  
Tempaku-cho, Toyohashi, Aichi, 441-8580 Japan

\*dolgovatv@my.msu.ru

Ultrafast optical control of light-matter interaction is a key goal in modern nanophotonics and magnetophotonics, with potential applications ranging from signal processing to neuromorphic computing. Dynamic elements and metasurfaces that are engineered two-dimensional materials with tunable resonances, offer a route to such control both in the optical and terahertz regimes, despite practical limitations in their scalability and performance. Laser heating with high peak power pulses has a nonlinear effect on the optical response of both homogeneous materials and metasurfaces. Such a pulse heats the electron gas in the metal, leading to a change in the dielectric constant. This process is commonly described using the two-temperature model, in which the metal is treated as comprising two subsystems (electrons and phonons) in internal equilibrium but at different temperatures. The model assumes that at the beginning the electron gas is heated under the influence of the incident pulse, remaining all the time in an equilibrium state. However, this approximation often fails to capture the complexity of relaxation dynamics in resonant plasmonic and hybrid metal-dielectric systems, where deviations from the model predictions are frequently observed. In this work, we study two distinct implementations of ultrafast reconfiguration mechanisms that share a common emphasis on femtosecond-scale modulation of optical and terahertz response. The following types of resonant systems are studied: a hybrid metal-dielectric metasurface consisting of gold nanospheres embedded in a yttrium-iron-garnet matrix; an all-nickel magnetoplasmonic crystal with surface modulation engineered to achieve critical coupling, and resonant one-dimensional plasmonic gratings photoinduced on a flat gallium arsenide surface by the structured laser illumination and supporting the excitation of surface plasmon in the THz range. Experimental results obtained using a pump-probe technique reveal distinctive features of the optical and magneto-optical relaxation dynamics. The observed behavior is analyzed within theoretical frameworks that go beyond the conventional two-temperature model.

The ultrafast control and pulse shaping has been demonstrated in the terahertz regime using photoinduced gratings. In these systems, spatially structured femtosecond laser pulses are used to generate transient carrier distributions in GaAs substrates, forming reconfigurable diffraction gratings with submillimeter resolution. These optically patterned structures support terahertz plasmonic resonances, enabling dynamic modulation of the amplitude and wavefront of terahertz radiation. A modified approach to time-domain spectroscopy has been developed to resolve and analyze individual terahertz pulses directly in the time domain, avoiding artifacts introduced by Fourier transformation and allowing precise analysis of field evolution in photoinduced plasmonic modes. A photocontrolled terahertz pulse shaping is demonstrated.

This work was supported by Russian Science Foundation (24-12-00210).

# **Metallic nanowires of various types-synthesis, structure, magnetic properties and possible applications**

D. Zagorskiy<sup>a,\*</sup>, I. Doludenko<sup>a</sup>, L. Panina<sup>b</sup>, D. Khairtadinova<sup>a,b</sup>, V. Kanevskiy<sup>a</sup>

<sup>a</sup> NRC "Kurchatov Institute", Moscow, Russia

<sup>b</sup> MISIS, Moscow, Russia

\*dzagorskiy@gmail.com

The main features of matrix synthesis technique were considered. Two types of frequently used host matrices, Porous Aluminum Oxide and Track Membranes, were compared. There are three main types of objects that can be obtained - mono-metal NWs, alloyed NWs and layered NWs. According to this, some different samples (Fe, Co, Ni, Cu; FeCo, FeNi, CoCu, NiCu and Co/Cu, Ni/Cu) were obtained by electrochemical method using the Track Membranes as template in this work. Specific features of these objects synthesis are presented: real-time control of synthesis, possibilities of changing the type of NWs by changing process parameters were demonstrated.

Combination of investigation techniques – Microscopy, XRD was applied to determine shape, phase composition. Combination of Vibration magnetometry, NMR, Mossbauer and MFM was used for investigation magnetic parameters of NW ensemble and single NW.

Dependence of hysteresis loops on surface density of Fe NWs was demonstrated. It was shown that saturation field and demagnetizing field exhibited a correlation with NW's density within the membrane, for the external field aligned along the preferential NW orientation. It was in quantitative agreement with calculations derived from the effective medium model.

For alloyed NWs (FeNi and FeCo) the difference between electrolyte and NW's composition takes place- the amount of Fe in NWs is higher than in the electrolyte. It was found that the effect is more pronounced for FeNi, for lower deposition voltage and for higher NW diameter. It could be explained by a so-called anomalous co-deposition of Fe. According to XRD data, a solid solution is formed for all types of NWs. Cell parameter  $a$  depends on concentration according to Vegard law. Unit cell type of solid solutions depends on the Fe concentration. For Fe-rich samples unit cell type is *bcc*, while for Ni -rich samples *fcc* type is observed. It is Interesting that Co-rich samples also have *fcc* structure, Instead of *hcp*, which is typical for bulk samples. For these alloyed NWs the possibility of changing the magnetic properties in wide range was demonstrated: FeNi (permalloy ) NWs with small diameter (30 nm) demonstrate hard magnetic properties. The reasons for synthesis of three-components NWs was discussed.

For layered NWs the approaches were supposed for control of length, composition and flat interfaces for thin layers (down to 7-10 nm). The following methods were considered: passed charge control, using of reference electrode and reducing of deposition speed. The orientation of easy magnetization axes depends on the ratio of thicknesses of magnetic and copper layers as well as on interwire distances.

Possible applications of all these types of NWs were also discussed: generation of THz irradiation (using nets of NWs with heterojunctions); catalytic and emission properties determined by specific shapes of samples; in medicine: magnetic nano-sized particles for drug-delivery and hyperthermia.

The work was carried out within the state assignment of NRC "Kurchatov Institute". The magnetic measurements were held and supported by NUST MISIS.

## Multifunctional and multimodal contrast agents containing iron oxide nanoparticles

E. Moiseeva<sup>a</sup>, V. Skribitsky<sup>b</sup>, D. Tsiurko<sup>a</sup>, S. German<sup>a</sup>, A. Lipengolts<sup>b</sup>, D. Gorin<sup>a,\*</sup>

<sup>a</sup> Skolkovo Institute of Science and Technology, 121205, Bolshoy Boulevard, 30, bld. 1, Moscow, Russia

<sup>b</sup> N.N. Blokhin National Medical Research Center of Oncology, 115522, Moscow, Russia

\*d.gorin@skoltech.ru

Theranostics is a highly promising current trend in medicine that combines the pathological tissue imaging and therapeutic effect. One of the conventional methods of the pathological tissue imaging is MRI. This method has many advantages including a relatively high resolution, suitable penetrating to the human body and feasibility of image contrast enhancement. Nevertheless, elaborating the contrast agents that can combine both functionalities such as imaging and therapy is a clinically relevant goal. The widely used gadolinium (Gd) based contrast usually provides only  $T_1$  contrast. A good alternative to Gd-contrast agent is the contrast agent based on iron oxide nanoparticles. Traditionally, iron oxide nanoparticle-based contrast agent demonstrates  $T_2$  contrast. It was established earlier that the maghemite nanoparticles at size  $3.2 \pm 0.7$  nm exhibit the  $T_1$  contrast ability as well at the level compared to the commercially available contrast agent [1]. The maghemite nanoparticles were synthesized using the automatic reactor TetraQuant CR-1. The synthesis as well as colloidal and magnetic properties, MRI contrast were described in [2]. It is necessary to remark that iron oxide nanoparticle-based drug has been already approved by FDA for clinical applications for anemia treatment. The colloidal stability of maghemite nanoparticles stabilized with citric acid in PBS buffer and PBS buffer with protein was explored. The presence of proteins decreases the colloidal stability of maghemite nanoparticles. Nonetheless, the size of the nanoparticle is still stable until 6 hours of incubation in PBS buffer or PBS buffer with proteins [1]. The significant difference in cell toxicity was shown for maghemite nanoparticles incubated for 6 and 24 hours. Maghemite nanoparticles after incubation lasting for 6 hours are not toxic until the concentration 2 mg/ml, while after incubation for 24 hours exhibits the pronounced toxicity at concentrations starting with 0.125 mg/ml [1]. *In vivo* MRI contrast enhancement of cancer tissue after 5 min of intravenous injection was demonstrated. The acceptable level of MRI contrast enhancement remained until 48 hours after intravenous administration [1]. It was demonstrated that the light induced photodissolution of maghemite nanoparticles. Iron ions have the ability to switch on the ferroptosis of pathological cells. Therefore, it allows us to combine the MRI contrast with the light triggered ferroptosis.

[1] E. Moiseeva et al, Nanomedicine: Nanotechnology, Biology, and Medicine 65, 102811(2025)

[2] E. Moiseeva et al, Journal of Magnetism and Magnetic Materials, 608, 172447 (2024)

# Polymeric Materials for Medicine: Biocompatibility and Efficiency in Biological Systems

E. Nikolskaya<sup>\*</sup>, M. Sokol, M. Mollaeva, M. Chirkina, I. Gulyaev, M. Klimenko, O. Kamaeva,  
N. Yabbarov

N. M. Emanuel Institute of Biochemical Physics of Russian Academy of Sciences, 119334, Kosygina 4,  
Moscow, Russia

<sup>\*</sup>elenanikolskaja@gmail.com

Bioresorbable polymers are one of the most intensively studied materials in recent years due to their possible application as artificial scaffolds for tissue engineering and drug delivery systems. Polymer scaffolds, nano- and microparticles should be biocompatible and biodegradable. The use of drug delivery systems based on medical polymers approved by the regulatory authorities of different countries, can significantly improve the efficacy of many medicinal substances by preventing their untimely metabolism, reducing the level of drug interaction with inappropriate targets by altering the mechanisms of accumulation, and optimizing the drug release rate.

Natural and synthetic polymers are widely used for the development of various delivery systems. They can be modified to impart with certain properties (smart polymers) and parameters (size, surface morphology, etc.), improve the biocompatibility, and provide controlled drug release at a specified dose. Among natural polymeric biomaterials applied in wound healing materials we should emphasize collagen, gelatin, silk fibroin, and polysaccharides (sodium alginate, chitosan, cellulose, hyaluronic acid, etc.). However, most of them are characterized with limited physicochemical flexibility restraining final materials formulation process and potential application. Moreover, most of them cannot withstand the sterilization and demand special environment, particularly in combination with growth factors. In this regard, the synthetic biodegradable polymers are especially popular – poly(lactic acid) (PLA), poly(lactic-co-glycolic acid) (PLGA), poly( $\epsilon$ -caprolactone) (PCL), polyethylene glycol (PEG), polyvinyl alcohol (PVA), poly-3-hydroxybutyrate (PHB).

Nanoparticles based on the copolymer of lactic and glycolic acids (PLGA) are widely used as drug delivery systems. When particles are introduced into the internal environment of the body, a protein crown is formed on their surface - a set of proteins adsorbed from the biological environment of the body. It is known that the protein crown affects the biodistribution, pharmacokinetics and therapeutic functionality of the particles. Our objective was to obtain modified PLGA nanoparticles featuring various polymeric ligands and to develop methods for isolating these nanoparticles from blood plasma. We developed a technique for surface modification of PLGA nanoparticles using zwitterionic, positively charged, and negatively charged polymeric ligands. These included poly(carboxybetaine acrylamide), poly(2-ethyl-2-oxazoline), poly(N-isopropylacrylamide), poly(ethyl-ethylene-phosphate), and chitosan.

The main question is the degradation process of polymers in a living organism. It is known that the degradation of polymeric materials is associated with the hydrolysis of ester bonds of polymer chains, which kinetics depends on many factors. The hydrolysis rate depends on environmental conditions and catalysts (including biological ones), as well as on the chemical and enantiomeric composition of polymers. The development and application of biomaterials requires technologies capable of characterizing and monitoring the properties and microstructure of polymer scaffolds both *in vitro* and *in vivo*.

Thus, the study of the influence of the polymer type, the physicochemical properties of the object of study, as well as its life cycle in biological environments is an important stage of the work.

The research was supported by the Russian Science Foundation (project № 24-25-00095), <https://rscf.ru/project/24-25-00095/>

# Application of Raman mapping for determining heterogeneous phases in PVDF polymer films

A. Burko<sup>a\*</sup>, H. Bandarenka<sup>a</sup>, P. Ershov<sup>b</sup>

<sup>a</sup> Belarusian State University of Informatics and Radioelectronics, 220030, P. Brovki 6, Minsk, Belarus

<sup>b</sup> Immanuel Kant Baltic Federal University, 236004, Nevskogo 14, Kaliningrad, Russia

\*a.burko@bsuir.by

Polyvinylidene fluoride (PVDF) is one of the promising polymer materials for various applications, which combines high strength and resistance to deformation as well as tolerance to temperature and aggressive chemical environments. The unique features of PVDF open up its prospects for use in such devices as piezoelectric sensors and lithium-ion battery membranes. At the same time, PVDF has several phases that determine its physical and mechanical properties. For example, the  $\alpha$ -phase offers high stability, chemical resistance, and low dielectric permeability but completely lacks the piezoelectric effect. On the other hand, the  $\beta$ -phase is characterized by lower chemical resistance but pronounced piezoelectric properties. Often, fabrication of PVDF films is accompanied by formation of a structure composed of several phases in varying ratios (Figure 1a), which can lead to unstable polymer properties.

In this regard, there is an urgent need for study of the phase composition distribution in the PVDF films to control and tune their properties. Raman spectroscopy is a powerful technique that allows for the determination of the phase composition of polymer structures. Currently, systems combining Raman spectrometer and a confocal microscope or a scanning probe microscope are gaining in popularity. This combination makes it possible to analyze the phase distribution at the microscale, and in some cases even at the submicron level. This opens new possibilities for studying and controlling phase formation in polymer films. Additionally, these Raman systems are equipped with automated precision stages or galvanometer scanners, allowing the measurement region to be shifted with an accuracy of up to 100 nm.

The present study demonstrates the capability to identify and differentiate regions with various phase compositions in PVDF films produced by the doctor blade method (Figure 1, b), achieving microscale spatial resolution.

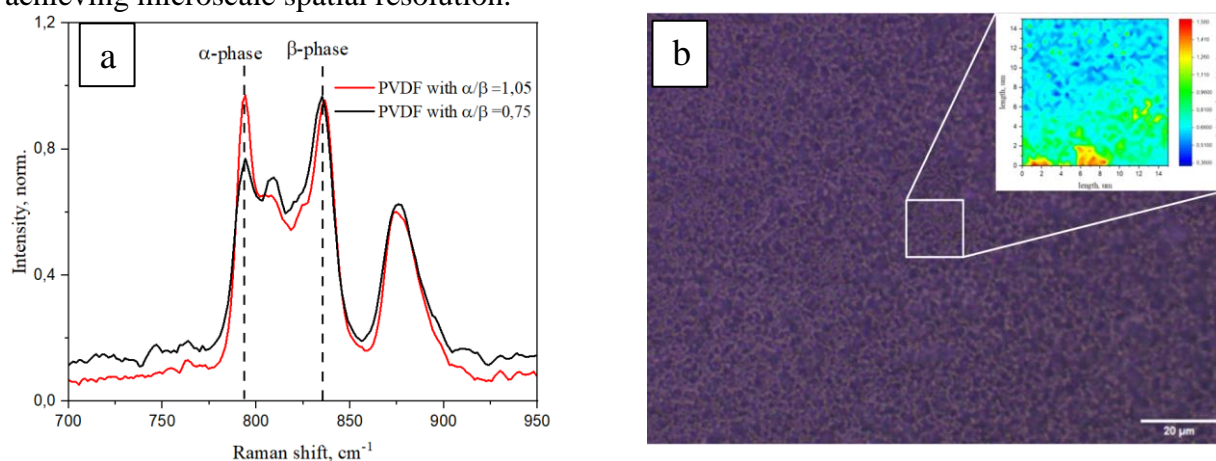


Figure 1. Raman spectra of PVDF film with different (a) phase ratio and (b) Raman imaging the PVDF film revealing the phase distribution in its surface

[1] R. Dallaev, Polymers. 14, 4793(2022)

[2] M. T. Riosbaas, Proc. of SPIE 9061, 0610Z-1 (2014)

# Influence of Size and Shell Fraction on Exchange Bias and Coercivity in Core/Shell Ferrite Nanoparticles

Atiane Quetly Silva<sup>a</sup>, Franciscarlos Gomes da Silva<sup>a,\*</sup>, Bárbara Pereira<sup>a</sup>, Rafael Cabreira Gomes<sup>c</sup>,  
Guilherme Gomide<sup>a</sup>, Renata Aquino<sup>b</sup>, Marianna Vasilakaki<sup>c</sup>, Kalliopi N. Trohidou<sup>c</sup>, Regine  
Perzynski<sup>d</sup>, Jérôme Depeyrot<sup>a</sup>

<sup>a</sup> Laboratório de Fluidos Complexos, Instituto de Física, Universidade de Brasília, Brasília (DF), Brazil

<sup>b</sup> Laboratório de Nanociência Ambiental e Aplicada, FUP-UnB, Universidade de Brasília, Brasília (DF),  
Brazil

<sup>c</sup> Departamento de Física, Universidade Federal de Santa Catarina, Santa Catarina, Brazil

<sup>d</sup> Sorbonne Université, CNRS, PHENIX, Paris, France

<sup>e</sup> Institute of Nanoscience and Nanotechnology, NCSR “Demokritos”, Athens 15310, Greece

\*fcarlos857@gmail.com

In recent decades, magnetic ferrite nanoparticles have been extensively studied for applications like magnetohyperthermia, which uses their ability to convert magnetic field energy into heat for treating certain cancers [1,2]. At the nanoscale, their magnetic properties are governed by the collective magnetic ordering of the core and by size and surface effects, in particular surface disorder. At low temperatures, the magnetic structure of these nanoparticles can be seen as an ordered core surrounded by a shell of disordered spins, resembling a spin-glass-like (SGL) structure. The coupling between the ordered spins of the core and the disordered spins of the shell leads to an exchange bias (EB) field, observed as a shift in hysteresis loops after a field cooling procedure [3,4]. In this work, we investigate the size and shell fraction dependency of the exchange anisotropy field in hard/soft core/shell ferrite nanoparticles. We synthesized three samples of ultrasmall  $\text{CoFe}_2\text{O}_4@ \gamma\text{-Fe}_2\text{O}_3$  nanoparticles ( $\sim 3\text{--}4$  nm): two with the same size but different maghemite shell fractions, and one with a different size and fixed shell volume fraction. Low-temperature magnetic hysteresis loops were recorded under various cooling fields, allowing determination of both exchange anisotropy and coercivity fields. Both EB and coercive fields were found to be enhanced in smaller particles with larger shell volume fractions. A mesoscopic-scale Monte Carlo (MC) approach [5] was employed to simulate diluted assemblies, incorporating inter- and intraparticle interactions along with particle size polydispersity. The numerical results agree with experimental data and support our interpretation of the observed magnetic behaviors.

[1] S. Beji et al., Chem. Mater. 22, 5420–5429 (2010)

[2] D. Pilati et al., J. Phys. Chem. C 122, 3028–3038 (2018)

[3] R. Cabreira-Gomes et al., J. Magn. Magn. Mater. 368, 409 (2014)

[4] F. G. Silva et al., J. Phys. D: Appl. Phys. 46, 285003 (2013)

[5] F. G. Silva et al., Nanoscale Adv. 4, 3777–3785 (2022)

# Antiferromagnetism, Symmetry and Nonlinear Optics

V. Pavlov\*

Ioffe Institute, 194021, Politekhnicheskaya 26, St. Petersburg, Russia

\*pavlov@mail.ioffe.ru

Antiferromagnets not only make up the vast majority of magnetically ordered substances, but also possess many specific physical properties unique to them [1, 2]. These materials attract significant research interest due to their potential for modern technologies, including antiferromagnetic spintronics, opto-spintronics, and memory devices [3, 4]. The second harmonic generation (SHG) is the simplest nonlinear optical process among various optical phenomena associated with frequency conversion [5]. SHG is described by the second-order nonlinear susceptibility, therefore it is sensitive to specific details of the crystallographic or magnetic structures, and to the local symmetry of electric charges and spins.

This talk is devoted to nonlinear magneto-optical phenomena associated with SHG in several antiferromagnets with different symmetries. Work [6] proposed a simple classification of antiferromagnets with respect to symmetry operations that allow the antiferromagnetic vector to be inverted. In this classification antiferromagnets are divided into three classes – magnetoelectrics (well known example is  $\text{Cr}_2\text{O}_3$ ), ordinary antiferromagnets (like  $\text{NiO}$ ) and altermagnets (for example,  $\text{CoF}_2$ ). In the electric dipole (ED) approximation, SHG is allowed only in noncentrosymmetric materials. SHG is also allowed in centrosymmetric media in the magnetic dipole (MD) or electric quadrupole approximations. In the classical magnetoelectric antiferromagnet  $\text{Cr}_2\text{O}_3$ , the spatial inversion is violated due to the spin order below the Néel temperature  $T_N$ , therefore ED SHG can be observed in the temperature range below  $T_N$  [7]. A new magnetic-field-induced mechanism of SHG is associated with the magnetoelectric effect [8]. In centrosymmetric antiferromagnet  $\text{NiO}$  the SHG is due to the nonlinear optical susceptibility of the MD type [7]. A novel nonlinear optical susceptibility of the MD type can be observed in altermagnetic  $\text{CoF}_2$  [9]. Materials, that can have both ferroelectric and antiferromagnetic order parameters simultaneously, are multiferroics. Hexagonal manganites  $\text{RMnO}_3$  ( $R = \text{Sc}, \text{Y}, \text{Ho}, \text{Er}, \text{Tm}, \text{Yb}, \text{Lu}$ ) belong to this group of antiferromagnets. In  $\text{RMnO}_3$  SHG is associated with a nonlinear optical polarization of the ED type, being a bilinear function of two order parameters [7]. The interference of various SHG contributions can be used to visualize antiferromagnetic domains that are invisible in linear optics. Thus, SHG technique makes it possible to reveal a new information, that can't be retrieved using linear optical methods.

Support by the Russian Science Foundation (project No. 24-12-00348) is acknowledged.

- [1] R.R. Birss, *Symmetry and Magnetism*, North-Holland, Amsterdam, 1966
- [2] Е.А. Туров, А.В. Колчанов, В.В. Меньшенин, И.Ф. Мирсаев, В.В. Николаев, *Симметрия и физические свойства антиферромагнетиков*, Физматлит, Москва, 2001
- [3] V. Baltz, et al., *Rev. Mod. Phys.* 90, 015005 (2018)
- [4] P. Němec, M. Fiebig, T. Kampfrath, A.V. Kimel, *Nat. Phys.* 14, 229 (2018)
- [5] R.W. Boyd, *Nonlinear optics*, Academic, London, 1992
- [6] A.V. Kimel, Th. Rasing, B.A. Ivanov, *J. Magn. and Magn. Mater.* 598, 172039 (2024)
- [7] M. Fiebig, V.V. Pavlov, R.V. Pisarev, *J. Opt. Soc. Am. B*, 22, 96 (2005)
- [8] V. V. Pavlov, et al., *Phys. Rev B*, 111, 004400 (2025)
- [9] P. A. Usachev, R. V. Pisarev, V. V. Pavlov, to be published (2025)

# Modern magnetic composite materials, their properties and application prospects

N. Perov<sup>\*</sup>, L. Makarova, D. Karpenkov

Lomonosov Moscow State University, 119991, Leninskie gory 1, Moscow, Russia

<sup>\*</sup>perovns@my.msu.ru

Composite materials (composites) are artificially created materials consisting of two or more components with different physical and chemical properties. When they are combined, a new material is obtained that is superior to the original components in terms of strength, stiffness, resistance to wear and tear and other characteristics. Composites are widely used in aviation, astronautics, automotive industry, construction, medicine and other high-tech industries. Their demand in modern technologies is determined by their unique properties. In particular, synergistic effects have been observed in composite materials, opening new perspectives for their applications.

A special place among composites is occupied by magnetic composites, which combine the advantages of traditional magnets with new possibilities such as lightness, corrosion resistance and controllable electromagnetic characteristics [1]. Magnetic liquids and magnetic elastomers, composite multiferroics and permanent magnets, materials with giant magnetic resistance have become widely known.

The peculiarities of such materials are related not only to the methods of their production, but also to the subsequent processing. Unique and controllable physical properties constantly open new perspectives for their applications.

Large coercivity and maximum magnetization are important for permanent magnets. Various technologies are used for their production. In recent years, additive technologies based on 3D printing have become more and more widespread. When using them, it is possible to obtain complex spatial configurations of the permanent magnetic field, which can significantly improve the efficiency of electrical machines.

Magnetic elastomers, which are polymer matrices with magnetic filler, are constantly expanding their capabilities. In the XXI century, they are used to develop elements of actuators, including those for robotics and electronics, medical technologies, systems of various sensors and transducers [2]. A distinctive feature of magnetic elastomers is their manufacturability and the possibility of creating biocompatible structures.

In conclusion, we would like to remind about composite structures with the effect of giant magnetoresistance.

[1] Shuai Wu et al, Multifunct. Mater. 3, 042003 (2020)

[2] D. V. Savelev et al, Polymers, **16**, 7, pp. 928–928 (2024)



# A comparative study of magneto-optical effects in the mixed ferrite $\text{Zn}_{1-x}\text{Co}_x\text{Fe}_2\text{O}_4$ and $\text{Mg}_{1-x}\text{Co}_x\text{Fe}_2\text{O}_4$ nanoparticles

A. Sokolov<sup>a,\*</sup>, I. Edelman<sup>a</sup>, O. Ivanova<sup>a</sup>, R. Ivantsov<sup>a</sup>, D. Petrov<sup>a</sup>,

Yu. Knyazev<sup>a</sup>, A. Thakur<sup>b</sup>, P. Thakur<sup>b</sup>

<sup>a</sup> Kirensky Institute of Physics, Federal Research Center KSC SB RAS, 660036, Krasnoyarsk, Russia

<sup>b</sup> Amity University Haryana, Gurugram, Haryana, 122413 India

\*alexeys@iph.krasn.ru

Faraday rotation and magnetic circular dichroism (MCD) spectral dependences were investigated for the nanoparticles (NPs) of the  $\text{Me}^{2+}_{1-x}\text{Co}_x\text{Fe}_2\text{O}_4$  where  $\text{Me}^{2+}$  was Zn or Mg with  $x$  changing from zero to 0.6 in comparison with the Mossbauer spectroscopy data. Ferrite nanoparticles were obtained by an identical technology using the self-combustion method with the citrate precursor [1,2]. The Fig 1 shows the MCD spectra for some identical cobalt concentrations in both compounds. A significant difference between the spectra is visible, the maximum for the initial compounds when  $x=0$ . If in the case of  $\text{ZnFe}_2\text{O}_4$  the MCD is practically absent, in accordance with the distribution of  $\text{Fe}^{3+}$  ions by positions then in the case of  $\text{MgFe}_2\text{O}_4$  in the region of 2-4 eV it reaches a significant value and demonstrates a complex structure. This type of spectrum does not correspond at all to the data on the Mössbauer effect (Table 1), which may be due to the skew of the magnetic moments of the  $\text{Fe}^{3+}$  ions, similar to iron borate or hematite. When  $\text{Co}^{2+}$  ions are added, strong changes occur in the spectra. At  $x = 0.2$  in the first case, two very wide maxima of very small amplitude can be seen. In the second case, at this concentration of cobalt, a clear structure of the spectrum is also visible. With further increase in  $x$ , a strong negative peak appears centered near 1.75 eV in both cases.

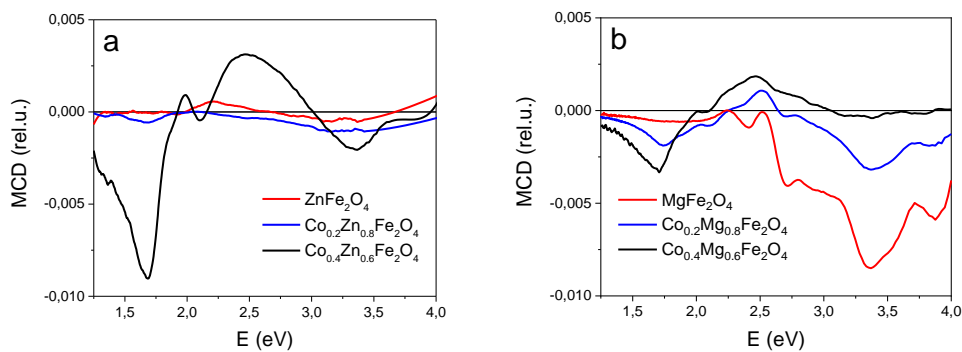


Figure 1. MCD spectra

Tables 1. The data of the Mössbauer effect spectroscopy

$x=0$	$(\text{Zn}_{0.76}\text{Fe}_{0.24}) [\text{Zn}_{0.24}\text{Fe}_{1.76}]\text{O}_4$	$(\text{Fe}_{0.95}\text{Mg}_{0.05})[\text{Fe}_{1.05}\text{Mg}_{0.95}]\text{O}_4$
$x=0.2$	$(\text{Co}_{0.08}\text{Zn}_{0.80}\text{Fe}_{0.12}) [\text{Co}_{0.12}\text{Fe}_{1.88}]\text{O}_4$	$(\text{Fe}_{0.93}\text{Mg}_{0.07})[\text{Fe}_{1.07}\text{Mg}_{0.73}\text{Co}_{0.2}]\text{O}_4$
$x=0.4$	$(\text{Co}_{0.24}\text{Zn}_{0.60}\text{Fe}_{0.26}) [\text{Co}_{0.26}\text{Fe}_{1.74}]\text{O}_4$	$(\text{Fe}_{0.94}\text{Mg}_{0.06})[\text{Fe}_{1.06}\text{Mg}_{0.54}\text{Co}_{0.4}]\text{O}_4$

The observed structure of the spectra and its change with changing  $x$  are discussed from the point of view of electronic transitions in  $\text{Co}^{2+}$  and  $\text{Fe}^{3+}$  ions.

[1] A. Thakur et al, JMR 39 (2024) 3029

[2] O. Ivanova et al, Jetp Lett. 119 (2024) 104

## Biointerfaces based on laser-induced carbon composite materials

A. Gerasimenko<sup>a, b\*</sup>

<sup>a</sup> National Research University of Electronic Technology - MIET, 124498, Zelenograd, Moscow, Russia

<sup>b</sup> I.M. Sechenov First Moscow State Medical University, 119991, Moscow, Russia

\*gerasimenko@bms.zone

Recent studies have demonstrated the efficacy of bioelectronic devices in addressing cognitive disorders, pain syndromes, and other diseases of the nervous system. Devices that interact with the nervous system have emerged as an alternative to pharmacological treatments, thereby inaugurating a new era of implantable interfaces [1]. These devices possess the capacity to receive electrical impulses from nerve tissue and to transmit them in response to stimulation. The implantation of these devices in the dorsal region serves to regulate the transmission of nociceptive signals to the brain. The electrodes of these devices function as a biosimilar interface, thereby facilitating the communication between the generator or receiver of electrical signals and the nervous tissue of the spinal cord. The interfaces are fabricated with specific dimensions and geometry, as well as electrical and mechanical properties, to meet biological requirements in terms of invasiveness, selectivity, and performance [2]. A microelectrode array (MEA) constitutes an advantageous biosimilar interface topology. This is due to the fact that the MEA is a thin layer that carries embedded conductor structures. The dense arrangement of charge carriers enables the activation of a greater number of discrete neurons or groups of neurons. High-performance biosimilar interfaces should be characterized by low impedance, high conductivity and charge injection capacity for sensing and recording as well as safe and reversible stimulation. This necessitates an augmentation in the specific surface area of the interface, which is accomplished by forming the surface from composite layers based on carbon nanomaterials. The sp<sup>2</sup>-hybridized structure exhibits a high degree of mechanical strength and stability, a high aspect ratio, controlled electrical conductivity, and a structure comparable to the main proteins of the extracellular matrix. The creation of oriented framework structures was achieved through the utilization of external exposure to electromagnetic radiation, employing compounds that exhibit sp<sup>3</sup>-hybridization characteristics on the surface and within the volume of biopolymers [3-5]. A method for the formation of neurointerfaces of flat and cylindrical shapes with a given micro- and nanostructure has been developed. During the process of electrical stimulation, it is imperative to deliver a charge to activate the action potential at close contact between the interface and the nervous tissue. This phenomenon is contingent upon the existence of a mutual correspondence of structures on both sides. Under the action of pulsed laser radiation on the medical steel substrate, a microstructured surface was formed due to the ablation process. Furthermore, the interaction of deposited layers of albumin biopolymer, reduced graphene oxide flakes, and single-walled carbon nanotubes resulted in the formation of vertically oriented structures providing charge injection capacity up to 2 mC/cm<sup>2</sup> [6]. Such structures demonstrated the absence of cytotoxicity, and when connected to a pulse generator provided electrostimulation of neural tissue cell growth.

[1] E. Mankin, *Neuron*, 106, 218 (2020)

[2] C. Bohler, *Biomaterials* 67, 346 (2015)

[3] A. Gerasimenko, *Spectrochimica Acta Part A: Mol. and Biomol. Spectr.*, 227 (117682), 1 (2020)

[4] A. Gerasimenko, *Nanomaterials*, 12, 2812 (2022)

[5] A. Gerasimenko, *Polymers*, 14(9), 1866 (2022)

[6] M. Savelyev, *Polymers*, 17(10), 1300 (2025)

# Oral talks

# Dielectric photonic metasurfaces for analog optical image processing

A. Fedyanin<sup>a,\*</sup>

<sup>a</sup> Lomonosov Moscow State University, 119991, Leninskie gory 1, Moscow, Russia

<sup>\*</sup>fedyanin@nanolab.phys.msu.ru

Image processing is used in a wide range of applications, such as objects detection and identification, evaluation of geometric transformations, noise filtering, image restoration, etc. These tasks are usually solved by rasterization of the image and its further digital processing. However, in the case of intensive workloads, this approach brings about significant power and time consumption overhead. The problem can be solved using analog image analysis. For this, before entering the camera, the input image passes through the optical system performing preliminary processing, which simplifies further image analysis. One of the most popular approaches for input image processing is Fourier filtering, but the use of conventional elements such as spatial light modulators for wavefront shaping is a serious drawback due to their weight and large size. Metasurfaces open new possibilities for creating compact and versatile optical components. We perform numerical and experimental studies of the analog correlation analysis using an optical metasurface. For that, we design and fabricate a silicon-based device operating as a matched filter in the spatial Fourier filtering scheme

[1] V.V. Yushkov, V.A. Sitnyansky, A.S. Shorokhov, and A.A. Fedyanin, ACS Photonics 11, 2506 (2024)

# Investigation of nonlinear effects of spin waves in multilayer ferromagnetic structures with a periodic metallic shield

A. Ptashenko\*, A. Sadovnikov

Saratov State University

\*andrey.po3@mail.ru

Nonreciprocal effects of spin waves (SW) in multilayer ferromagnetic structures are of significant interest for applications in magnonics and spintronics. This study investigates the behavior of SW in bilayer yttrium iron garnet (YIG) films with a periodic copper overlay, which exhibit lower losses compared to traditional YIG/metal structures [1]. The structure consists of two YIG layers with different thicknesses ( $d_2=9\text{ }\mu\text{m}$ ,  $d_1=7\text{ }\mu\text{m}$ ) and saturation magnetizations ( $M_1=904\text{ Gs}$ ,  $M_2=1738\text{ Gs}$ ), placed in an external magnetic field ( $H_0=670\text{ Oe}$ ) oriented perpendicular to the SW propagation plane to excite surface magnetostatic waves (SMSW) [2].

Numerical modeling was performed using HFSS and COMSOL MULTIPHYSICS tools, solving Maxwell's equations with the finite element method (FEM) [3]. The amplitude-frequency characteristics (AFC) reveal two transmission bands in the low-frequency (2.82–2.9 GHz) and high-frequency (3.53–3.75 GHz) ranges (Fig. 1a), confirmed by dispersion analysis (Fig. 1b). Adding a periodic copper overlay induces Bragg forbidden zones in the high-frequency region, demonstrating effective control over SW propagation.

The results highlight the potential of multilayer ferromagnetic films for designing devices with tunable SW properties, advancing magnonic technologies [4].

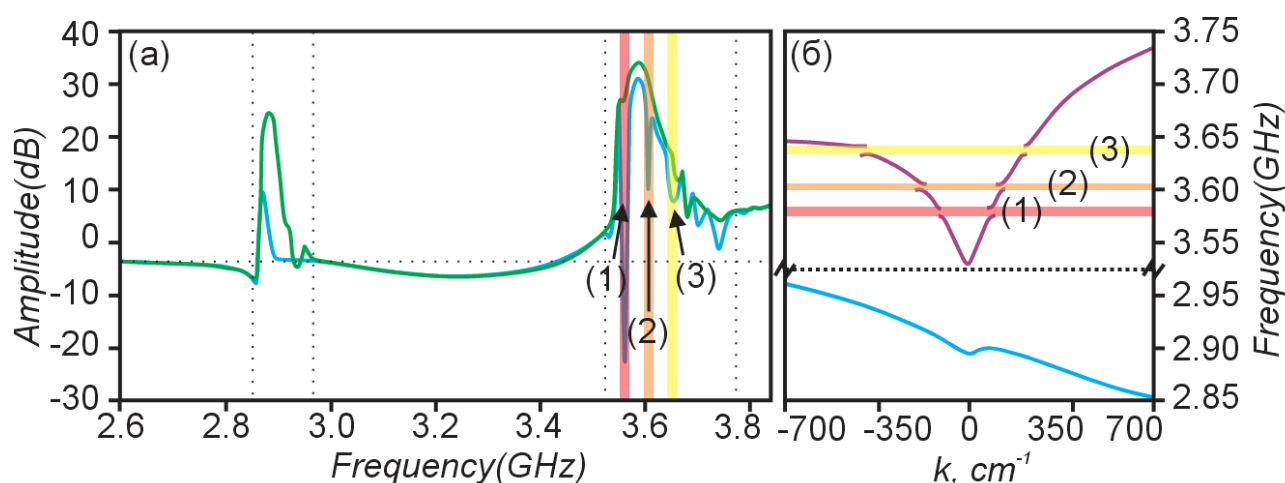


Figure 1.(a) Amplitude-frequency characteristic of SW. (b) Dispersion characteristics of SW

The work was supported by the Russian Science Foundation grant (No. 23-79-30027)

[1] Nikitov S.A., Safin A.R., Kalyabin D.V., Sadovnikov A.V., Beginin E.N., Logunov M.V., Morozova M.A., Odintsov S.A., Osokin S.A., Sharayevskaya A.Yu., Sharayevsky Yu.P., Kirilyuk A.I., UFN 190 1009–1040 (2020). Chumak A.V., Vasyuchka V.I., Serga A.A., and Hillebrands B. Nature Phys 11, 453–461 (2015)

[2] Rozhnev A.G. Modeling the propagation of magnetostatic waves in one-dimensional magnonic crystals. // Proceedings of Higher Educational Institutions. Applied Nonlinear Dynamics. 2012. V.20(1). P.143–159

[3] Damon R.W. and Eshbach J.R. J. Phys. Chem. Solids. 19, 308 (1961)

[4] Chumak A.V., Vasyuchka V.I., Serga A.A., and Hillebrands B. Nature Phys 11, 453–461 (2015)

# Resonant-like magneto-optical spectra in the Ta(2 nm)/Co<sub>50</sub>Pt<sub>50</sub>(4.6 nm)/Ta(2 nm) nanostructure

I. Gladyshev<sup>a</sup>, M. Yashin<sup>a\*</sup>, A. Yurasov<sup>a</sup>, M. Simdyanova<sup>a,b</sup>, I. Lobov<sup>c</sup>, M. Makarova<sup>c</sup>, J. Park<sup>d</sup>,

Y. Kim<sup>d</sup>, A. Telegin<sup>c</sup>, A. Granovsky<sup>b,e</sup>

<sup>a</sup> MIREA-Russian Technological University, Moscow, 119454 Russia

<sup>b</sup> Lomonosov Moscow State University, Moscow 119991, Russia

<sup>c</sup> M.N. Mikheev Institute of Metal Physics, Ural Branch of the Russian Academy of Sciences, Yekaterinburg, 620108, Russia

<sup>d</sup> Department of Materials Science and Engineering, Korea University, Seoul 02841, Republic of Korea

<sup>e</sup> Institute for Theoretical and Applied Electrodynamics, Russian Academy of Sciences, Moscow, 125412 Russia

\*alexey\_yurasov@mail.ru

The Ta(2 nm)/Co<sub>50</sub>Pt<sub>50</sub>(4.6 nm)/Ta(2 nm) nanostructure was fabricated on silicon substrate by magnetron sputtering. Structural properties were studied by X-ray reflectometry and diffraction. Magnetic measurements showed soft magnetic behavior and in-plane magnetization. Magneto-optical spectra were obtained in the transverse Kerr effect (TKE) geometry in magnetic fields up to 10 kOe in the spectral range from 0.5 to 4.5 eV. All measurements were performed at room temperature. The unusual behavior of TKE was found with resonant-like features around 1.0 and 3.0 eV, where the TKE parameter reached  $10^{-2}$  (Fig.1) .

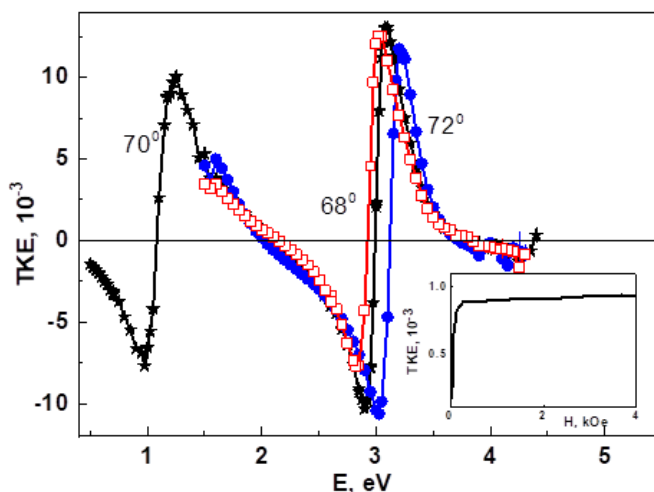


Figure 1 Spectral dependences of the Kerr effect (TKE) for the Co<sub>50</sub>Pt<sub>50</sub> nanostructure at various angles of incidence of radiation in a magnetic field of 2.2 kOe. The insert shows the field dependence of the TCE for an angle of incidence of 70 degrees at a radiation energy of 2 eV.

The modeling using the Fresnel formulas and the parameters for thick CoPt samples and Ta showed that this behavior is not related to interference effects. We suggested that the observed resonant features are due to the quantum size effect in thin Co<sub>50</sub>Pt<sub>50</sub> layer, which leads to resonant magneto-optical transitions. Our modeling using transfer-matrix method and assuming resonant levels in non-diagonal dielectric permeability confirms this explanation.

# Nucleation of magnetic skyrmions by spin-polarized current injection

T. Taaev<sup>a,\*</sup>, V. Antonov<sup>a,b</sup>, K. Khizriev<sup>a</sup>

<sup>a</sup> H. Amirkhanov Institute of Physics DFRC RAS, 367003, M.Yaragskii 94, Makhachkala, Russia

<sup>b</sup> Institute of High Technologies and Advanced Materials, Far Eastern Federal University, 690922, Ajax Bay 10, Russky Island, Vladivostok, Russia

\*taaev89@mail.ru

Magnetic skyrmions are among the most promising candidates for the creation of next-generation magnetic memory devices due to their nanoscale size (down to several nanometers), topological protection and high mobility under of spin-polarized currents [1-3]. Currently, the key challenges in the study of magnetic skyrmions are controlling their nucleation and motion. Structural inhomogeneities in thin films and various defects, which are always present at the micro- and nanoscale, play a crucial role in these processes. The stability of skyrmions in the presence of non-magnetic defects was studied in detail by using transition state theory [4], which demonstrated that skyrmion nucleation and annihilation are energetically favorable at non-magnetic defects.

In this work, we propose a model of a magnetic racetrack with structural defects for the stable nucleation of skyrmions using spin-polarized current injection. Micromagnetic simulations were performed using the MuMax3 package, which solves the Landau-Lifshitz-Gilbert equation [5] to calculate magnetization dynamics:

$$\frac{\partial \vec{m}}{\partial t} = \gamma \frac{1}{1 + \alpha^2} \left( \vec{m} \times \vec{H}_{eff} + \alpha \left( \vec{m} \times (\vec{m} \times \vec{H}_{eff}) \right) \right) + \tau_{ZL}, \quad (1)$$

where  $\tau_{ZL}$  is the Zhang-Li spin-transfer torque term [6]:

$$\tau_{ZL} = \frac{b}{1 + \alpha^2} \{ \vec{m} \times (\vec{m} \times (\vec{j} \cdot \nabla) \vec{m}) + (\beta - \alpha) (\vec{m} \times (\vec{j} \cdot \nabla) \vec{m}) \}, \quad (2)$$

where  $\gamma$  is the gyromagnetic ratio,  $\alpha$  is the damping parameter,  $m$  is the normalized magnetization vector,  $H_{eff}$  is the effective field,  $j$  is the vector of the current density,  $\beta$  is the nonadiabatic factor, and  $b = P\mu_B / eM_s (1 + \beta^2)$  with  $P$  the polarization of the current density,  $\mu_B$  is the Bohr magneton and  $e$  is the electron charge.  $H_{eff}$  is the effective magnetic field given by the functional derivative of the free energy  $E$  with respect to the magnetization:

$$\vec{H}_{eff} = - \frac{1}{\mu_0 M_s} \frac{\delta E}{\delta \vec{m}}. \quad (3)$$

The conditions for the magnetic skyrmion nucleation were determined as functions of both size of the defect and spin-polarized current magnitude. We demonstrated the feasibility of a binary data storage system, where skyrmions act as information bits controlled by adjusting the amplitude and pulse duration of the spin-polarized current density.

The research was supported by the Russian Science Foundation (project No.25-22-20086).

- [1] S. Muhlbauer, et al. Science. 323, 915(2009)
- [2] C. Back, et al. J. Phys. D: Appl. Phys. 53, 363001 (2020)
- [3] S.S.P. Parkin, et al. Science. 320, 190 (2008)
- [4] P.F. Bessarab, et al. Computer Physics Communications. 196, 335 (2015)
- [5] A. Vansteenkiste, et al. AIP Advances. 4, 107133 (2014)
- [6] R.M. Menezes, et al. Physical Review B. 99, 104409 (2019)

# A magnetic bubble domain making: electric field-controlled blowing and splitting

D. Volkova, E. Nikolaeva, A. Pyatakov\*

<sup>a</sup> Lomonosov Moscow State University, 119991, Leninskie gory 1, Moscow, Russia

<sup>b</sup> MIREA — Russian Technological University, 119454 Vernadsky Avenue, 78 Moscow, Russia

\*PyatakovAP@my.msu.ru

Recently in iron garnet films the electric-field control of magnetic structure was demonstrated [1], as an electrostatic interaction between charged electrode and electrically polarized magnetic domain walls. In particular, it makes possible to nucleate the bubble domain at positively charged tip in homogeneously magnetized media (Figure 1).

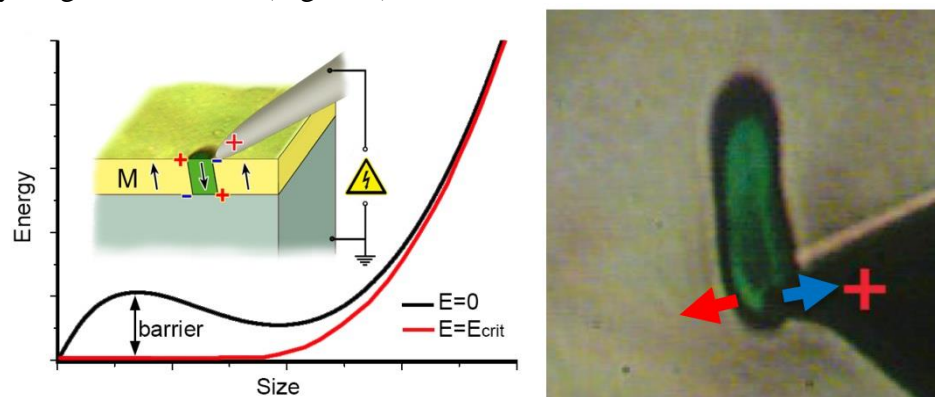


Figure1. The electric field-induced magnetic bubble domain blowing: a) the mechanism of domain nucleation: the electrostatic interaction flattens the potential barrier for bubble nucleation; b) the magneto-optical image of bubble domain generated at the electrically biased cantilever tip of scanning probe microscope. The forces of Coulomb attraction and repulsion to the positively charged tip are shown with arrows. [1].

In this work we report the reverse effect of bubble domain splitting by negatively charged tip electrode (Figure 2).

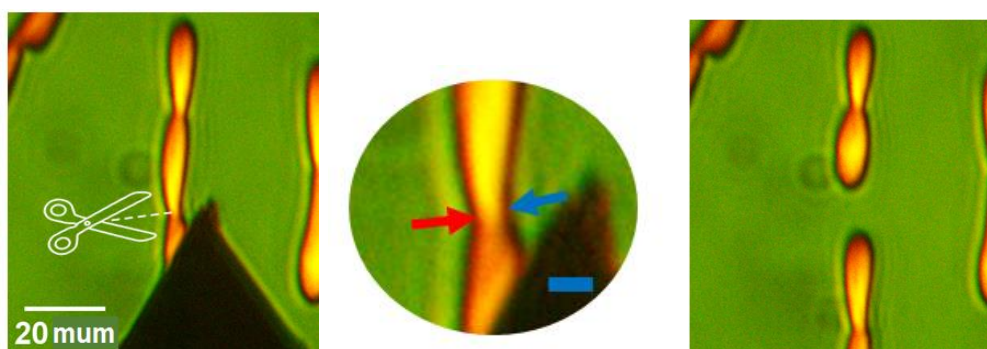


Figure 2. The process of stripe domain splitting by tip electrode. The forces of Coulomb attraction and repulsion to the negatively charged tip are shown with arrows.

The work is supported by Russian Science Foundation grant #25-79-30019.

[1] A. Pyatakov, Physica B: Condensed Matter 542 (2018) 59–62



# Magnetic properties of Fe-*Me* (*Me* = Ga, Ge) alloys with low *Me* content: Insights from *ab initio* and Monte Carlo

M. Zagrebin<sup>a,\*</sup>, A. Kuznetsov<sup>a</sup>, M. Matyunina<sup>a</sup>, V. Sokolovskiy<sup>a</sup>, V. Buchelnikov<sup>a</sup>

<sup>a</sup> Chelyabinsk State University, 454001, Brat'ev Kashirinykh Str. 129, Chelyabinsk, Russia

\*miczag@mail.ru

Multifunctional iron-based compounds are of interest due to their unusual mechanical, magnetic, electrical and magnetostrictive properties [1]. The addition of non-magnetic Al, Ga, and Ge atoms to the  $\alpha$ -Fe structure leads to a significant increase in magnetostriction value in alloys of relatively pure iron [2]. In the range of non-magnetic atom content from 0 to 10 at.%, the phase diagrams of the Fe-*Me* alloy (*Me* = Al, Ga, Ge) have a similar appearance and are characterized by the presence of a disordered structure A2 (symmetry group No. 229), in which the Curie temperature decreases slightly [3]. In this paper, the effect of the crystal lattice parameter on the magnetic properties of Fe<sub>100-*x*</sub>Me<sub>*x*</sub> alloys (*Me* = Ga, Ge 0 ≤ *x* ≤ 14) is analyzed. All calculations were performed using the density functional theory implemented in the SPR-KKR package (spin-polarized relativistic Korringa-Kohn-Rostoker code) [4]. For the exchange-correlation potential, a generalized gradient approximation in the form of the PBE functional (Perdew-Burke-Ernzerhof) was used [5]. The disordered structure of A2 was investigated in the work. Calculations were carried out for the values of the crystal lattice parameter 2.7 ≤ *a* ≤ 3.0 Å and the content of Fe atoms 0 ≤ *x* ≤ 14 at.%. In Fig. 1 the distributions of the magnetic exchange interaction parameters between the nearest-neighboring Fe atoms in Fe-Ge alloy in dependence on the crystal lattice parameter *a* and the Fe content *x* is depicted. It is evident from the figure that the value of the magnetic exchange interaction parameters has a nonlinear character of dependence on both the Fe content and the crystal lattice parameter.

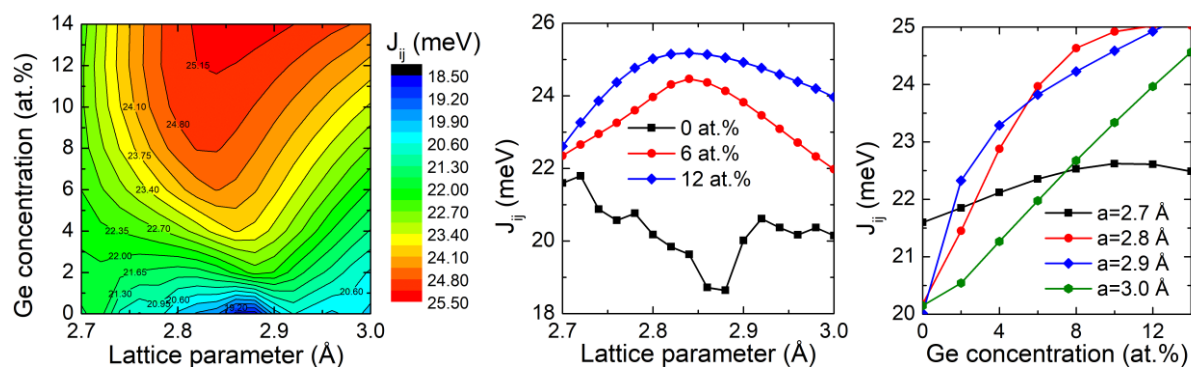


Figure 1. Distribution of the magnetic exchange interaction parameters between the nearest neighboring Fe atoms depending on the crystal lattice parameter *a* and the Fe content *x* in Fe-Ge alloy.

This work was supported by Russian Science Foundation (project # 24-22-20086, <https://rscf.ru/project/24-22-20086/>).

- [1] I. S. Golovin et al. Phys. Met. Metallogr. 121, 937 (2020)
- [2] A.E. Clark et al. IEEE Trans. Magn. 36, 3238 (2000)
- [3] O. Kubaschewski. Iron-Binary phase diagrams. Springer-Verlag (1982)
- [4] H. Ebert et al. Rep. Prog. Phys. 74, 096501 (2011)
- [5] J.P. Perdew et al. Phys. Rev. Lett. 77, 3865 (1996)

# Magneto-optical Spectroscopy of CoFeB–LiNbO<sub>3</sub> Nanocomposite Films

E. Ganshina<sup>a</sup>, M. Simdyanova<sup>a,b,\*</sup>, I. Pripechenkov<sup>a</sup>, S. Nikolaev<sup>c</sup>, V. Rylkov<sup>c,d</sup>, I. Bykov<sup>d</sup>,  
A. Dorofeenko<sup>d</sup>, A. Sitnikov<sup>e</sup>, A. Yurasov<sup>b</sup>, A. Granovsky<sup>a,d,\*\*</sup>

<sup>a</sup> Faculty of Physics, Lomonosov Moscow State University, Moscow, 119991, Russia

<sup>b</sup> MIREA-Russian Technological University, Moscow, 119454 Russia

<sup>c</sup> National Research Center «Kurchatov Institute», Moscow, 123182 Russia

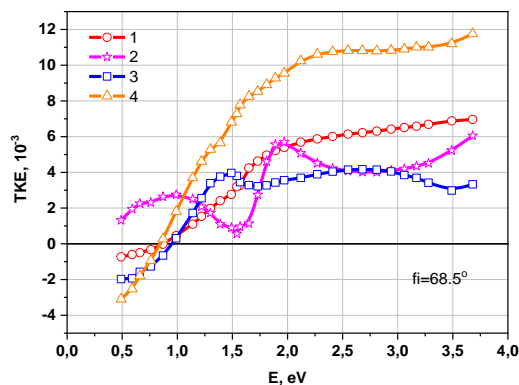
<sup>d</sup> Institute for Theoretical and Applied Electrodynamics, Russian Academy of Sciences, Moscow, 125412  
Russia

<sup>e</sup> Voronezh State Technical University, Voronezh, 394026 Russia

\*marina.simdyanova3103@mail.ru

\*\*gran60@mail.ru

We present results on field and spectral dependences of the transverse Kerr effect (TKE) for (Co<sub>40</sub>Fe<sub>40</sub>B<sub>20</sub>)<sub>x</sub>(LiNbO<sub>3</sub>)<sub>100-x</sub> nanocomposite films with x=43, 47, 55 and 59 at.% deposited on silicon substrates and with x=59 at.% on glass-ceramic, silicon and quartz substrates. It is shown that the magneto-optical spectroscopy can help to find the critical concentration for the metal-insulator transition, superferromagnetic state, and difference of magnetic properties of samples with the same composition but fabricated on different substrates. For example, Fig.1 shows TKE spectra for (Co<sub>40</sub>Fe<sub>40</sub>B<sub>20</sub>)<sub>59</sub>(LiNbO<sub>3</sub>)<sub>41</sub> thin films fabricated on glass-ceramic substrate (curve 1), Si (curve 2) and SiO<sub>2</sub> (curve 3). It is shown also for comparison the TKE spectra for the film without boron - (Co<sub>50</sub>Fe<sub>50</sub>)<sub>59</sub>(LiNbO<sub>3</sub>)<sub>41</sub> (curve 4).



Experimental TKE spectra of nanocomposites (CoFeB)<sub>59</sub>(LiNbO<sub>3</sub>)<sub>41</sub> on various substrates: Glass-ceramic (circles), Si (squares), SiO<sub>2</sub>/Si (stars); and nanocomposite (CoFe)<sub>59</sub>(LiNbO<sub>3</sub>)<sub>41</sub> on the Si substrate (triangles).

The experimental results are analyzed using data for structural properties, resistivity, anomalous Hall effect, optical properties, and using calculations within the framework of the effective medium theory generalized to take into account the granular size.

# Prediction of magnetic properties for nanoparticles with machine learning

K. Kapranova, J. Razlivina, N. Shirokiy, D. Kaldko\*

ITMO University, Saint-Petersburg 191002, Russian Federation

\*kladko@scamt-itmo.ru

Magnetic nanoparticles underpin a wide range of applications—biomedicine, biosensing, data storage, petroleum engineering, and catalysis—thanks to their tunable magnetic responses (coercivity, remanence, and saturation magnetization) and other task-specific attributes that can be engineered to meet functional requirements. Mapping these behaviors to structural, compositional, and morphological features is, however, highly nonlinear. Consequently, data-driven and machine-learning (ML) approaches are increasingly used to predict magnetic performance from known descriptors. While prior ML studies have successfully modeled intrinsic properties such as magnetocrystalline anisotropy and Curie temperature for well-defined materials families [1,2], far fewer connect synthesis conditions to magnetic outcomes. In practice, nanoparticle magnetism is strongly dictated by parameters like temperature, solvent, precursors, and reaction time. This synthesis–structure–property triad remains underexplored computationally, leaving forward and inverse prediction of synthesis routes a major open challenge.

Here we present an AI-driven platform for the design of magnetic nanoparticles that combines ML models with an LLM-based multi-agent system. We curated a multimodal dataset of ~2,000 entries capturing synthesis conditions and resulting properties, and trained models to predict coercivity, saturation magnetization, and remanent magnetization. Among tree-based boosting methods, CatBoost was the most consistent performer ( $R^2 = 0.82$ ; RMSE = 0.27), outperforming HistGradientBoosting and LightGBM. We further employ retrieval-augmented generation (RAG) to optimize the selection of synthesis protocols for target magnetic properties. In its forward mode, the system ingests a curated database of synthesis records—structured numerical descriptors such as reaction temperature, precursor ratios, particle size, shape, and surface coating—and applies machine-learning models to accurately predict the key magnetic properties, including coercivity, saturation magnetization, and remanent magnetization. Conversely, in its inverse mode, the same database of paired synthesis protocols and measured properties is mined to train predictive algorithms that, given a set of desired magnetic targets, can propose the most promising synthesis parameters and structural features needed to achieve them. By uniting these two capabilities in an LLM-based platform, researchers can not only anticipate nanoparticle performance before experimentation but also streamline the design of novel materials by directly translating performance goals into actionable synthetic blueprints.

[1] S. Mal, G. Seal, P. Sen, J. Phys. Chem. Lett. 2024, 15, 3221.

[2] C. J. Court, A. Jain, J. M. Cole, Chem. Mater. 2021, 33, 7217.

# Magnetic resonance in nanogranular composites: Observation of “double-quantum” excitations in ferromagnetic particles

A. Drovosekov<sup>a,\*</sup>, M. Dmitrieva<sup>a,b</sup>, A. Sitnikov<sup>c</sup>, S. Nikolaev<sup>d</sup>, V. Rylkov<sup>d,e,f</sup>

<sup>a</sup> Kapitza Institute for Physical Problems, RAS, 119334, Moscow, Russia

<sup>b</sup> National Research University Higher School of Economics, 101000, Moscow, Russia

<sup>c</sup> Voronezh State Technical University, 394026, Voronezh, Russia

<sup>d</sup> National Research Centre Kurchatov Institute, 123182, Moscow, Russia

<sup>e</sup> Institute of Theoretical and Applied Electrodynamics, RAS, 125412, Moscow, Russia

<sup>f</sup> Kotelnikov Institute of Radio Engineering and Electronics, Fryazino Branch, RAS, 141190, Fryazino, Moscow region, Russia

\*drovosekov@kapitza.ras.ru

Films of metal-insulator nanogranular composites  $M_xD_{100-x}$  with different compositions and percentage of metallic and dielectric phases ( $M = \text{Fe, Co, Ni, CoFeB}$ ;  $D = \text{Al}_2\text{O}_3, \text{SiO}_2, \text{ZrO}_2, \text{LiNbO}_3$ ;  $x \approx 10\text{--}80$  at.%) were studied by magnetic resonance. The experiments were carried out in a wide range of frequencies ( $f = 7\text{--}38$  GHz) and temperatures ( $T = 4.2\text{--}360$  K) at different orientations of the magnetic field with respect to the film plane.

It was found that at concentrations of the metallic ferromagnetic (FM) phase below the percolation threshold, the experimental spectra, besides the usual signal of the FM resonance (FMR), contain an additional absorption peak characterized by a double effective g-factor  $g_{\text{eff}} \approx 4$ . Furthermore, the observed peak demonstrates a number of other unusual properties:

- 1) It is better manifested in the longitudinal geometry of the resonance excitation.
- 2) With an increase of the FM phase content, the peak demonstrates an additional frequency shift depending on the orientation of the external field with respect to the film plane.
- 3) The temperature dependence of the peak intensity has a non-monotonic character with a maximum in temperature. This maximum shifts to higher temperatures with an increase of the FM phase content.

The appearance of such a peak in the resonance spectra can be explained within the framework of the “giant spin” model [1] by excitation of “forbidden” (“double-quantum”) transitions inside the FM nanogranules with a change in the spin projection  $\Delta m = \pm 2$ . Within the framework of this approach, it is possible to explain the better manifestation of the  $g_{\text{eff}} \approx 4$  peak in the longitudinal geometry of the resonance excitation, as well as the anomalous temperature dependence of its intensity [1–3]. The unusual frequency-field and orientational dependencies observed for the  $g_{\text{eff}} \approx 4$  peak are well described taking into account the presence of effective dipolar fields inside the film: the “demagnetization field” and the “Lorentz fields” [4].

[1] N. Noginova, T. Weaver, E. P. Giannelis, A. B. Bourlinos, V. A. Atsarkin, V. V. Demidov, Phys. Rev. B 77, 014403 (2008)

[2] M. Fittipaldi, R. Mercatelli, S. Sottini, P. Ceci, E. Falvo, D. Gatteschi, Phys. Chem. Chem. Phys. 18, 3591 (2016)

[3] A.B. Drovosekov, M.Yu. Dmitrieva, A.V. Sitnikov, S.N. Nikolaev, V.V. Rylkov, Zh. Eksp. Teor. Fiz. 166, 383 (2024)

[4] A. B. Drovosekov, N. M. Kreines, D. A. Ziganurov, A. V. Sitnikov, S. N. Nikolaev, V. V. Rylkov, J. Exp. Theor. Phys. 137, 562 (2023)

# Fabrication of Magnetoelectric PVDF/CFO Composites Using FDM and DIW 3D Printing Techniques

P. Ershov<sup>a,\*</sup>, A. Omelyanchik<sup>a</sup>, V. Savin<sup>b</sup>, A. Amirov<sup>a</sup>, A. Ignatov<sup>a</sup>, A. Zhansitov A<sup>b</sup>, I. Musov, I. Vindokurov<sup>c</sup>, M. Tashkinov<sup>c</sup>, V. Salnikov<sup>a</sup>, E. Sergeev<sup>a</sup>, S. Vorontsov<sup>a</sup>, V. Kolesnikova<sup>a</sup>, P. Vorontsov<sup>a</sup>, L. Panina<sup>a,d</sup>, V. Rodionova<sup>a</sup>

<sup>a</sup> Immanuel Kant Baltic Federal University, 236004, Nevskogo 14, Kaliningrad, Russia

<sup>b</sup> Kabardino-Balkarian State University named after H.M. Berbekov, Nalchik, Russia

<sup>c</sup> Perm National Research Polytechnic University, 614990, Perm, Russia

<sup>d</sup> National University of Science and Technology, MISiS, 119049 Moscow, Russia

\*pershov@kantiana.ru

This study explores the fabrication of magnetoelectric (ME) composites polyvinylidene fluoride (PVDF) and cobalt ferrite (CFO) nanoparticles using two 3D printing techniques: fused deposition modeling (FDM) and direct ink writing (DIW). Optimized DIW inks—based on a dimethyl sulfoxide (DMSO)/acetone solvent blend and polyethylene glycol (PEG)-coated CFO nanoparticles—enabled the formation of PVDF with up to 50% electroactive phase content, enhancing the ME coupling coefficient to  $10 \text{ mV} \cdot \text{cm}^{-1} \cdot \text{Oe}^{-1}$ . In comparison, FDM-printed samples showed the same electroactive phase content (~52%) and a reduced ME coefficient ( $\sim 2.6 \text{ mV} \cdot \text{cm}^{-1} \cdot \text{Oe}^{-1}$ ), influenced by the thermal processing route and melt crystallization behavior.

A comparative evaluation of DIW and FDM printing methods revealed distinct trade-offs. DIW-printing facilitated superior nanoparticle dispersion and electroactive phase development due to its solvent-based, low-temperature processing; however, it is constrained by slower throughput and structural instability during printing. FDM-printing, while introducing more thermal defects and lower electroactivity, benefits from greater scalability, shape fidelity, and material reuse. Strategies to address DIW's scalability include the development of rapid solvent evaporation systems, multi-nozzle printing arrays, and ink formulations with tunable rheology and low toxicity solvents. FDM's limitations may be offset through tailored filament compositions, incorporation of nucleating agents, or in-line thermal annealing to improve  $\beta$ -phase yield and mitigate phase degradation during extrusion.

The continued development of diverse fabrication methods for magnetoelectric (ME) composites is essential, as each technique presents distinct advantages. DIW- printing enables the use of thermally sensitive compositions that would degrade during high-temperature processes like FDM-printing. Conversely, thermal printing offers significantly faster fabrication of three-dimensional objects by eliminating the time-consuming solvent evaporation step required in liquid-based approaches. Consequently, the advancement of this technology hinges on the intelligent combination of these manufacturing methods. Fabricating ME objects from PVDF/CFO polymer composites will require further investigation to refine and optimize these synergistic printing strategies.

This work was supported by the Russian Science Foundation (RSF) according to the research project No. 21-72-30032.

## Magnetic nanoparticles and nanocomposites for modern technologies of diagnostics (mrt, mpi) and treatment (mht)

A. Kamzin

Ioffe Institute RAS, 194021, 26 Politekhnicheskaya, St-Petersburg, Russia

\*ASKam@mail.ioffe.ru

The first stable colloidal ferrofluid was created in 1938 [1]. The heating ability of nanoparticles in an alternating magnetic field was first used for therapeutic purposes in 1957 [2]. Ferrofluids have been included in a number of industrial applications such as encapsulation, transformer cooling, loudspeaker damping and cooling, and hazardous waste treatment. Over the past few decades, nanomaterials with sizes less than 100 nm possess unique properties in terms of high surface–volume ratios, tunable properties, enhanced thermal conductivity, which have made these nanomaterials highly useful in a wide range of applications in various fields including large-scale biomedical applications. such as targeted drug delivery, hyperthermia treatment (HT), MRT contrast agents, etc. [3]. In 2000, a new method of visualizing human organs was proposed, called magnetic powder imaging (MPI) [3]. Magnetic nanoparticles (MNP) and magnetic nanocomposites (MNC) are used in the listed methods of diagnostics and treatment of humans. If at the beginning of the stages of applying the MRI and MHT methods, MNP of hematite ( $\alpha\text{-Fe}_2\text{O}_3$ ), magnetite ( $\text{Fe}_3\text{O}_4$ ), were used, which are the most biologically compatible with a living organism, since they are present in the blood. At present, medicine requires MNP and MNC with high magnetic characteristics to reduce the dose of the administered magnetic fluid. The MPI method imposes significantly higher requirements on the properties of MNP.

Currently, MNP and MNC intended for use in the above-mentioned methods of diagnostics and treatment are being studied. MNCs are materials consisting of two or more components with different, and often opposite, properties, such as hard magnetic and soft magnetic materials (HM/SM), graphene oxide and ferrites (GO/Ferr), core/shell MNCs (C/S). The core has high magnetic characteristics, but is often toxic, so the core is coated with a biocompatible material. Combining components with completely different properties and characteristics allows us to obtain materials with new unique properties, which opens up new broad opportunities for their diverse applications.

The report presents the works on the creation of MNP and MNC with high magnetic and structural characteristics that satisfy both the well-known MRT method and the new method of visualization and diagnostics of MPI, as well as the treatment (MHT) of human diseases.

[1] Gilchrist RK, Medal R, Shorey WD, Hanselman RC, Parrott JC, Taylor CB. Selective inductive heating of lymph nodes. *Ann Surg* 1957;146:596.

[2] X. Li, J. Niu, L. Deng, Y. Yu, L. Zhang, Q. Chen, J. Zhao, B. Wang, H.Gao, *Acta Biomater.* **2024**, 173, 432.

[3] B. Gleich, J. Weizenecker, *Nature* **2005**, 435, 1214

# Effect of mobility and distribution of particles in magnetic elastomers on magnetoelectric effect in layered composites

L. Makarova<sup>a,\*</sup>, S. Kirgizov<sup>b</sup>, M. Musaev<sup>a</sup>, R. Makarin<sup>a</sup>, A. Kharlamova<sup>a</sup>,

M. Kalandia<sup>a</sup>, S. Kostrov<sup>c</sup>, O. Kuvandikov<sup>b</sup>, E. Kramarenko<sup>a,c</sup>, N. Perov<sup>a</sup>

<sup>a</sup> Lomonosov Moscow State University, 119991, Leninskie gory 1, Moscow, Russia

<sup>b</sup> Samarkand State University named after Sharof Rashidov, 140100, University Boulevard 15, Samarkand, Uzbekistan

<sup>c</sup> A.N. Nesmeyanov Institute of Organoelement Compounds of Russian Academy of Sciences, 119334, Vavilova St., 28, Moscow, Russia

\*la.loginova@physics.msu.ru

The magnetoelectric effect (MEE) is a physical phenomenon that involves the induction of electric polarization in an external magnetic field. The MEE has been observed in multiferroics, materials that exhibit several types of ferro-properties simultaneously; in composite multiferroics, the effect is observed up to several  $\text{V}\cdot\text{cm}^{-1}\cdot\text{Oe}^{-1}$ , which has attracted the interest of researchers. The applications of multiferroics are extensive, encompassing a broad range of technological domains, including microwave devices, sensors, multiple-state memories and antennas, etc. Autonomous energy harvesting represents an exemplification of the application of multiferroics. Flexible magnetoelectrics have been identified as a key development area, with the potential to advance both the field of flexible electronics and the field of biocompatible magnetoelectrics. The latter is particularly significant for the creation of biomedical sensors, which are crucial for medical research and healthcare applications.

One such example of a flexible and biocompatible multiferroic is a layered structure composed of a layer of piezopolymer film and a layer of magnetoelastomeric (MAE) film [1]. It has been demonstrated that such mechanically bonded structures are found to exhibit MEE due to the deformation of the MAE layer in the presence of a magnetic field. The MAE layer functions as a flexible magnetostrictive layer, and the piezopolymer layer, which possesses piezoelectric properties, is also flexible, thereby enabling the structure to maintain its overall flexibility. The employment of MAE facilitates the modulation of the MEE magnitude and resonance frequency. Varying the composition of MAE - filling with micro- or nanoparticles of different concentrations, changing the elastic modulus, - allows a more precise calibration of the control parameters. Furthermore, the possibility of simultaneous displacement and retraction of particles can also lead to changes in the MEE settings.

In this study, we analyze properties of MAE-based layered structures comprising iron microparticles with isotropic and anisotropic distribution within a polymer matrix, with varying elastic moduli. The mobility of particles in the polymer is clearly manifested in the magnitude of the magnetoelectric effect in structures with an isotropic MAE layer. Despite the isotropic distribution of particles and their equal concentration, the value of the MEE increases with decreasing elastic modulus. It is evident that the magnitude of the effect is not contingent on oil concentration for anisotropic samples, given the influence of particle mobility. It has been demonstrated that particle structures formed into chain-like structures from particles bound by strong dipole-dipole interactions are almost equally drawn into the field gradient without significant displacement. This results in an almost equivalent magnitude of MEE.

The work was supported by the Russian Science Foundation (Project No. 22-72-10137)

[1] L.A. Makarova et al., Polymers 15, 2262 (2023)

# Deformation and interaction of ferroliquid drops in a magnetic field

A. Zakinyan, D. Kononenko

Federal State Autonomous Educational Institution for Higher Education, 355017, Pushkin 1, Stavropol,  
Russia

\*daryna.kononenko@yandex.ru

The dynamics of the deformation process of liquid droplets, as well as their interactions in an external field, are of considerable scientific interest [1, 2]. In particular, one of the traditional problems in the physics of ferrofluids is the study of equilibrium shapes of droplets in a magnetic field. The equilibrium configurations and the dynamics of shape changes of individual ferrofluid droplets have been studied in detail [3]. However, the behavior of these processes in systems of interacting droplets remains insufficiently explored. The characteristics of these processes are determined by factors such as magnetic interactions, interfacial tension, and hydrodynamic forces.

This paper examines the processes of dynamics formation in a system of two and three interacting ferrofluid drops when a stationary magnetic field source is applied to them. It is shown that, at the initial stage of exposure to the external field, droplet shape oscillations are observed (Fig. 1). These oscillations are caused by inertial effects and are most pronounced when the droplets are close together, where hydrodynamic interaction influences their relative motion.

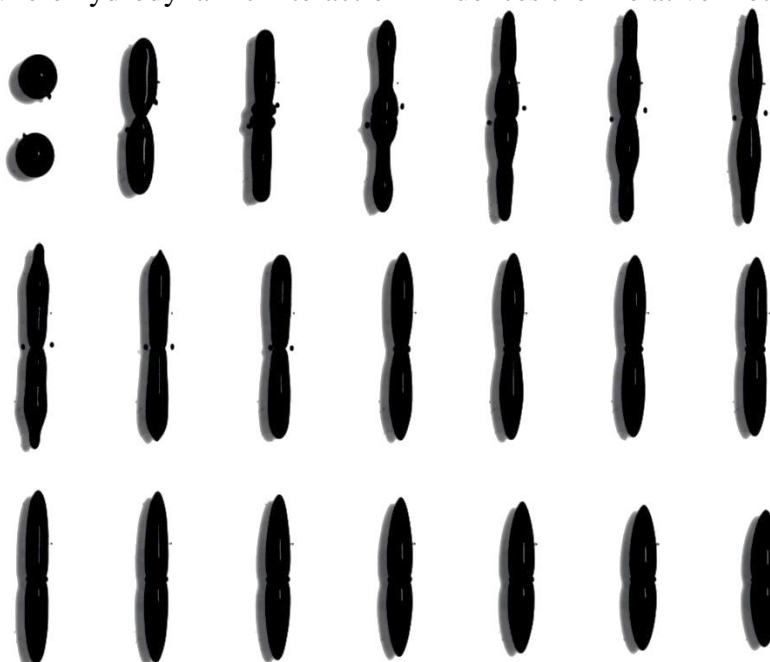


Figure 1. Monolayer of ferrofluid droplets at successive moments of time after application of a uniform magnetic field.

- [1] S. Torza, R.G. Cox, S.G. Mason, Electrohydrodynamic deformation and burst of liquid drops, *Philos. Trans. R. Soc. London, Ser. A* 269 (1971) 295–319, <https://doi.org/10.1098/rsta.1971.0032>
- [2] P.M. Vlahovska, Electrohydrodynamics of drops and vesicles, *Annu. Rev. Fluid Mech.* 51 (2019) 305–330, <https://doi.org/10.1146/annurev-fluid-122316-050120>
- [3] E. Blums, A. Cebers, M.M. Maiorov, *Magnetic Fluids*. de Gruyter, New York, 1997



# Investigation of magnetoresistance of CoFeB/SiO<sub>2</sub> composite in magnetic fields of 1 and 5 T at temperatures of 2-400 K

A. Utkin<sup>a,\*</sup>, L. Kotov<sup>a</sup>, A. Sitnikov<sup>b</sup>, Yu. Kalinin<sup>b</sup>

<sup>a</sup> Syktyvkar State University, Syktyvkar, Russia

<sup>b</sup> Voronezh State Technical University, Voronezh, Russia

\* utych@yandex.ru

Composite metal-dielectric films like CoFeB/SiO<sub>2</sub>, containing dielectric and magnetic granules with randomly oriented magnetic moments, are promising materials for magnetoelectronics, spintronics, and sensors due to their tunable electrical resistance in magnetic fields [1]. Properties such as magnetoresistance (MR) depend strongly on particle size, shape, distribution, and film structure [2], but achieving optimal MR, particularly large negative values, requires further study [3-5]. This work investigates CoFeB/SiO<sub>2</sub> films with varying metal concentrations ( $x = 0.45-0.83$ ) over a wide temperature range of 2-400 K and in magnetic fields up to 9 T to better understand these relationships.

Films were fabricated by ion bombardment of CoFeB and SiO<sub>2</sub> targets onto Laysan (PET) substrates. MFM analysis revealed a clear dependence of film structure on the metal concentration  $x$  [4, 5]. Films with  $x = 0.45-0.49$  showed a granular structure, potentially with small percolation regions. At  $x = 0.56-0.72$ , a stripe magnetic domain structure was observed. For  $x = 0.8-0.83$ , the structure consisted of a metallic matrix with embedded dielectric particles. Conductivity measurements indicated semiconductor-like transport, with resistance decreasing linearly as temperature increased. Calculated activation energies reflected the structural changes, being 0.22 eV for granular films ( $x = 0.45$ ) and 0.02 eV for  $x = 0.49$  films [4, 5]. Magnetotransport property studies [4, 5] highlighted a strong dependence on this microstructure. Granular films ( $x = 0.45$ ) exhibited the most significant effects: a peak negative MR of 230% was observed at 400 K in a 1 T field. The  $x = 0.45$  sample also exhibited an exponential MR increase above 370 K in weak fields (possibly thermal ordering) and, at 5 T, showed both a 50% negative MR peak and a transition from positive to negative MR around 270 K, potentially due to changing scattering mechanisms. Compared to granular films, stripe ( $x = 0.56-0.72$ ) and matrix ( $x > 0.8$ ) structures exhibited much weaker MR effects up to 9 T (potentially involving Lorentz contributions for stripes), while  $x = 0.49$  films showed pronounced field dependence at 100 K indicative of spin transport.

These findings suggest that MR formation in CoFeB/SiO<sub>2</sub> involves several competing mechanisms, with Lorentz and tunneling effects likely playing key roles [4, 5]. The analysis indicates that the overall MR magnitude and sign depend critically on the balance between these effects. This balance is governed by temperature, magnetic field strength, and crucially, the film's specific microstructure, such as the ratio and connectivity of metallic versus granular regions.

The work was carried out with the support of a grant from the Russian Science Foundation, project No. 25-72-20063.

[1] S. Yang, J. Zhang, *Chemosensors*, 9(8), 211 (2021)

[2] V.V. Rylkov, A.V. Emelyanov, S.N. Nikolaev, K.E. Nikiruy, A.V. Sitnikov, E.A. Fadeev, V.A. Demin, A.B. Granovsky, *J. Exp. Theor. Phys.*, 131, 160-176 (2020)

[3] L. Yang, N. Shipp, Y. Pu, Y. Chen, Y. Chen, L. He, X. Ruan, W. Liu, Y. Xu, *Appl. Phys. Lett.*, 115, 072407 (2019)

[4] L.N. Kotov, A.A. Utkin, Yu.E. Kalinin, A.V. Sitnikov, *15* (4), 85–92 (2023)

[5] L. Kotov, V. Vlasov, P. Kovalev, A. Utkin, Y. Kalinin, A. Sitnikov, V. Ustygov, 2023 International Conference on Next Generation Electronics (NEleX), Vellore, India, 2023

## Spin valves for THz emitter/modulator

E. Mishina<sup>a,\*</sup>, M. Sapozhnikov<sup>a,c</sup>, A. Buryakov<sup>a</sup>, V. Preobrazhensky<sup>a,b</sup>

<sup>a</sup> MIREA - Russian Technological University, 119454, Moscow, Russia

<sup>b</sup> Prokhorov General Physics Institute of RAS, Moscow 119991, Russia

<sup>c</sup> Institute for Physics of Microstructures RAS, Nizhny Novgorod, 603950, Russia

\*mishina\_elena57@mail.ru

Over the past decade, intensive development of terahertz (THz) spintronics has focused on investigating efficient THz emitters and sensitive detectors. It has now become that for the comprehensive use of THz range for spectroscopy and imaging, it is necessary to create a full line of complementary THz wave operation devices, including polarization control devices, modulators, amplifiers, and saturable absorbers. Spintronic emitters with in-plane anisotropy of magnetic layer provide full 360° polarization rotation with constant THz amplitude and high optic-to-THz conversion efficiency [1]. Spin valves, which are two magnetic layers separated by a nonmagnetic spacer, provide the existence of additional (from two to multiple) states and increased functioning and are used in various applications such as magnetic sensors, read heads for hard disk drives, and non-volatile magnetic memory devices such as MRAM. Recently, a spin valve was suggested as a spintronic emitter providing amplitude control (modulation) while polarization remains constant [2].

Here, we present the results of experimental studies of two types of spin valves used as spintronic THz emitters. The first one is based on two unequal-thickness magnetic emitting structures FeCo/TbCo<sub>2</sub>/FeCo separated by a nonmagnetic copper layer (FM1/Cu/FM2). The second one is formed by two cobalt layers separated by a Pt layer (Co/Pt/Co); in one of the Co layer magnetization is pinned by adjacent antiferromagnetic IrMn layer. In both spin valves, an in-plane magnetic anisotropy is established as a fine tool to tune the properties of magnetic nanostructures. In-plane magnetic field control their functional properties. In both structures, the spin current is excited by a femtosecond optical pulse through ultrafast electron heating followed by magnetically asymmetrical relaxation, and the charge current is produced by inverse spin-Hall effect (ISHE). However, the resulting behavior of the THz wave in these two structures is different. This is due to different localization of charge current. In the first structure, the Cu separating layer does not possess charge-orbit coupling, then each FeCo/TbCo<sub>2</sub>/FeCo structure acts as an independent source of charge current. Then the emitted THz wave is the result of interference of two THz waves from these two different sources. In the second structure, the non-magnetic Pt layer between two magnetic Co layers possesses a strong charge-orbital coupling, and it is Pt that is the source of the charge current. This current arises due to ISHE at two opposite interfaces. Therefore, in this case, we can talk about the summation of charge currents with two opposite directions or a kind of "interference" of two currents. THz conversion efficiency as well as the amplitude modulation efficiency is much higher in the Co/Pt/Co/IrMn structure.

Modeling of magnetization and THz field was performed. For the (FM1/Cu/FM2) structure, due to different thickness of FM1,2 structures, one of them was considered as magnetically soft, while the other as magnetically hard; the interaction between these two layers was absent. For the (Co/Pt/Co) structure, interaction between two layers was taken into account. The results of modeling the magnetization and the THz field amplitude hysteresis loops fit well with the experimental results.

The work was supported by the Russian Science Foundation under Grant No. 23-19-00849 (<https://rscf.ru/en/project/23-19-00849/>).

[1] D. Khusyainov, Scientific Reports 11, 697 (2021)

[2] M. Fix, Appl. Phys. Lett. 117, 132407 (2020)

# Effect of Ferromagnets on Coherent Transport in Josephson Hybrid Nanostructures

V. Ryazanov<sup>a,b\*</sup>

<sup>a</sup> Moscow Institute of Physics and Technology, State University, 141700, Institutskiy per. 9, Dolgoprudny, Moscow Region, Russia

<sup>b</sup> Institute of Solid State Physics, Russian Academy of Sciences, 142432, Akademik Ossipyan 2, Chernogolovka, Moscow region, Russia

\*valery.ryazanov@gmail.com

Currently, there is great interest in hybrid nanostructures with coherent transport through various Josephson barriers made of normal metals, ferromagnets, topological insulators, etc. Our group has carried out pioneering experiments with the flow of superconducting current through layers of weak ferromagnets [1,2] and layers of normal metals in contact with ferromagnets [3,4]. The presence of ferromagnets significantly changes the relation between the superconducting current and the superconducting phase difference at a Josephson barrier, up to the transition of the Josephson structure to a state with an inverse current-phase relation, the  $\pi$ -state.

The talk discusses experimental studies of two types of Josephson  $\pi$ -contacts: Josephson superconductor-ferromagnet-superconductor sandwiches (Josephson SFS contacts) and planar submicron Josephson S-N/F-S structures, with a contact of a normal metal and a ferromagnet in the Josephson barrier. The most attention is paid to the features of “Andreev” coherent transport in the presence of injection and diffusion of spin-polarized carriers into the Josephson barrier [3,4] due to the contact of a normal metal and a ferromagnet in the barrier.

Josephson hybrid structures based on ferromagnetic layers (SFS  $\pi$ -junctions) have prospects for use in digital and quantum electronics [5].

- [1] V.V. Ryazanov, V.A. Oboznov, A.Yu. Rusanov et al, Phys. Rev. Lett. 86, 2427 (2001)
- [2] V. A. Oboznov, V.V. Bol'ginov, A.K. Feofanov et al, Phys. Rev. Lett. 96, 197003 (2006)
- [3] T.E. Golikova, F. Hübner, D. Beckmann et al, Phys. Rev. B 86, 064416 (2012)
- [4] T.A. Golikova, M.J. Wolf, D. Beckmann et al, Supercond. Sci. Technol. 34, 095001 (2021)
- [5] A.K. Feofanov, V.A. Oboznov, V.V. Bol'ginov et al, Nature Physics 6, 593 (2010)

# The Effect of Argon Ion Irradiation on the Electrical Resistivity and Magnetotransport Properties of Topological Weyl Semimetal WTe<sub>2</sub>

A. Perevalova<sup>a,\*</sup>, B. Fominykh<sup>a</sup>, S. Naumov<sup>a</sup>, K. Shalomov<sup>b</sup>, E. Marchenkova<sup>a</sup>, N. Gushchina<sup>b</sup>,  
V. Ovchinnikov<sup>b</sup>, V. Marchenkov<sup>a</sup>

<sup>a</sup> M.N. Mikheev Institute of Metal Physics, Ural Branch of the Russian Academy of Sciences, 620108,  
S. Kovalevskaya str., 18, Ekaterinburg, Russia

<sup>b</sup> Institute of Electrophysics, Ural Branch of the Russian Academy of Sciences, 620016, Amundsen str., 106,  
Ekaterinburg, Russia

\*domozhirova@imp.uran.ru

Tungsten ditelluride has been found to belong to the class of topological Weyl semimetals [1]. The presence of Weyl nodes in the band spectrum of this compound provides its outstanding electronic properties. The formation of defects as a result of irradiation with charged particles can cause significant changes in transport characteristics. For example, the paper [2] demonstrates the influence of Ga<sup>+</sup> implantation on the electronic structure and transport properties of WTe<sub>2</sub>. This opens up a new direction in the study of the physical properties of topological semimetals, as well as new possibilities for practical applications of such compounds. The purpose of this work is to study the effect of argon ion irradiation on the electrical resistivity and magnetotransport of WTe<sub>2</sub>.

WTe<sub>2</sub> single crystals were grown by the chemical vapor transport method. Ion beam treatment was carried out with continuous beams of Ar<sup>+</sup> ions with an energy of 40 keV and various fluences from 10<sup>15</sup> to 5·10<sup>17</sup> cm<sup>-2</sup>. X-ray diffraction analysis, scanning electron microscopy, and energy-dispersive X-ray spectroscopy were used for structural characterization of the pristine and irradiated samples. Electrical resistivity and galvanomagnetic properties were measured at temperatures from 2 to 300 K and in magnetic fields up to 9 T.

As a result of argon irradiation, the destruction of the crystalline structure of the surface of the studied single crystals was observed. At the same time, the electrical resistivity of the samples increases with increasing temperature and fluence. Shubnikov-de Haas oscillations were detected in magnetoresistivity. Variations in the concentration and mobility of current carriers were observed, estimated from the analysis of both quantum oscillations and the Hall effect using a two-band model. These effects are due to the appearance of additional scattering centers, as well as a possible change in the Fermi surface. Thus, argon ion irradiation is an effective tool for tuning the electrical resistivity and magnetotransport characteristics of WTe<sub>2</sub>.

The research was supported by the Russian Science Foundation (project No. 24-72-00168).

[1] P. Li, Y. Wen, X. He, et al., Nat. Commun. 8, 2150 (2017)

[2] D. Fu, B. Zhang, X. Pan, et al., Sci. Rep. 7, 12688 (2017)

# Noninvasive Deep Brain Stimulation Using Magnetoelectric Core–Shell Nanotransducers

R. Chernozem<sup>a,\*</sup>, A. Romashchenko<sup>a,b</sup>, A. Urakova<sup>a</sup>, P. Chernozem<sup>a</sup>, A. Ibraeva<sup>a,b</sup>, M. Surmeneva<sup>a</sup>,

R. Surmenev<sup>a</sup>

<sup>a</sup> National Research Tomsk Polytechnic University, 634050, Lenin av. 30, Tomsk, Russia

<sup>b</sup> FRC Institute Cytology and Genetic, SB RAS, 121205, ac. Lavrentieva ave. 10, Moscow, Russia

\*romanchernzoem@gmail.com

**Introduction.** Magnetoelectric (ME) nanomaterials and nanotechnology have attracted considerable attention for biomedical applications, particularly in treating neurodegenerative disorders and neurotrauma [1]. Core-shell nanoparticles (NPs) with strong ME coupling are widely employed to fabricate ME nanostructures. Recently, ME core-shell NPs based on biocompatible magnetic  $\text{MnFe}_2\text{O}_4$  (MFO) cores and a perovskite  $\text{Ba}_{(1-x)}\text{Ca}_x\text{Zr}_\gamma\text{Ti}_{(1-\gamma)}\text{O}_3$  (BCZT) shell were reported [2]. However, their surface functionalization and implications for biomedicine remain underexplored. Moreover, a detailed analysis of the physical properties of stable colloidal MFO@BCZT NPs and their influence on biological functions is lacking. This study investigates the surface characteristics, structure, and physical properties of colloidal ME MFO@BCZT NPs, as well as their biological activity *in vitro* and *in vivo* under external magnetic fields (MF).

**Materials and Methods.** ME core-shell NPs were synthesized via *in situ* microwave-assisted hydrothermal synthesis as previously described [3]. Citric acid (CA) and pectin (PEC) were used for surface functionalization to stabilize colloidal dispersions. Post-synthesis, NPs were washed thoroughly with deionized water using magnetic separation. Structural and phase analyses were performed via X-ray diffraction (XRD) and Raman spectroscopy; morphology was examined by transmission electron microscopy (TEM). Surface chemistry and elemental composition were characterized by X-ray photoelectron spectroscopy (XPS) and energy-dispersive X-ray spectroscopy (EDX). Magnetic properties were assessed by pulsed-field magnetometry, while piezoelectric and ME responses were evaluated by piezoresponse force microscopy (PFM) with and without MF. Zeta potential was measured by dynamic light scattering. Biocompatibility, neuronal activity, and axonal transport were assessed *in vitro*, *ex vivo*, and *in vivo*.

**Results and Discussion.** TEM, EDX, XRD, and Raman analyses confirmed the formation of a 2–5 nm BCZT (COD #96-210-085) shell on MFO cores (COD #96-152-831) with a core size of  $23 \pm 9$  nm. XPS analysis verified successful surface functionalization with CA and PEC. The NPs exhibited strong magnetic ( $>5$  emu/g), piezoelectric ( $>10$  pm/V), and ME ( $>8 \times 10^5$  mV·cm<sup>-1</sup>·Oe<sup>-1</sup>) properties. *In vitro* assays demonstrated excellent biocompatibility and revealed the ability of the NPs to modulate calcium flux, enabling bidirectional control of cell proliferation. *Ex vivo* and *in vivo* experiments showed enhanced NP accumulation in the mouse brain under MF application. These findings highlight the potential of ME NPs for noninvasive, targeted modulation of neuronal behavior and axonal transport.

**Acknowledgments.** This work was supported by the Russian Science Foundation (№ 24-43-00171). The authors thank Dr. D.V. Wagner and Dr. E.Yu. Gerasimov for their assistance with magnetic and microstructural characterization.

[1] S. Kopyl et al., Mater. Today Bio 12, 100149 (2021)

[2] R.V. Chernozem et al., Small 19 (42), 2302808 (2023)

[3] P.V. Chernozem et al., ACS Appl. Mater. Interfaces 17, 21614-21629 (2025)

# Antisite-Defect-Driven Magnetic Phase Transition in Sb-Doped $\text{MnBi}_2\text{Te}_4$

A. Tarasov<sup>a,b\*</sup>, A. Frolov<sup>b,c</sup>, D. Usachov<sup>a,b</sup>

<sup>a</sup> St. Petersburg State University, 199034, 7/9 Universitetskaya nab., St. Petersburg, Russia

<sup>b</sup> Center for Advanced Mesoscience and Nanotechnology, Moscow Institute of Physics and Technology,  
141700, Dolgoprudny, Russia

<sup>c</sup> Lomonosov Moscow State University, 119991 Moscow, Russia

\* artem.tarasov@spbu.ru

$\text{MnBi}_2\text{Te}_4$  is a layered magnetic topological insulator whose A-type antiferromagnetic (AFM) ground state and strong spin-orbit coupling make it an ideal platform for realizing exotic quantum phases such as the quantum anomalous Hall and axion insulator states [1]. Importantly, achieving a ferromagnetic (FM) ground state in this material class is of particular interest, as it enables access to the Weyl semimetal (WSM) phase - a topologically nontrivial state characterized by Weyl nodes carrying opposite chiral charge. These phases exhibit a range of unconventional electronic properties, including the chiral anomaly, anomalous Hall and spin Hall effects, and large negative magnetoresistance, and are considered promising for realizing Majorana fermions in unconventional superconductivity [2]. A key mechanism for driving the AFM–FM transition in  $\text{MnBi}_2\text{Te}_4$  involves the formation of  $\text{Mn}_{\text{Bi}}$  antisite defects, which locally alter exchange pathways and can induce ferrimagnetic or FM alignment [3]. Previously, it was suggested that such defects can tip the balance of interlayer exchange interactions, driving a transition from the AFM ground state to a FM one and thereby enabling access to the WSM phase under broken inversion and time-reversal symmetries [4].

To quantify the role of antisite defects in Sb-substituted  $\text{MnBi}_2\text{Te}_4$ , we employed photoelectron diffraction (PED) within the multiple scattering (MS) approximation to extract element-specific structural information from angular distributions of photoelectron intensity. These measurements provided direct estimates of  $\text{Mn}_{\text{Bi}}$  concentrations as a function of Sb content. Complementary to this, we performed first-principles calculations of exchange coupling parameters between Mn atoms in the magnetic layers and Mn atoms at Bi sites, modeling the evolution of magnetic interactions with increasing defect concentration.

The PED results confirmed that the concentration of antisite  $\text{Mn}_{\text{Bi}}$  defects increases systematically with Sb content. The calculated exchange interactions reveal that when the  $\text{Mn}_{\text{Bi}}$  concentration exceeds ~17% - typically at Sb substitution levels above 40% - the dominant interlayer coupling switches from AFM to FM, signaling a robust transition of the magnetic ground state. Importantly, our calculations show that structural changes alone are insufficient to induce this magnetic transition: the FM state still emerges even when the lattice geometry is held fixed, indicating that it is the antisite defects - not structural distortion - that act as the primary driving force. These findings establish a microscopic mechanism for magnetic phase control in Sb-doped  $\text{MnBi}_2\text{Te}_4$  and provide a pathway for engineering the WSM phase via defect modulation.

The authors acknowledge Saint-Petersburg State University for a research project 125022702939-2.

- [1] M. Otrokov et al., *Nature*. 576, 416–422 (2019)
- [2] C. Zhang et al., *Nat. Commun.* 7, 10735 (2016)
- [3] M. F. Islam et al., *Adv. Mater.* 35, 2307767 (2023)
- [4] A. M. Shikin et al., *Sci. Rep.* 15, 1741 (2025)

# Photothermal therapy utilizing star-shaped Au@Fe<sub>3</sub>O<sub>4</sub> nanoparticles induces cell death in human hepatocarcinoma

S. Pshenichnikov<sup>a</sup>, A. Anikin<sup>a</sup>, A. Motorzhina<sup>a</sup>, M. Albino<sup>a,b</sup>, V. Rodionova<sup>a</sup>, C. Sangregorio<sup>a,b</sup>,  
L. Panina<sup>a,d</sup> and K. Levada<sup>a\*</sup>

<sup>a</sup>REC Smart Materials and Biomedical Applications, Immanuel Kant Baltic Federal University,  
Kaliningrad, Russia

<sup>b</sup>Institute of Chemistry of Organometallic Compounds – C.N.R., Sesto Fiorentino (FI), Italy

<sup>c</sup>Department of Chemistry ‘Ugo Schiff’ & INSTM, University of Florence, Sesto Fiorentino (FI), Italy\*

<sup>d</sup>National University of Science and Technology MISIS, Moscow, Russia

\*kateryna.levada@gmail.com

Photothermal therapy (PTT) provides wide opportunities for cancer treatment due to ability of nanomaterials to effectively convert near-infrared (NIR) laser irradiation into heat. However, the efficacy of PTT is highly dependent on the photothermal performance of nanomaterials [1]. We present a study of previously fabricated [2] star-shaped magnetic-plasmonic Au@Fe<sub>3</sub>O<sub>4</sub> nanostars (NSs) as an agent for PTT. A series of *in vitro* experiments was performed on a human hepatocarcinoma cell line (Huh7) over a wide range of concentrations (1–100 µg/mL). Cytotoxicity analysis demonstrated that NSs induce concentration-dependent toxic effect on Huh7 cells after 24 h treatment (data not shown). PTT significantly decreased the survivability of cells (Fig. 1 A) in comparison with only NSs-treatment.

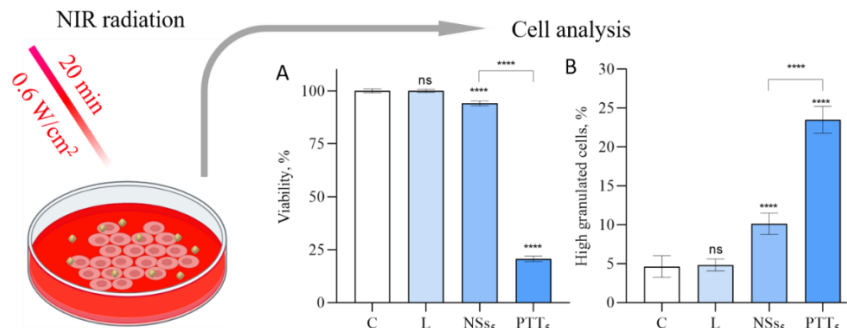


Figure 1. (A) PTT greatly decreased viability of Huh7 cells; (B) Number of high granulated cells in Huh7 subpopulations was significantly increased after PTT. C - control cells, L - cells treated via laser irradiation for 20 min, NSs<sub>5</sub> - cells treated with 5 µg/ml NSs for 24 h, PTT<sub>5</sub> - cells cultivated with 5 µg/ml NSs for 24 h and treated with PTT for 20 min. Cell viability was analyzed using Guava ViaCount Reagent via flow cytometry. Data values were normalized to the control. Statistical significance levels between control and experimental values are represented by asterisks (“\*\*\*\*” for p value < 0.0001, ns – no significant differences). Data values are represented as mean ± SE.

Further analysis demonstrated that amount of high granulated cells in Huh7 subpopulations significantly increases after PTT and NSs treatment at concentration 5 µg/ml (Fig. 1 B).

The obtained results exhibit the development of nano-sized tools for PTT, which may enable novel approaches in cancer treatment and inspire further research.

This work was supported by the Russian Science Foundation, grant 21-72-20158-II.

[1] S. Duan, RSC Adv. 13, 14443(2023)

[2] B. Muzzi, ACS Appl. Mater. Interfaces 14, 29087(2022)

# Tuning the Electronic Structure of Surface States at the Au/MnBi<sub>2</sub>Te<sub>4</sub> Interface

V. Anferova\*, A. Shikin, A. Tarasov

St. Petersburg State University, 198504, Universitetskaya emb. 7-9, St. Petersburg, Russia

\*st085003@student.spbu.ru

Magnetic topological insulators (MTIs) are electronic materials that combine nontrivial band topology with intrinsic magnetic order. A key factor for the development of next-generation functional electronic devices based on these materials is the size of the energy gap in the topological surface states (TSS), as it significantly affects the emergence of the quantum anomalous Hall effect [1]. One of the most thoroughly studied MTIs is the antiferromagnetic topological insulator MnBi<sub>2</sub>Te<sub>4</sub>. The gap in TSS is theoretically estimated to lie in the range of 80 – 88 meV [2], yet subsequent experimental studies have revealed a strong dependence of this gap on sample conditions, with reported values typically ranging from 50 – 70 meV down to 12 – 15 meV, and in some cases indicating a nearly gapless TSS dispersion [3]. This can be attributed to the presence of structural imperfections. In particular, uncompensated surface charges arising from them on the sample surface have been shown to contribute to a reduction in the gap [4].

This study investigates the influence of Au adlayer on the electronic structure of MnBi<sub>2</sub>Te<sub>4</sub>, focusing on its impact on the TSS. The presence of heavy Au adatoms can induce charge redistribution and lead to band hybridization [5]. On the other hand, Au is a heavy element, which results in strong spin-orbit coupling – one of the key factors necessary for the emergence of Rashba-like states [6]. All of which may modify the electronic structure and spin texture of the surface states. In this context, the primary aim of the work is to theoretically assess the possibility of tuning the gap in TSS for MnBi<sub>2</sub>Te<sub>4</sub> using the deposition of an Au adlayer, within the framework of density functional theory. The analysis considers several key parameters: the configuration of the deposited Au atoms, their surface concentration, and the interlayer distance between the Au adlayer and the MnBi<sub>2</sub>Te<sub>4</sub> surface.

The Au/MnBi<sub>2</sub>Te<sub>4</sub> interface demonstrate that interface configuration plays a decisive role in shaping the system's electronic properties. Investigation into the dispersion relations of these interfaces revealed that the TSS are preserved if the electronic states of the Au adlayer lie above or below the Dirac point or if the adlayer is sufficiently distant from the surface to prevent hybridization between the Au bands and the TSS. However, if the adlayer states are near the Dirac point and close enough to enable hybridization with the TSS, the TSS are destroyed. As the distance between the adlayer and the crystal decreases, the energy bands of Au shift upward, and the EG in the TSS increase by a factor of 2-3. Further analysis of the spin texture shows that Rashba-like states emerge within the bulk gap in the fcc configuration. This suggests the potential for stabilizing quantum Hall effect-like phases in such engineered systems [7]. In the hcp configuration, a strong s<sub>z</sub>-polarization is observed in the states within the bulk gap. Taken together, these findings highlight the promise of Au/MnBi<sub>2</sub>Te<sub>4</sub> interfaces for applications in electronics, spintronics, and quantum technologies.

The authors acknowledge Saint-Petersburg State University for a research project 125022702939-2.

- [1] Y. Deng, et al., Science 367, 895–900 (2020)
- [2] M. M. Otrokov, et al., Nature 576, 416–422 (2019)
- [3] A. Shikin, et al., Physica B: Condens. Matter 649, 414443 (2023)
- [4] A. M. Shikin, et al., Phys. Rev. B 104, 115168 (2021)
- [5] O. Clark, et al., npj Quantum Materials 7, 36 (2022)
- [6] C. Tusche, A. Krasnyuk, J. Kirschner, Ultramicroscopy 159, 520–529 (2015)
- [7] M. M. Wysokinski, W. Brzezicki, Phys. Rev. B 108, 035121 (2023)



## Effect of magnetoelectric stimulation on mesenchymal stem cell condensation and differentiation

V. Antipova\*, E. Vlasyuk, V. Frolova, V. Salnikov, P. Vorontsov, K. Levada, V. Rodionova

Immanuel Kant Baltic Federal University, 236004, Nevskogo 14, Kaliningrad, Russia

\*valya.antipova24@gmail.com

Conservative treatments of large defects (more than 2-3 cm) have their limitations, such as the risk of infection and the possibility of an immune response. In this regard, the use of functional substrates that not only support cell growth, but also contribute to their transformation into osteogenic ones is becoming increasingly important in tissue engineering. It is optimal to use biocompatible materials, the mechanical and topographic properties of which are similar to those of the natural extracellular matrix of bone, since they are able to modulate cellular behavior and promote their osteogenic differentiation. In addition to the mechanical and topographic characteristics of the cellular microenvironment, the behavior of cells can be influenced by various types of stimulation, such as electrical and mechanical. However, these approaches have their limitations and disadvantages. For example, electrical stimulation requires direct contact of electrodes with cells, which can lead to tissue damage. And for the successful application of mechanical stimulation, it is necessary to solve the problem of effective transmission of forces to cells and tissues. In this paper, a method of cell stimulation is proposed that combines a non-invasive approach and targeted mechanoelectric stimulation with a magnetic field based on magnetoelectric substrates for accelerated osteogenic differentiation.

PVDF-based nanocomposites modified with  $\text{CoFe}_2\text{O}_4$  nanoparticles served as magnetoelectric substrates. Biological tests of nanocomposites were carried out on a culture of human mesenchymal stem cells (FetMSC). The cells were stimulated daily for 30 minutes for 21 days. Osteogenic differentiation of stem cells was studied using alizarin red staining (ARS).

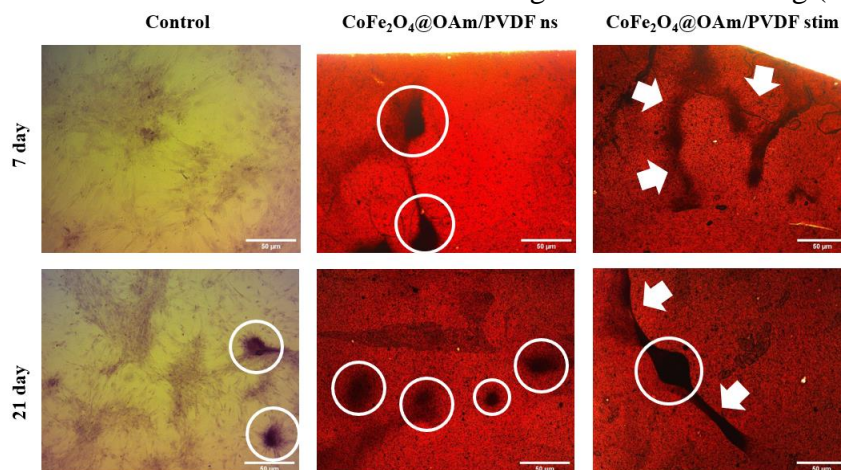


Figure 1. Representative images of ARS staining results. White circles indicate the foci of mineralization. The arrows mark the areas of mesenchymal condensation. The bar scale - 50 µm.

It was found that the presence of nanocomposites (with and without magnetoelectric stimulation) promotes an earlier manifestation of mesenchymal condensation (day 7), as well as control (Fig.1). At the same time, the largest number of mineralization foci were found in groups of stimulated cells, which indicates a more active course of cell differentiation processes. The results obtained demonstrate the potential of using these substrates in bone tissue engineering.

# Magnetic Phase Diagrams of Antiferromagnet DyB<sub>12</sub> with Jahn-Teller Lattice Instability and Electron Phase Separation

A. Azarevich<sup>a,\*</sup>, A. Bogach<sup>a</sup>, K. Krasikov<sup>a</sup>, S. Gabani<sup>b</sup>, K. Flachbart<sup>b</sup>, S. Gavrilkin<sup>c</sup>, A. Tsvetkov<sup>c</sup>,  
N. Sluchanko<sup>a</sup>

<sup>a</sup> Prokhorov General Physics Institute, Russian Academy of Sciences, Vavilov str. 38, Moscow 119991, Russia

<sup>b</sup> Institute of Experimental Physics, Slovak Academy of Sciences, Watsonova 47, SK-04001 Košice, Slovakia

<sup>c</sup> Lebedev Physical Institute, Russian Academy of Sciences, Moscow, Leninsky Prospect 53, 119991 Russia

\*azarevich@lt.gpi.ru

The origin of charge transport and magnetization anisotropy was studied in the DyB<sub>12</sub> antiferromagnetic (AF) metal (the Neel temperature  $T_N \approx 16.3$  K) with both cooperative Jahn-Teller distortions of the *fcc* crystal structure and nanoscale electronic instability (dynamic charge stripes). The  $H$ - $T$  antiferromagnetic phase diagrams of DyB<sub>12</sub> obtained here for the first time (Fig. 1a-c). Moreover, from the angular resolved magnetoresistance and magnetization measurements the butterfly-type pattern of  $H$ - $\phi$  magnetic phase diagram in the (110) plane was also reconstructed, including a number of different magnetic phases separated from each other by radial and circular boundaries (Fig. 1d-e). Several positive and negative contributions to magnetoresistance are separated and analyzed in the study, providing with arguments in favor of spin density wave *5d*-component in the magnetic structure of AF state.

We argue that charge fluctuations in stripes are responsible for the suppression of the Ruderman-Kittel-Kasuya-Yoshida (RKKY) indirect exchange between the nearest neighbored Dy<sup>3+</sup> ions located along the same  $\langle 110 \rangle$  directions as charge stripes producing the magnetic phase diversity and butterfly-type anisotropy in DyB<sub>12</sub>, which is similar to that one detected recently for ErB<sub>12</sub> [1].

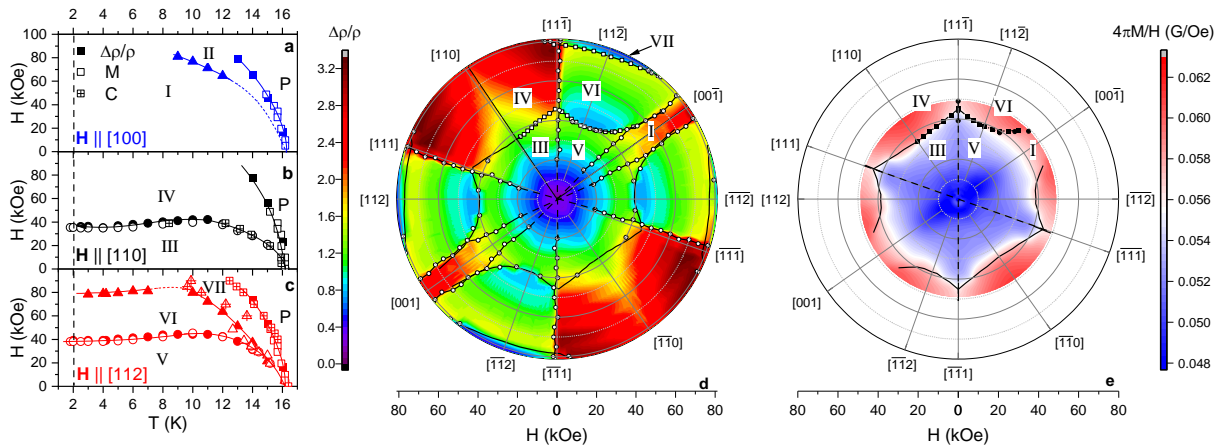


Figure 1. Magnetic phase  $H$ - $T$  (panels (a-c)) and  $H$ - $\phi$  (d-e) diagrams of DyB<sub>12</sub>.

[1] K. M. Krasikov, A. V. Bogach, S. V. Demishev, V. V. Voronov, N. Yu. Shitsevalova, V. B. Filipov, and N. E. Sluchanko, J. Magn. Magn. Mat. 545, 168796 (2022)

## Ti<sub>3</sub>C<sub>2</sub>T<sub>x</sub> MXenes obtained by the MILD method induce cytotoxic effect on liver cancer cells

S. Pshenichnikov\*, E. Korepanova, N. Shilov, A. Motorzhina, V. Rodionova and K. Levada

REC Smart Materials and Biomedical Applications, Immanuel Kant Baltic Federal University, Kaliningrad, Russia

\*SPshnikov@gmail.com

Ti-based MXenes have been extensively studied for biomedical applications due to their unique combination of properties: biocompatibility, hydrophilicity, efficient light-to-heat conversion, mechanical flexibility, and superior optical absorption with higher photothermal conversion efficiency compared to other 2D nanomaterials. These advantages have generated widespread interest in MXenes as highly promising materials for biomedical uses, particularly in photothermal therapy (PTT).

In the current study, we propose MXenes Ti<sub>3</sub>C<sub>2</sub>T<sub>x</sub> produced by selective etching of the aluminum layer of their precursor MAX-Phase Ti<sub>3</sub>AlC<sub>2</sub> using the MILD method. MXenes obtained by this method have significantly fewer -F groups on the surface, which should have a positive effect on cell viability. Cytotoxicity analysis performed using WST-1 assay demonstrated, that obtained MXenes induce cytotoxic effect on human hepatocarcinoma cells at wide range of concentrations (Fig. 1).

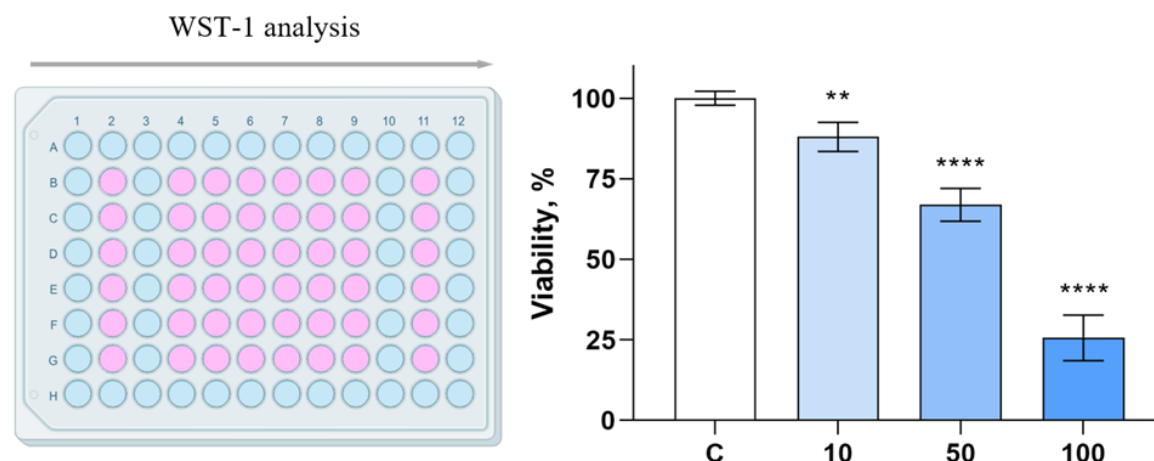


Figure 1. MXenes induce concentration-dependent toxic effect on Huh7 cells after 24 h treatment. Cell viability was analyzed using WST-1 viability assay. Data values were normalized to the control values. Statistical significance levels between control and experimental groups are represented by asterisks (“\*\*\*\*” for p value < 0.0001, “\*\*” for p value < 0.01). Data values are represented as mean ± SE.

MXenes demonstrate prospective physical properties for application as PTT agents, provided their cytotoxicity remains low under both *in vitro* and *in vivo* conditions [1]. The results demonstrated that MXenes can be effectively applied when their cytotoxicity is sufficiently minimized. Additionally, the selectivity of MXenes-based treatment can be enhanced by combining active targeting (e.g., antibody conjugation) with localized NIR irradiation, utilizing the EPR effect and stimulus-responsive drug release.

This work was supported by the Russian Science Foundation, grant 25-22-00433.

[1] N. Li et al., Small 20, 2305645 (2024)

## Overshoots of electrical resistivity of magnetic elastomers

A. Zubarev

Ural Federal University, 620000, Lenin Ave., 51, Ekaterinburg, Russia

\*a.j.zubarev@urfu.ru

Experiments [1] demonstrate sharp overshoots of electrical resistance of soft magnetic elastomers after stepwise sample compression or decompression along the electrical current direction. The similar overshoots also were observed after instantaneous either activation or deactivation of a magnetic field aligned along the current. Characteristic time of the resistance peaks, in the order of magnitude, coincides with the time of viscoelastic relaxation of the host polymer medium. These effects present interest both from the point of view of basic research of the soft magnetic composites and from the viewpoint of their practical applications in fast alternating conditions.

The proposed work deals with physical explanation of the overshoot effects. The explanation is based on the concept that the particles of the magnetic filler form percolating clusters, which provide the macroscopic conductivity of the composite. The particles in the clusters are not in a physical contact but separated by ultrathin polymer layers. The interparticle conductivity is provided by the tunnel current through these layers. As well known, the tunnel resistivity strongly depends on the interparticle distance. After the instantaneous mechanical as well as magnetic impacts, loading as well as disloading of the sample, activation and deactivation of the field, the relative motion of the particles in the clusters first leads to change of the interparticle distances and provokes fast increase, and then – relatively decrease of the macroscopic resistivity till the stationary values.

Theoretical results, in the order of magnitude, reproduce the experimental ones.

[1] Stepanov G.V., Semerenko D.A., Raikher Yu.L., Bakhtiarov A.V., Lobanov D.A., Storozhenko P.A.// Smart Mater. Struct. V.33, P.115001 (2024)

# Magnetic phase transitions in decorated square kagomé lattice antiferromagnets of nabokoite family

V. Glazkov<sup>a,\*</sup>, Ya. Rebrov<sup>a,b</sup>, M. Markina<sup>c</sup>, A. Murtazoev<sup>c</sup>, P. Berdonosod<sup>c</sup>, A. Vasiliev<sup>c</sup>

<sup>a</sup> P. Kapitza Institute for Physical Problems, Kosygin str. 2, 119334 Moscow, Russia

<sup>b</sup> Faculty of Physics, HSE University, Myasnitskaya str. 20, 101000 Moscow, Russia

<sup>c</sup> Lomonosov Moscow State University, Leninskie gory 1, 119991, Moscow, Russia

\*glazkov@kapitza.ras.ru

Kagomé lattice antiferromagnet is one of the corner-stone models of frustrated magnetism. Square kagomé lattice (SKL) featuring alternating square and octagonal voids is a development of this model [1]. Antiferromagnet on an ideal equilateral 2D SKL is predicted to form a gaped spin-liquid ground state [2], while variety of possible ordered phases is considered for a more realistic lattices with distorted exchange bonds [2].

While ideal 2D SKL remains evasive, mineral nabokoite and the family of related compounds  $\text{ACu}_7(\text{TeO}_4)(\text{SO}_4)_5\text{B}$  ( $\text{A}=\text{Na, K, Cs, Rb}$ ;  $\text{B}=\text{Cl, Br}$ ) presents interesting case of *decorated* SKL: six copper ions form distorted SKL layers, while seventh ion takes inter-layer positions. Thermodynamic measurements [3] reveal Curie-Weiss temperatures above 150 K for compounds, while magnetic ordering forms at temperatures below 5 K, which is in agreement with formation of spin-liquid state as expected for SKL layers.

We present results of the detailed electron spin resonance study nabokoite family compounds at the frequencies from 9 to 150 GHz and at the temperatures from 1.7 to 200 K.

We have observed broad (line-width about 1 T) paramagnetic absorption in the paramagnetic phase which transforms to characteristic antiferromagnetic resonance at the ordering temperature. Absolute magnitude of this paramagnetic absorption corresponds to the 1/7 of all copper ions in the sample. This observation is a direct experimental evidence that “decorating” copper ions in inter-layer positions orders at magnetic phase transition. It also allows to separate unambiguously contribution of SKL layers to static magnetic susceptibility. The later turns out to freeze out on cooling supporting predictions of gaped magnetic excitations in SKL antiferromagnet [2].

Antiferromagnetic resonance in the ordered phase revealed that light alkali-ions nabokoites ( $\text{A}=\text{Na, K}$ ) form non-collinear antiferromagnetic order, while heavy alkali-ion compounds ( $\text{A}=\text{Cs, Rb}$ ) orders collinearly. Non-collinear ordering correlates with the observation of high-temperature dielectric anomaly [4], indicating that lattice (dielectric) degrees of freedom play important role in the choice of the magnetic ground state. Analysis of the powder antiferromagnetic data allowed to extract magnon gaps values and temperature dependences, revealing also two-stage ordering in some of the compounds.

Nabokoite family compounds turn out to be an interesting case combining magnetic frustration and lattice degrees of freedom with staircased phase transitions and possible co-existence of the ordering in the sub-system of “decorating” copper ions with the gaped spin-liquid in SKL layers.

The work was supported by RSF grant No. 22-12-00259-II (V.G. and Ya. R., ESR experiments).

[1] R. Siddharthan, A. Georges, Phys. Rev. B **65**, 014417 (2001)

[2] J. Richter, O. Derzhko, J. Schnack, Phys. Rev. B **105**, 144427 (2022); M. Gembé, H.-J. Schmidt, C. Hickey et al. Phys. Rev. Research **5**, 043204 (2023); J. Richter, J. Schnack, Phys. Rev. B **107** (2023) 245115

[3] A.F. Murtazoev, K.A. Lyssenko, M.M. Markina et al. ChemPhysChem **24**, e202300111 (2023); M.M. Markina, P.S. Berdonosov, T.M. Vasilchikova et al. Mat. Chem. Phys. **319**, 129348 (2024)

[4] Ya.V. Rebrov, V.N. Glazkov, A.F. Murtazoev et al. JMMM **592**, 171786 (2024)

# Computer Simulation of FORC Diagrams for Ellipsoidal Multicore Nanoparticles

V. Zverev<sup>a,\*</sup>, A. Kuznetsov<sup>b</sup>

<sup>a</sup> Ural Federal University, 620000, Turgeneva 4, Ekaterinburg, Russia

<sup>b</sup> University of Vienna, 1090, Sensengasse 8/18, Vienna, Austria

\*vladimir.zverev@urfu.ru

Recently, advances in bioengineering and medicine have renewed focus on developing nanotextured materials. These materials have properties that can be controlled by external stimuli, such as a magnetic field [1]. One example is magnetic liquids. They consist of magnetic single-domain nanoparticles suspended in a non-magnetic liquid medium. Additionally, more complex magnetic objects, like magnetic multinucleated nanoparticles, have been proposed as alternatives to single-domain magnetic particles.

This work discusses the properties associated with the FORC diagram of multicore magnetic nanoparticles (MMN). We assume that the nanoparticles have an ellipsoidal shape. MMN is modeled as a collection of spherical subparticles. These subparticles have fixed spatial positions relative to one another. This arrangement is similar to embedded nanoparticles in a non-magnetic polymer or another rigid matrix.

Computer simulations were performed using the ESPResSo molecular dynamics software. This software accounts for magnetic anisotropy. The simulations were based on a proposed approach that involves solving the stochastic Landau-Lifshitz-Gilbert equation [2]. This is done in a particle frame stationary with respect to the nanoparticle. During this process, the precession and Barnett effects are eliminated. We formed a set of single-domain particles in such a manner that their combined convex hull approximated an elongated ellipsoid of revolution. This ellipsoid has a predetermined ratio of semiaxes. This setup allows for comparison of the resulting behavior to that of spherical particles. The findings are consistent with prior computational experiments [3].

Research supported by the Russian Science Foundation Grant No. 25-22-00338.

[1] S.Trisnanto et al, Journal of Applied Physics, 130 (2021)

[2] M. Shliomis et al., Journal of magnetism and magnetic materials, 122 (1993)

[3] E. Pyanzina, Journal Molecular Liquids, 126842 (2025)

# Purification of argon from oxygen-containing impurities using MXenes of the composition $\text{Ti}_3\text{C}_2\text{T}_x$

N. Shilov<sup>\*</sup>, K. Magomedov<sup>a</sup>, K. Sobolev<sup>b</sup>, P. Shvets<sup>a</sup>, I. Mallphanov<sup>a</sup>, Ch. Gritsenko<sup>a</sup>, V. Rodionova<sup>a</sup>

<sup>a</sup>Immanuel Kant Baltic Federal University, 236004, Nevskogo 14, Kaliningrad, Russia

<sup>b</sup>Department of Materials Engineering, Ben Gurion University of the Negev, 8410501, P.O. Box 653,  
Beer- Sheva

\*nikolayshilov2002@gmail.com

Inert gases are elements of Group VIII of the main subgroup. These gases have no taste, color, or odor. The electron shells of their atoms are completely filled, which makes them stable and practically incapable of forming stable chemical bonds.

The Earth's atmosphere consists primarily of nitrogen (78.1%) and oxygen (20.9%); noble gases, including argon (0.9%), neon (0.0018%), helium (0.0005%), krypton (0.0001%) and xenon (0.000009%), are present only in trace amounts. Obtaining these gases in pure form is quite a laborious task, as they are by-products of the separation of air into its constituent gases.

Among all the inert gases, argon is the most frequently used in scientific research, industry, medicine and nanotechnology due to its excellent thermal characteristics and low cost compared to other noble gases. In this regard, the problem of purifying argon from impurities remaining in the gas during its production is relevant. One of the promising directions for its solution is the use of MXenes.

MXenes are a new class of two-dimensional materials that have a number of unique properties (hydrophilicity, metallic conductivity, negatively charged surface, etc.) [1,2]. Thanks to these properties, they have found various applications. For example, MXenes have been used in the sorption of heavy metals, antibiotics, and dyes, where they show promise for use as sorbents. Recently, studies have begun to appear showing the ability of MXenes to also be used for the sorption of various gases [3,4].

The aim of this work was to conduct an experiment on the sorption of impurity gases (oxygen, carbon dioxide, and water vapor) from argon using a two-dimensional nanomaterial— $\text{Ti}_3\text{C}_2\text{T}_x$  MXene. The MXenes obtained in this work were comprehensively characterized and then used to sorb oxygen-containing impurities. It was shown that MXenes absorb water vapor best, resulting in a sorption capacity of 0.035 g/g (MXenes). The sorption capacity of MXenes for carbon dioxide molecules was also obtained, which amounted to 0.386 mmol/g (MXenes), which is 2.5 times higher than previously obtained experimentally [4]. In addition, the sorption capacity of MXenes with respect to oxygen molecules was obtained experimentally for the first time, which amounted to 0.675 mmol/g (MXenes).

[1] Y. Gogotsi and Q. Huang, *ACS Nano*, 15 (2021) 5775–5780. <https://doi.org/10.1002/10.1021/ACSNANO.1C03161>

[2] B. Anasori and Y. Gogotsi, *Graphene and 2D Materials* 7 (2022) 75–79. <https://doi.org/10.1007/S41127-022-00053-Z>

[3] F. Liu, et al., *Adsorption*, 22 (2016) 915–922. <https://doi.org/10.1007/S10450-016-9795-8>.

[4] D. I. Petukhov, et al., *J Memb Sci*, 621 (2021) 118994. <https://doi.org/10.1016/J.MEMSCI.2020.118994>



# Influence of nanoscale magnonic crystal geometry on spin magnetization

V. Balaeva \*, D. Romanenko, M. Morozova

Saratov State University, 410012, Astrakhanskaya, 83, Saratov, Russia

\*vkonda2000@mail.ru

One of the most promising structures of magnonics studied in micro- and nanoelectronics are magnonic crystals (MC) [1-3]. Magnonic crystals are structures with periodically changing magnetic properties and are used to control the characteristics of spin waves (SW) in signal processing devices. Band gaps (BG) are formed in MC – bands of non-transmission in the spectrum of spin waves, due to which MCs are functionally flexible and have great capabilities for controlling SW characteristics.

In this research, the features of SW propagation in MC based on a ferromagnetic film of iron-yttrium garnet (YIG) of the 100 nm thickness with a periodic system of grooves on the surface are investigated. The simulation is performed in the micromagnetic modeling environment MuMax3.

It has been found that in MCs, the signal propagates better in grooves than in ridges, which leads to an uneven magnetization distribution (fragmentation). The features of magnetization fragmentation are influenced by the parameters such as signal frequency, ratio of ridge to groove widths  $a/b$  (Fig. 1), grooves depth and the MC period length. An increase in the signal frequency in a certain frequency range leads to a decrease in signal suppression in ridges and, as a result, to a decrease in the fragmentation effect. As the MC period decreases, the fragmentation becomes less uneven and closer to harmonic-type for the signal envelope, especially at the lower wavenumbers of SW.

It is established that additional modes on the dispersion characteristic for MC are formed near each width mode as a result of the interaction of forward and backward waves of different orders. The ratio of ridge and groove widths affects the energy distribution between the main and additional modes and their cutoff frequency. As the waveguide width increases, the influence of the ridge/groove value on the dispersion characteristics weakens. The influence of the ridge/groove on the band gaps formation is analyzed. The most pronounced BGs is observed for large ridge/groove values, especially when ridge width twice as much as groove one. Also, an increase in the ridge/groove and in the grooves depth leads to an increase in a number of pronounced Bragg resonances.

*This work was supported by Russian Science Foundation (grant № 23-79-30027).*

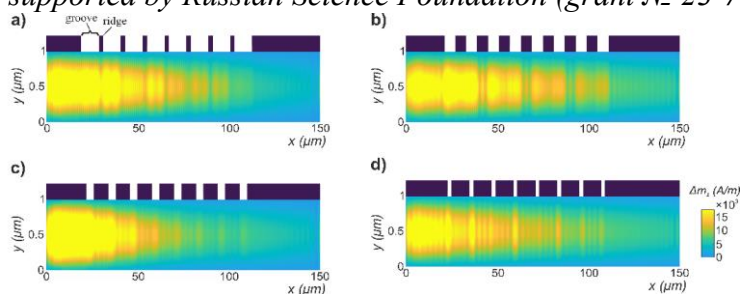


Figure 1. Maps of the spatial magnetization distribution with the structure profile at different ridge/groove (a/b): (a)  $a/b = 2/10$ ; (b)  $a/b = 6/6$ ; (c)  $a/b = 8/4$ ; (d)  $a/b = 10/2$ . Grooves depth  $h = 20$  nm, signal frequency  $\nu = 4.895$  GHz, MC period  $\Delta = 12$   $\mu\text{m}$ , structure length  $L = 150$   $\mu\text{m}$  and width  $w = 1$   $\mu\text{m}$ .

- [1] S.A. Nikitov, P. Tailhades, C.S. Tsai, JMMM Vol. 236, №. 3, pp. 320-330 (2001)
- [2] V.V. Kruglyak et al., Metamaterial, Ed. London: InTech, Ch. 14, pp. 341-370 (2012)
- [3] A.V. Chumak, A.A. Serga, B. Hillebrands, J. Phys.: Appl. Phys. Vol. 50, № 24, p. 244001 (2017)



# Critical behavior of the antiferromagnetic Potts model on a bcc lattice

D. Kurbanova\*, M. Magomedov, M. Ramazanov, A. Murtazaev

Amirkhanov Institute of Physics, Daghestan Federal Research Centre RAS, 367015, Makhachkala, Russia

\*d\_kurbanova1990@mail.ru

The Potts model with competing exchange interactions is recently widely studied due to the occurrence of unusual magnetic orderings. The basis for the emergence of unique states of low-dimensional spin systems is the absence or difficulty of long-range order formation [1]. The phase diagrams of such systems have a rich structure and demonstrate effects such as a change in the type of phase transition, critical points, order-disorder transitions, reversible phase transitions, phase separation.

In present work, on basis Monte Carlo replica algorithm, we investigate the exchange interaction competition influence on phase transitions and critical properties of the antiferromagnetic 3-state Potts model on a body-centered cubic lattice.

Hamiltonian of the model:

$$H = -J_1 \sum_{\langle i,j \rangle, i \neq j} \delta(S_i, S_j) - J_2 \sum_{\langle i,k \rangle, i \neq k} \delta(S_i, S_k) \quad (1)$$

where  $S_i = 1, 2, \dots, q$  can be in different  $q$  states and  $\delta_{S_i, S_j}$  is the Kronecker  $\delta$  function. The first sum is over pairs of the nearest-neighbor spins, and the second sum is over pairs of next-nearest-neighbor spins,  $J_1$  and  $J_2$  are the parameters of the exchange interactions of the first ( $J_1 = -1$ ) and second ( $J_2 < 0$ ) nearest-neighbor. The calculations were carried out for systems with periodic boundary conditions and linear dimensions  $2 \times L \times L \times L = N$ ,  $L = 8 \div 60$  in the range  $-1 \leq J_2 \leq 0$ . A nature of phase transitions is estimated using the methods of the histogram analysis and the fourth order Binder cumulants.

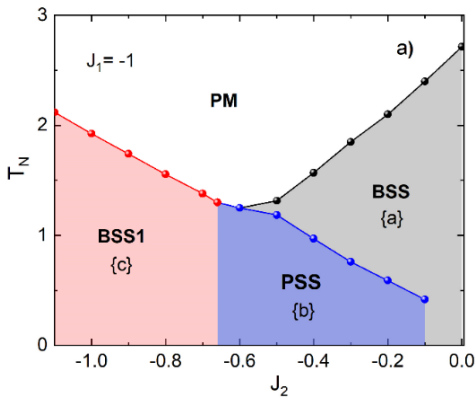


Fig. 1. Phase diagram of the 3-state Potts model on a bcc lattice. All phase transitions are first order except the BSS-PM transition which is

were established.

The study was performed by grant of the Russian Science Foundation Project No. 25-12-20029, <https://rscf.ru/en/project/25-12-20029/>

[1] F.Y. Wu, Rev. Mod. Phys. 54, 235 (1982)

# Micromagnetic structure and topological magnetic states in thin Co/Pd ferromagnetic films

M. Dorokhin<sup>a,\*</sup>, M. Ved<sup>a</sup>, I. Kalentyeva<sup>a</sup>, P. Demina<sup>a</sup>, A. Zdoroveyshchev<sup>a</sup>, D. Zdoroveyshchev<sup>a</sup>,  
A. Kudrin<sup>a</sup>, D. Tatarskiy<sup>a,b</sup>, R. Kriukov<sup>a</sup>, S. Zubkov<sup>a</sup>

<sup>a</sup> Lobachevsky State University, 603950, Gagarin ave. 23, Nizhniy Novgorod, Russia

<sup>b</sup> Institute for Physics of Microstructures RAS, 603087, GSP-105, Nizhniy Novgorod, Russia

\*dorokhin@nifti.unn.ru

Thin ferromagnet/heavy metal multilayer films are considered as prospective media for a magnetic recording and Co/Pd films are a good example of such materials. An important factor that determines the possibility of practical application of Co/Pd is the formation of room temperature stable magnetic states, such as skyrmions [1,2] with the spatial size at the nanometer scale. A series of papers [3,4] was devoted to studying the effects at Co/Pd interfaces giving rise to formation skyrmions of so-called Bloch-Neel type. It is believed that the Dzyaloshinskii-Moriya interaction is responsible for stabilizing these configurations. Bloch-Neel type spin textures combine both achiral Bloch and a chiral Neel component of the domain wall which allows reducing the demagnetization field at the surface of the film [4].

In this work, we studied the magnetic properties and micromagnetic structure of Co/Pd multilayer films with different bilayer thicknesses ( $[\text{Co}(0.3 \times t \text{ nm})/\text{Pd}(0.5 \times t \text{ nm})] \times 10$ ), but with the same ratio Co vs Pd. The Co/Pd ferromagnetic films were fabricated by electron beam evaporation in vacuum at 300°C on Si, GaAs, or 50 nm thick Si<sub>3</sub>N<sub>4</sub> membranes. To form Co/Pd layers, Co and Pd targets were alternately evaporated by an electron beam in a high vacuum. A weight piezoelectric sensor was used to control the thickness of the grown layers in the Co/Pd multilayer structure. The values of the layer thickness were set by changing the tooling coefficient  $t$  (a special adjustment factor of the technological unit). Since the value of the tooling coefficient remained constant during the growth of the sample, the thickness of the individual Co and Pd layers, as well as the ratio of Co to Pd also remained constant, although the overall film thickness varied in different samples.

Transmission electron microscopy and X-ray diffraction studies allow us to suppose that the investigated films are highly mixed alloys. Magnetic force microscopy and Lorentz transmission electron microscopy showed the presence of various micromagnetic features in the films. Along with skyrmions which are well-known magnetic topological artefacts some new features were revealed which were interpreted as 360 ° domain walls, skyrmioniums and the combination of the above two. It has been found that the type and density of micromagnetic features strongly depend on the bilayer thickness parameter ( $t$ ). The effect is associated with the peculiarities of interfacial magnetic interactions in the samples with highly mixed interfaces. The tooling coefficient represents a useful tool of the electron beam evaporation technique enabling wide manipulation of micromagnetic particles, in particular, skyrmioniums which are currently considered a prospective media for current driven magnetic recording.

- [1] A. Fert, Nat. Rev. Mater. 2, 17031 (2017)
- [2] C. Kind, Appl. Phys. Lett. 116, 022413(2020)
- [3] J.A. Garlow, Phys. Rev. Lett. 122, 237201 (2019)
- [4] J.A. Garlow, Phys. Rev. B. 102, 214429 (2020)

## Research of the structure and magnetic properties in Pt/Co/MgO and WTe<sub>x</sub>/Pt/Co/MgO films

A. Prikhodchenko<sup>a,\*</sup>, M. Kuznetsova<sup>a</sup>, F. Meng<sup>b</sup>, Y. Feng<sup>b</sup>, Y. Wang<sup>b</sup>, A. Kozlov<sup>a</sup>

<sup>a</sup> Far Eastern Federal University, 690041, Ajax 10, Vladivostok, Russia

<sup>b</sup> Dalian University of Technology, 116024, Dalian, China

\* prikhodchenko.av@dvfu.ru

In the field of spintronics, two-dimensional materials and ultra-thin magnetic films containing transition metal dichalcogenides (TMDs) are intensively studied [1]. It is known that the magnetic characteristics are directly determined by the structure of the materials [2]. Thus, the aim of this work was to determine the changes in the structural characteristics of Pt/Co/MgO films after the application of a WTe<sub>x</sub> underlayer and following identification of the effect of the structure on the magnetic properties.

The objects of the study were three series of samples in which the Pt thickness was varied. Series №1: SiO<sub>2</sub>/Pt(2-10 nm)/Co(0,9 nm)/MgO(2 nm)/SiO<sub>2</sub> (4 nm); series №2: SiO<sub>2</sub>/WTe<sub>x</sub> (7 nm)/Pt(2-10 nm)/Co(0,9 nm)/MgO(2 nm)/SiO<sub>2</sub> (4 nm); series №3: Al<sub>2</sub>O<sub>3</sub>/WTe<sub>x</sub> (7 nm)/Pt(2-10 nm)/Co(0,9 nm)/MgO(2 nm)/SiO<sub>2</sub> (4 nm). All samples were grown by magnetron sputtering with subsequent annealing at 300°C. Structural studies were carried out using a Colibri (Burevestnik) X-ray diffractometer using X-ray diffraction (XRD) and X-ray reflectometry (XRR) methods. The vibrating-sample magnetometer (7410 VSM, LakeShore) was used to study the magnetic parameters of the samples.

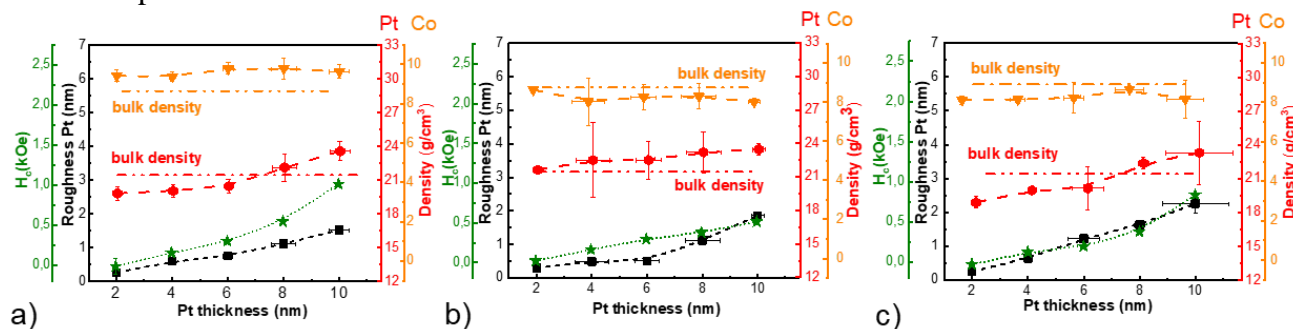


Figure 2. Graphs of the dependences of the coercive force ( $H_c$ ), roughness of the Pt layer, density of Pt and Co for series a) №1, b) №2, c) №3 on the thickness of Pt.

Based on the XRD spectra, it was found that series №2 demonstrated the highest growth rate of Pt grains. As a result of the analysis of the XRR curves, the interface roughness and material density were determined, and dependences on the Pt thickness were plotted (Fig. 1). Series №1 (Fig. 1a), demonstrates the Co density higher than the bulk value, which leads an increasing of  $H_c$  over the entire range of thicknesses. The addition of a WTe<sub>x</sub> underlayer grown on SiO<sub>2</sub> leads to the fact that the  $H_c$  value in series №2 (Fig. 1b) at a Pt thickness of 10 nm is half that of series №1.

As a result, adding a WTe<sub>x</sub> underlayer changes the growth mode of Pt. The differences in the structure of the underlying layers affect the growth of the Co layer, which in turn changes the magnetic parameters of the system.

*The authors thank the Russian Scientific Foundation, Project No 23-42-00076*

[1] Qidong Xie, Weinan Lin, Baishun Yang et al Giant Enhancements of Perpendicular Magnetic Anisotropy and Spin-Orbit Torque by a MoS<sub>2</sub> Layer // Advanced Materials 2019 V.31

[2] В.О. Васьковский, М.Н. Волочаев, А.Н. Горьковенко Структурные особенности и магнитные свойства пленок Co-W // Физика твердого тела, 2021, том 63, вып. 7 с.915-922

# MRFM studies of the gyrotropic mode in the ferromagnetic-antiferromagnetic system

E. Skorokhodov\*, E. Karashtin, I. Fedotov, I. Pashenkin, M. Sapozhnikov

The Institute for Physics of Microstructures of the Russian Academy of Sciences, 603087, Akademicheskaya Str., 7, Afonino, Russia

\*evgeny@ipmras.ru

Patterned ferromagnetic nanostructures are promising in terms of creating new information processing and storage systems, detecting weak magnetic fields, and generating electromagnetic radiation. One of the most promising compact on-chip sources of electromagnetic radiation are vortex spin-transfer nanoscillators (VSTNO), which represent a magneto-resistive contact in which one of the ferromagnetic layers (the free layer) is in a vortex magnetic state. The operation of these devices is based on the phenomenon of gyrotropic mode self-oscillations under the action of spin-polarized electric current. The frequencies of the gyrotropic mode lie in the range 0.1-1 GHz. Frequency tuning in vortex nanooscillators is carried out in the range (from 0.1 to 1 GHz) due to changes in the magnitude of the current or external magnetic field. The limitation of frequency range tuning is due to the existence of a critical current value, exceeding which leads to attenuation of self-oscillations. There is also a limit value for the external magnetic field, above which the vortex state collapses. However, for many applications, a range of more than 1 GHz may be of interest. An alternative way to adjust the generation frequency is to implement imprinting of the vortex state of the free layer into an antiferromagnet, which occurs when the sample is annealed at a temperature exceeding the Neel temperature of the antiferromagnet [1,2]. Theoretical estimates show that a strong exchange interaction between a ferromagnet and an antiferromagnet leads to a significant change in the generation frequency, thereby increasing the scope of application of nanoscillators. The additional resonance frequency shift due to the exchange interaction between the ferromagnet and antiferromagnet can be estimated using the following formula.

$$\omega_{exch} \approx \gamma H_{exch} \ln \left( \frac{R}{\bar{d}} \right)$$

At the same time, the magnitude of this interaction can be controlled by changing the thickness of the magnetic layers.

In this work we experimentally study gyrotropic modes in a ferromagnet coupled to an antiferromagnet. Ferromagnetic film Fe(0.5)NiFe(12)Ta(5) and antiferromagnetic-ferromagnetic film Ta(20)IrMn(5)Fe(0.5)NiFe(12)Ta(5) were obtained by magnetron sputtering. Then, by electron lithography and ion etching, micron-diameter disks were formed from the obtained films. The structures made from an antiferromagnet-ferromagnet film were subjected to thermal annealing at a temperature of 350 C, as a result of which the imprinting of the vortex state from a ferromagnet into an antiferromagnet was realized. The report will present the results of studies of the frequency of the gyrotropic mode in the obtained structures using magnetic resonance force microscopy (MRFM) and numerical modeling.

The work was supported by RSF Grant No. 25-72-20055.

[1] J. Sort, K. S. Buchanan, V. Novosad, et al., PRL 97, 067201 (2006)

[2] G. Salazar-Alvarez, J. J. Kavich, J. Sort, et.al., APPLIED PHYSICS LETTERS 95, 012510 (2009)

# Modelling of $\text{Ti}_3\text{C}_2\text{T}_x$ –MXene Functionalization by Citric Acid and Lysin

K. Magomedov<sup>a</sup>, S. Drach<sup>a</sup>, E. Tarasova<sup>a</sup>, N. Shilov<sup>a</sup>, K. Sobolev<sup>b</sup>, V. Rodionova<sup>a</sup>

<sup>a</sup> Immanuel Kant Baltic Federal University, 236004, Nevskogo 14, Kaliningrad, Russia

<sup>b</sup> Ben-Gurion University, Be'er Sheva, Israel

\*m\_kurban@mail.ru

Two-dimensional MXene  $\text{Ti}_3\text{C}_2\text{T}_x$  ( $\text{T}_x = -\text{O}, -\text{OH}, -\text{F}$ ) combines high metallic conductivity, large specific surface area, and a negatively charged surface, making it a versatile platform for surface functionalization. Recent studies have shown that grafting organic acids onto  $\text{Ti}_3\text{C}_2\text{T}_x$  can induce partial localization of electronic states and approach semiconducting behavior. In particular, modification with phenylsulfonic acid produced a  $\sim 1.5$  eV band gap (Hu et al., 2023). This work generalizes that approach by modelling, via density functional theory (DFT) in VASP, the adsorption of citric acid (citrate ion) and L-lysine onto  $\text{Ti}_3\text{C}_2\text{T}_x$ , aiming to assess their binding modes and impact on electronic structure.

## Objectives.

1. Determine equilibrium adsorption geometries of citrate and lysine on  $\text{Ti}_3\text{C}_2\text{T}_x$ .
2. Compute adsorption energies and analyze charge transfer mechanisms.
3. Evaluate changes in density of states (DOS) near the Fermi level and band gap.
4. Provide guidelines for using these functionalized MXenes in optoelectronic and catalytic applications.

## Expected Findings.

- **Citrate** is expected to form multiple Ti–O bonds via its  $\text{COO}^-$  groups, leading to a relatively strong adsorption energy. This multi-center coordination is anticipated to induce pronounced hybridization between Ti d and O p states, which may partially deplete the DOS at the Fermi level and create localized mid-gap states.
- **Lysine**, with a single  $\text{NH}_3^+$  site per molecule, is expected to exhibit moderate adsorption strength via N p–Ti d interaction, producing smaller perturbations in the DOS but still potentially reducing the metallic character near the Fermi level.
- Both ligands may lead to changes in the near-Fermi DOS, suggesting the possibility of semiconducting behavior under certain conditions.
- Charge transfer analyses will be conducted to understand the electron donation from the MXene to the ligand and vice versa, which will help elucidate the stabilization mechanism.

## Conclusions and Outlook.

This modelling framework aims to demonstrate that organic ligands with multiple coordination sites, such as citrate, or protonated amino groups, such as lysine, can tune the electronic properties of  $\text{Ti}_3\text{C}_2\text{T}_x$ , potentially transitioning it from metallic to quasi-semiconducting behavior. The multi-dentate binding of citrate is particularly promising for inducing localized states and enhancing light–matter interactions, which could be beneficial for applications in photodetectors or catalysis. Lysine-functionalized MXene may find uses in biosensing or pH-responsive applications due to its amino functionalities. Future work will involve hybrid functional calculations to refine band-gap estimates and ab initio molecular dynamics in aqueous environments to assess ligand stability under realistic conditions.

[1] Hu C. et al., *Adv. Funct. Mater.* 33 (2023) 2302188. <https://doi.org/10.1002/adfm.202302188>

[2] Naguib M. et al., *Adv. Mater.* 23 (2011) 4248–4253. <https://doi.org/10.1002/adma.201102306>

# Neuromorphic Functionality of Thin-Film GMI Structure in a Nonlinear Mode of The Current Excitation

G. Demin<sup>\*</sup>, N. Djuzhev

National Research University of Electronic Technology (MIET), 124498, Shokin sq., bld. 1, Zelenograd,  
Moscow, Russia

<sup>\*</sup>gddemin@gmail.com

Due to the intensive development of information technologies, new computing systems are required that are capable of quickly and efficiently processing large amounts of data and solving a wide range of cognitive tasks, such as text and graphics recognition, machine translation, object classification, etc. As the complexity level and the number of logical operations performed increase, the time delay for data transfer between the processor and memory in the classical von Neumann architecture grows significantly, which leads to an overall decrease in its performance.

One of the solutions to the problem above is the development of a new neuromorphic architecture based on artificial neurons and synapses combined into a single neural network. The concept of a convolutional neural network based on magnetic tunnel junctions (MTJs) was proposed recently in [1]. The magnetodynamic response of MTJ to the spin-polarized current makes it possible to successfully simulate the behavior of neurons and synapses, the minimum dimensions of which are scaled down to 10 nm and below, and the energy consumption is at the level of several  $\mu\text{W}$  [2].

The dependence of the magnetic permeability of amorphous ferromagnetic (FM) structures on the frequency and amplitude of the exciting alternating current in a non-magnetic (NM) bus allows us to implement a similar approach to imitate both neural and synaptic functionality using a simpler technology and a lower amplitude of operating frequencies - in the region of tens of MHz [3].

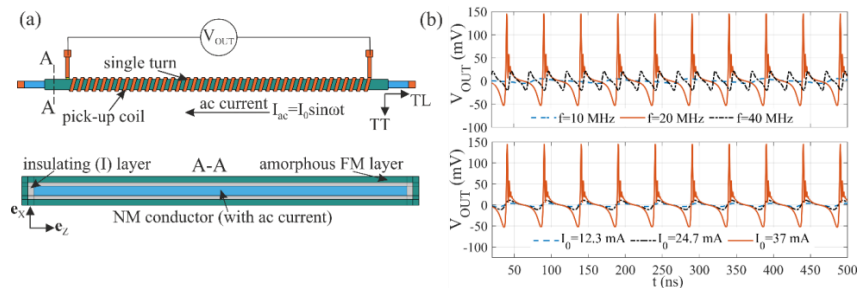


Figure 3. (a) Schematic of the thin-film GMI structure. (b) Output voltage signal at different frequency and amplitude of the current.

We have analyzed the neuromorphic functionality of thin-film FM-insulator-NM-insulator-FM structures, which exhibit the giant magnetoimpedance (GMI) effect under a weak magnetic field aligned parallel/perpendicular (TT/TL) to the anisotropy axis of the FM film (Figure 1). Based on the micromagnetic model, the shift in the output voltage with the frequency and amplitude of alternating current in the nonlinear mode of operation was estimated, which can be responsible for the synaptic plasticity. At a certain amplitude and frequency of the current, the output signal has a resonant shape similar to the action potential (spike) of an activated neuron. The results obtained can be used in the fabrication of a new type of neuromorphic devices based on the GMI effect. This work was supported by the RF Ministry of Science and Higher Education (State assignment No. FSMR-2024-0004).

[1] N. Leroux et al., Neuromorph Comput. Eng., 2, 034002 (2022)

[2] B. Jinnai et al., Appl. Phys. Lett., 116, 160501 (2020)

[3] L. Jamilpanah et al., Sci. Rep., 13, 8635 (2023)

## Microscopy techniques for study of graphene sensors

D. Sobola<sup>a,\*</sup>, F. Orudzev<sup>b,c</sup>, Sh. Ramazanov<sup>b</sup>, D. Dadagishiev<sup>c</sup>

<sup>a</sup> Department of Physics, FEEC, Brno University of Technology, 61200, Technicka 10, Brno, Czechia

<sup>b</sup> Amirkhanov Institute of Physics, Dagestan Federal Research Center, Russian Academy of Sciences,  
Makhachkala 367003, Russia

<sup>c</sup> Smart Materials Laboratory, Dagestan State University, Makhachkala 367000, Russia

\*sobola@vut.cz

Scanning probe microscopy techniques play a pivotal role in characterizing the unique electronic, structural, and surface properties of graphene-based sensors. Their nanometer-scale spatial resolution enables detailed mapping of doping profiles, local charge distributions, and environmental influences that affect graphene's sensing performance. Among these, Kelvin probe force microscopy (KPFM) has emerged as an essential tool, providing direct insight into local work function variations and electrostatic potential landscapes that underpin the operation and sensitivity of graphene sensors.

In this study, KPFM is utilized to visualize the spatially resolved electronic characteristics of graphene surfaces. The method generates contact potential difference (CPD) maps that capture the electrostatic potential needed to balance the work function difference between the tip and the sample. These maps reveal local variations in doping, charge transfer, and trapped charges, thus differentiating p-type and n-type domains. By calibrating the tip's work function, CPD data are converted into quantitative work function maps, highlighting how adsorbed molecules or fields modify the electronic structure of the sensor. Donor molecules reduce the work function (signaling n-type doping), while electron-withdrawing species raise it (indicating p-type behavior).

These measurements also allow for carrier density mapping by relating Fermi level shifts to local electron or hole concentrations, revealing the dynamic doping landscape of the graphene sensor. Additionally, calculating spatial derivatives of CPD data yields in-plane electric field maps, pinpointing high-field regions at domain boundaries or defect sites that influence charge carrier mobility. The study further explores environmental effects, showing how water vapor exposure introduces dipolar layers that electrostatically shift the vacuum level, enhancing p-type doping. As a result, changes in humidity lead to measurable increases in the work function and carrier density.

Overall, KPFM-derived mapping techniques offer a comprehensive and spatially detailed understanding of how intrinsic and extrinsic factors modulate graphene's sensing behavior. Such insights are vital for optimizing the performance and reliability of next-generation graphene-based sensor technologies.



# Magnetic tunnel junctions with perpendicular magnetic anisotropy

I. Pashenkin<sup>a\*</sup>, N. Gusev<sup>a</sup>, M. Sapozhnikov<sup>a</sup>, D. Zdoroveishchev<sup>b</sup>

<sup>a</sup>Institute for Physics of Microstructures RAS, 603950, Nizhny Novgorod, Russia

<sup>b</sup>Lobachevsky State University, 603022, Nizhny Novgorod, Russia

\*pashenkin@ipmras.ru

Recently, investigations of magnetic tunnel junctions (MTJ) with perpendicular magnetic anisotropy (PMA) in the application of magnetoresistive random-access memory (MRAM) have gained significant attention. In HM/CoFeB/MgO/CoFeB/HM (HM – heavy metal) systems, in which the giant tunnel magnetoresistance (TMR) effect is observed, the PMA in ferromagnetic layers is provided by the spin-orbit interaction at the boundaries with the MgO layer and the heavy metal layer. The use of W layers as HM makes it possible to obtain record-high TMR values in such systems [1]. In addition, MTJs with W layers have good thermal stability, which is a critical requirement for integration with CMOS technology. For the proper MRAM cell operation, it is necessary that the magnetic layers of the MTJ have significantly different anisotropy energy and switching fields. It is possible to use a multilayer FM/NM/FM structure with an antiferromagnetic coupling, called a synthetic antiferromagnet (SAF) layer, as a fixed (reference) layer of MTJ.

In this work, we developed a fabrication process of Ta(30)/W(3)/CoFeB(1)/MgO(2)/CoFeB(1.5)/W(3)/Ta(2)/Pt(10) MTJs (the thickness is given in nm) with PMA, showing a magnetoresistance  $\sim 50\%$  at room temperature (Figure 1, b). Multilayer structures were grown by magnetron sputtering at room temperature. Circular MTJs with a 3  $\mu\text{m}$  diameter were formed using optical lithography and ion milling. The magnetic properties of the film structures were studied by Kerr magnetometry and by measuring the anomalous Hall effect. The difference in switching fields of layers in films (Figure 1a) and patterned MTJs (Figure 1b) is attributed to the MTJ size is smaller than the magnetic domain, which is confirmed by MFM studies. We also obtained multilayer SAF structures Ta(10)/Pt(10)/[Co(0.7)/Pt(1)]<sub>2</sub>/Co(0.7)/Ru(0.7)/ [Co(0.7)/Pt(1)]<sub>3</sub>/Pt(5) with perpendicular magnetic anisotropy, in which the effective field of antiferromagnetic coupling was about 3 kOe at 325 K (Figure 1c).

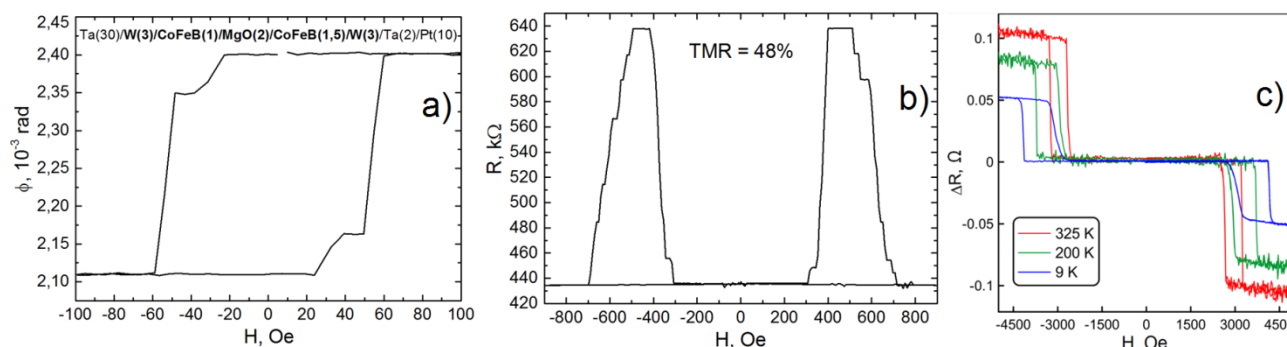


Figure 1.a) –magnetization reversal loop of Ta(30)/W(3)/CoFeB(1)/MgO(2)/CoFeB(1.5)/W(3)/Ta(2)/Pt(10) MTJ structure; b) – magnetoresistive curve of 50 MTJs, connected in a series, after thermal annealing at 330 °C for 1 h.; c) – anomalous Hall effect curves of Ta(10)/Pt(10)/[Co(0.7)/Pt(1)]<sub>2</sub>/Co(0.7)/Ru(0.7)/[Co(0.7)/Pt(1)]<sub>3</sub>/Pt(5) SAF-structures.

The work was supported by the Russian Science Foundation (project No. 25-72-20055).

[1] M. Wang, Nat. Commun **9**, 671 (2018)



## Single-molecule magnets and how to compute their properties

V. Yushankhai<sup>a,\*</sup>, A. Syurakshin<sup>b</sup>

<sup>a</sup> Joint Institute for Nuclear Research, 141980, Joliot-Curie 6, Dubna, Moscow Region, Russia

<sup>b</sup> Institute of Mathematical Problems of Biology, 142290, Prof. Vitkevich St. 1, Pushchino, Moscow Region, Russia

\*yushankh@theor.jinr.ru

In a brief introduction, basic physical properties of a broad family of single-molecule magnets are characterized and their potential for practical applications is revealed. In particular, molecular magnets can serve as elements of magnetic memory, quantum bits and molecular refrigerants.

To relate the observable characteristic of single-molecule magnets with their internal electronic structure and magnetic anisotropy, the multi-electron wave functions should be calculated by solving Schrodinger equation for a general all-electron Hamiltonian of the system. This is done for mononuclear complexes such as metal-organic molecule, based on explicitly correlated (multiconfigurational) ab initio quantum chemical calculations. The computational methodology is presented at a general level accessible to non-specialists.

[1] E. Coronado, *Nature Reviews Materials*, 5 (2) 87-104 (2019)

[2] A. Raza, M. Perfetti, *Coordination Chemistry Reviews*, 490, 215213 (2023)

[3] L. Chibotaru, in *Computational Modelling of Molecular Nanomagnets* (ed. G. Rajaraman), Springer, 2023

# Effect of Se-S substitution on the crystal structure and physical properties of high coercivity $\text{Fe}_{0.25}\text{TaX}_2$ ( $\text{X} = \text{S}, \text{Se}$ )

N. Nosova<sup>a,\*</sup>, N. Selezneva<sup>a</sup>, N. Baranov<sup>b</sup>

<sup>a</sup> Ural Federal University, 620062, Mira 19, Ekaterinburg, Russia

<sup>b</sup> M.N. Miheev Institute of Metal Physics, UB of RAS, 620108, Sofya Kovalevskaya 18, Ekaterinburg, Russia

\*toporova.natalia@urfu.ru

In recent years, layered transition metal dichalcogenides (TMDCs) and intercalation complexes based on TMDCs have been extensively studied. The bonding between the *Ch-T-Ch* triple layers is weak and allows for the insertion of a wide variety of foreign atoms and molecules. Such insertion into the structure of transition metal dichalcogenides may give rise to dramatic changes in the physical properties of parent compounds [1].

The layered compounds  $2\text{H-TaS}_2$  and  $2\text{H-TaSe}_2$  are known to exhibit metallic conductivity and density-wave phase transitions, as well as transitions to the superconducting state [2]. The intercalation of iron atoms between  $\text{S-Ta-S}$  sandwiches leads to the appearance of extremely high coercivity ( $H_c \sim 27 - 70$  kOe), huge magnetocrystalline anisotropy (anisotropy field  $H_a \sim 600$  kOe) and ferromagnetic ordering, which is strongest at Fe concentrations around  $\sim 25\%$  due to the formation of the Fe superstructure [3, 4]. Significant magnetic hysteresis and field-induced magnetic phase transitions were observed in another intercalated system  $\text{Fe}_{0.5}\text{Ti}(\text{S},\text{Se})_2$ , in which sulfur was replaced by selenium [5].

The aim of the present work was to systematically study the effect of anionic substitution on the crystal structure and physical properties of  $\text{Fe}_{0.25}\text{TaS}_{2-y}\text{Se}_y$  ( $0 \leq y \leq 2$ ) materials at a constant iron content. The  $\text{Fe}_{0.25}\text{TaS}_{2-y}\text{Se}_y$  compounds were prepared by solid-state reactions using a single-stage technology at a temperature of  $T = 700$  °C. The X-ray diffraction was performed using a Bruker D8 Advance diffractometer. The magnetization was measured by using a SQUID-magnetometer at temperatures from 2 K to 350 K and in magnetic fields up to 70 kOe.

In this work, we have synthesized, for the first time, a system of polycrystalline compounds  $\text{Fe}_{0.25}\text{TaS}_{2-y}\text{Se}_y$ ,  $y \leq 2$ . The replacement of sulfur by selenium leads to the anisotropic expansion of the crystal lattice and dramatically affects the magnetization behavior with temperature and magnetic field. It was found that all the  $\text{Fe}_{0.25}\text{TaS}_{2-y}\text{Se}_y$  compounds are characterized as Ising-type ferromagnets with a giant coercive field in the range 40 – 60 kOe at low temperatures. A jump-like behavior of the magnetization at 2 K is observed for substituted compounds across the entire concentration range. The change in  $H_c$  with the Se content in  $\text{Fe}_{0.25}\text{TaS}_{2-y}\text{Se}_y$  correlates with the concentration dependence of the Curie temperature in this system, which means that coercivity in these materials is determined more by the exchange energy than by the magnetocrystalline anisotropy.

This work was supported by the Prioritet-2030 program.

- [1] S.S.P. Parkin, Phil. Mag. B. 41, 65–93 (1980)
- [2] D.C. Freitas, Phys. Rev. B. 93, 184512 (2016)
- [3] M. Arai, Appl. Phys. Lett. 107, 103107 (2015)
- [4] W.J. Hardy, Phys. Rev. B. 91, 054426 (2015)
- [5] N.V. Baranov, Phys. Rev. B. 100, 024430 (2019)

# Effect of Magnetic and Elastic Anisotropy on Adiabatic Potential Energy of a Jahn-Teller Complex in Dilute Semiconductors

V. Gudkov<sup>a,\*</sup>, N. Averkiev<sup>b</sup>, M. Sarychev<sup>a</sup>, I. Zhevstovskikh<sup>a,c</sup>, S. Zherlitsyn<sup>d</sup>, Yu. Korostelin<sup>e</sup>

<sup>a</sup> Ural Federal University, Institute of Physics and Technology, 620002, Mira st. 21, Ekaterinburg, Russia

<sup>b</sup> Ioffe Institute, RAS, 194021, Politekhnikeskaya st. 26, St. Petersburg, Russia

<sup>c</sup> M.N. Mikheev Institute of Metal Physics, UB RAS, 620137, S. Kovalevskaya st. 18, Ekaterinburg, Russia

<sup>d</sup> Hochfeld-Magnetlabor Dresden (HLD-EMFL), Helmholtz-Zentrum Dresden-Rossendorf, Dresden D-01314, Germany

<sup>e</sup> P.N. Lebedev Physical Institute, RAS, 119991, Leninsky Avenue 53, Moscow, Russia

\* v.v.gudkov@urfu.ru

Ultrasonic experiments provide unique information about characteristics of the Jahn-Teller (JT) complexes in dilute magnetic crystals. First experiments in this field were dated by 1960<sup>th</sup> and deal with dynamic properties, i.e., relaxation mechanisms of the JT subsystem [1]. The energy characteristics of the complexes were studied further on, namely the adiabatic potential energy (APE) as a function of symmetrized coordinates (see [2] and references therein). Influence of magnetic field on APE was revealed in ZnSe (sphalerite) and CdSe (wurtzite) crystals doped with Cr<sup>2+</sup> ions and described [3] in the framework of the linear  $T \times (e + t_2)$  problem and spin Hamiltonian which was used for interpretation of the results of optical [4] and ESR [5] experiments. The main conclusion of this description is influence of the magnetic field on the global (former equivalent) minima of the APE surface (APES) and re-distribution of the structure elements of the JT subsystem over these minima. In an ultrasonic experiment, this re-distribution manifests itself as increase or cancellation of the wave attenuation in strong magnetic field dependent on magnetic field orientation with respect to the principal crystal axes. This property is an evidence of magnetic anisotropy of the JT complexes. Such a clear situation took place in a sphalerite ZnSe:Cr<sup>2+</sup> crystal in which CrSe<sub>4</sub> represents a tetrahedral complex which is described similar to a cubic one. An important feature is: the axes of a cube (in which the tetrahedron is embedded) are parallel to the principal axes of the host (cubic) matrix. Recent theoretical treatment of a hexagonal (wurtzite) CdSe:Cr<sup>2+</sup> crystal revealed additional form of anisotropy, namely, elastic anisotropy of the JT complex. This anisotropy originates from lower crystal symmetry of the matrix with respect to the symmetry properties of the tetrahedral complex [6]. Dependent on the magnitudes of the primary force constants which characterize the JT complex, one of the global minima of the APES is lifted or lowered with respect to the others. This is an analogy of the magnetic field effect dependent on its orientation. As a result, in CdSe:Cr<sup>2+</sup> two types of anisotropy, magnetic and elastic ones, compete and provide the final result of the APES formation. Support by the Ministry of Science and Higher Education of the Russian Federation (the basic part of the state assignment, project no. FEUZ-2023-0013) is acknowledged.

[1] M.D. Sturge, J.T. Krause, E.M. Gyorgy, *et al.*, Phys. Rev. 155, 218 (1967)

[2] M.N. Sarychev, W.A.L. Hosseny, I.V. Zhevstovskikh, *et al.*, JETP 135, 473 (2022)

[3] M.N. Sarychev, I.V. Zhevstovskikh, Yu.V. Korostelin, *et al.*, JETP 136, 803 (2023)

[4] J.T. Vallin, G.A. Slack, S. Roberts, *et al.*, Phys. Rev. B 2, 4313 (1970)

[5] J.T. Vallin, G.D. Watkins, Phys. Rev. B 9, 2051 (1974)

[6] V.V. Gudkov, N.S. Averkiev, I.V. Zhevstovskikh, *et al.*, JETP Letters 119, 503 (2024)

# First-Principles Analysis of The Magnetic Properties of Co-Ni-Fe Alloy Depending on Its Crystal Structure and Composition

G. Demin<sup>a,\*</sup>, R. Tikhonov<sup>b</sup>, N. Djuzhev<sup>a</sup>

<sup>a</sup> National Research University of Electronic Technology (MIET), 124498, Shokin sq., bld. 1, Zelenograd, Moscow, Russia

<sup>b</sup> SMC “Technological Center” MIET, 124498, Shokin sq., bld. 1/7, Zelenograd, Moscow, Russia

\*gddemin@gmail.com

To achieve record sensitivity of magnetic sensors based on the tunnel magnetoresistive effect (up to 4000%/mT and beyond), thin-film magnetic flux concentrators (MFCs) are currently used, which locally enhance the magnetic field (MF) in the region of the magnetic tunnel junction [1]. Typically, MFCs are made of soft magnetic films that have high magnetic permeability and a low demagnetization factor. This allows for MF enhancement of up to 400 times or more [2]. One of such promising materials for MFC is the Co-Ni-Fe alloy, which has high magnetic permeability and low coercivity. The magnetic properties of Co-Ni-Fe films are determined by their crystal structure and atomic composition, which controls the volume fractions of the fcc and bcc phases in the crystal lattice.

Based on the first-principles approach and using the local spin density approximation (LSDA), the saturation magnetization ( $M_s$ ) of the Co-Ni-Fe alloy (Figure 1a) was estimated as a function of the concentrations of Co and Ni atoms at a fixed Fe content. It was shown that an increase in the content of Co atoms (volume fraction of the fcc phase) leads to an increase in  $M_s$  and magnetic permeability  $\mu$ , which is typical for Co-rich magnetic alloys and consistent with the experimental data from [3].

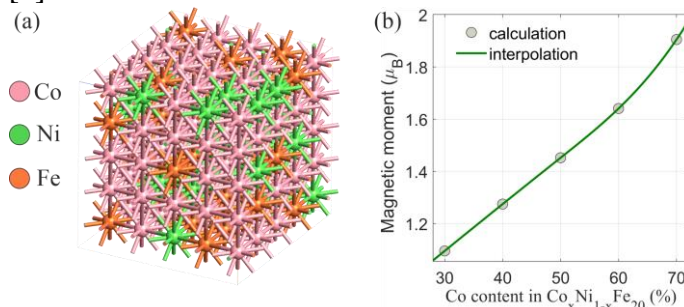


Figure 4. (a) Crystal structure of the Co-Ni-Fe alloy ( $\text{Co}_{60}\text{Ni}_{20}\text{Fe}_{20}$ ). (b) Magnetic moment of  $\text{Co}_x\text{Ni}_{1-x}\text{Fe}_{20}$  as a function of Co content(x).

A series of amorphous Co-Ni-Fe films of different thickness (above 1  $\mu\text{m}$ ) and atomic content (Co, Ni, Fe) were formed by electrochemical deposition. According to the results of GI-XRD analysis, the structure of Co-Ni-Fe films with increased Co content (more than 50%) has a polycrystalline fcc phase with a predominant reflection in the  $\langle 111 \rangle$  direction. The variation of the coercive force  $H_C$  and the maximum magnetic permeability  $\mu = \mu_{\text{MAX}}$  of Co-Ni-Fe films were experimentally studied depending on the atomic content. For  $\text{Co}_{58.5}\text{Ni}_{27.4}\text{Fe}_{14.1}$ , we obtained  $\mu_{\text{MAX}} = 12320$  and  $H_C = 1.64$  Oe, while the measured lattice parameter  $a = 3.52$  Å is in a good agreement with simulated diffraction patterns generated by CrystalDiffra for this composition ( $a \approx 3.55$  Å). The results can be used in the formation of Co-Ni-Fe films for MFCs with improved magnetic properties. This work was supported by the RF Ministry of Science and Higher Education (State assignment No. FSMR-2023- 0003).

[1] Y. Yang et al., IEEE Trans. Magn., 59(1), 4400107 (2023)

[2] S. Manceau et al., Appl. Phys. Lett., 123(8), 082405 (2023)

[3] G. Shamsutdinov, et al., Sci. Rep., 12, 1957 (2022)

# FORC-analysis study of magnetic interactions in ferrite oxides

V. Kolesnikova<sup>a\*</sup>, V. Salnikov<sup>a</sup>, A. Nikitin<sup>b</sup>, A. Omelyanchik<sup>a,c,d</sup>,

L. Panina<sup>a,b</sup>, V. Rodionova<sup>a</sup>

<sup>a</sup> Immanuel Kant Baltic Federal University, Kaliningrad, Russia

<sup>b</sup> National University of Science and Technology MISIS, 119991, Moscow, Russia

<sup>c</sup> Dipartimento di Chimica e Chimica Industriale (DCCI), Università degli Studi di Genova, Italy

<sup>d</sup> ISM-CNR, nM2-Lab, Area della Ricerca Roma Monterotondo Scalo (RM), Italy

\*VGKolesnikova1@kantiana.ru

The FORC analysis method (FORC: First Order Reversal Field) is a powerful method for studying magnetic interactions of the complex systems. The FORC analysis method is based on the mathematical model of Preisach hysteresis, in which a unit of magnetic domain is described by a magnetic hysteron. The hysteron is a Preisach distribution function  $P(H_c, H_u)$ , describing an ideal rectangular hysteresis loop depending on the switching field (coercivity in the case of a rectangular loop) -  $H_c$  and on the interaction field -  $H_u$ . In a system of a set of hysterons, it is the presence of a hysteron shift in magnitude on the axis of the external applied magnetic field ( $H$ ) that indicates that the system is subject to a magnetic effect. If for a multiphase system we construct distribution functions in the coordinates of the switching fields and interaction fields, we obtain a magnetic interaction diagram - the Preisach diagram [1,2].

In this work, FORC-analysis was applied to study magnetic interparticle interactions in cobalt ferrites ( $\text{CoFe}_2\text{O}_4$ ) magnetic nanoparticles, focusing on the effect of the particle crystallization during surfactant-assisted hydrothermal synthesis in the presence of sodium dodecyl sulfate (SDS). SDS served as both a growth-controlling agent [3], and a capping agent, stabilizing the nanoparticles in aqueous solutions for applications such as dye sorption [4] and hyperthermia [5]. For each sample, 150 FORC curves were measured at room temperature on a vibrating sample magnetometer, complemented by X-ray diffraction and transmission electron microscopy to probe microstructural evolution as a function of hydrothermal synthesis.

As a result, a transition was obtained from an ensemble of particles with soft magnetic properties to a harder one with a parallel decrease in saturation magnetization from ~71 to 61 emu/g and an increase in coercivity from ~0.80 to 1.17 kOe.

This study was funded by the Russian Science Foundation under Project no. 25-72-30009, <https://rscf.ru/en/project/25-72-30009/>.

[1] A. Stancu, C. Pike, L. Stoleriu, P. Postolache, D. Cimpoesu, Micromagnetic and Preisach analysis of the First Order Reversal Curves (FORC) diagram, J. Appl. Phys. 93 (2003) 6620–6622.

[2] I.D. Mayergoyz, G. Friedman, Generalized preisach model of hysteresis (invited), IEEE Trans. Magn. 24 (1988) 212–217.

[3] A. Omelyanchik, K. Levada, S. Pshenichnikov, M. Abdolrahim, M. Baricic, A. Kapitunova, A. Galieva, S. Sukhikh, L. Astakhova, S. Antipov, B. Fabiano, D. Peddis, V. Rodionova, Green synthesis of co-zn spinel ferrite nanoparticles: Magnetic and intrinsic antimicrobial properties, Materials (Basel). 13 (2020) 1–13.

[4] M. Singh, H.S. Dosanjh, H. Singh, Surface modified spinel cobalt ferrite nanoparticles for cationic dye removal: Kinetics and thermodynamics studies, J. Water Process Eng. 11 (2016) 152–161.

[5] M.A. Kashi, K. Heydaryan, A comparative study on characterization and hyperthermia properties of  $\text{CoFe}_2\text{O}_4$  nanoparticles synthesized with different surfactants, J. Mater. Sci. Mater. Electron. 34 (2023).

# Magnetic field-induced tunable optical spatial differentiator based on magnetoplasmonic crystals

A. Nerovnaya<sup>\*</sup>, A. Frolov, A. Fedyanin

Lomonosov Moscow State University, 119991, Leninskie gory 1, Moscow, Russia

<sup>\*</sup>nerovnayaaa@my.msu.ru

In recent years, analog optical computing has attracted significant attention due to its high performance and low energy consumption. The miniaturization of such computing devices down to subwavelength scales has been achieved through the use of metasurfaces. Previously, it was demonstrated that spatial differentiation of an input signal can be realized in thin plasmonic films through the interference between direct reflection at the interface and the leakage radiation of surface plasmon polaritons (SPPs) [1]. Most metasurfaces possess a specific optical response tailored for a particular mathematical operation. To enhance the functionality of these structures, approaches of actively modulating their optical response are being developed, for example, to enable switching between different differentiation modes [2]. In this work, we experimentally investigate the optical spatial differentiation using magnetoplasmonic crystals, which allows modulation of the optical response under an external magnetic field.

The key condition for optical spatial differentiation is achieving a near-zero reflectance that is proportional to the value of the in-plane wavevector of the incident light in the vicinity of resonance incident angles. A nickel plasmonic crystal with a period of 575 nm and a corrugation depth of 116 nm was used. Figure 1 presents the image of a slit's edges captured with a CMOS camera at a resonance incidence angle of  $22^\circ$ , where the reflection coefficient approaches almost zero. As the incidence angle deviates from the resonance, the visibility of the edges diminishes until it disappears. Figure 2 shows that the edges of the slit exhibit higher intensity compared to the surrounding areas, confirming the realization of optical spatial differentiation. A magnetic field-induced modulation of the spatial intensity profile of approximately 3% was observed.

The demonstrated capabilities of magnetoplasmonic crystals pave the way for the development of a new generation of ultrafast, compact, and energy-efficient computing devices based on magnetic field-induced tunability.

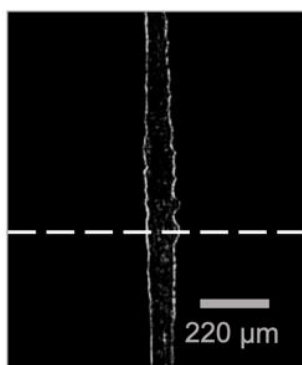


Figure 1. Image of slit edges on the CMOS camera

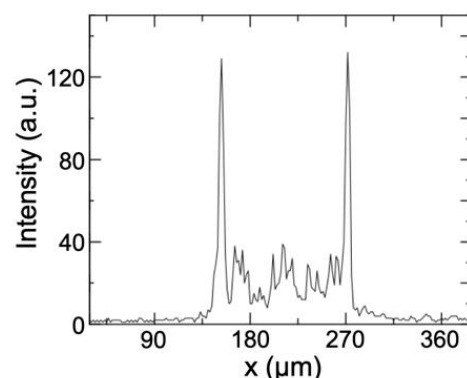


Figure 2. The spatial cross-section of the image corresponding to the white dashed line in Fig. 1

[1] T. Zhu, Nat. Commun. 8, 15391(2017)

[2] M. Cotrufo, Nat. Commun. 15, 4483(2024)

# Modeling of multiferroic composites properties via FEM

A. Ignatov<sup>a,\*</sup>, Y. Raikher<sup>b,a</sup>, O. Stolbov<sup>b,a</sup> and V. Rodionova<sup>a</sup>

<sup>a</sup> Immanuel Kant Baltic Federal University, 236004, Nevskogo 14, Kaliningrad, Russia

<sup>b</sup> Institute of Continuous Media Mechanics, Russian Academy of Sciences, Ural Branch, Perm 614018, Russia

\*artem.ignatov98@gmail.com

Composite magnetoelectric materials are capable of converting magnetic energy into electric energy (direct effect) and vice versa (inverse effect). This effect is due to the mechanical connection between their ferromagnetic and piezoelectric components. The key advantages of composites over single-phase multiferroics are a significantly stronger magnetoelectric response (an order of magnitude higher) [1] and flexibility in designing properties due to varying the phase composition. High conversion efficiency makes them suitable for creating sensitive elements of magnetic/electric field sensors [2,3], energy harvesting [3], smart scaffolds for regenerative medicine [4] and other devices.

One of the methods for studying multiferroic composites is the numerical calculation of the properties of such materials using FEM. For example, such a method helped to establish the comparability of the contribution to the magnetoelectric effect of the phenomenon of magneto-deformation compared to magnetostriction [5].

This paper will present the results of FEM calculations of some properties of multiferroic composites.

This research was supported by funds provided through the Russian Federal Academic Leadership Program “Priority 2030” at the Immanuel Kant Baltic Federal University, project number 123120700040-2

- [1] Pereira N., Lima A.C., Lanceros-Mendez S., Martins P. *Materials*. 2020. V. 13. Art. no. 4033.
- [2] Vidal J.V., et al. *IEEE Transactions on Ultrasonics and Ferroelectrics, Frequency Control*. 2020. V. 67. P. 1219.
- [3] Pereira N., et al. *Materials*. 2020. V. 13. Art. no. 1729.
- [4] Omelyanchik A., et al. *Nanomaterials*. 2021. V. 11. Art. no. 1154.
- [5] Stolbov O.V., Raikher Yu.L. *Nanomaterials*. 2024. V. 14. Art. no. 31.
- [6] B. Brown, *EPJ* 33, 255 (2011)

# Magneto-Optical Effects Enhancement at the Bound States in the Continuum Resonances

M. Gavryushina\*, A. Musorin, A. Fedyanin

Lomonosov Moscow State University, 119991, Leninskie gory 1, Moscow, Russia

\*gavryushinams@my.msu.ru

This work focuses on dielectric metasurfaces supporting high-Q resonances associated with bound states in the continuum (BIC) — modes that belong to the radiation spectrum but do not radiate [1]. In realistic systems, symmetry breaking transforms ideal BIC into quasi-BIC with finite but extremely high quality factors, making them accessible to external excitation [2]. BIC in all-dielectric metasurfaces enable ultra-high-Q resonances, making them a powerful platform for enhancing light–matter interactions. Such metasurfaces are particularly advantageous due to their minimal absorption losses compared to plasmonic structures. While the configuration based on symmetric quadrumers in silicon demonstrates the excitation of high-Q quasi-BIC via translational lattice perturbation [3], magneto-optical (MO) effects were not considered in that context, despite the relative simplicity of fabrication.

The originality of this work lies in applying this lattice-scaling approach to a magnetic dielectric material, Bi-substituted yttrium iron garnet (Bi:YIG), for enhancing MO effects such as Faraday rotation. In previous studies, quasi-BIC were implemented in magneto-optical metasurfaces based on asymmetric nanodisks with a displaced air hole — a geometry that is more challenging to fabricate [4]. It was shown that such structures help to enhance the Faraday rotation up to  $0.7^\circ$  due to the excitation of high-Q quasi-BIC resonances.

In studying metasurface based on a quadrumer voids in Bi:YIG layer with lattice-period-induced symmetry breaking, the Faraday rotation reaches  $\Theta = -2.66^\circ$  for a 210 nm thick of the magnetic material. The structure, deposited on a gold (Au) substrate (fig. 1), is numerically analyzed using the finite-difference time-domain (FDTD) method. The simulations reveal a resonance at a wavelength of 844 nm for a lattice period of 767 nm, confirming the presence of high-Q quasi-BIC modes responsible for the observed MO enhancement.

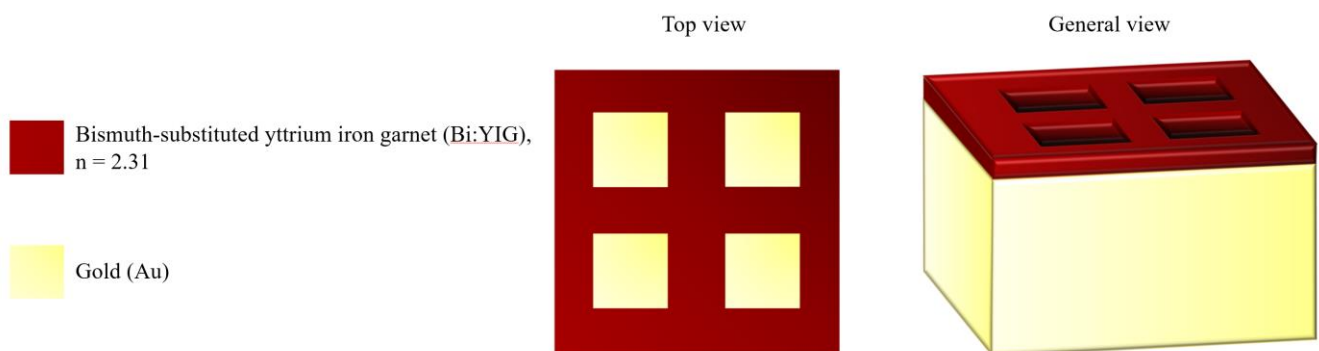


*Figure 1. Schematics of the sample supporting BIC resonance.*

- [1] C. Hsu, Nat. Rev. Mater. 1, 16048(2016)
- [2] K. Koshelev, Phys. Usp. 66, 494(2023)
- [3] M. Zhou, Sci. China Phys. Mech. Astron. 66, 124212(2023)
- [4] A. Chernyak, JETP Lett. 111, 40(2020)



# Extracting anisotropic exchange in spin Hamiltonians with quantum chemical cluster calculations for complex transition metal oxides

L. Siurakshina

Joint Institute for Nuclear Research, 141980, Joliot-Curie 6, Dubna, Moscow Region, Russia

siuraksh@jinr.ru

Theoretical treatment of the exchange coupling between the spin magnetic moments in the wide family of transition metal-based oxides (TMOs) with the unfilled electronic 3d shell (including cuprates, vanadates, nickelates and other) can be successfully done using the analytical perturbative methods of Anderson's superexchange theory. When passing to heavier elements, such as iridium, with an unfilled 5d shell of valence electrons, the electronic spin-orbit interaction within the 5d shell increases and the nature of the TM magnetic moments, as well as the exchange coupling between neighboring TM ions change dramatically. Then, an accurate quantitative characterization of the above-mentioned local magnetic characteristic is possible only based on the ab initio quantum chemical cluster calculations.

The quantum-chemical cluster approach [1-3] we have developed includes three main procedures:

(a) for the central part of the cluster containing a pair of neighboring exchange-coupled TM ions, the calculation of many-electron wave functions (configurations) is performed taking into account electron correlations in a high-level computational scheme (CASSCF, MRCI, etc),

(b) the ion-covalent chemical bonds between the central part of the cluster and the rest of crystalline medium are treated in the Hartree-Fock approximation, i.e. without including electron correlations, and

(c) the calculated low-energy configurations are mapped onto the limited state space of an effective spin Hamiltonian for a pair of neighboring exchange-coupled TM ions; this pair spin Hamiltonian generates its lattice analog using the underlying translational symmetry of the system under consideration.

The model spin Hamiltonians thus obtained are applied to study the macroscopic properties of magnetic systems, for instance, to predict their phase diagrams and magnetic excitation spectra.

In particular, the cluster method of quantum chemical calculations is of exceptional importance for the quantitative analysis of heavy transition metal systems such as iridium oxides, in which the strong spin-orbit interaction between the valence electrons in the unfilled 5d shell leads to the dominance of the anisotropic over the isotropic Heisenberg exchange.

[1] L. Xu, R. Yadav, V. Yushankhai, L. Siurakshina et al., Phys. Rev. B 99, 115119(2019)

[2] Z. Porter, P.M. Sarte et al., Phys. Rev. B 106, 115140(2022)

[3] Л.А.Сюракшина, В.Ю. Юшанхай, Известия РАН. Серия физическая 89, № 10 (2025)

# Electric field as a new tool in ultrafast magnetism

N. Khokhlov\*, T. Gareev, A. Kimel

Radboud University, 6525 AJ, Heyendaalseweg 135, Nijmegen, The Netherlands

\*nikolai.khokhlov@ru.nl

Ultrafast magnetism explores spin dynamics and eventually spin switching in magnets excited by ultrashort (sub-100 ps) stimuli [1]. The progress in the field is predominantly driven by experimental research, where ultrafast spin dynamics is typically triggered by femtosecond laser pulses and investigated as a function of parameters of laser excitation, temperature and magnetic field. Here, we show that also electric field, whose effect on magnets is often ignored, can have a substantial effect on ultrafast spin dynamics and result in spin switching, in particular.

First, we demonstrate the impact of an electric field on laser-induced magnetization dynamics in ferrimagnetic iron garnet ( $\text{BiLu}_3(\text{FeGa})_5\text{O}_{12}$ ). For the experiments we employed epitaxially grown iron garnet film on  $\text{Gd}_3\text{Ga}_5\text{O}_{12}$  substrate with (110)-orientation [2]. Applying an E-field of 0.5 MV/m, we observe remarkable changes in oscillations amplitude, frequency and damping (Fig. 1a).

In the second experiment, we employed antiferromagnetic  $\text{Cr}_2\text{O}_3$ , which is known to be an archetypical magneto-electric material [3]. Particularly, its magnetic state could be defined by the combination of electric and magnetic fields  $\mathbf{E} \cdot \mathbf{B}$ . We used the fact to manipulate AFM domain wall in c-cut crystal of  $\text{Cr}_2\text{O}_3$  with thickness of 0.5 mm. In the experiments, we applied uniform B-field and localized E-field in the vicinity of the wall. As a result, the direction of wall motion and covered distance depend on the sign and magnitude of dot product  $\mathbf{E} \cdot \mathbf{B}$  (Fig. 1 b,c). Furthermore, we established the combination of E, B fields and sample temperature for robust writing of antiferromagnetic patterns with a single laser pulse. Further, studies of electrically gated spin dynamics in  $\text{Cr}_2\text{O}_3$  are presently in progress.

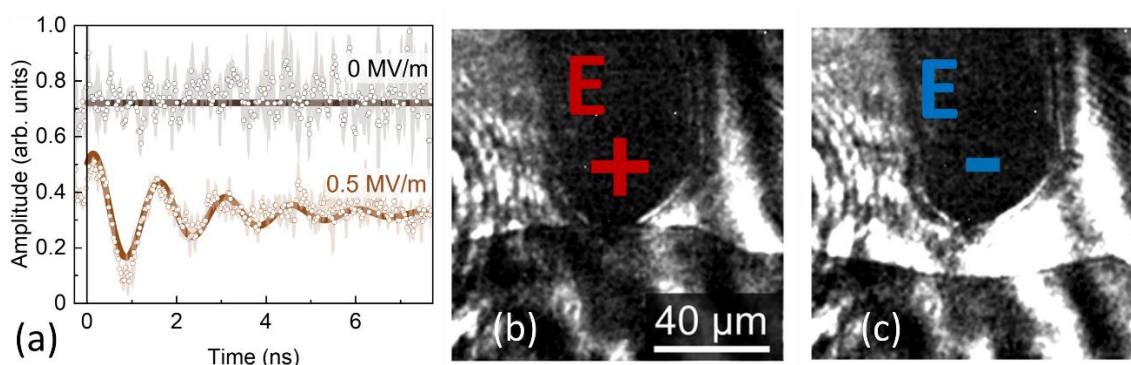


Figure 1. Electric field as a tool in magnetic dynamics. (a) Ultrafast laser-induced spin dynamics as detected via the magneto-optical Faraday effect in electrically gated  $(\text{BiLu})_3(\text{FeGa})_5\text{O}_{12}$ . (b,c) Antiferromagnetic domains in  $\text{Cr}_2\text{O}_3$  visualized with the help of second harmonic generation. A combination of electric and magnetic fields can cause a displacement of the domain wall. An external E-field of opposite polarities, applied locally with a non-magnetic charged tip (dark elongated area at the top) shifts the wall in mutually opposite directions.

- [1] A. Kimel, A. Zvezdin, S. Sharma, et al. Journal of Physics D, 55(46), 463003 (2022)
- [2] N.E. Khokhlov, A.E. Khranova, E.P. Nikolaeva, et al. Sci. Rep., 7, 264 (2017)
- [3] K. Du, X. Xu, C. Won, et al., npj Quantum Mater., 8, 17 (2023)

# Structural and magnetic properties of ternary alloyed FeCoCu nanowires

D. Khairetdinova<sup>a,b,c,\*</sup>, I. Doludenko<sup>b</sup>, D. Ulybyshev<sup>a</sup>, I. Volchkov<sup>b</sup>, L. Panina<sup>a,c</sup>

<sup>a</sup> National University of Science and Technology MISIS, 119049, Leninskiy avenue 4, Moscow, Russia

<sup>b</sup> National Research Centre “Kurchatov Institute”, 119333, Leninskiy avenue 59, Moscow, Russia

<sup>c</sup> Immanuel Kant Baltic Federal University, 236004, Alexander Nevsky st 14, Kaliningrad, Russia

\*khairetdr@gmail.com

FeCoCu nanowires (NWs) obtained by the matrix synthesis method may be of great interest as functional material for nanoelectronics and biomedical applications [1]. The addition of different amounts of Cu to binary FeCo solid solutions can change the magnetic anisotropy and improve optical properties for magneto-plasmonic applications. Furthermore, it is possible to produce layered NWs FeCoCu/Cu for magnetically controlled photothermia, since Cu as a plasmonic metal covers a wide spectral range [2].

In this work, FeCoCu NWs were obtained by electrodeposition into the pores of polymer track-etched membranes with pore diameters  $d$  of 30 and 100 nm. A series of samples with different Cu concentrations were prepared by applying a deposition potential in the range of 1 to 2 V. The morphology and elemental composition were studied by SEM and EDX, and XRD was used for structural analysis. The hysteresis loops of the NWs were measured by VSM and optical properties were modelled within effective medium theory of conductivity of a infinite cylinder.

For NWs with  $d = 100$  nm, the Cu content tends to decrease with increasing the deposition voltage, leading to an increase in Fe and Co concentrations, which reach a plateau at  $U = 1.4$  V. The minimum Cu content (5 at.%) was obtained at  $U = 1.8$  V, while the Fe and Co contents were 36 at.% and 59 at.%, respectively. NWs with  $d = 30$  nm show a similar tendency, but the concentration dependence reaches a plateau more quickly and the minimum of Cu content is around 2 at. %.

The XRD study has revealed the presence of a number of phases, including the FeCo phase, which has the most intense peak (110) corresponding to a bcc solid solution, and some smaller peaks corresponding to CoCu and FeCu phases.

The VSM study of NWs was carried out at two different magnetic field positions: out of plane (OOP) and in plane (IP) of the samples. Regardless of a diameter, there is a general tendency for both  $H_c$  and  $M_r/M_s$  to decrease with increasing Cu-content, which is important for biomedical applications. For other applications, enhanced values of  $H_c$  and  $M_r/M_s$  are important, which can be achieved with lower Cu-concentrations of about 5 at.%. The value of  $H_c$  was 370 Oe, which is nearly 100 Oe higher than that of binary FeCo NWs with similar Fe:Co ratio. For NWs with  $d = 30$  nm,  $H_c$  and  $M_r/M_s$  values are higher for the OOP direction, indicating a strong impact of the shape anisotropy. The dependence of magnetic parameters on Cu content is similar to that of NWs with  $d = 100$  nm, but the values of  $H_c$  and  $M_r/M_s$  increase considerably ( $H_c = 1350$  Oe at 11 at. % Cu). This may be due to the formation of a finely dispersed Cu phase, which can alter the domain wall propagation processes in NWs, or to the increase in magnetocrystalline anisotropy values in such structures.

Tuning the constituent concentrations of Fe and Co also affects the plasmonic behavior of Cu-based hybrids. The resonant wavelength of layered FeCo/Cu NWs changes from 765 to 1200 nm with the increase of the aspect ratio of the Cu segment. This corresponds to the transparency window of tissues.

The work is supported by grant RSF 21-72-20158.

[1] N. Lupu, Electrodeposited Nanowires and Their Applications, 144 (2010)

[2] Yue Xin et al, Advanced Materials, 2008145 (2021)

## Optical clearing technology in antitumor photothermal therapy

E. Genina<sup>a,\*</sup>, I. Serebryakova<sup>a</sup>, Yu. Surkov<sup>a</sup>, V. Genin<sup>a</sup>, M. Kirillin<sup>b,c</sup>, D. Kurakina<sup>b</sup>,  
A. Bucharskaya<sup>d</sup>, N. Navolokin<sup>d</sup>, N. Shushunova<sup>d</sup>, B. Khlebtsov<sup>e</sup>, and V. Tuchin<sup>a,f,g</sup>

<sup>a</sup> Saratov State University, 410012, Astrakhanskaya Str. 83, Saratov, Russia

<sup>b</sup> FRC “A.V. Gaponov-Grekhov Institute of Applied Physics of the Russian Academy of Sciences”, 603950,  
Ul’yanov Str. 46, Nizhny Novgorod, Russia

<sup>c</sup> Lobachevsky State University, 603022, Prospekt Gagarina 23, Nizhny Novgorod, Russia

<sup>d</sup> Saratov State Medical University, 410012, B. Kazachya Str. 112, Saratov, Russia

<sup>e</sup> Institute of Biochemistry and Physiology of Plants and Microorganisms, FRC “Saratov Scientific Centre of  
the Russian Academy of Sciences”, 410049, Prospekt Entuziastov 13, Saratov, Russia

<sup>f</sup> Institute of Precision Mechanics and Control, FRC “Saratov Scientific Centre of the Russian Academy of  
Sciences”, 410028, Rabochaya Str. 24, Saratov, Russia

<sup>g</sup> National Research Tomsk State University, 634050, Lenin Ave. 36, Tomsk, Russia

\*geninae@sgu.ru

The effectiveness of phototherapy as a cancer treatment method is confirmed by numerous studies [1]. The use of light, which is a strength of phototherapy, is also its weakness, since it is associated with a limited depth of light penetration into biological tissue due to scattering. One of the new directions in the development of the method is a combination of photothermal (PTT) and photodynamic (PDT) therapy with optical clearing [2]. Diffuse reflectance spectra measured in vivo provide information on the content of hemoglobin [3] and water [4] in tissues, which can be useful in the development of safe phototherapeutic procedures.

We present the results of modeling changes in light propagation in a multilayer tumor model with intratumorally introduced gold nanorods during plasmonic PTT with preliminary optical clearing of the skin and monitoring changes in blood and water in tissues in vivo during this procedure. Twenty laboratory outbred male rats were included in the study. The PC-1 cholangiocarcinoma model was generated by subcutaneous inoculation of the cell suspension into the interscapular region. Gold nanorods (GNRs) with an aspect ratio of 4:1 were used for PTT. Tumors were irradiated with an 808 nm diode laser at a power density of 2.3 W/cm<sup>2</sup> 24 h after GNR injection. An optical clearing agent (a mixture of 70% aqueous glycerol and 5% dimethyl sulfoxide) was applied topically to the skin over the tumor before therapy. Skin heating was monitored using an IR visualizer. Diffuse reflectance spectra were recorded before and after the procedures in the spectral range of 400-2100 nm.

PTT caused an increase in local heating temperature and corresponding changes in the reflectance spectra. Erythema and water content indices were calculated for different maximum temperatures achieved. A reduction in skin dehydration and thermal damage was observed with optical pre-clearing compared to PTT without optical clearing.

The work was supported by the RSF grant no. 23-14-00287.

[1] M. Kim, J.H. Lee, J.M. Nam, *Adv. Sci.* 6(17), 1900471 (2019)

[2] Zh. Hao, J. Xu, J. Wan et al. *Nano Today* 36, 101058 (2021)

[3] O.A. Zyuryukina, Y.P. Sinichkin *Opt. Spectrosc.* 127, 555–563 (2019)

[4] D.A. Davydov, G.S. Budylin, A.V. Baev et al. *JBO* 28(5) 057002 (2023)

# Phase transition in $\text{Fe}_{45}\text{Co}_{30}\text{Si}_{10}\text{B}_{15}$ and $\text{Co}_{83}\text{Fe}_7\text{C}_1\text{Si}_7\text{B}_2$ micro-wires in the temperature dependence of the ESR spectrum

A. Shestakov<sup>a,\*</sup>, I. Fazlizhanov<sup>b</sup>, R. Eremina<sup>b</sup>,

S. Demishev<sup>c</sup>, V. Rodionova<sup>d</sup>, V. Kolesnikova<sup>d</sup>

<sup>a</sup> Prokhorov General Physics Institute of the RAS, 119991, Vavilova 38, Moscow, Russia

<sup>b</sup> Zavoisky Physical-Technical Institute, FRC KazSC of RAS, 420029, Sibirsky tract, 10/7 Kazan, Russia

<sup>c</sup> Institute for High Pressure Physics of the RAS, 108840, Kaluga highway 14, Troitsk, Moscow, Russia

<sup>d</sup> Immanuel Kant Baltic Federal University, 236004, Nevskogo 14, Kaliningrad, Russia

\*ALEKSEIVSHESTAKOV@GMAIL.COM

Thin ferromagnetic metallic glass-coated microwire of compositions  $\text{Co}_{83}\text{Fe}_7\text{C}_1\text{Si}_7\text{B}_2$  ( $d/D=38/41 \mu\text{m}$ ) and  $\text{Fe}_{45}\text{Co}_{30}\text{Si}_{10}\text{B}_{15}$  ( $d/D=19.1/26.2 \mu\text{m}$ ) was produced by the Taylor-Ulitovsky method under water or air cooling. They demonstrated various types of magnetization reversal behaviors, including bistable, stepwise, and S shape with a highly enhanced coercivity [1]. It was found that a system of Co-based microwires with nearly zero magnetostriction coefficient exhibits a step-like hysteresis loop [2]. The hysteresis loops of magnetostrictive microwires show strong sensitivity to the  $d/D$  ratio [3]. The influence of post-processing conditions on the magnetic properties of amorphous and nanocrystalline microwires is carefully analyzed, with special attention paid to the influence of magnetoelastic, induced and magnetocrystalline anisotropies on the hysteresis loops of Fe-, Ni- and Co-rich microwires [4]. Using the EPR equipment (Varian-12, X-band 9.48 GHz), first derivative of microwave absorption spectra was obtained at temperatures from 290 to 773 K and in magnetic fields up to 10 kOe (Figure 1a). The microwire was located vertically in the central part of the cylindrical resonator ( $\text{TE}_{102}$ ), i.e. along the magnetic component of microwaves. Three lines are observed in the spectrum of the microwire (Figure 1a) associated with the components of the  $g$ -tensor ( $g_x$ ,  $g_y$ ,  $g_z$ ) of ferrimagnetic resonance. At temperatures above 510 K, the three lines of  $\text{Co}_{83}\text{Fe}_7\text{C}_1\text{Si}_7\text{B}_2$  merge into a single line, and the phase transition from ferromagnetic to paramagnetic was observed (Figure 1a). The phase transition temperature of the  $\text{Fe}_{45}\text{Co}_{30}\text{Si}_{10}\text{B}_{15}$  microwire was approximately estimated to be in the region of about 870 ÷ 890 K by extrapolation from  $g$ -value temperature dependencies (Figure 1b).

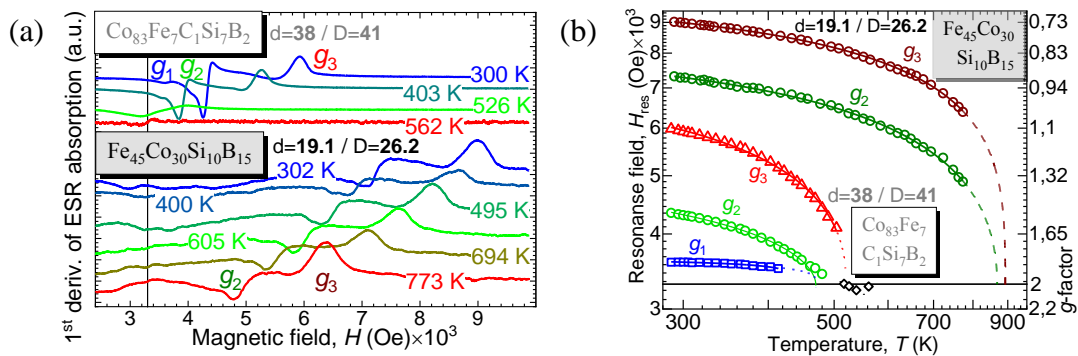


Figure 1. (a) Temperature evolution of the ESR spectra; (b) temperature dependence of the  $g$ -tensor components for  $\text{Co}_{83}\text{Fe}_7\text{C}_1\text{Si}_7\text{B}_2$  ( $d/D=38/41 \mu\text{m}$ ) and  $\text{Fe}_{45}\text{Co}_{30}\text{Si}_{10}\text{B}_{15}$  ( $d/D=19.1/26.2 \mu\text{m}$ ).

- [1] V.V. Rodionova, I.A. Baraban, L.V. Panina *et.al*, IEEE Trans. of Magn. **99**, 1-6 (2018)
- [2] V.V. Rodionova, K. Chichay, V. Zhukova, *et.al*, J Supercond Nov Magn. **28**, 977-981 (2014)
- [3] A. Zhukov, M. Ipatov, V. Zhukova, Abstarct II-Moscow Readings (MISIS), **62** (2011)
- [4] V. Zhukova, P. Corte-Leon, L. González-Legarreta, *et.al.*: Opt. of Magn. Properties of Magn. Microwires by Post-Processing **8**, 1006 (2020)

## Magnetic microdisks as an agent for combined photothermal and magnetomechanical therapy

A. Motorzhina<sup>a\*</sup>, A. Anikin<sup>a</sup>, D. Zinnyatulina<sup>a</sup>, I. Shamanov<sup>a</sup>, S. Pshenichnikov<sup>a</sup>, L. Panina<sup>a,b</sup>,

K. Levada<sup>a</sup>

<sup>a</sup> Immanuel Kant Baltic Federal University, 236004, Nevskogo 14, Kaliningrad, Russia

<sup>b</sup> National University of Science and Technology «MISIS», 119049, Leninskiy av. 4, Moscow, Russia

\*AMotorzhina1@kantiana.ru

One of the most promising areas of research in anti-cancer treatment methods is the development of therapies that exhibit reduced invasiveness and fewer adverse effects in comparison to conventional treatment modalities such as chemotherapy, surgery, and radiation therapy [1]. Such innovative methods include photothermal therapy (PTT) and magnetomechanical therapy (MMT). In PTT, the application of laser irradiation to tumour areas containing noble metal nanoparticles (NPs) results in the induction of localised hyperthermia, which exceeds the threshold required for cell damage. This process leads to the destruction of cellular structures and thermal cell death [1]. In complex diseases such as cancer, PTT is often selected as one component of a combination treatment strategy rather than as a stand-alone universal therapy.

The present study puts forward a hypothesis that combines the use of PTT with MMT, with the aim of achieving greater efficiency in the action on cancer cells. This is achieved by means of layered magnetic microdisks made of gold and iron. MMT constitutes a mechanical action on the cell membrane by moving magnetic NPs in an alternating magnetic field of low frequency (approximately 1-10 Hz), which has the capacity to trigger cell death processes. The fabrication of layered magnetic microdisks was achieved through the utilisation of electron-beam lithography and magnetron sputtering techniques. In comparison with spherical NPs, microdiscs exhibit a higher mechanical moment and can be utilised effectively for combined MMT and PTT.

The present study investigates the impact of gold-iron-gold (AFA) and iron-gold-iron (FAF) microdisks on human hepatocarcinoma cells (Huh7) before and after PTT and/or MMT. The investigation into the viability of the culture was conducted by means of the WST-1 test. The relative viability of Huh7 cells after 24 hours of exposure to AFA and FAF microdisks significantly decreased by 7% and 10%, respectively, at the maximum concentration of 100 µg/ml that was studied. The combination of PTT and MMT at the same concentration resulted in a 50% decrease in culture viability compared to the control group.

The present study was supported by the Russian Science Foundation, grant number 21-72-20158-II.

[1] Fan, W., Yung, B. et al. Chem Rev, 117, (2017)

# Spectral response of circular magnetization in Co-rich amorphous microwires

A. Pashnina<sup>a,\*</sup>, N. Yudanov<sup>a</sup>, L. Panina<sup>a</sup>

<sup>a</sup> National University of Science and Technology «MISIS», 119049, Leninskiy Avenue 4, Moscow, Russia

\*alionapashnina@gmail.com

Co-rich amorphous wires are excellent soft magnetic materials with a unique circular magnetic structure. They are considered to be among the most promising materials for the fabrication of sensitive magnetoimpedance (MI) sensors. The MI phenomenon is based on a pronounced change in the circular magnetisation under various external factors. At frequencies much lower than those used in MI sensors, in the range of 50-200 kHz, a circular magnetic field generated by an alternating current can move circular domain walls. An additional sharp voltage pulse is then generated across the wire ends, the spectrum of which contains higher order harmonics (with respect to the fundamental frequency of the excitation current). This is due to a strong non-linear dependence of the magnetisation on the circular magnetic field. The present study investigates the circular magnetisation processes and the harmonic spectrum under the influence of an axial DC magnetic field. This provides insight into the circular domain structure and suggests potential applications in inductive spectroscopy, for example in the detection and identification of magnetic particles.

Microwires of the composition  $\text{Co}_{66,6}\text{Fe}_{4,28}\text{B}_{11,51}\text{Si}_{14,48}\text{Ni}_{1,44}\text{Mo}_{1,69}$  with a metal core diameter of 14.2 microns and a total diameter of 25.8 microns, were used in this study. To enhance the circular anisotropy, the wire was subjected to current annealing (15 mA). An alternating current with a frequency of 100 to 250 kHz and an amplitude of 15 mA was applied to the wire, causing its circular magnetisation. In order to eliminate the resistive component of the voltage, the technology of a balanced bridge circuit was used, allowing only the inductive contribution to be filtered out.

The circular magnetization of the wire results in the generation of an additional voltage of inductive origin across the wire. Integration of this voltage produces a circular hysteresis loop, as shown in Fig. 1a in the presence of an axial magnetic field  $H_b$ . Initially, the squareness ratio increases with increasing  $H_b$ , indicating a spiral-type of easy anisotropy. However, with a further increase in  $H_b$ , the loop becomes tilted and is characterised by reduced magnetic susceptibility, as the axial field suppresses the circular magnetisation processes. The voltage pulse is characterised by its harmonic spectrum, which can be easily measured up to the 15th harmonic, as shown in Fig.1b. Furthermore, the harmonic amplitude is sensitive to  $H_b$ , which can also be used to detect magnetic objects, since the symmetry of the excitation field is different from that of any stray fields.

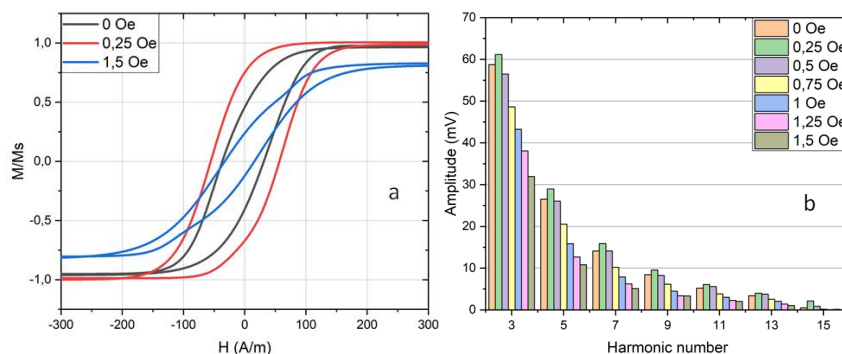


Figure 1. Circular hysteresis loops (a) and harmonic response (b) of a microwire with the composition  $\text{Co}_{66,6}\text{Fe}_{4,28}\text{B}_{11,51}\text{Si}_{14,48}\text{Ni}_{1,44}\text{Mo}_{1,69}$  in the presence of an axial dc field.

The work was supported by RSF grant No 25-72-30009



# Magnetization reversal in Low Curie amorphous microwires for wireless sensors

A. Acuna<sup>a,\*</sup>, L. Panina<sup>a</sup>, N. Yudanov<sup>a</sup>

<sup>a</sup> National University of Science and Technology (MISiS), 119049, Leninsky Avenue 4, Moscow, Russia

\*adrian.acuna1992@gmail.com

Amorphous microwires with a low Curie temperature ( $T_c$ ) are of interest for temperature measurements. With an increase in the temperature, the saturation magnetization  $M_s$  and other magnetic parameters, such as the anisotropy and magnetostriction, decrease near  $T_c$  [1]. The sensing operation of these microwires can be based on the generation of high frequency harmonics of the voltage pulse induced during remagnetization [2]. The present work is devoted to the study of the magnetization reversal process in amorphous microwires of two compositions with a low  $T_c$ .

The amorphous microwires used in the study were prepared by the Taylor–Ulitsky method [3], and had the following compositions:  $\text{Co}_{27.4}\text{Fe}_5\text{B}_{12.26}\text{Si}_{12.26}\text{Ni}_{43.08}$  (sample 1, negative magnetostriction,  $T_c=48^\circ\text{C}$ ) and  $\text{Co}_{64.82}\text{Fe}_{3.9}\text{B}_{10.2}\text{Si}_{12}\text{Cr}_9\text{Mo}_{0.08}$  (sample 2, positive magnetostriction,  $T_c=61^\circ\text{C}$ ). For the second type of microwires, the value of  $T_c$  was decreased to  $57^\circ\text{C}$  by current annealing.

The results show that, sample 1 has an inclined hysteresis loop and sample 2 shows a nearly rectangular loop, which is dictated by the sign of magnetostriction. The form of both hysteresis remains largely unchanged with an increase in temperature up to  $T_c$ . During the process of remagnetization under the influence of a periodic excitation field, a sequence of voltage pulses is produced. Employing lock-in techniques, the harmonic spectrum of these pulses is identified, extending up to the 15th harmonic, as shown in Figure 1(a) for sample 1. The harmonics amplitudes and the area  $S$  under the induced voltage exhibit a pronounced decline as the temperature approaches  $T_c$ . In the case of sample 1, the higher order harmonics have a non-monotonic dependence on  $T_c$ . However, lower-number harmonics monotonically decrease with increasing temperature showing a close proportionality to  $M_s$  and area  $S$  under the voltage pulse (Figure 1(b)). The wires with different Curie temperatures can be used together to enhance the temperature sensitivity and extend the sensitive temperature range. Figure 1(c) compares the amplitude of the 3-d harmonic of sample 1, annealed sample 2 and their pair. It is seen that the temperature-sensitive range was widened to be between  $35^\circ\text{C}$  and  $57^\circ\text{C}$ . The results obtained demonstrate the potential for these microwires to be used as temperature-sensing elements with remote operation.

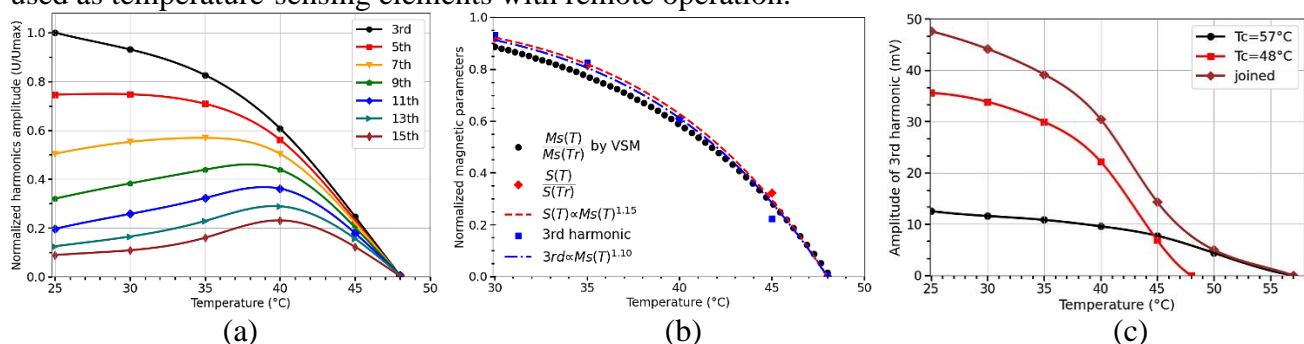


Figure 1: Temperature dependence of magnetic parameters. In (a), harmonics amplitudes for sample 1. In (b), saturation magnetization  $M_s$  (measured by VSM), area ( $S$ ) under the induced voltage and the third harmonic of induced voltage for sample 1. In (c), the 3rd harmonic amplitude for sample 1, annealed sample 2 and their pair.

[1] J. Alam et al., PMM, 124(1), 1–7 (2023)

[2] L. Panina et al., Sen., 19(23), 5089 (2019)

[3] H. Chiriac, MSEA, 304–306(1), 166-171 (2001)



# **On methods of direct measurement of magnetocaloric effect in the temperature range of 4-400 K under AC magnetic fields**

A. Aliev, A. Mukhuchev

Amirkhanov Institute of Physics of Dagestan Federal Research Centre of RAS, 367003, M.Yaragskogo 94,  
Makhachkala, Russia

\*lowtemp@mail.ru

The magnitude of the magnetocaloric effect (isothermal change in entropy  $\Delta S_M$  and/or adiabatic change in temperature  $\Delta T_{ad}$ ) can be estimated by indirect methods, or the  $\Delta T_{ad}$  value can be measured by direct methods. In recent years, methods for measuring  $\Delta T_{ad}$  in alternating magnetic fields using Lock-in detection have been increasingly used. Significant advantages of this method are high temperature sensitivity, the possibility of measuring in weak fields, and the possibility of measuring the MCE in small-sized samples. But such methods also have significant disadvantages and limitations. For example, alternating magnetic fields induce an EMF in a thermocouple, which affects the measured MCE value. If in the area of room temperatures or even in the area of nitrogen temperatures these signals can be dealt with by twisting the thermocouple and extension wires bifilarly, then in the area of helium temperatures this method does not give the desired result, since against the background of decreasing sensitivity of the thermocouple with decreasing temperature, even a small induced EMF can lead to significant changes in the measured signal. In the area of helium temperatures other problems can arise. For example, the use of external alternating magnetic fields can lead to a significant change in the temperature of the entire system (cryostat + sample) due to Foucault currents in the copper screen of the cryogen free helium cryostat. The use of linear actuators for input and output of the temperature insert with the sample can also lead to the impossibility of temperature stabilization. Therefore, it is necessary to look for new methods of periodic action of the magnetic field on the sample.

In this paper, various methods of creating alternating magnetic fields acting on the material under study are considered, including using superconductors. The advantages and disadvantages of each method are discussed. The results of direct measurements of adiabatic temperature changes in materials with different temperatures of magnetic phase transitions, including in the region of helium temperatures, using different methods are presented.

The study was supported by a grant from the Russian Science Foundation (No. 24-12-00362).

## **Composite materials based on polyether ether ketone and natural magnetite**

A. Vindizheva<sup>a,\*</sup>, A. Khashirov<sup>a</sup>, P. Ershov<sup>b</sup>, V. Salnikov<sup>b</sup>, I. Simonov-Yemelyanov<sup>c</sup>,

S. Khashirova<sup>a</sup>

<sup>a</sup> Kabardino-Balkarian State University named after H.M. Berbekov, 360004, Chernyshevskogo 173, Nalchik, Russia

<sup>b</sup> Immanuel Kant Baltic Federal University, 236004, Nevskogo 14, Kaliningrad, Russia

<sup>c</sup> MIREA - Russian University of Technology, 119454, Vernadsky Ave. 78, Moscow, Russia

\* amina.vindizheva@mail.ru

Composite materials attract considerable attention due to their ability to offer innovative solutions with unique characteristics. These include polymer composites with magnetic properties, which represent a promising area of materials science with wide possibilities for various applications. Magnetic polymer materials are widely used in medical practice due to their unique qualities: controllability using a magnetic field, functionalization capabilities and controlled magnetic properties. Particular attention is paid to the study of composite materials based on polyether ether ketone (PEEK) and natural magnetite.

The structure of natural magnetite and its magnetic characteristics are studied. Various methods for obtaining magnetite powders are considered, and their sizes are analyzed. The polymer composition is modified with natural magnetite powder in a volume of 5-25 volume fractions (vol.f.), and the physical-mechanical, magnetic, thermal and thermophysical properties of the obtained composite materials are studied.

The results of the conducted studies demonstrated that the saturation level of magnetization of natural magnetite differs from the empirically established value and is 83.97 emu/g. Composite materials have residual magnetization, which creates the possibility of preserving magnetic properties even after the external magnetic field ceases to act. Using scanning electron microscopy, it was found that magnetite particles are mainly represented by irregularly shaped agglomerates. A technique for producing magnetite powder with a monomodal particle distribution has been developed. A study of the physicomachanical properties of the obtained composite materials based on PEEK and magnetite showed that the addition of magnetite leads to a uniform increase in the elastic modulus and bending strength, while elongation and impact toughness decrease, which is expected for rigid fillers.

Thus, natural magnetite turned out to be an effective modifier for creating polymer composite materials with magnetic properties. In addition, its non-toxicity opens up new possibilities for practical application, in particular, in the field of medicine.

The work was carried out within the framework of the state assignment of the Ministry of Science and Higher Education of the Russian Federation, mnemonic code FZZR-2023-005. Work on measuring and characterizing magnetic hysteresis loops was carried out within the framework of the RSF grant №. 21-72-30032.

# Low-temperature Hall effect in magnetocaloric Ni-Mn-Sb-Al alloys

S. Emelyanova<sup>a,\*</sup>, V. Marchenkov<sup>a,b</sup>

<sup>a</sup> M.N. Mikheev Institute of Metal Physics of the Ural Branch of the Russian Academy of Science, 620108, Kovalevskaya street 18, Ekaterinburg, Russia

<sup>b</sup> Ural Federal University, 620002, Mira street 19, Ekaterinburg, Russia

\*emelyanova@imp.uran.ru

It is well known that Heusler alloys exhibit a number of different effects, for example, they can demonstrate a giant anomalous Hall effect [1]. Despite this, there are currently several works devoted to investigation of the Hall effect in Heusler alloys based on Ni-Mn-Z ( $Z = \text{Ga, In, Sn, Sb}$ ) systems. In [2] such studies were carried out for the  $\text{Ni}_{45.4}\text{Mn}_{40}\text{In}_{14.6}$  alloy, this work is one of the few where the concentration  $n$  and mobility  $\mu$  of charge carriers were determined. In addition, there are similar studies for four-component alloys, for example,  $\text{Ni}_{50}\text{Mn}_{17}\text{Fe}_8\text{Ga}_{25}$  [3] and Ni-Mn-In-B [4]. It should be noted that for  $\text{Ni}_{50}\text{Mn}_{35}\text{Sb}_{15-x}\text{Ge}_x$  ( $x = 0, 1, 3$ ) [5] and  $\text{Ni}_{47-x}\text{Mn}_{41+x}\text{In}_{12}$  ( $x = 0, 1, 2$ ) [6] alloys a relationship between the electronic transport characteristics (which are the coefficients of normal  $R_0$  and anomalous  $R_S$  Hall effect and the concentration of charge carriers  $n$ ) and the phase transition temperatures was found. In this work an attempt to detect a similar relationship in the Ni-Mn-Sb-Al alloys was made.

The  $\text{Ni}_{50}\text{Mn}_{35}\text{Sb}_{15-x}\text{Al}_x$  ( $x = 0, 1, 2, 4$ ) ingots were prepared by arc melting in inert atmosphere and subsequently subjected to annealing at 1100 K for 24 h. The structural analysis was performed at the Collaborative Access Center “Testing Center of Nanotechnology and Advanced Materials” of the Institute of Metal Physics, UB RAS. The chemical composition of all alloys corresponds to the real one with good accuracy. Was demonstrated that at room temperature the alloys are practically single-phase with a predominance of cubic  $L2_1$ -crystal structure.  $M(H)$  dependences were measured in magnetic fields of up to 10 kOe at 4.2 K, dependences of  $M(T)$  were measured in the temperature range from 50 to 330 K. The electrical resistivity and the Hall effect were obtained using the standard four-probe method at direct current. Dependences of  $\rho(T)$  were received in the temperature range from 75 to 375 K, the Hall effect was measured at 4.2 K in magnetic fields of up to 80 kOe.

The temperature dependences of electrical resistivity  $\rho(T)$  and magnetization  $M(T)$  clearly demonstrate the presence of temperature hysteresis, that is, the coexistence region of the austenitic and martensitic phases, which confirm realization of the first-order phase transition in the studied alloys. The phase transition temperatures were determined from this dependences using the method of tangents [7], the obtained values are in good agreement with each other. It has been established that the values of the coefficient of normal  $R_0$  Hall effect for all investigated alloys are negative, therefore, electrons are the main charge carriers. The coefficients of the anomalous  $R_S$  Hall effect turned out to be positive. The relationship between the concentration of charge carriers  $n$  and the phase transition temperatures was established.

The work was carried out within the framework of the state assignment of the Ministry of Science and Higher Education of the Russian Federation for the IMP UB RAS.

- [1] I. Dubenko, A.K. Pathak, S. Stadler et al., Physical Review B 80, 092408 (2009)
- [2] S. Konoplyuk, A. Kolomiets, J. Prokleska et al., Physica Scripta 96, 125833 (2021)
- [3] Z. Zhu, S.W. Or, G. Wu, Applied Physics Letters 95, 032503 (2009)
- [4] M. Blinov, A. Aryal, S. Pandey et al., Physical Review B 101, 094423 (2020)
- [5] V.V. Marchenkov, S.M. Emelyanova, Low Temperature Physics 47, 55 (2021)
- [6] V.V. Marchenkov, S.M. Emelyanova, E.B. Marchenkova, Materials 16(2), 672 (2023)
- [7] N.N. Kuranova, A.V. Pushin, A.N. Uksusnikov et al., Technical Physics 62, 1189 (2017)

# Enhanced Piezoelectric Response of Glycine-loaded Poly(3-hydroxybutyrate) Scaffolds for Nerve Tissue Engineering

L. Shlapakova, M. Surmeneva, R. Surmenev\*

National Research Tomsk Polytechnic University, 634050, Lenina 30, Tomsk, Russia

\*rsurmenev@mail.ru

Nerve injury poses a threat to the mobility and sensitivity of a nerve, leading to permanent function loss due to the low regenerative capacity of mature neurons. To date, the most widely clinically applied approach to bridging nerve injuries is autologous nerve grafting, which faces challenges such as donor site morbidity, donor shortages, and the necessity of a second surgery [1]. An effective therapeutic strategy is urgently needed worldwide to overcome the current limitations. Piezopolymers allow to generate exogenous electric potentials close to that of endogenous ones, inherent to the nervous tissues, to promote tissue regeneration [2]. Poly(3-hydroxybutyrate) (PHB) has gained particular attention due to its natural origin, exceptional biocompatibility, slow biodegradability, and mechanical stability; however, the inherent piezoelectric response of PHB is weak, and there is a need to improve it while preserving the scaffold's biocompatibility. Electrospinning is an ideal fabrication technique for nanofibrous nerve–tissue-mimetic scaffolds or conduits of tailorable strength, elasticity, crystalline structure, and piezoresponse. Herein, we have managed to increase the piezoresponse of electrospun nanofibrous PHB scaffolds by incorporation of homogeneously distributed crystals of piezoactive  $\beta$ -glycine (Gly). We have successfully optimized the electrospinning parameters to prepare composite PHB fibers with varied Gly content of 5, 15, 20, and 30 wt%. Gly incorporation creates nanoporous textured surface of the polymer fibers, which allows to improve surface wettability and free surface energy of the originally hydrophobic PHB scaffolds. X-ray diffraction and Raman spectroscopy revealed that electrospinning of PHB-Gly solutions produces the electroactive  $\beta$ -phase of Gly due to the practically instant solvent evaporation resulting in the  $\beta$ -Gly crystals that are “sealed” in a polymeric matrix preventing them from transformation in more stable phases. In addition, Gly crystals act as nucleators for PHB crystallization, diminishing the polymer crystallite size and increasing its crystallinity degree from 40% for pure PHB to 46% for PHB-Gly-30. DFT calculations revealed that the interaction of Gly molecule with PHB surfaces occurs predominantly through hydrogen bonding. Hydrophilicity and free surface energy of PHB-Gly scaffolds dramatically increased compared to those of the pristine PHB one due to the hydrophilic amino- and hydroxyl groups of Gly adsorbed on the PHB surface via hydrogen bonding as well as the capillary effect of the nanopores on the composite fibers' surface.

By applying a novel in-point approach to piezoelectric force microscopy, we have obtained distributions of piezoelectric response along the fibers, uncovering a considerable increase in the average piezoresponse for PHB scaffolds with 30 wt% Gly (from 0.1 to 2.4 pm/V) due to (i) the presence of piezoelectric  $\beta$ -Gly phase and (ii) the higher PHB crystallinity.

The findings of this study open novel fundamental insights into straightforward one-step engineering of numerous material properties, including morphology, wetting behavior, and piezoelectric response, and each of them can tremendously affect cell activities *in vitro* and tissue growth *in vivo*. The synergistic benefits of Gly-loaded scaffolds make them a promising candidate as a highly biocompatible, biodegradable, and electroactive material that can be reformed into an effective nerve guidance conduit.

The work is supported by the Russian Science Foundation (№ 25-13-20058) and TPU development program Priority 2030.

[1] Y. Yan, *Bioact. Mater.* 11, 57–76 (2022)

[2] Y. Ma, *CEJ.* 452, 139424 (2023)

## Structure and magnetic properties of FeRh microflakes

D. Kanurin<sup>a,b\*</sup>, A. Amirov<sup>a</sup>, A. Komlev<sup>a,b</sup>, N. Tabachkova<sup>a</sup>, A. Turutin<sup>a</sup>, Yu. Parkhomenko<sup>a</sup>,  
A. Tishin<sup>b</sup>

<sup>a</sup> National University of Science and Technology MISIS, 119049, Leninskiy Prospekt 4, Moscow, Russia

<sup>b</sup> Lomonosov Moscow State University, 119991, Leninskie gory 1, Moscow, Russia

\*kanurin.da18@physics.msu.ru

FeRh-based alloys have recently attracted attention as promising functional magnetic materials for biomedical applications due to their unique magnetic properties, *giant* magnetocaloric effect, and low cytotoxicity at physiological temperatures [1,2]. The main challenges in the development of FeRh alloys for biomedical use are related to the fabrication of micro(nano)-sized materials with an ordered CsCl-type structure.

Magnetic FeRh particles in the form of microflakes were fabricated using a mechanical method from a bulk FeRh alloy sample ordered in the CsCl-type (B2) structure. For this purpose, an Fe<sub>50</sub>Rh<sub>50</sub> alloy was synthesized by arc melting in a helium atmosphere (0.013 Pa) from high-purity rhodium (Rh, 99.9%) and iron (Fe, 99.98%) powders. The microflakes were produced by mechanical filing followed by heat treatment. SEM analysis revealed that the resulting particles had flake-like shapes with sizes ranging from 100 to 400 μm. XRD analysis of the FeRh microflakes indicated a predominant ordered B2 phase, corresponding to a body-centered cubic (bcc) crystal structure, with traces of an iron-containing impurity phase formed during the filing process.

Magnetization measurements as a function of temperature in the 100–800 K range showed two magnetic phase transitions: the first from an antiferromagnetic (AFM) to a ferromagnetic (FM) state between 200 and 400 K, and the second from the FM to a paramagnetic (PM) state at approximately 670 K.

The broad character of the AFM–FM transition is attributed to the mechanical treatment of the Fe<sub>50</sub>Rh<sub>50</sub> microflakes during fabrication, which affects the magnetic properties and leads to a gradual change in magnetization.

The Fe<sub>50</sub>Rh<sub>50</sub> microflakes partially retain the properties of the initial bulk material. The parameters of the AFM–FM transition can be tuned by varying the heat treatment protocol, including annealing temperature and cooling rate.

This work was supported by the Russian Science Foundation (project no. 24-19-00782, <https://rscf.ru/en/project/24-19-00782/>).

[1] A. M. Tishin. Magnetic Materials and Technologies for Medical Applications. Woodhead Publishing (2022)

[2] A. Amirov et.al. ACS Appl. Eng. Mater. 3(2), 410 (2025)

# Shape memory effect in 3D-printed biocompatible composite poly(lactic acid)-based scaffolds for bone tissue engineering

A. Fetisova<sup>\*</sup>, A. Firoz, V. Rybakov, L. Shlapakova, Y. Mukhortova, M. Surmeneva, R. Surmenev

National Research Tomsk Polytechnic University, 634050, Lenina Avenue 30, Tomsk, Russia

<sup>\*</sup>zerospace25@gmail.com

Critical-sized bone defects resulting from trauma, tumors, or infection remain a major clinical challenge. Although autologous bone grafts are the current gold standard, their limitations, including donor site morbidity and limited availability, have driven the search for alternatives. Shape-memory scaffolds, particularly those responsive to external stimuli such as magnetic fields, offer exciting prospects for minimally invasive implantation and spatially guided tissue regeneration.

The aim of this work was to fabricate PLA/Fe<sub>3</sub>O<sub>4</sub> composite scaffolds with a triply periodic minimal surface gyroid structure at various infill densities (100%, 70%, 50%, and 30%), and to investigate the effect of magnetite incorporation on their structural and mechanical properties. In this study, biodegradable and magnetically responsive scaffolds were successfully developed using fused deposition modeling. Polylactic acid (PLA) was blended with citric acid-coated magnetite nanoparticles (Fe<sub>3</sub>O<sub>4</sub> NPs), and scaffolds were 3D-printed with controlled infill densities. The gyroid structure was chosen due to its optimal combination of mechanical stability and porosity, while the addition of Fe<sub>3</sub>O<sub>4</sub> nanoparticles was intended to enhance both stiffness and magnetic functionality.

Scaffolds composition and structure were characterized using XRD, Raman spectroscopy, SEM and EDS. Thermal behavior and filler effects were assessed using DSC. Mechanical properties (Young's modulus, compression, and tensile strength) were evaluated through tensile-strength and compressive tests. Shape memory performance was quantified through shape fixity ( $R_f$ ) and recovery ratio ( $R_r$ ) obtained via bending tests in a hot water bath at 80 °C. Cytocompatibility was assessed via MTT assays using NIH/3T3 fibroblasts.

XRD revealed enhanced crystallinity in PLA/Fe<sub>3</sub>O<sub>4</sub> composites compared to pure PLA. DSC indicated crystallinity values of 4.7% for pure PLA and 5.6% for PLA/Fe<sub>3</sub>O<sub>4</sub>. Raman spectroscopy confirmed molecular interactions between Fe<sub>3</sub>O<sub>4</sub> NPs and the PLA matrix, including reactions between ester groups of PLA and metallic cations of Fe<sub>3</sub>O<sub>4</sub>, as well as hydrogen bonding between PLA ester groups and carboxyl groups of the citric acid coating.

Mechanical testing showed that Fe<sub>3</sub>O<sub>4</sub> incorporation increased Young's modulus by ~23% (from  $3.15 \pm 0.22$  to  $3.88 \pm 0.32$  GPa) in 100% infill scaffolds and by ~39% (from  $1.64 \pm 0.05$  to  $2.27 \pm 0.44$  GPa) in 70% infill scaffolds. Compressive strength ranged from 10.17 MPa (30% infill) to 64.09 MPa (100% infill). The 50% infill PLA/Fe<sub>3</sub>O<sub>4</sub> scaffold exhibited optimal tensile strength (16.02 MPa), aligning with the mechanical properties of human cancellous bone.

All scaffolds showed excellent shape fixity ( $R_f > 99\%$ ) and good recovery ( $R_r > 74\%$ ), with the highest recovery (85%) observed in 30% infill PLA/Fe<sub>3</sub>O<sub>4</sub>. Enhanced recovery in lower-density scaffolds is attributed to increased chain mobility and structural flexibility, further accelerated by Fe<sub>3</sub>O<sub>4</sub> induced physical crosslinking.

MTT assays confirmed the non-cytotoxicity of both PLA and PLA/Fe<sub>3</sub>O<sub>4</sub> scaffolds after 72 h.

In summary, the 3D-printed PLA/Fe<sub>3</sub>O<sub>4</sub> scaffolds demonstrate tunable mechanical properties, magnetic responsiveness, and efficient shape recovery, establishing them as a promising minimally invasive platform for bone tissue engineering.

*This research was supported by the Russian Science Foundation (№ 25-13-20055) and TPU development program Priority 2030.*

[1] A.b. Firoz, Adv Compos Hybrid Mater 8, 95 (2025)

# Magnetoelectric effect in the region of torsional and longitudinal-shear modes in the structure of lithium niobate / AMAG

I. Markov\*, O. Sokolov, M. Bichurin

Polytechnic Institute, Yaroslav-the-Wise Novgorod State University, 173003,

Bolshaya Sankt-Peterburgskaya 41, Veliky Novgorod, Russia

\*ivanmarckov02@mail.ru

In recent years, much attention has been paid in periodicals to studies of the magnetoelectric (ME) effect in composites in connection with the prospect of its practical application [1]. The ME effect is mainly studied in experiments in the region of one of the electromechanical resonance (EMR) modes, since in this case the effect increases by 1-2 orders of magnitude [2]. Of particular interest is the magnetoacoustic resonance (MAR) mode, when one of the EMR modes and the ferromagnetic resonance in the ME structure coincide. In this case, the theory predicts a further increase in the ME effect [2]. In this report, the authors present the results of a study of the ME effect in the region of torsional and longitudinal-shear modes in the structure of monomorph lithium niobate / AMAG and in the region of torsional modes in the structure of bimorph lithium niobate/AMAG, performed with a view to their identification and possible further application in the MAR mode. In [3], it was found that a longitudinal-shear mode and a torsional mode occur in an asymmetric Metglas / GaAs composite, and the magnitude of the stress coefficient in the longitudinal-shear mode is an order of magnitude greater than in the torsional mode, so the resonant value of the ME coefficient in the torsional mode is difficult to determine experimentally. To exclude the longitudinal-shear mode, it was proposed to use a bimorph LN Zyl + 45°, in which two layers of the same thickness are polarized in opposite directions along the thickness, and in this case, only the ME effect from the torsional mode can be observed in the experiment. Two ME structures were made for the experiment. The first is the symmetrical structure of AMAG-225 / monomorph LN Zyl + 45° / AMAG-225, the second is the asymmetrical structure of AMAG-225 / bimorph LN Zyl + 45°. The ME effect was measured on a stand where an alternating magnetic field was directed along the length of the ME composite, and a constant one along its width. As a result, the desired electrical signal was removed from the LN Zyl + 45° plates. The results of [4] were used as the basis for the theoretical calculation of the ME voltage coefficient. The experimental frequencies of the longitudinal-shear and torsional modes were 359 and 458 kHz, and the theoretical frequencies were 362 and 456 kHz, respectively. The maximum of the experimental ME voltage coefficients were 496 and 30.4 V/A, and the theoretical ones were 530 and 30.9 V/A, respectively. In the end, the results of theory and experiment showed a good match.

*The research was carried out at the expense of a grant from the Russian Science Foundation No. 24-15-20044, <https://rscf.ru/project/24-15-20044/>.*

- [1] M. I. Bichurin, V. M. Petrov, R. V. Petrov, A. S. Tatarenko. Magnetoelectric Composites, Pan Stanford Publishing Pte. Ltd. Singapore, 280 (2019)
- [2] M. I. Bichurin, V. M. Petrov, O. V. Ryabkov, S. V. Averkin, G. Srinivasan, Phys. Rev. B.72, 060408 (2005)
- [3] S. V. Ivanov, O. V. Sokolov, M. I. Bichurin, M. A. Zakharov, R. V. Petrov. Vestnik of NovSU, 5(134), 743 (2023)
- [4] M. I. Bichurin, O. V. Sokolov, S. V. Ivanov, V. S. Leontiev, D. A. Petrov, G. A. Semenov, V. N. Lobekin. Sensors, 22(13), 4818 (2022)

# **Nanocomposite sensitive element in the industrial internet of things**

S. Voronina<sup>\*</sup>, E. Tomberg

Reshetnev Siberian State University of Science and Technology, 660037, Krasnoyarsky Rabochy Ave 31,  
Krasnoyarsk, Russian Federation

<sup>\*</sup>simkina\_svetlana@mail.ru

The Industrial Internet of Things (IIoT) is a complex system of networks and industrial equipment supplemented with specialized software and embedded sensors. The sensor elements of such devices can be fabricated using polymer-based nanomaterials and employed in structural health monitoring systems. These systems are part of the IIoT and are designed to collect data on deformations and stresses occurring within structures. The development of strain-sensitive elements based on polymer nanocomposites represents one of the current directions in modern sensor technology and materials science. This work investigates the structure of a conductive element formed on the basis of epoxy resin reinforced with carbon nanostructures. The use several type carbon nanomaterials provides a pronounced synergistic effect, contributing to a significant increase in the electrical conductivity and sensitivity of the composite to mechanical deformations, even at low filler concentrations.

At Reshetnev Siberian State University of Science and Technology, an advanced pre-failure condition monitoring system was developed, based on a sensor element made from a polymer-based nanocomposite material. Data obtained from the sensor element are processed by a digital system that analyzes multiple indicators characterizing the level of deformation. In the event of detecting a hazardous deformation, the system automatically transmits the data via a GSM channel, enabling operators to take preventive measures against emergency situations. The sensor element samples consist of composite materials based on epoxy resin modified with carbon nanostructures.

The sensitive effect was identified by measuring changes in the electrical resistance of the polymer composite material under mechanical tensile strain. A digital multimeter was used to quantitatively assess the variations in resistance of the samples during deformation.

Future research prospects include optimizing the composition of nanofillers, improving dispersion techniques, and comprehensively studying the influence of external factors such as temperature, humidity, and mechanical loads on the functional characteristics of the strain-sensitive elements. These studies will not only enhance existing technologies but also expand the application scope of strain-sensitive materials. The use of hybrid nanofillers in various polymer matrices opens new opportunities for the development of innovative electronic devices, including flexible electronics. Given these properties, such composites can be effectively employed as electrode materials in batteries and capacitors, as well as in conductive films and sensor systems, providing high sensitivity and operational reliability.



# **Influence of small lanthanum additions on the structural and electromagnetic properties of lithium ferrite**

Yu. Elkina\*, E. Lysenko, V. Vlasov

Tomsk Polytechnic University, 30, Lenin Avenue, Tomsk 634050, Russia

\*ysm7@tpu.ru

Lithium ferrites ( $\text{LiFe}_5\text{O}_8$ ) have unique electromagnetic properties and are used in microwave devices, lithium-ion batteries and gas sensors[1]. However, despite the high values of saturation magnetization and Curie temperature, the use of unsubstituted lithium ferrite in a number of industrial areas is limited by its electrophysical characteristics. In this regard, a relevant area is the modification of lithium ferrites with small additives of various ions, including rare earth elements[2], such as lanthanum.

This paper studies the structural and magnetic properties of lithium ferrite modified with lanthanum hydroxide. These samples were obtained by solid-phase synthesis of  $\text{Fe}_2\text{O}_3/\text{Li}_2\text{CO}_3/\text{La}(\text{OH})_3$  chemical reagents in a certain weight ratio (1.5-14 mass%  $\text{La}(\text{OH})_3$ ) at a temperature of 900 °C for 240 minutes, and then sintered in a laboratory furnace at 1150 °C [3].

The aim of this work is to study the effect of different lanthanum concentrations on the structural, electrical and magnetic characteristics of lithium ferrite. Particular attention is paid to finding the optimal lanthanum content to maximize electrical resistance with minimal loss of magnetic properties.

XRD showed that the introduction of lanthanum leads to the formation of a two-phase structure: the spinel phase  $\text{LiFe}_5\text{O}_8$  and the perovskite-like phase  $\text{LaFeO}_3$ . Lanthanum is not incorporated into the ferrite crystal lattice, but is completely consumed to form  $\text{LaFeO}_3$ . Lanthanum additives reduce grain size and increase porosity. Small lanthanum additives significantly increase specific electrical resistance without reducing saturation magnetization. Thermogravimetric and differential scanning calorimetric studies have shown that the introduction of lanthanum significantly affects the Curie temperature during high-temperature sintering of lithium ferrite. Based on the data obtained, it can be concluded that the introduction of small lanthanum additives opens up new possibilities for the use of lithium ferrites modified with lanthanum in modern electronics.

This research was supported by TPU development program Priority 2030.

[1] M. Mahmoudi, M. Kavanlouei, H. Maleki-Ghaleh, Powder Metall. Met. Ceram. 54, 31 (2015)

[2] E. N. Lysenko, V. A. Vlasov, et al., J. Therm. Anal. Calorim. 148, 1445 (2023)

[3] Yu. S. Elkina et al., Fine Chem. Technol. 20, 156 (2025)

# Double step magnetization reversal in 2D magnetoplasmonic crystals based on permalloy

Ch. Gritsenko<sup>\*</sup>, Z. Grigoreva, V. Belyaev, V. Rodionova

Immanuel Kant Baltic Federal University, 236004, Nevskogo 14, Kaliningrad, Russia

<sup>\*</sup>KByrka@kantiana.ru

Currently, one of the important request in the field of magnetic sensorics is to continue research in increasing a sensor sensitivity, miniaturization and integration into devices, eliminating interference and filtering signals, increasing stability and durability, three-dimensional mapping of magnetic fields, as well as increasing accuracy in changing environmental conditions [1]. The solution to these problems can positively affect of magnetic field sensors in such areas as biomedical detection, electromagnetic pollution control, electromagnetic compatibility measurement and equipment fault diagnostics [2, 3]. Conducting studies of magnetic properties of thin films, such as the micromagnetic structure, stray fields distribution, as well as the behavior of magnetization in an external magnetic field allows us to obtain information about magnetic anisotropy and magnetic interactions in the sample. This is important when developing sensor elements and tuning their functional properties.

In this work, samples of two-dimensional magnetoplasmonic crystals based on  $\text{Ni}_{80}\text{Fe}_{20}$  were studied using magneto-optical method of the Kerr magnetometry. The relief elements height of the diffraction grating was  $85 \pm 10$  nm. The lateral dimensions of the lattice elements varied depending on the change in the exposure dose of the electron resist from  $200 \mu\text{C}/\text{cm}^2$  to  $600 \mu\text{C}/\text{cm}^2$  used in the electron beam lithography during sample preparation.

As a result, double step magnetic hysteresis behavior was observed for the samples depending on the exposure dose. Increasing the dose led to the magnetization reversal steps occurring, meaning various reversal phases arising, which can be used for further functionalization in an application.

[1] Qiu, Yulin, et al. "Integrated sensors for soft medical robotics." *Small* 20.22 (2024): 2308805

[2] Origlia, Cristina, et al. "Review of microwave near-field sensing and imaging devices in medical applications." *Sensors* 24.14 (2024): 4515

[3] Ma, Yufei, et al. "A Survey on Magnetic Sensing and Communication: Technologies, Sensors, and Applications." *IEEE Communications Surveys & Tutorials* (2025)

# The Interplay of Magnetic Anisotropy and Interactions in Magnetic Nanoparticle Assemblies

A. Omelyanchik<sup>a,b,\*</sup>, D. Peddis<sup>a,b</sup>

<sup>a</sup> Department of Chemistry and Industrial Chemistry & INSTM ru, University of Genova, nM2-Lab,  
Via Dodecaneso 31, 16146, Genova, Italy

<sup>b</sup> Institute of Structure of Matter, National Research Council, nM2-Lab,  
Via Salaria km 29.300, Monterotondo Scalo, 00015, Roma, Italy

\* Aleksander.Omelyanchik@ext.unige.it

Nanoparticles are intricate and unique physical entities whose properties markedly differ from their bulk counterparts. In addition, the collective magnetic behaviour of a nanoparticle ensemble is driven by interparticle interactions, which can be either dipole–dipole interactions or exchange coupling between surface atoms. The complex interplay of individual and collective properties drives the magnetic behavior of nanoparticle assemblies, leading to complex "supermagnetic" regimes and others [1-3].

This talk delves into the intricate relationship between magnetic anisotropy and interparticle interactions in nanoparticle ensembles, particularly focusing, as a model system, on spinel ferrite nanoparticles of different sizes and compositions, including core/shell structures. As a first example, we examined the chemical engineering of cationic distribution in  $\text{CoFe}_2\text{O}_4$  nanoparticles substituted with  $\text{Zn}^{2+}$  and  $\text{Ni}^{2+}$  [4]. Further, we synthesized bi-magnetic core/shell nanoparticles comprising hard  $\text{CoFe}_2\text{O}_4$  cores with soft nickel ferrite ( $\text{NiFe}_2\text{O}_4$ ) shells, and vice versa [5].  $\text{NiFe}_2\text{O}_4$  was selected as the soft material for its superior chemical stability and relatively invariant inversion degree with particle size, making it an ideal model system to reduce degrees of freedom in the study. Strong exchange coupling at the core/shell interface was confirmed, demonstrating the potential to modulate magnetic anisotropy through nano-architecture design.

These studies advance our understanding of how structural and compositional modifications at the nanoscale can precisely control the magnetic properties of nanoparticles, opening new avenues for applications in biomedicine and data storage. However, in our view, a lot of open questions still exist in this direction:

1. What are the mechanisms by which interparticle interactions are influenced by intraparticle magnetic interaction and vice versa?
2. How do different types of interparticle interactions, such as dipolar interactions or exchange interactions, contribute to the overall magnetic behavior of nanoparticle assemblies?
3. How does the architecture of core/shell nanoparticles, including the selection of materials for the core and shell, the size of both layers, the molecular coating, and the shape and other features affect their macroscopic magnetic properties?
4. How can the understanding of the interplay between magnetic anisotropy and interparticle interactions in nanoparticle assemblies be applied to the design of new materials with tailored magnetic properties?

[1] García-Acevedo, P. et al. *Adv. Sci.* 10, 1–15 (2023).

[2] López-Ortega, A. et al. *Nanoscale* 4, 5138 (2012).

[3] Muzzi, B. et al. *ACS Appl. Nano Mater.* 5, 14871–14881 (2022).

[4] Baričić, M. et al. *Phys. Chem. Chem. Phys.* 26, 6325–6334 (2024).

[5] Omelyanchik, A. et al. *Nanoscale Adv.* 3, 6912–6924 (2021).

## **(In,Mn)As quantum dot p-i-n structures**

A. Bouravleuv<sup>a-c,\*</sup>

<sup>a</sup> Ioffe Institute, Ioffe Institute, 194021, Polytechnicheskaya 26, St.Petersburg, Russia

<sup>b</sup> Saint-Petersburg Electrotechnical University “LETI”, 197022, Popova 5, St.Petersburg, Russia

<sup>c</sup> Institute for Analytical Instrumentation, 198095, Ivana Chernykh 31-33, St.Petersburg, Russia

\* alxsb@mail.ru

Nanoscale ferromagnetic semiconductor (FS) structures, e.g.  $A_3B_5$  semiconductor compounds doped with Mn, are one of the most promising candidates for controlling spin interactions using various techniques, such as electrical and optical methods. Their implementation could lead to the development of novel spin-based devices, including spin light-emitting diodes (spin-LEDs).

Typically,  $(A_3,Mn)B_5$  FS layers are grown at relatively low temperatures in order to avoid phase separations. It results in formation of various structural defects. We have elaborated the novel technique for the growth of (In,Mn)As quantum dots at relatively high temperatures [1-2]. It based on the Mn-atom selective doping of central parts of InAs quantum dots by molecular beam epitaxy. The detailed investigation of the structures obtained demonstrates that, despite relatively high growth temperature, the (In,Mn)As quantum dot structures have a high crystalline quality.

Such (In,Mn)As quantum dots were used as an active layers for the creation of p-i-n diode structures. Their optoelectronic properties were investigated using both optical and electric pumping techniques.

[1] Appl. Phys. Lett., 105 232101(2014)

[2] Nanotechnology, 27 425706(2016)

## Influence of annealing on the microstructure and magnetic properties of Mn-substituted cobalt ferrite nanoparticles

V. Salnikov<sup>a,\*</sup>, G. Petrovskaya<sup>b</sup>, A. Novakova<sup>b</sup>, S. Panfilov<sup>b</sup>, A. Omelyanchik<sup>a</sup>, V. Rodionova<sup>a</sup>

<sup>a</sup> Immanuel Kant Baltic Federal University, 236004, Nevskogo 14, Kaliningrad, Russia

<sup>b</sup> Faculty of Physics, Lomonosov Moscow State University, 119991, Leninskie gory 1, Moscow, Russia

\*vdmsalnikov2@kantiana.ru

Nanostructures are a crucial component of modern technologies, with applications spanning from data storage to biomedicine. Magnetic nanoparticles based on spinel ferrites attract particular attention due to the diversity of their physical and chemical properties [1]. Among them, ferrites of the composition  $\text{Mn}_x\text{Co}_{1-x}\text{Fe}_2\text{O}_4$  stand out because of the similarity of ionic radii and electronic structures of the constituent metal atoms. Compared to cobalt and iron, manganese possesses a higher magnetic moment, and substituting cobalt with manganese could significantly enhance the magnetic properties of ferrites in this system. One promising application for such nanoferrites is the development of cost-effective permanent magnets to fill the gap between conventional ferrite magnets and rare-earth-based magnets such as NdFeB [2,3].

In this study,  $\text{Mn}_x\text{Co}_{1-x}\text{Fe}_2\text{O}_4$  nanoparticles were synthesized using the sol–gel method, self-combustion reaction with heating up to 350 °C. After cooling, the samples were annealed in the temperature range from 500 to 700 °C. The manganese concentration was varied within the range  $x = 0.15\text{--}0.35$ .

The resulting materials were characterized using magnetic measurements, X-ray diffraction (XRD), and Mössbauer spectroscopy. It was found that manganese incorporation alters the distribution of metal cations among the spinel sublattices, leading to a non-monotonic change in magnetic properties. Additionally, an increase in manganese concentration, combined with annealing at temperatures up to 600 °C, promotes the segregation of hematite from the ferrite structure. This segregation results in a decrease in the saturation magnetization of the ferrite nanoparticles.

- [1] Silva, F. G. da *et al.* Structural and Magnetic Properties of Spinel Ferrite Nanoparticles. *J. Nanosci. Nanotechnol.* **19**, 4888–4902 (2019)
- [2] López-Ortega, A., Lottini, E., Fernández, C. D. J. & Sangregorio, C. Exploring the Magnetic Properties of Cobalt-Ferrite Nanoparticles for the Development of a Rare-Earth-Free Permanent Magnet. *Chem. Mater.* **27**, 4048–4056 (2015)
- [3] Quesada, A. *et al.* Energy Product Enhancement in Imperfectly Exchange-Coupled Nanocomposite Magnets. *Adv. Electron. Mater.* **2**, 1500365 (2016)

# Weyl semimetal and axion insulator phases in $\text{MnBi}_2\text{Te}_4$ -based systems

A. Eryzhenkov<sup>\*</sup>, A. Tarasov, A. Shikin

Saint Petersburg State University, 199034, Universitetskaya emb. 7–9, Saint Petersburg, Russia

<sup>\*</sup>st037623@student.spbu.ru

Antiferromagnetic topological insulators (AFM TI) of the  $\text{MnBi}_2\text{Te}_4$  family represent well-known universal platform for either quantum anomalous Hall effect (QAHE) observation or investigating exotic quantum phases such as axion insulators [1] and magnetic Weyl semimetals (WSM) [2]. Depending on various effective parameters such as exchange field strength or spin-orbit coupling (SOC) strength, these systems may exhibit topological phase transitions (TPTs) between a variety of topological phases.

When these systems are brought close to TPT points, they may display exotic behavior potentially detectable by experimental means, for example, the topological magnetoelectric effect (TME). However, the case of magnetic WSM is particularly interesting since WSM phase is characterized by certain bulk behavior which is reflected mainly by the enhanced QAHE where the anomalous Hall conductance is directly proportional to the Weyl point separation in the reciprocal space. The WSM phase is not trivially destructible since it bears topological protection and Weyl nodes with opposite chirality must be brought together to annihilate in order to destroy the WSM phase. Any generic external perturbations cause only produce a shift of Weyl nodes, hence the larger the Weyl point separation, the more robust and pronounced the WSM phase is.

In this work a variety of TPTs was studied using combined approach including the density functional theory (DFT) as well as experimental methods such as angle-resolved photoemission spectroscopy (ARPES).

It was found [2] by DFT and confirmed by ARPES that  $\text{Mn}_{1-x}\text{Ge}_x\text{Bi}_2\text{Te}_4$  experiences a TPT for approximately half substitution ( $x \approx 50\%$ ). It is important that this system has a lower spin-flop threshold for greater Ge concentrations which allows a more realizable transition into the ferromagnetic (FM) phase which admits the WSM phase on its topological phase diagram which is rather robust under perturbations modeled in our DFT calculations using SOC strength variation, magnetic moment variation or uniaxial  $c$ -strain applied to the system [3].

A specific type of Mn/Ge substituted system  $\text{Mn}_{0.625}\text{Ge}_{0.375}\text{Bi}_2\text{Te}_4$  was presented in [3] and compared to its  $\text{Fe}_{0.625}\text{Ge}_{0.375}\text{Bi}_2\text{Te}_4$  counterpart to find that ferrimagnetic (FIM) ordering which ensues due to Mn/Ge and Fe/Ge substitutions leads to WSM phase such that obtaining complete FM remagnetization of Mn (Fe) layers is not needed; moreover, Fe-based WSM phase appears to be more robust from the Weyl point separation standpoint.

A more real case of approaching TPTs that are often modeled by SOC variation is given in [1] by an example of  $\text{MnBi}_2\text{Te}_2\text{Se}_2$  system where Te/Se substitution makes the effective SOC strength lower. This system may be used as a platform to implement axion insulator phases and observe corresponding physical phenomena.

The obtained results are valuable for both fundamental physics and material study, aiding understanding of TPTs into various topological phases and potential ways of their implementation and usage in real materials for spintronic devices.

This work was supported by the Russian Science Foundation grant No. 23-12-00016.

[1] A.M. Shikin, A.V. Eryzhenkov, A.V. Tarasov et al. Sci Rep 13 (2023), 16343

[2] A.M. Shikin, A.V. Eryzhenkov, A.V. Tarasov et al. Sci Rep 15 (2025), 1741

[3] A.M. Shikin, A.V. Eryzhenkov, A.V. Tarasov et al. (to be published)

## Radiation Effects on Magnet Properties of Ferrites

E. Shipkova<sup>a,\*</sup>, N. Perov<sup>a</sup>, R. Makarin<sup>a</sup>, A. Punda<sup>b</sup>, V. Zhivulin<sup>b</sup>, D. Vinnik<sup>b,c,d</sup>, M. Salakhitdinova<sup>e</sup>,

E. Ibragimova<sup>f</sup>, A. Granovsky<sup>a,e,g</sup>

<sup>a</sup> Lomonosov Moscow State University, 119991, Leninskie gory 1, Moscow, Russia

<sup>b</sup> South Ural State University (National Research University), 454080, Lenin pr. 76, Chelyabinsk, Russia

<sup>c</sup> Moscow Institute of Physics and Technology (National Research University), 117303, Institutsky 9,  
Dolgoprudny, Russia

<sup>d</sup> Saint Petersburg State University, 199034, Universitetskaya naberezhnaya 7/9, Saint Petersburg, Russia

<sup>e</sup> Samarkand State University, 140104, University blv. 15, Samarkand, Uzbekistan

<sup>f</sup> Institute of Nuclear Physics of the Academy of Sciences, 100214, Huroson 1, Tashkent, Uzbekistan

<sup>g</sup> Institute of Theoretical and Applied Electrodynamics of the Russian Academy of Sciences, 125412,  
Izhorskaya 13, Moscow, Russia

\*Shipkova\_liza@mail.ru

Ferrites are widely demanded in industry class of materials [1]. They are used in many modern products – microwave electronics devices, transformers and antennas, magnetic field shielding devices, satellites, information storage and recording devices, etc. Particular interest is the study of changes in the magnetic properties of ferrites under non-standard conditions – under the exposure of radiation [2]. The implementation of the correct operation of spacecraft, stations, satellites equipped with complex and sensitive equipment requires a detailed study of the effect of radiation on the magnetic properties of ferrite materials.

The solid-phase synthesis method was used to obtain molded ceramics from which 14 pieces of BaFe<sub>12</sub>O<sub>19</sub> and SrFe<sub>12</sub>O<sub>19</sub> hexaferrite plates were manufactured. The samples were irradiated with gamma rays from a <sup>60</sup>Co radioactive source at a temperature of 323 K with a total irradiation dose of 0.8 to 17 MR at a dose rate of 84 R/s. Magnetic properties of the samples were measured on a VSM LakeShore 7407 series magnetometer at T = 300 K in a field of up to 16 kOe.

According to the results of X-ray structural analysis of the initial samples, the number and position of reflections on the diffraction pattern correspond to the structure of hexaferrites BaFe<sub>12</sub>O<sub>19</sub> and SrFe<sub>12</sub>O<sub>19</sub>. In the irradiated samples, the appearance of defects and the formation of secondary phases were observed, which indicates a change in its structure.

The results of magnetic measurements for the samples are the values of saturation magnetization (M<sub>s</sub>), residual magnetization (M<sub>r</sub>) and coercivity (H<sub>c</sub>). For samples of both compositions, the dependence of M<sub>s</sub> on the dose (time) of irradiation is non-monotonic. This nature of the dependences can be associated with the displacement of atoms from their original positions, namely Fe<sup>3+</sup> and Ba<sup>2+</sup>/Sr<sup>2+</sup> ions under irradiation and, as a consequence, a change in intralattice and interlattice exchange interactions. Since the superexchange interaction Fe<sup>3+</sup> – O<sup>2-</sup> – Fe<sup>3+</sup> is dominant, it can be assumed that the type of dependence of M<sub>s</sub> on the dose is determined by its weakening/strengthening. The type of H<sub>c</sub> on the dose (time) of irradiation also does not have a uniform dependence for the two sample compositions. Since its nature is largely determined by the magnitude of magnetic anisotropy, it can be assumed that the change in H<sub>c</sub> during irradiation is a consequence of its modification.

E.D. Shipkova is a scholarship holder of the Foundation for the Development of Theoretical Physics and Mathematics "BASIS" (grant # 24-2-2-15-1).

[1] Vinnik D. A. et al. JMMM. – 2024. – V. 605. – P. 172344

[2] Assar S. T., et al. JMMM. – 2017. – V. 421. – P. 355-367

# Influence of temperature on optical properties of magnetic fluid with aggregates of nanoparticles

V. Vivchar\*, C. Yerin

North-Caucasus Federal University, Stavropol, 355017 Russia

\*vicklyh74@gmail.com

Experiments and numerous computer simulations have shown a significant effect of particle aggregates on the physical properties of magnetic fluids. Aggregates of nanoparticles effects on optical properties, for example significantly increase the amplitude and relaxation time of the birefringence effect, anisotropic light scattering, transparency or even the color of the colloid. Heating the sample can lead to a change in the average size of the aggregates.

In this paper, we present the results of studies of the optical properties of magnetic fluid in transmitted and scattered light at different temperatures of the sample under study. Aggregate-unstable magnetic fluid of the magnetite-in-kerosene type stabilized by oleic acid produced by the Magnetic Liquids Scientific and Technical Center, Naro-Fominsk (vol. concentration 0.05 and 0.1%).

Fig. 1 shows the results of studies of the effect of temperature on the magnetic field-induced change in the intensity of light scattered at an angle of 90 degrees. With increasing temperature, the magnitude of the effect of changing the intensity of scattered light decreases significantly.

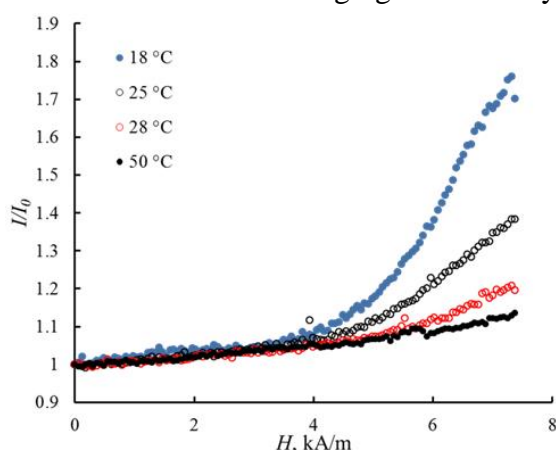


Figure 1.

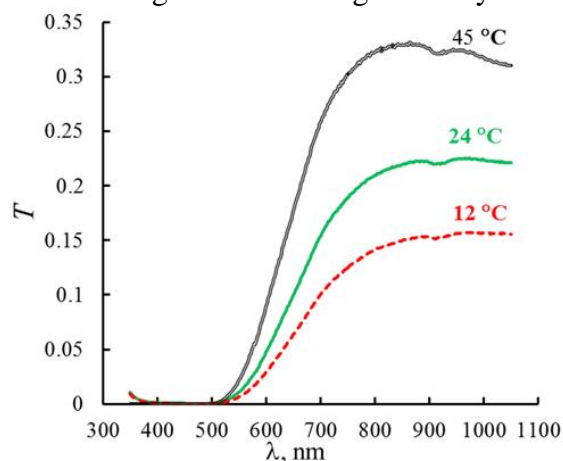


Figure 2.

The same effect can be observed in transmitted light. Fig. 2 shows the transmission spectra of a magnetic fluid with aggregates under the influence of a magnetic field of 30 kA/m. The dependence of the spectra on temperature has been established. With an increase in temperature, the transparency of the magnetic fluid increases significantly, and with a decrease in temperature, it decreases.

The interpretation of these features of optical effects can be related to the change in the size of the aggregate due to temperature changes. An increase in temperature leads to a partial disintegration of the aggregates and a decrease in their average size. This affects the amount of scattering and transmission of light through the parameters of the scattering and absorption cross sections of light. In the absence of aggregates, only the refractive index is temperature-dependent, the changes in which in the studied temperature range, are very small (do not exceed several %). Thus, the effect of temperature on the optical properties of aggregated magnetic fluids during heating and cooling can only be explained by a change in the average size of the aggregates under the action of thermal motion of individual nanoparticles.



# Uniaxial Tension-Induced Phase Transitions in PVDF/CFO Composites

P. Vorontsov\*, V. Salnikov, V. Savin, P. Ershov, V. Rodionova

Immanuel Kant Baltic Federal University, 236004, Nevskogo 14, Kaliningrad, Russia

\*pavorontsov@kantiana.ru

Poly(vinylidene fluoride) (PVDF) exhibits a range of crystalline phases, among which the  $\beta$ -phase imparts superior ferro-, pyro-, and piezoelectric properties, making PVDF-based composites excellent candidates for magnetoelectric applications [1-3].

This work explores phase transitions in PVDF/CoFe<sub>2</sub>O<sub>4</sub> (CFO) nanocomposites subjected to uniaxial tensile deformation at elevated temperature. Composite films containing CFO nanoparticles (10wt%) were synthesized and stretched at 100, 200, and 300% at 100°C (Fig. 1). Structural evolution was monitored via X-ray diffraction and Fourier-transform infrared (FTIR) spectroscopy, while differential scanning calorimetry (DSC) and mechanical testing provided information on crystallinity and tensile strength. The study reveals a controlled and efficient transition from the  $\alpha$  and  $\gamma$  phases to the electroactive  $\beta$ -phase, with  $\beta$ -phase content increasing from 1% in unstretched samples to 91% after 300% elongation. The fraction of electrically active phases increased from 74% to 92%. Simultaneously, the crystallinity decreased from 61% to 44%, and the ultimate tensile strength rose from 35.7MPa to 85.0MPa.

These findings demonstrate that mechanical stretching is a practical approach for tuning the phase composition and enhancing the mechanical and functional properties of magnetoelectric PVDF-based composites, highlighting their promise for advanced device and biomedical applications [4].



Figure 1. Photographs of stretched and stretched samples at 100, 200 and 300% at 100°C (S0, S100, S200 and S300)

- [1] P. Saxena and P. Shukla, Adv. Compos. Hybrid Mater. 4, 8 (2021)
- [2] R. Dallaev, T. Pisarenko, D. Sobola, et al., Polymers (Basel) 14 (22), 1 (2022)
- [3] Y. P. Su, L. N. Sim, X. Li, et al., J. Memb. Sci. 620, 118818 (2021)
- [4]. H. Alibakhshi, H. Esfahani, and E. Sharifi, Ceram. Int. 50 (5), 8017 (2024)

# Correlation of light-to-heat conversion coefficient and SAR in photothermal and magnetothermal studies of nanoparticle solutions

A. Anikin<sup>\*</sup>, V. Salnikov<sup>a</sup>, D. Petrukhin<sup>a</sup>, V. Khanadeev<sup>b</sup>, V. Belyaev<sup>a</sup>, V. Rodionova<sup>a</sup>

<sup>a</sup> REC Smart Materials and Biomedical Applications, Immanuel Kant Baltic Federal University, Kaliningrad, Russia

<sup>b</sup> Institute of Biochemistry and Physiology of Plants and Microorganisms, Saratov Scientific Centre of the Russian Academy of Sciences, Saratov, Russia

<sup>\*</sup> anikinanton93@gmail.com

Magnetic hyperthermia and photothermal therapy are methods of local heating by external fields of cancerous tumors with introduced nanoparticles. Magnetic hyperthermia involves heating magnetic nanoparticles in a high-frequency magnetic field [1]. Photothermal therapy involves heating the nanoparticles using infrared radiation [2]. The efficiency of heating nanoparticle solutions in the two therapies is assessed differently. Magnetic hyperthermia uses the specific absorption rate (SAR), which is numerically equal to the heating power of the nanoparticle solution, related either to the total mass of the nanoparticles or to the mass of magnetic ions. To assess photothermal efficiency, the photothermal conversion coefficient ( $\eta$ ) is most often used, which denotes the share of the energy of the infrared radiation attenuated by the solution that is converted into heat.

Currently, attempts to combine both therapies so that the heating of the nanoparticles occurs due to both the magnetic field and the infrared radiation are of interest. Combining the two contributions will reduce the concentration of nanoparticles required to achieve a therapeutic effect. To assess the efficiency of heating a nanoparticle solution under combined action, the most suitable parameter is SAR. Experimental determination of SAR consists in determining the rate of heating of the solution under external fields near the initial moment of heating. The use of SAR is justified when the external influence is uniform at each point of the solution, which can be considered feasible in magnetic hyperthermia, but is not possible in photothermia.

The report will consider the features of the experimental determination of SAR during photothermal heating. An assessment will be made of the influence of the laser beam geometry and the optical density of the solution on the extracted SAR based on the experimental data obtained using gold nanoparticles. An alternative version of determining SAR using the photothermal conversion coefficient is proposed.

The study was supported by the Russian Federal Academic Leadership Program “Priority 2030” at the Immanuel Kant Baltic Federal University, project № 123101900024-9.

[1] Xiaoli Liu et al., *Theranostics*, **10**(8), 3793 (2020)

[2] Moustafa R. K. Ali et al., *J. Phys. Chem. C*, **123**, 15375 (2019)

# **Polymer-based Free-standing Composites Fullerene/PVDF With Controlled $\beta$ -Phase: Formulation and Quantum Chemical Simulation**

D. Petrukhin<sup>a,\*</sup>, V. Salnikov<sup>a</sup>, K. Magomedov<sup>a</sup>, V. Antipova<sup>a</sup>, V. Kolesnikova<sup>a</sup>, A. Ignatov<sup>a</sup>,  
N. Romanova<sup>b</sup>, A. Goryunkov<sup>b</sup>, R. Usmanov<sup>c</sup>, M. Lomova<sup>d</sup>, A. Omelyanchik<sup>a</sup> and V. Rodionova<sup>a</sup>,

<sup>a</sup> REC Smart Materials and Biomedical Applications, Immanuel Kant Baltic Federal University, 236004,  
Nevskogo 14, Kaliningrad, Russia

<sup>b</sup> Department of Chemistry, Lomonosov Moscow State University, 119991, Moscow,  
Russia.

<sup>c</sup> A.E Favorsky Irkutsk Institute of Chemistry, Siberian Branch of the Russian Academy of Sciences, 664033,  
Favorsky 1, Irkutsk, Russia.

<sup>d</sup> Science Medical Centre, Saratov State University, Saratov, 410012, Russia.

\*DAPetruhin@stud.kantiana.ru

Free-standing polymer platforms fullerene/PVDF with  $\beta$ -phase for future biosensor devices and tissue engineering systems with unique physicochemical properties have been derived using trifluoromethylation, and the perfect convergence of their properties between experiment and quantum chemical simulation has been shown for the first time. The incorporation of carbon fillers into polymer matrices is difficult due to weak adhesion at the interface but is necessary for wide variation of active groups on the surface of coatings and improvement of composite properties. We propose using modified fullerenes to strengthen intermolecular interactions in polyvinylidene fluoride (PVDF). Two series of PVDF-based composites with variable C<sub>60</sub> and trifluoromethyl[C<sub>60</sub>]fullerenes in the form of S<sub>6</sub>-C<sub>60</sub>(CF<sub>3</sub>)<sub>12</sub> concentrations (0.0–0.7 wt%) by the solution casting technique were fabricated. Our experimental results show that the presence of C<sub>60</sub> molecules induces the formation of PVDF  $\beta$ -phase in unstretched films, while the content of  $\gamma$ -phase decreases, and this process can be controlled by trifluoromethylation. Experimental data correlate with the quantum chemical simulation, during which it revealed an increase in interaction of PVDF with functionalized fullerenes.

Additionally, an initial biological validation of the composites on human mesenchymal stem cell culture was performed to assess the applicability of these materials in the field of regenerative medicine and tissue engineering.

# Experimental evidence of IR radiation absorption due to spin-flip transitions in a helical ferromagnet

E. Karashtin<sup>a,b,c,\*</sup>, N. Gusev<sup>a</sup>, D. Kuritsyn<sup>a</sup>, L. Naumova<sup>d</sup>

<sup>a</sup>Institute for Physics of Microstructures RAS, Nizhny Novgorod, 603950, Russia

<sup>b</sup>Lobachevsky State University, Nizhny Novgorod, Russia, 603950

<sup>c</sup>MIREA - Russian Technological University, Moscow, Russia, 119454

<sup>d</sup>Institute of Metal Physics of the Ural Branch of the Russian Academy of Sciences (IMP UB RAS),  
Ekaterinburg 620108, Russia

\*eugenk@ipmras.ru

It is known that transitions of conduction electrons between spin subbands accompanied by absorption or emission of electromagnetic wave are forbidden in a uniform ferromagnet. This restriction may be cancelled if either a spin-orbit interaction is taken into account or a non-uniform non-collinear ferromagnet is considered [1]. A special case of non-collinear magnetization distribution is magnetic helicoid (or Bloch type spiral):  $\mathbf{M} = \mathbf{e}_x \cos qz + \mathbf{e}_y \sin qz$ . This type of magnetization structure is realized due to long-range exchange coupling in rare-earth metals (Ho, Dy) or due to the Dzyaloshinskii-Moriya spin-orbit interaction in some non-centrosymmetric media (MnSi, FeGe) at low temperature. The IR absorption peak was detected in a holmium monocrystal a while ago [2]. Theoretical explanation of this absorption allowed to determine the s-f exchange coupling constant to be  $J_{Ho} = 0.185$  eV [3]. It was shown that the effect crucially depends on the spiral step  $L$  ( $\sim L^{-2}$ ) and on the wave polarization (the electric field of the wave should be along the spiral axis). After that, there were no such experiments published in literature.

In current investigation, we experimentally detect IR wave absorption due to spin-flip electron transitions in Dy. The Dy films of different thickness (5 to 30nm) were obtained by magnetron sputtering on  $Al_2O_3$  substrates with a Ta(5nm) buffer and capping layer. It was shown previously [4] that there is a component in which the magnetic helicoid axis lies in the film plane. The IR transition spectra were measured with the use of Bruker Vertex 80V Fourier-transform spectrometer at different temperature (11 to 200K). We found that the transition to antiferromagnetic state occurs approximately at  $T_N = 155K$ , while the transition to a uniform ferromagnetic state was not observed. A clear IR transmission minimum (or absorption peak) is observed below  $T_N$  at a frequency corresponding to 0.405eV, which gives the s-f exchange constant  $J_{Dy} = 0.202$ eV. Observed temperature dependence of the absorption peak may be explained by the temperature dependence of the spiral period in Dy.

The possibility to manipulate equilibrium magnetic state of a helical ferromagnet (such as Dy or Ho) by applying an external magnetic field or via the exchange coupling with a neighbouring ferromagnetic layer is also discussed. This opportunity may allow to control the direction of magnetic helicoid axis in the experiment in order to observe the IR radiation absorption.

The work was supported by RSF Grant No. 25-72-20055.

- [1] E. Karashtin, J. Magn. Magn. Mater. 552, 169193 (2022)
- [2] P. Weber, M. Dressel, J. Magn. Magn. Mater. 272-276, E1109 (2004)
- [3] E.A. Karashtin and O.G. Udalov, J. Exp. Theor. Phys. 113, 6, 992-999 (2011)
- [4] L.I. Naumova, R.S. Zavornitsyn, M.A. Milyaev et al., Fiz. Met. Metalloved. 124, 8, 692 (2023)

## Microdiffraction gratings tuned by external magnetic field

A. Frolov\*, A. Buldakova, K. Kaver, V. Tolmacheva, M. Sharipova, A. Fedyanin

Lomonosov Moscow State University, 119991, Leninskie gory 1, Moscow, Russia

\*frolovay@my.msu.ru

The development of active optical devices offers a way to control light properties. One of the powerful approaches is the fabrication of optical elements from magnetic composite polymers. This allows the creation of compact magnetic field sensors [1], tunable lense focusing [2], and endoscopes [3] that are driven by an external magnetic field. The induced magnetic forces actuate the optical devices, and the induced deformation and movement significantly modify the optical response.

In this work, we demonstrate the fabrication of the magnetic microdiffraction gratings with a tunable period in external magnetic field. The gratings are created using two-photon photopolymerization technique (Fig. 1(a)). For the fabrication, we use a developed magnetic composite photopolymer based on the commercially available photoresist SZ-2080 and  $\text{Fe}_3\text{O}_4$  nanoparticles. To ensure homogeneous distribution of the  $\text{Fe}_3\text{O}_4$  nanoparticles in the photopolymer they are functionalized with oleic acid. The period of the microdiffraction gratings is  $3\text{ }\mu\text{m}$  and the number of the periods is twelve. The overall size of the grating is length= $75\text{ }\mu\text{m}$ , width= $40\text{ }\mu\text{m}$  and height= $5\text{ }\mu\text{m}$ . When light with a wavelength of  $1064\text{ nm}$  is focused onto these gratings, they produce diffraction patterns. By applying an external magnetic field, the microgratings can be stretched (Fig. 1(b)), compressed, and inclined allowing us to tune the diffraction angles. The developed gratings have protentional application in microdevices that control the angles of light propagation.

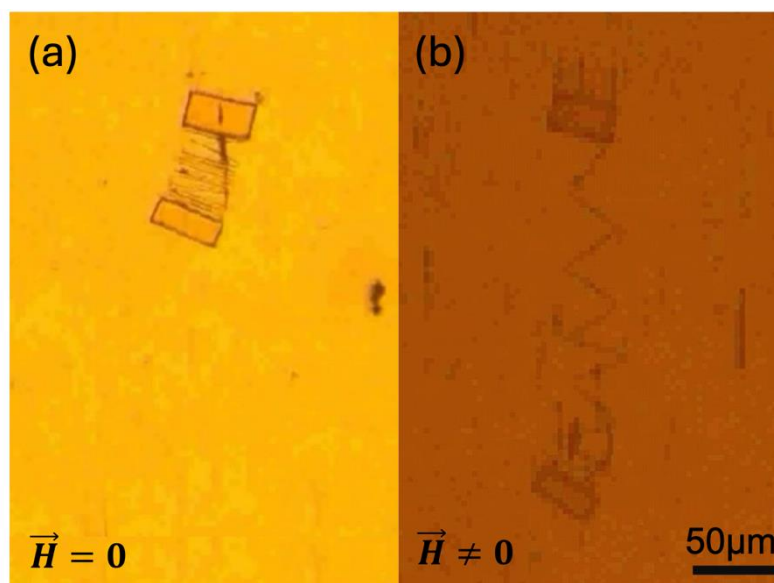


Figure 1. The optical microscope images of the fabricated microdiffraction grating without (a) and with (b) application of the external magnetic field.

The work is supported by RSF grant № 24-72-00042

[1] H. Huang, ACS Photonics 10, 6 (2023)

[2] V. Vieille, Adv. Mater. Technol. 5, 10 (2020)

[3] F. Rothermel, Comms. Eng. 4, 69 (2025)

# Magnetoplasmonic crystal based DC and AC magnetic field sensor

V. Belyaev\*, D. Murzin, V. Rodionova

Immanuel Kant Baltic Federal University, 236004, Nevskogo 14, Kaliningrad, Russia

\*vbelyaev@kantiana.ru

The ubiquitous use of magnetic materials in electromagnetic and micromagnetic systems is primarily attributed to their inherent stability, cost-effectiveness, and application simplicity. To ensure the optimal functionality of post-assembled magnetic systems, a wide range of sensors can be used, including those with optical readout for contactless and electromagnetic interference-free monitoring. These sensors can be made using nanostructured materials supporting the excitation of surface plasmon-polaritons (SPPs) that enhance magneto-optical effects. Such sensing elements made of combined magnetic and plasmonic materials, known as magnetoplasmonic crystals (MPCs).

Here we demonstrate the fabrication of the magnetic field sensing elements based on 1D and 2D magnetoplasmonic crystals prepared using e-beam lithography and magnetron sputtering methods. Magnetoplasmonic crystals consist of square lattice diffraction gratings with varying filling factors layered with Ag, Ni<sub>80</sub>Fe<sub>20</sub>, and Si<sub>3</sub>N<sub>4</sub> layers. Based on the magnetic, optical, and magneto-optical studies, the magnetoplasmonic crystal allowing for both high transverse Kerr effect and isotropic in-plane magnetic properties along the diffraction grating vectors was determined.

Here we demonstrate 1D and 2D permalloy-based MPCs can be used as a magnetic field probes for magnetic field mapping and measurements of AC and DC magnetic field magnitude. For DC measurements it was shown that magnetic field sensors based on one-dimensional magnetic field sensors have a sensitivity of 21.9 mV/Oe with a maximum measurable field amplitude of about 1.1 Oe, while magnetic field sensors based on two-dimensional diffraction gratings allow measurements of two orthogonal components of the external magnetic field with a sensitivity of  $0.67 \times 10^{-3}$  mV/Oe with a maximum measurable field amplitude of about 60 Oe. For AC measurements of non harmonic shape signals the sensors sensitivity can reach 30 mOe in frequency range from 0.1 to 100 Hz [3].

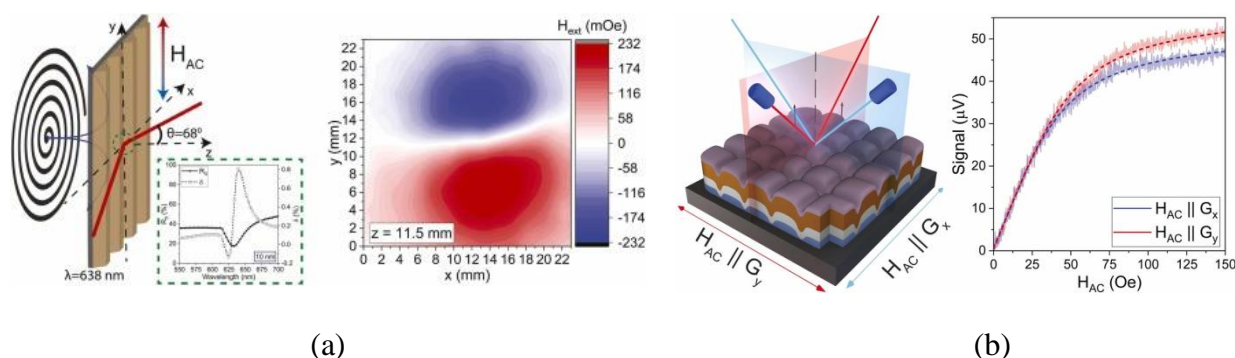


Figure 1. Magnetic field mapping (a) and magnitude (b) measurement concepts [1, 2].

- [1] D. Murzin et al, Sens. Actuator A-Phys 377 (2024) 115773
- [2] D. Murzin et al, Sens. Actuator A- Phys 376 (2024) 115552
- [3] V.K. Belyaev et al, Phys. Met. Metallogr. 3, 126, (2025) 264–272

# Change in the type of magnetic anisotropy in $\text{GdMn}_2(\text{Ge}_{1-x}\text{Si}_x)_2$ compounds

P. Terentev<sup>a,b,\*</sup>, N. Mushnikov<sup>a</sup>, E. Gerasimov<sup>a,b</sup>, V. Gaviko<sup>a,b</sup>

<sup>a</sup> M.N. Mikheev Institute of Metal Physics of Ural Branch of Russian Academy of Sciences, 620108, Sofia Kovalevskaya 18, Yekaterinburg, Russia

<sup>b</sup> Yeltsin Ural Federal University, 620062, Mira 19, Yekaterinburg, Russia

\*terentev@imp.uran.ru

The structure and magnetic properties of  $\text{GdMn}_2(\text{Ge}_{1-x}\text{Si}_x)_2$  intermetallic compounds have been investigated. The Si and Ge atoms form a solid solution in the 4e sites of the  $\text{ThCr}_2\text{Si}_2$ -type structure. Magnetization measurements on quasi-single crystals revealed that with increasing  $x$  the total magnetization vector gradually reorients from the  $c$ -axis to the basal plane. For  $x = 0.1$  the spin reorientation occurs also with increasing temperature.

Detailed analysis of magnetic structures and magnetic phase transitions has been performed with a three-sublattice model with negative exchange interactions between the sublattices. For  $\text{GdMn}_2\text{Ge}_2$  (Figure 1) and  $\text{GdMn}_2(\text{Ge}_{0.9}\text{Si}_{0.1})_2$ , using available experimental data, the field dependences of the magnetic moment along the main crystallographic directions were calculated. For the field applied along the  $c$ -axis, seven different magnetic structures were predicted, including two angular structures considered for the first time. Our analysis showed that, in order to explain the spin-reorientation in  $\text{GdMn}_2(\text{Ge}_{1-x}\text{Si}_x)_2$  system through the angular magnetic phase, it is necessary to take into account magnetic anisotropy of Mn sublattices with a large negative second-order anisotropy constant  $K_2$ . The origin of the appearance of  $K_2$  in  $\text{RMn}_2\text{X}_2$  is not clear at present and requires additional studies.

The research was supported by RSF project No. 23-12-00265 (<https://rscf.ru/en/project/23-12-00265/>).

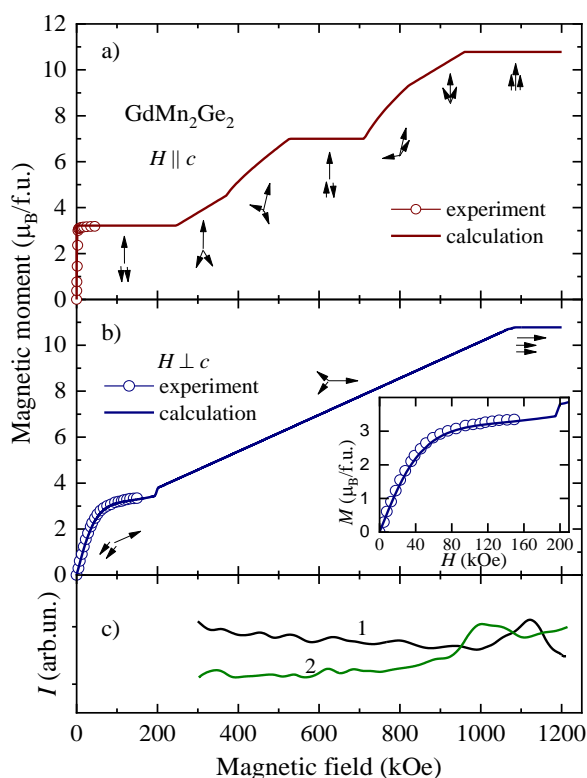


Figure 1. Field dependences of magnetic moment of  $\text{GdMn}_2\text{Ge}_2$  in magnetic fields applied parallel to the  $c$ -axis (a) and in the basal plane (b). Symbols are the experimental data [33], solid lines are the results of calculation. The arrows schematically show the mutual orientations of the three magnetic sublattices for different magnetic field intervals. Inset in panel (b) shows  $M(H)$  dependence on a larger scale. (c) – field dependences of the magnetic signal  $I$  induced in experiments with a single-turn coil [36] on polycrystalline  $\text{GdMn}_2\text{Ge}_2$  sample: 1 – increase in field, 2 – decrease in field.

# Crystal structure and magnetocrystalline anisotropy of $Y_2(Fe_xCo_{1-x})_{17}H_y$ compounds

A. Sinkevich<sup>a,\*</sup>, A. Karpenkov<sup>a</sup>, M. Lyakhova<sup>a</sup>, E. Semenova<sup>a</sup>, D. Karpenkov<sup>b</sup>, R. Makarin<sup>c</sup>

<sup>a</sup> Tver State University, 170100, Zhelyabova 33, Tver, Russia

<sup>b</sup> National University of Science and Technology “MISIS”, 119049, Leninskiy prospekt 4, Moscow, Russia

<sup>c</sup> Lomonosov Moscow State University, 119991, Leninskie gory 1, Moscow, Russia

\*artem.sinkevich2602@gmail.com

Rare-earth intermetallic compounds of the  $R_2M_{17}$  type ( $R$  – rare-earth element;  $M = Fe, Co$ ) are of considerable interest as functional materials that form a basis for high-energy permanent magnets. However, a number of compounds of this type have “easy plane” magnetocrystalline anisotropy (MCA) type, which limits both their study and practical use. It was shown [1] that the small cobalt-to-iron sublattice replacement for these compounds leads to change of MCA type to “easy axis”, which persists over a wide compositional range.

In the present study we focused on the investigation of such quasi-binary intermetallic compounds with the yttrium  $Y_2(Fe_xCo_{1-x})_{17}$ . Samples of initial  $Y_2(Fe_xCo_{1-x})_{17}$  and hydrogenated  $Y_2(Fe_xCo_{1-x})_{17}H_y$  compounds in a wide compositional range  $x = 0.03 - 0.53$  were investigated. The complete crystal structure and MCA analysis of the samples was carried out to understand the effect of the hydrogenation process on these compounds.

The original  $Y_2(Fe_xCo_{1-x})_{17}$  as-cast samples were prepared by induction melting under a high purity argon atmosphere. Hydrogenated  $Y_2(Fe_xCo_{1-x})_{17}H_y$  samples were obtained based on the original samples. Hydrogenation was carried out at the temperature of 300 °C during 15 h in molecular hydrogen flux with the speed of 0.037 L per minute in 2 atm pressure. The crystal structure of the samples was determined by powder x-ray diffraction (XRD) at room temperature. The XRD patterns were recorded at a  $2\theta$  scanning step of 0.02 on a DRON-7.0 powder diffractometer with  $CuK\alpha$  radiation. Magnetization measurements were carried out in a vibrating-sample magnetometer in the fields up to 2.5 T in a wide temperature range of  $T = 100 - 923$  K.

From the XRD study, it was found that  $Y_2(Fe_xCo_{1-x})_{17}$  and  $Y_2(Fe_xCo_{1-x})_{17}H_y$  samples crystallize in a rhombohedral  $Th_2Zn_{17}$  and a hexagonal  $Th_2Ni_{17}$  type of structure with a transition point at around  $x = 0.22$ . The hydrogenation process for all studied samples leads to the unit cell expansion in the basal plane (lattice parameters  $a$  and  $b$  increase) with a small reduction of the cell along the  $c$  axis (lattice parameter  $c$  slightly decreases). Analysis of the XRD results and comparison with the literature data for the  $Y_2Fe_{17}H_y$  compound allowed us to estimate the amount of hydrogen absorbed by the lattice.

The values of MCA constants were calculated from the experimental magnetization curves using the Sucksmith-Thompson approach [2]. The obtained saturation magnetization temperature dependences  $M_s(T)$  were analyzed using the Kuz'min expression [3] to evaluate the change in the temperature stability of the magnetic properties of the samples after the hydrogenation process. The resulting temperature dependences of the MCA constants  $K_{1,2}(T)$  were processed using the classical Zener approach [4].

[1] H. Chen, J. Magn. Magn. Mater. 78, 203-207 (1989)

[2] W. Sucksmith, Proceedings of the Royal Society of London. Series A. 225, 362-375 (1954)

[3] M.D. Kuz'min, Phys. Rev. Lett. 94, 107204 (2005)

[4] C. Zener, Phys. Rev. 96, 1335 (1954)



# **Ultrasensitive detection of cancer and cardiac disease markers in saliva using graphene and magnetic bioconjugates**

A. Kudriavtseva<sup>a,b</sup>, J. Malkerov<sup>a,c</sup>, A. Skirda<sup>a,b</sup>, A. Orlov<sup>a</sup>, I. Bobrinetskiy<sup>b</sup>, P. Nikitin<sup>a,\*</sup>

<sup>a</sup> Prokhorov General Physics Institute of the Russian Academy of Sciences

38 Vavilov str., Moscow 119991, Russia

<sup>b</sup> Moscow Institute of Physics and Technology, Dolgoprudny, Russia

\*nikitin@kapella.gpi.ru

For biochemical *in vitro* medical diagnostics, saliva sampling is very attractive as a non-invasive, comfortable for patients, and less risky method of sample collection. However, the concentration of many informative biomarkers of cancer and heart diseases in saliva is about a thousand times lower than in blood, so highly sensitive methods are still needed for analysis [1,2].

To address these goals, we have developed and tested several novel approaches. The first one is based on using graphene (G) grown by chemical vapor deposition and reduced graphene oxide (rGO) in combination with aptamers on top of a liquid-gated field-effect transistor (FET), yielding GFET and rGO-FET biosensors, respectively. The miniature immersible rGO-FET aptasensors have been developed for the non-invasive analysis of natural human fluids such as saliva by measuring the concentration of N-terminal pro-B-type natriuretic peptide (NT-proBNP), which is an early-stage marker of heart failure. The aptasensors offer high selectivity and sensitivity for rapid detection of NT-proBNP at a record concentration level of 41 fg/ml (~4.6 fM). In the presence of corresponding biorecognition receptors at the surface, such sensor can be effectively used to monitor a variety of other biomarkers, e.g., CYFRA 21-1, a fragment of cytokeratin 19, which is a predominant molecular biomarker for cancers of epithelial origin, such as non-small cell lung cancer, squamous cell carcinoma of the lungs, and muscle-invasive bladder carcinoma. The developed GFET aptasensors have also been successfully tested for detection of ultra-low concentrations of ochratoxin A in wine with a record detection limit of 1.4 pM and a response time of 10 s [3].

To reduce the cost of consumables, we have developed a paper-based biosensing technique using magnetic nanoparticles (MP) obtained by traditional colloidal chemistry or genetic cell-assisted biosynthesis of well-calibrated MP [4]. The MP conjugated with antibody serve as labels for the lateral flow assay (LFA), in which they are counted by the magnetic particle quantification (MPQ) technique [5]. The next generation of MPQ readers have been designed based on low-current electronic components that have low intrinsic noise and provide an optimal signal-to-noise ratio. The developed LFA have demonstrated the limit of detection of 9 pg/mL for the CYFRA 21-1 tumor marker concentration. Remarkably, due to the exceptional sensitivity of the system, the analysis can be carried out with non-invasively collected saliva samples [6] rather than solely for venous blood samples. Furthermore, the LFA based on magnetic bioconjugates was also tested for measuring ultra-low concentrations of mycotoxins in food products, e.g., in barley flour samples contaminated with *Fusarium graminearum* [7]. The detection limits of 2.3 pg/ml zearalenone and 11 pg/ml ochratoxin A were shown with a 20-min analysis time, which are at the level of the best analytical techniques.

The research was funded by Russian Science Foundation, grant No 25-12-00373.

- [1] A. Kudriavtseva, et al., Biosensors, 14, 215 (2024)
- [2] S. Jaric, et al., Microchemical Journal, 196, 109611 (2024)
- [3] N. Nekrasov, et al., Biosensors and Bioelectronics, 200, 113890 (2022)
- [4] A. N. Gabashvili, et al., Pharmaceutics, 15(10), 2422 (2023)
- [5] A.V. Orlov, et al., Doklady Physics, 68 (7), 214-218 (2023)
- [6] A.M. Skirda, et al., Biosensors 14 (12), 607 (2024)
- [7] A.V. Orlov, et al. Toxins, 16, 5 (2024)

# Synthesis of intermetallic powder with hard magnetic phase

## □-MnAl by calcium thermal reduction

M. Gorshenkov<sup>\*</sup>, S. Yudin, T. Morozova, A. Fortuna, E. Khusainova

National University of Science and Technology MISIS, Moscow, 119049, Russia

<sup>\*</sup>mvg@misis.ru

In this work, we investigated the parameters of MnAl(C) powder synthesis in the region of formation of a metastable hard magnetic phase ( $\tau$ -MnAl) by the method of calcium-thermal reduction from aluminum oxide ( $\text{Al}_2\text{O}_3$ ) and manganese monoxide (MnO) powders. To alloy the intermetallic compound with carbon, pure graphite was added to the batch during synthesis. The selection of synthesis parameters included varying the ratio of aluminum and manganese oxide in the mixture, amount of  $\text{CaH}_2$ , as well as batch compaction methods - manual (without pressure) or pressing under a pressure of 56 MPa have been investigated. The synthesis was carried out in pre-evacuated steel containers at a temperature of 1250°C for 6 hours. The ratios of aluminum and manganese oxides were selected in order to obtain the desired near equiatomic alloy composition with the slight manganese excess  $\text{Mn}_{54}\text{Al}_{46}$ . The parameters of the process of intermetallic powder extraction from the charge material were selected. The influence of the oxide ratio on the composition of the resulting intermetallic powder was studied. It was shown that in order to obtain powder in the desired composition range, it is necessary to add an excess of aluminum from 20 to 50% in terms of aluminum oxide. Phase composition and magnetic properties measurements revealed that content of the magnetically hard phase in the resulting powder is insignificant, the maximum magnetization of the powder was about 6-8 emu/g. Additional development of the process - water quenching of the container from the 950°C led to the formation of about 50 vol. % metastable hard magnetic phase ( $\tau$ -MnAl) in the powder. The powder could be also interesting for additive technologies – 3D printing of a MnAl based permanent magnets.

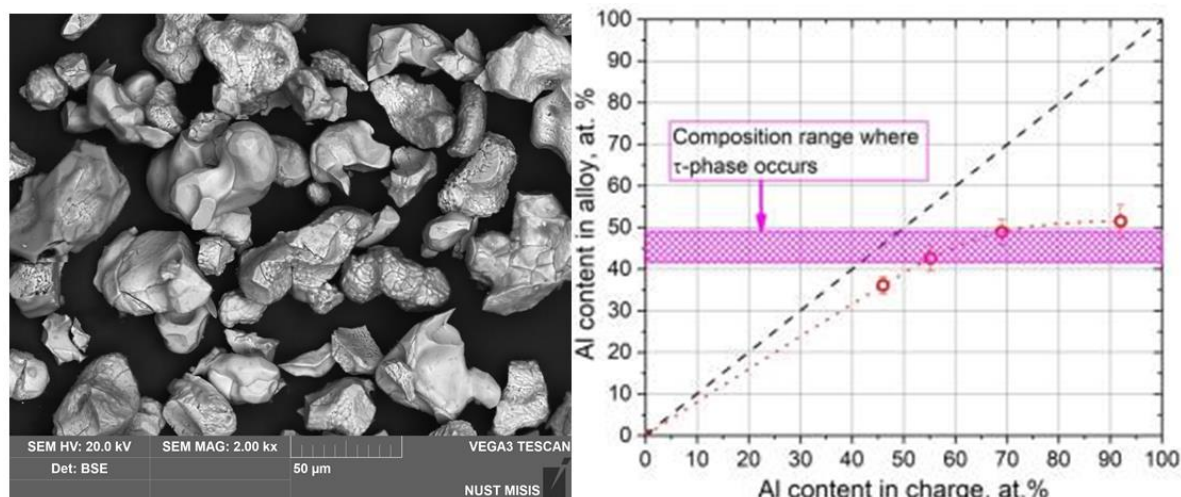


Figure 1. SEM image of the MnAl powder obtained by calcium thermal reduction method (a), and dependence of the Al content in the alloy on the Al content in the charge

The research was carried out with support from the Ministry of Science and Higher Education of the Russian Federation within the framework of State Assignment No. FSME-2023-0007.

# Optical properties of adipose tissue in a rat model of diabetes mellitus

I. Yanina<sup>a,b\*</sup>, D. Tuchina<sup>a,b</sup>, N. Shushunova<sup>a</sup>, A. Bucharskaya<sup>c</sup>, A. Mylnikov<sup>c</sup>, N. Navolokin<sup>c</sup>,  
V. Tuchin<sup>a,b,d</sup>

<sup>a</sup> Saratov State University, 83 Astrakhanskaya str., 410012, Saratov, Russia

<sup>b</sup> Tomsk State University, 36 Lenin's av., 634050, Tomsk, Russia

<sup>c</sup> Saratov State Medical University, 112 B Kazachaya str., 410012, Saratov, Russia

<sup>d</sup> Institute of Precision Mechanics and Control, FRC "Scientific Research Centre of the Russian Academy of Sciences," 24 Rabochaya str., 410028, Saratov, Russia

\*irina-yanina@list.ru

The incidence of diabetes mellitus (DM) is growing annually, and experts believe that if the situation continues to develop at the same rate, then by 2025 the number of patients will double, and in 2030 this disease will become the seventh leading cause of death worldwide.

DM is associated with a violation of carbohydrate metabolism, characterized by high glucose levels in the blood [1]. A distinction is made between type 1 and type 2 diabetes. Despite the different mechanisms of pathogenesis, both types of the disease are accompanied by hyperglycemia, which causes serious complications. Since glycation of biological molecules occurs throughout the body, including vital organs, then by studying the structural and chemical changes associated with prolonged hyperglycemia in the body, it is possible to obtain information about the degree of glycation of not only hemoglobin, but also proteins and lipids in various tissues. This should directly indicate the risks of serious complications in the development of DM. Not only amino acid residues of proteins, lipoproteins as lipid-carrying protein macromolecules, but also lipids are subject to glycation. Aminophospholipids react directly with glucose, forming the end products of glycolysis, which are then oxidized by reactive oxygen species [2, 3].

The aim is to study the optical properties such as absorption coefficient, scattering coefficient, of abdominal fat tissue of healthy and type 1 and 2 DM animals at different stages.

The experiments were carried out on 20 white male Wistar rats weighing 200-250 g. The model of DM type 1 was reproduced by intraperitoneal administration of alloxan (at a dose of 90 mg/kg). The non-genetic form of experimental DM type 2 was modeled by alloxan with preliminary (15 min) administration of nicotinamide (intraperitoneally - 230 mg/kg).

The spectra of total transmittance and diffuse reflectance of the samples were measured in the wavelength range of 350–2500 nm using a spectrophotometer UV-3600 with an integrating sphere LISR-3100 (Shimadzu, Japan). A multi-wavelength Abbe refractometer Atago DR-M2 1550 (Atago, Japan) has been applied for the quantitative assessment of refractive index.

Data on the optical properties of tissues in combination with histological analysis provide information on structural changes occurring in biological tissues and their components, which must be taken into account in diagnostics [4]. This study shows significant differences in absorption coefficient, scattering coefficient, and scattering anisotropy factor of abdominal adipose tissue of healthy and diseased animals.

The study was supported by a grant Russian Science Foundation No. 24-44-00082, <https://rscf.ru/project/24-44-00082/>.

[1] O. Mookpaksacharoen, S. Choksakunwong, R. Lertwattanak, BMC Endocr. Disord. 24 (1), 114 (2024)

[2] J. W. Baynes, S. R. Thorpe, Free Radic Biol Med. 28 (12), 1708-1716 (2000)

[3] V. N. Titov, N. V. Khokhlova, Yu. K. Shiryayeva, Clin. Med. 3, 15-24 (2013)

[4] D.K. Tuchina and V.V. Tuchin, in *Handbook of Tissue Optical Clearing: New Prospects in Optical Imaging*, CRC Press, Boca Raton, FL (2022), pp. 517-538.

# Alloyed Rapidly Quenched $\tau$ -MnAl Ribbons: Microstructure and Magnetic Properties

A. Fortuna<sup>a,\*</sup>, N. Vazhinskii, K. Nechaev, D. Karpenkov<sup>b</sup> and M. Gorshenkov

<sup>a</sup> National University of Science and Technology MISIS, 119049, Leninskiy prospekt 4, Moscow, Russia

<sup>b</sup> Lomonosov Moscow State University, 119991, Leninskie gory 1, Moscow, Russia

\*fortuna.as@misis.ru

$\tau$ -MnAl alloys, containing a metastable ferromagnetic  $\tau$ -phase (lattice  $L1_0$ , P4/mmm, tP2, with a homogeneity region in the binary alloy of 51-58 at.% Mn), are promising hard magnetic materials for use in electric motors for cars and personal mobility devices. However, the use of these alloys is complicated by several problems, including the difficulty in obtaining a  $\tau$ -phase with an optimal microstructure, and a decrease in the saturation magnetization of the alloy due to disorder in the arrangement of Mn atoms in the lattice. These problems can both be solved through alloying. Alloying the  $\tau$ -phase with Ga and V has shown promise. The aim of this study was to investigate the magnetic properties and defect microstructure of  $Mn_{55}Al_{36}Ga_9$  and  $Mn_{53}Al_{44}V_3$  rapidly quenched ribbons.

Ribbons of the  $Mn_{55}Al_{36}Ga_9$  and  $Mn_{53}Al_{44}V_3$  compositions were produced by rapid quenching of pre-melted ingots. The rapid quenching process was conducted by spinning on the copper wheel at a linear rotation speed of 10 m/s for  $Mn_{55}Al_{36}Ga_9$  and 30 m/s for  $Mn_{53}Al_{44}V_3$ . After quenching, the  $Mn_{55}Al_{36}Ga_9$  ribbons were annealed at a temperature of 700 °C (20 min). The  $Mn_{53}Al_{44}V_3$  samples were studied in their rapidly quenched state. The phase transition temperatures were determined using differential scanning calorimetry (DSC) with a heating rate of 10 °C/min. X-ray diffraction (XRD) analysis and transmission electron microscopy (TEM) were used to study the microstructure. Magnetic hysteresis loops were measured at a field of 6 T, while thermomagnetic curves were obtained at a field of 0.5 T during heating to 400 °C and subsequent cooling.

After annealing, the  $Mn_{55}Al_{36}Ga_9$  ribbons acquired the following structure:  $\tau$ -phase - 88.2%, ( $\beta$ -Mn) - 7.7%, and  $\gamma_2$  - 4.1%. The specific saturation magnetization of the  $\tau$ -phase was measured and found to be 102 A·m<sup>2</sup>/kg, which is approximately 85% of the saturation magnetization experimentally obtained for a bulk sample of  $Mn_{55}Al_{39.6}Ga_{6.4}$ , as presented in [1]. A TEM study revealed that the  $\tau$ -phase grains had a planar dislocation structure with a high dislocation density. Based on the results of dark-field analysis, these dislocations had a Burgers vector of  $[111]$ . When these dislocations slip in the  $L1_0$  lattice, antiphase boundaries are formed. It is likely that the presence of these high-density antiphase boundaries leads to a decrease in magnetization, as the exchange interaction between Mn atoms at the antiphase boundaries is antiferromagnetic.

The rapidly quenched  $Mn_{53}Al_{44}V_3$  ribbons were characterized by the presence of the  $\tau$ -phase (87.9%), with a small amount of the  $\epsilon$ -phase (12.1%). The microstructure of the  $\tau$  phase possessed a large number of twins with an average thickness of 8 nm. XRD and DSC studies showed that the  $\tau$ -phase decomposed into equilibrium  $\beta$ -Mn and  $\gamma_2$ , which underwent decomposition at a temperature of 559 °C. There were no other exothermic reactions observed in the heat flow versus temperature curve. The only endothermic reaction was observed at 281 °C. XRD analysis of a sample annealed at 300 °C showed no changes in the phase composition, so the observed effect could be correlated with the Curie temperature of the alloy. Thermomagnetic measurements up to 400 °C, below the temperature at which the  $\tau$ -phase decomposed, revealed a hysteresis in the Curie temperature, with values of 350 and 230 °C for heating and cooling, respectively. Such an effect has not been observed previously in  $\tau$ -MnAl alloys with other compositions. The specific saturation magnetization of the  $\tau$  phase in the  $Mn_{53}Al_{44}V_3$  ribbon was 122 A·m<sup>2</sup>/kg, which is higher than the previously best value of 117 A·m<sup>2</sup>/kg achieved in the  $(Mn_{0.55}Al_{0.45})_{98}C_2$  alloy [2].

[1] T. Mix, F. Bittner, K.-H. Müller e a., Acta Mater. 128, 160-165 (2017)

[2] H. Fang, S. Kontos, J. Ångström e a., J. Solid State Chem., 237, 300-306 (2018)

## Using Biosensors Based on MXenes and DNA Aptamers for the Quantitative Determination of Coronavirus RBD Protein

A. Amosov<sup>\*</sup>, A. Fedorova, N. Shilov, K. Magomedov, K. Levada

Immanuel Kant Baltic Federal University, 236004, Nevskogo 14, Kaliningrad, Russia

<sup>\*</sup>[alexeyamosov92@gmail.com](mailto:alexeyamosov92@gmail.com)

Biosensors based on DNA aptamers and MXenes represent an effective tool for the quantitative and qualitative analysis of molecules due to their high sensitivity, selectivity, and ease of use. In these sensors, DNA aptamers are used as selective protein-binding elements, providing high specificity towards target proteins, while MXenes act as conductors of the electrical signal. In this study, a sensor based on aptamers and MXenes was used for the quantitative analysis of the coronavirus receptor-binding domain (RBD). MXenes ( $\text{Ti}_3\text{C}_2\text{T}_x$ ) are a novel class of two-dimensional nanomaterials, obtained from a precursor (MAX phase) by etching the aluminum layer with hydrofluoric acid or a mixture of hydrochloric acid and lithium fluoride. They possess high potential for surface modification, allowing for their efficient functionalization with DNA aptamers. DNA aptamers are selected for the target protein using the SELEX (Systematic Evolution of Ligands by Exponential Enrichment) method and are oligonucleotides 20-60 nucleotides long. After sequencing, the aptamers can be re-synthesized with the necessary modifications. Aptamers can selectively bind to the target protein, immobilizing it on the surface of the MXenes, which serve as conductors of the electrical signal. The interaction of the RBD protein with the DNA aptamers causes changes in the electrochemical properties of the MXene surface, which are recorded using a potentiostat-galvanostat. For the quantitative analysis of the RBD protein, silver electrodes connected in a three-electrode configuration to a potentiostat-galvanostat were used. Two layers of MXenes functionalized with aptamers were applied to the working electrode. As a result of the measurements, voltammetric characteristics of the biosensor were obtained; characteristic peaks were observed on the graphs at a potential of about 100 mV, changing depending on the protein concentration in the sample. Experiments were conducted on a multi-channel potentiostat-galvanostat P-20X8 (Russia) in potentiostatic mode with a potential range up to 6 V and a scan rate of 0.01 V/s. The developed biosensor demonstrates high sensitivity and selectivity in the quantitative analysis of the coronavirus RBD protein. This method of biosensor production can be adapted for the determination of other protein biomarkers, opening prospects for their application in medical research.

## **Pulsed Non-Destructive Facility for Studying Material Properties in Fields up to 60 T**

O. Surdin<sup>a,b,\*</sup>, Yu. Kudasov<sup>a,b</sup>, V. Platonov<sup>a,b</sup>, I. Makarov<sup>a</sup>, D. Maslov<sup>a,b</sup>, I. Strelkov<sup>a</sup>,

R. Kozabaranov<sup>a</sup>, P. Katenkov<sup>a</sup>, A. Korshunov<sup>a</sup>, P. Repin<sup>a</sup>, A. Filippov<sup>a</sup>

<sup>a</sup> Russian Federal Nuclear Center – VNIIEF, Sarov, Russia, 607188

<sup>b</sup> Sarov Physics and Technology Institute, NRNU “MEPhI”, Sarov, Russia, 607186

\*surdin@ntc.vniief.ru

The paper presents the results of upgrading a compact, non-destructive facility designed to generate pulsed magnetic fields up to 60 T with millisecond duration [1]. The characteristics, operational features, and prospects for further development of multi-turn solenoid technology to increase the magnetic field amplitude up to 75 T are discussed. The facility is equipped with a number of optical measurement techniques that allow research in the temperature range from 77 to 300 K in fields up to 50 T in the visible, mid- and far-IR ranges. A description of the measurement techniques currently under development is provided. The methods and results of cyclotron resonance and magnetotransport measurements in CdHgTe quantum well heterostructures [2], as well as Faraday rotation in YBiFeGaAlO films [3], are discussed.

The work was carried out within the framework of the scientific program of the National Center of Physics and Mathematics, direction No. 7 “Research in high and ultrahigh magnetic fields”.

[1] Platonov V.V. et al., High Magnetic Field Facility for Cyclotron Resonance Investigation in Semiconductors // IEEE TRANSACTIONS ON PLASMA SCIENCE, VOL. 43, NO. 1, 2015, doi: 10.1109/TPS.2014.2375637

[2] Ikonnikov A.V. et al., Temperature-dependent magnetospectroscopy of HgTe quantum wells // PHYSICAL REVIEW B 94, 155421, 2016, doi: 10.1103/PhysRevB.94.155421

[3] Yu. B. Kudasov et al., Giant widening of interface magnetic layer in almost compensated iron garnet. Appl. Phys. Lett. 21 March 2022; 120 (12): 122403. <https://doi.org/10.1063/5.0086067>

## **Natural biologically active agents with anti-inflammatory properties for ENT-surgery**

P. Serbun\*, R. Shaikenov, P. Snetkov, S. Morozkina

Institute of Advanced Data Transfer Systems, ITMO University, 197101, Kronverkskiy Prospekt, 49, Bldg.

A, Saint-Petersburg, Russia

\*polina\_serbun@itmo.ru

Otorhinolaryngological surgery (Ear, Nose, Throat and surgery) is a branch of medicine dealing with the diagnosis and treatment of diseases of the ear, throat and nose. Currently, one of the most actual areas is surgery of the ear region. The pathology of this area directly affects the hearing function, which also affects the quality of life of patients. One of the most frequent types of interventions are operations on the eardrum, such as myringoplasty and tympanoplasty. The result is the restoration of the integrity of the eardrum when it is perforated, which improves hearing and reduces the risk of serious complications such as the spread of infection to the inner ear or brain. Thanks to technological advances and a multidisciplinary approach, ear surgery is becoming increasingly effective, allowing personalized treatment and sustainable outcomes for patients.

Inflammation is one of the important problems in the complex development of otorhinolaryngological diseases and subsequently arising surgical interventions. The ear, nose and throat regions are specific regions of the body, due to anatomical features and exposure to external environments. For example, the external ear reacts acutely to inflammation because it is in an open anatomical position, which reduces protection from environmental factors.

In tympanic membrane surgery (tympanoplasty, myringoplasty), two inflammation mechanisms occur: infectious and aseptic. Infectious inflammation results from pathogenic bacteria or viruses entering the surgical site, causing acute or chronic inflammation with pain, swelling, hearing loss, and ear discharge, sometimes leading to purulent otitis media. It requires antibacterial treatment and in some cases surgical correction. Aseptic inflammation is a tissue reaction to mechanical damage during surgery without pathogens, characterized by edema, hyperemia, and pain without purulent discharge. It is usually temporary and resolves with healing but may worsen if secondary infection develops. Both types need timely diagnosis and treatment to prevent complications.

Biopolymers such as hyaluronic acid can be used to reduce inflammation. With its viscoelasticity, bacteriostatic and antioxidant properties, as well as stimulating angiogenesis and epithelialization through, it can suppress excessive inflammation in the wound healing phase [1].

Among natural compounds curcumin is one of the natural agents capable of inhibiting inflammation. It blocks the NF- $\kappa$ B, which triggers inflammatory processes in cells and reduces the production of pro-inflammatory cytokines (IL-1 $\beta$ , IL-6, IL-12, TNF- $\alpha$ ). It may also contribute to hepatoprotection by the suppression of ROS [2].

Natural polyphenol Resveratrol inhibits cyclooxygenase (COX) activity, reduces levels of pro-inflammatory markers such as C-reactive protein and tumour necrosis factor (TNF- $\alpha$ ), and increases anti-inflammatory cytokines (e.g. interleukin-10) [3].

The search of natural compounds with anti-inflammatory properties allows to reduce side-effects and enhance the treatment outcomes.

Acknowledgements: The study was supported by the Russian Science Foundation, project number 25-73-20141.

[1] P. Nabiyi, *fid.* 21, 42(2024)

[2] Y.S. Fu, *Biomed Pharmacother.* 141, 111888(2021)

[3] A. Olędzka, *IJMS.* 24, 4666(2023)

## Heavy metal dichalcogenides as promising materials for modern spintronics

A. Kozlov<sup>a,\*</sup>, Zh. Namsaraev<sup>a</sup>, A. Shishelov<sup>a</sup>, L. Davydenko<sup>a</sup>, M. Kuznetsova<sup>a</sup>, A. Prihodchenko<sup>a</sup>,  
N. Chernousov<sup>a</sup>, M. Bazrov<sup>a</sup>, P. Mushtuk<sup>a</sup>, I. Iliushin<sup>a</sup>, L. Afremov<sup>a</sup>, L. Likhoida<sup>a</sup>, R. Shestopalov<sup>a</sup>,  
A. Davydenko<sup>a</sup>, A. Ognev<sup>a,b</sup>, F. Meng<sup>c</sup>, Y. Feng<sup>c</sup>, Y. Wang<sup>c</sup>

<sup>a</sup> Institute of High Technologies and Advanced Materials, Far Eastern Federal University, Vladivostok, Russia

<sup>b</sup> Sakhalin State University, Yuzhno-Sakhalinsk, 693000, Russia

<sup>c</sup> Key Laboratory of Materials Modification by Laser, Ion and Electron Beams (Ministry of Education), School of Physics, Dalian University of Technology, Dalian, China

\*kozlov.ag@dvfu.ru

The widespread use of magnetic devices such as magnetic random-access memory (MRAM), logical memory, and neuromorphic computing devices requires efficient ways to control local magnetization. The success of modern spintronics is largely determined by the progress in the development of the science of functional nanomaterials and their unique properties. The basis of all developed spintronics devices are magnetic heterostructures, the key properties of which are determined by the phenomena and processes occurring both at the interfaces and in the volume of ultrathin layers of magnetic or nonmagnetic material. Magnetic heterostructures containing heavy metal at the boundary with a ferromagnet can demonstrate such useful properties as perpendicular magnetic anisotropy, Dzyaloshynskii-Moria interaction, etc. One of the most powerful tools for manipulating such spin structures and controlling local magnetization is spin-orbit torque, which can have both a bulk origin by the mechanism of the spin Hall effect and an interface origin due to the Rashba-Edelstein effect. The effect is to switch the magnetization by transferring spins into a ferromagnet from a bulk heavy metal. In both cases, a material with strong spin-orbit coupling is required.

One of the most promising classes of SOT materials are transition metal dichalcogenides [1-4] due to their topological properties and electronic structure features. To enhance compatibility with CMOS technologies, obtaining such materials by sputtering and epitaxy methods is the most preferable. In our work we focused on the development of technology for synthesis of heterostructures containing high quality heavy metal ditellurides, such as PtTe<sub>2</sub>, MoTe<sub>2</sub>, WTe<sub>2</sub>, by molecular beam epitaxy and magnetron sputtering methods, and we also investigated the influence of topological materials on ultrathin Pt/Co magnetic films with perpendicular magnetic anisotropy.

Magnetic heterostructures were prepared by magnetron sputtering or molecular beam epitaxy on Al<sub>2</sub>O<sub>3</sub> substrates. Ultraviolet photolithography was used to create nanostructures using standard templates for Hall structures and subsequent ion-plasma etching. The structure features of the layers and interface parameters were investigated by X-ray reflectometry. The magnetic hysteresis loops measured on VSM showed perpendicular magnetic anisotropy (PMA). Addition of a sublayer of TMDs leads to a halving of the coercivity and a slight decrease in PMA. SOT was investigated by the shift of the anomalous Hall effect loops.

The experimental results of the SOT study on the displacement of AHE loops showed a significant decrease in the switching current density. Obviously, the addition of the layer is accompanied by a significant increase in SOT. In addition, the SOT was investigated by Hall harmonic analysis. Hall harmonic analysis is a popular method for measuring damping-like (DL) and field-like (FL) torques. By analyzing the Hall voltage characteristics, the longitudinal and transverse effective fields induced by the DL and FL torques can be obtained, which are then converted into spin torque efficiencies. The spin-Hall conductivity for the combination of transition metal dichalcogenides sublayers was also investigated by ST-FMR. The prospects of using the proposed methods are shown in this work.

This work was financially supported by Russian Scientific Foundation, under the grant № 23-42-00076

- [1] Yi Wang, et al., Nature Communications 8 1364 (2017).
- [2] Fei Wang, et al., Nature Materials 23 768–774 (2024).
- [3] Zheyu Ren, et al., J. of Appl. Phys. 135 143904-1-7 (2024)
- [4] Cheng-Wei Peng, et al., Appl. Mater. Int. 13, 15950–15957 (2021)



## Nanomaterials based on natural polymers for ENT surgery

A. Kosova\*, P. Serbun, R. Shaikenov, P. Snetkov, S. Morozkina

Institute of Advanced Data Transfer Systems, ITMO University, 197101, Kronverkskiy Prospekt, 49,

Bldg. A, Saint-Petersburg, Russia

\*kosova@itmo.ru

One of the most actual areas of otorhinolaryngology (Ear, Nose, Throat surgery, ENT surgery) is surgery of the ear region, particularly the tympanic membrane - a thin film separating the external auditory canal from the tympanic cavity and serving to transmit sound vibrations to the auditory ossicles of the inner ear. When the tympanic membrane is damaged, an infectious inflammatory process develops and otitis media occurs, requiring tympanoplasty and antibiotic therapy. Despite the extensive range of modern ENT surgical techniques, some injuries cannot be reconstructed without biocompatible composite materials, which should facilitate the process of functional recovery and have antibacterial properties, as bacterial and/or fungal biofilms are formed on the surface of the material [1].

In the last decade, nanomaterials based on natural polymer matrices have attracted particular attention due to their excellent biocompatibility, biodegradability, immunomodulatory and antimicrobial activity [1]. They are well established in the treatment of various diseases, *in vivo* imaging, providing support in tissue regeneration, as well as targeted drug delivery and controlled drug release, which helps to reduce systemic drug toxicity.

Among the natural biopolymers used in ENT surgery are chitosan, pullulan, collagen, hyaluronic acid, the effectiveness of which is confirmed both on cellular and animal models. Chitosan, as N-deacetylated derivative of chitin, is known for its own antioxidant activity and antibacterial activity against Gram-negative and Gram-positive bacteria [2]. Hyaluronic acid is of particular interest due to its exceptional ability to hold 1000 times more water molecules than its own weight, thus creating a favourable environment for healing. Furthermore, it not only exhibits unique properties of high biocompatibility and biodegradability, but also serves as an effective matrix for natural antibacterial agents while playing a pivotal role in stimulating angiogenesis and epithelialization. This enables the creation of materials with synergistic effects and superior antimicrobial efficacy. [3]. Collagen, being the main structural protein of the connective tissue of the body, provides an ideal matrix for cell adhesion, migration and proliferation, accelerates tissue regeneration [4]. Pullulan, an environment friendly  $\alpha$ -glucan polysaccharide, exhibits significant antiviral and antibacterial activity, anticoagulant, antithrombotic and anti-inflammatory properties and can also be used as a carrier of drug agents [5].

Thus, the key advantages of natural polymers are effective suppression of inflammation, stimulation of tissue regeneration and the possibility of local controlled delivery of therapeutic agents. The creation of nanomaterials based on them provides improved long-term functional results of ENT surgery, accelerated recovery of patients and reduced risk of complications.

The study was supported by the Russian Science Foundation, project number 25-73-20141.

[1] J. Spalek, IJMS 23, 2575(2022)

[2] I.-V. Platon, IJMS 24, 4452(2023)

[3] P. Snetkov, Pharmaceutics, 14, 1186(2022)

[4] M. Chelu, Eng. Proc. 56, 158(2023)

[5] M. Rai, IJMS 22, 13596(2021)

# Poster presentations

## Peculiarities of signal propagation under the influence of spin current in structures of magnetic material-normal metal type

N. Lobanov\*, V. Balaeva, M. Morozova

Saratov State University, 410071, Astrakhanskaya 83, Saratov, Russia

\*nl\_17@mail.ru

Modern electronics based on charge current control faces fundamental limitations in miniaturization and energy efficiency, which drives the development of alternative approaches such as magnonics and spintronics that utilize spins and collective excitations in magnetic materials. Magnonics, studying spin waves (magnons) for information transfer without charge movement [1], and spintronics, manipulating the electron's spin to create energy-efficient devices [2], already demonstrate breakthrough applications—from magnetic memory (MRAM) [3] to neuromorphic systems that mimic synaptic connections [4]. The synthesis of these directions paves the way for post-silicon electronics, combining low energy consumption, high speed, and bionic functionality.

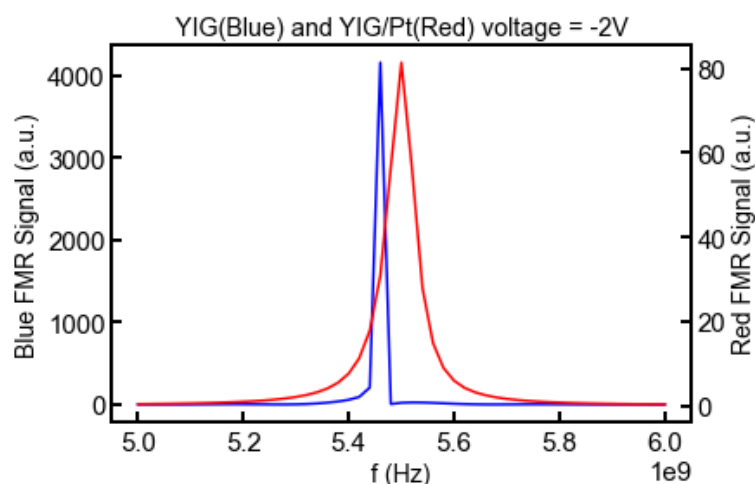


Figure 1. Dependence of the width and position of the band gaps on the ratio of the MC magnetizations.

In this work, micromagnetic modeling methods are used to study layered structures consisting of magnetic material (yttrium-iron garnet) and a normal metal (platinum). In particular, the influence of the spin current from the normal metal on the homogeneous precession in the magnetic material is considered, in other words, its impact on the ferromagnetic resonance curve.

On Figure 1, the ferromagnetic resonance lines for two cases are illustrated: a single layer of yttrium-iron garnet (YIG, blue curve) and a bilayer of yttrium-iron garnet/platinum (YIG/Pt, red curve) at negative voltage polarity on the metal. From the figure, it is evident that the ferromagnetic resonance curve for YIG/Pt, relative to that for YIG, is shifted to higher frequencies, the spectral width increases, and the resonance peak value decreases.

Thus, the use of an active layer expands the functionality of devices that can be used to create efficient elements of magnetic memory based on the principle of SOT (spin-orbit torque).

*This work was supported by the Russian Science Foundation (project № 23-79-30027).*

[1] V. V. Kruglyak, S. O. Demokritov, D. Grundler, J. Phys. D: Appl. Phys., 43(26), 264001(2010)

[2] S. D. Bader, S. S. P. Parkin, Annu. Rev. Condens. Matter Phys., 1(1), 71-88(2010)

[3] B. Dieny, et al., Nature Electronics, 3(8), 446-459(2020)

[4] J. Sinova, et al., Review of modern physics, 87(4), 1213-1260(2015)

# The effect of substrate selection on the structure and electronic properties of SrIrO<sub>3</sub> epitaxial thin films

A. Baydikova<sup>a,b,\*</sup>, I. Moskal<sup>a,c</sup>, N. Dubitskiy<sup>a,d</sup>, I. Moskal<sup>a</sup>, A. Petrzhik<sup>a</sup>, A. Shadrin<sup>a,c</sup>,

G. Ovsyannikov<sup>a</sup>

<sup>a</sup> Kotelnikov Institute of Radioengineering and Electronics of RAS, 125009, Moscow, Russia

<sup>b</sup> MIREA – Russian Technological University, 119454, Moscow, Russia

<sup>c</sup> MIPT (National Research University), 141701, Dolgoprudny, Moscow Region, Russia

<sup>d</sup> National Research University "Higher School of Economics", Faculty of Physics, 101000, Moscow, Russia

\*baydikova2001@mail.ru

Strontium iridate exhibits a strong spin-orbit interaction involving 5d iridium electrons, which leads to the formation of unusual electronic states. Strontium iridate possesses unique electronic and magnetic properties that can be used in the creation of new spintronic elements. These properties significantly depend on the synthesis method and the choice of monocrystalline substrates.

This work discusses the characteristics of thin films obtained by high-frequency magnetron sputtering from stoichiometric targets. Films were deposited on the following substrates: (001)SrTiO<sub>3</sub>, (110)NdGaO<sub>3</sub>, (001)(LaAlO<sub>3</sub>)<sub>0.3</sub>(Sr<sub>2</sub>TaAlO<sub>6</sub>)<sub>0.7</sub>, (011)Pb(Mg<sub>1/3</sub>Nb<sub>2/3</sub>)O<sub>3</sub>-PbTiO<sub>3</sub> (PMN-PT), (001)LaAlO<sub>3</sub>. The PMN-PT piezo substrate can significantly affect the electronic properties of the SrIrO<sub>3</sub> film deposited on it. Deposition occurred at a temperature of 730-770 °C in an Ar/O<sub>2</sub> atmosphere with a total pressure of 0.25 mbar. The growth parameter characteristics of the films were determined using X-ray diffraction and atomic force microscopy. Electrophysical measurements at T = 77-295 K allowed us to describe the temperature dependence of the conductivity.

Figure 1a shows a 2 $\Theta$ / $\omega$  diffractogram for a film grown on PMN-PT, which confirms single-phase growth. Figure 1b shows an atomic force microscope image of the surface morphology for SrIrO<sub>3</sub>/(110)NdGaO<sub>3</sub>. Root mean square (RMS) = 1.4 nm over an area of 5x5  $\mu\text{m}^2$  is typical for this series of samples.

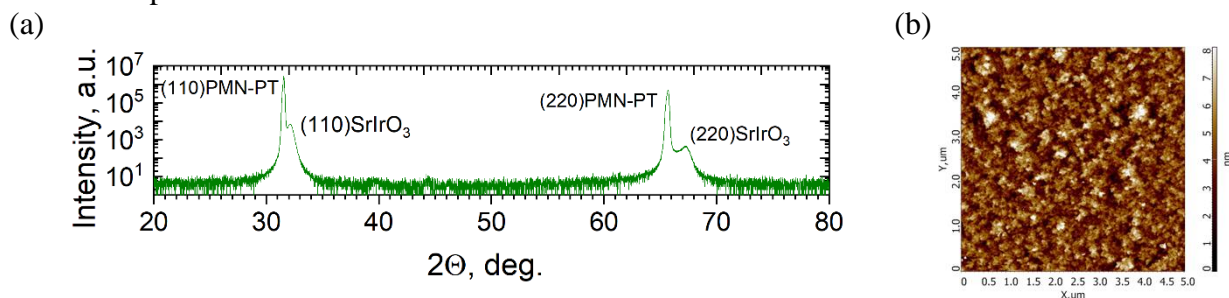


Figure 1. (a) 2 $\Theta$ / $\omega$  X-ray diffractogram for SrIrO<sub>3</sub>/(011)PMN-PT; (b) morphology of the surface of the SrIrO<sub>3</sub> thin film deposited on (110)NdGaO<sub>3</sub>.

Studies have shown a significant influence of synthesis parameters and substrate selection on the structural and electrophysical properties of SrIrO<sub>3</sub> epitaxial thin films.

The research was supported by the Russian Science Foundation grant No. 23-49-10006.

[1] V.A. Baydikova, N.V. Dubitskiy, I.E. Moskal et al., RENSIT 16(4), 509 (2024)

[2] I.E. Moskal, A.M. Petrzhik, Jr.V. Kislinskii et al., Bulletin of the Russian Academy of Sciences: Physics 88, 582 (2024)

# Study of ferromagnetic resonance and resistivity of multi-nanolayer films $\{[(\text{Co}_{40}\text{Fe}_{40}\text{B}_{20})_x(\text{SiO}_2)_{1-x}]/[\text{ZnO}]\}_{50}$ and their relationships

S. Gavriluk<sup>a,\*</sup>, L. Kotov<sup>a</sup>

<sup>a</sup> Syktyvkar state University, 167001, Oktyabrsky Ave., 55, Syktyvkar, Russia

\*Gavriluk-SI@yandex.ru

The study of conductivity and microwave magnetic resonance properties of multi-nanolayer films is of considerable interest for modern condensed matter physics and nanophysics [1]. Planar nanostructures based on magnetic composite and dielectric layers demonstrate unique magnetic and transport properties, which makes them promising for use in spintronics, magnetic field sensors and energy-efficient electronic devices. In this paper, we study the dependences of the parameters (width and position) of the ferromagnetic resonance (FMR) line and the specific conductivity of multi-nanolayer films  $\{[(\text{Co}_{40}\text{Fe}_{40}\text{B}_{20})_x(\text{SiO}_2)_{1-x}]/[\text{ZnO}]\}_{50}$  on a siall substrate, where 50 is the number of paired layers: composite - dielectric,  $x$  is the concentration of the metal alloy in the composite layer. Multi-nanolayer films on a glass-ceramic substrate were obtained by ion-beam sputtering of composite  $[(\text{Co}_{40}\text{Fe}_{40}\text{B}_{20})_x(\text{SiO}_2)_{1-x}]$  and ZnO dielectric films in an argon atmosphere, followed by deposition of particles of these films on glass-ceramic substrates, alternately occupying the deposition positions of the composite and ZnO dielectric [2]. Multi-nanolayer films on a glass-ceramic substrate consisted of composite (CoFeB+SiO<sub>2</sub>) layers and ZnO dielectric layers. The layer thickness varied from 0.2 to 3 nm. The dependences of the specific electrical resistance were measured by the four-probe method on direct current using a universal digital multimeter B7-78/1 along the plane of the film. Magnetic spectra in the field range from 0 to 0.7 T were recorded using a RE-1306 radio spectrometer at a frequency of 9.36 GHz [3]. Analysis of the obtained dependencies showed that the series of all 12 studied multi-nanolayer films and films can be divided into three parts. These three parts of the films characterize the initial, stable and final sections of the deposition of multi-nanolayer films. In the initial and final sections of the deposition of multi-nanolayer films, which are characterized by a strong change in the thickness of the composite and dielectric nanolayers, the functional relationship of the width  $\Delta B$  and the position of the FMR line  $B_r$  with the specific resistance is strongly nonlinear, and the physics of these dependencies in these areas still needs to be studied in more detail. For the middle part of the films, where the thickness of the film nanolayers remains practically constant, the line width  $\Delta B$  weakly depends on the specific resistance, and the position of the line  $B_r$  shifts towards larger magnetic fields from 0.27 to 0.29 T with an increase of two orders of magnitude in specific resistance. Taking into account the analysis of the obtained dependencies, it can be concluded that the width and position of the FMR line for these films have opposite dependencies on the specific electrical resistance.

The research was carried out with the support of the Russian Science Foundation grant, project No. 25-72-20063

- [1] P. Baranov, A. Kalashnikov, V. Kozub, Advances in the physical sciences. 189, № 8, 849 (2019)
- [2] A. Sitnikov, Y. Kalinin, V. Makagonov, V. Foshin, B. Volochaev., Physics of the Solid State. 66, issue 11, 1941 (2024)
- [3] L. Kotov, Z. Blinov, P. Kovalev, D. Zavarin, Yu Kalinin, A. Sitnikov, Bulletin RAS: Physics.88, Suppl.1, 80 (2024)

# Residual magnetization of a complex of carbon nanotubes and ferromagnetic nanoparticles

L. Ichkitidze<sup>a,b\*</sup>, V. Vagapov<sup>c</sup>, O. Demicheva<sup>c,d</sup>, M. Belodedov<sup>e</sup>, A. Gerasimenko<sup>a,b</sup>, D. Telyshev<sup>a,b</sup>,  
S. Selishchev<sup>b</sup>

<sup>a</sup> I.M. Sechenov First Moscow State Medical University, Trubetskaya str., 8, building 2, 119991, Moscow,  
Russia

<sup>b</sup> National Research University Moscow Institute of Electronic Technology (MIET), Zelenograd,  
Shokina square, 1, 124498, Moscow, Russia

<sup>c</sup> Russian New University, Moscow, st. Radio, 22, 105005, Moscow, Russia

<sup>d</sup> Research and Production Enterprise “Nanotechnology Center”, Aviamotornaya St. 55, Bldg. 31, 111124,  
Moscow, Russia

<sup>e</sup> Bauman Moscow State Technical University, 2th Baumanskaya St.5, Bldg. 1, 105005, Moscow, Russia

\*leo852@inbox.ru; ichkitidze\_l\_p@staff.sechenov.ru

Carbon nanotubes (CNTs) are widely used to create composite nanomaterials, including biocompatible composite nanomaterials exhibiting particularly high physical, mechanical or other characteristics that cannot be achieved by traditional means. However, the functional capabilities of nanomaterials containing magnetic nanoparticles (MNPs) and CNTs are significantly expanded, since the material simultaneously acquires electrically conductive and magnetic properties.

In this paper, we investigated composite nanomaterials containing a matrix of microcrystalline cellulose (MCC) or distilled water (H<sub>2</sub>O) with a filler in the form of multi-walled CNTs (MWCNTs) with embedded catalytic MNPs from Ni (MWCNTs MNPs Ni), or nanoparticles from Fe<sub>3</sub>O<sub>4</sub> (MNPs Fe<sub>3</sub>O<sub>4</sub>). In this case, in MWCNTs, the mass fraction of Ni MNPs was about 3 wt.%, in composite nanomaterials - also about 3 wt.% MNPs. The samples studied were in the form of powders, tablets, and suspensions. The powders were a stirred mixture of MCC and Ni MNPs (MCC//MWCNTs Ni MNPs); or MCC and Fe<sub>3</sub>O<sub>4</sub> MNPs (MCC//MWCNTs Fe<sub>3</sub>O<sub>4</sub>). The tablets were obtained by pressing the powders at a pressure of 300 bar, and the suspensions were obtained by diluting the specified powders in distilled water, which served as a matrix. All samples (powders, tablets, and suspensions) had the same composition: 97 wt %. MCC//3 wt %, MWCNTs Ni MNPs; 97 wt %. MCC//3 wt %. Fe<sub>3</sub>O<sub>4</sub> MNPs; 97 wt %. H<sub>2</sub>O //3 wt %; MWCNTs Ni MNPs; 97 wt %. H<sub>2</sub>O//3 wt %. Fe<sub>3</sub>O<sub>4</sub>.

The samples were magnetized in a constant vertical magnetic field of 500 G, the residual magnetic field was monitored by a Honeywell HMR2300 magnetometer with a resolution of ±0.1 mG. The methods of magnetic measurements and determination of residual magnetization coincide with those described in [1]. The specific residual magnetization was determined in units of G/g, and for all types of samples (powder, tablets, suspension) containing different magnetic particles (Fe<sub>3</sub>O<sub>4</sub> or Ni MNPs) it was in the range of 2÷5 G/g.

Therefore, along with MNPs Fe<sub>3</sub>O<sub>4</sub>, magnetic nanoparticles of MWCNTs and MNPs Ni can serve as magnetic agents in various applications. In particular, increasing the contrast of MRI, vector delivery of drugs in the body, or non-invasive monitoring of implants, such as neurostimulators, as well as non-invasive monitoring of nanomaterials in medical theranostics.

The work was carried out within the framework of the state assignment of the Russian Ministry of Education and Science (Project FSMR-2024-0003)

[1] Ichkitidze, L.P., et al. Springer Proceedings in Materials. PHENMA 2023. pp. 549–562

# Comparative study of inductive circuit configurations with planar coils for magnetic particle detection

A. Acuna<sup>a,b</sup>, A. Ignatov<sup>a\*</sup>, N. Yudanov<sup>a,b</sup>, A. Sobko<sup>a,b</sup>, L. Panina<sup>a,b</sup>, V. Rodionova<sup>a</sup>

<sup>a</sup> Immanuel Kant Baltic Federal University, 236004, Nevskogo 14, Kaliningrad, Russia

<sup>b</sup> National University of Science and Technology (MISiS), 119049, Leninsky Avenue 4, Moscow, Russia

\*a.ignatov@stud.kantiana.ru

Inductance-based magnetic sensors are widely utilized in diverse applications, including the measurement of magnetic fields, pressure, and temperature [1]. Their operational principle generally involves one or more coils incorporating a magnetic core, where the self-inductance or mutual inductance varies according to the physical parameter being sensed. One of the most used approaches is based on the measurement of the resonant frequency of an LC circuit containing the inductive sensor.

The presence of ferromagnetic materials alters the coil's inductance, thereby enabling detection of resonance frequency change in these systems. This functional mechanism is the basis for developing high-quality inductance measurement systems, offering high sensitivity, low cost, and strong selectivity [2,3]. However, for very high-sensitivity applications, this approach is compromised by the stability required for the oscillator circuit.

The present research compares several electronic circuit configurations for magnetic sensors based on inductive changes. The main circuit consists of three components: an oscillator, a filter, and a rectifier. The operational amplifier is employed for the oscillator due to its stability to temperature changes. The modification includes a Wheatstone bridge used to measure the imbalanced inductance, which is composed of two second-order differential filter circuits working at resonance conditions. In both circuits, a variable inductor is used to simulate the sensitive element, employing the Multisim program.

The objective of the comparison is to identify the most optimal characteristics, namely maximum output, stability, linearity, and high sensitivity, while ensuring an economical design. Both circuit variants have benefits and disadvantages in relation to each of the characteristics evaluated. high linearity, good sensitivity and stability are achieved with the first circuit. While the second circuit, despite not presenting high linearity, shows high sensitivity and good stability. However, optimization of these circuits in terms of resistance, capacitance and inductance is possible, depending on the specific application. The comparative study of different circuit configurations has led to an optimum design (in terms of both sensitivity and linearity) based on a second-order high pass filter. The simulation of this circuit leads to an overall maximum sensitivity of 8.86 V/mH.

The integration of inductive devices in Si technology has several potential advantages as compared to the macroscopic solenoids. However, planar inductors may have higher internal resistance due to intrinsic technological limitations when depositing the metal tracks using thin film technologies. This requires accurate modelling the inductance of the planar inductors to insure the resonant behavior. Here we developed a modelling method to calculate the planar coil inductance which is based on the calculation of total magnetic energy.

This work was supported by the Russian Science Foundation grant, project number 25-72-30009, <https://rscf.ru/project/25-72-30009/>

[1] E. Hristoforou et al., IEEE TM, 55(7), 1-14, (2019)

[2] S. Baglio et al., IEEE TIM, 56(5), 1590-1595, (2007)

[3] K. Diazde Lezana et al., Sens. Act. A: Phys., 91(1-2), 226-229, (2001)

# Microstructure and magnetic properties of Heusler alloy

## Ni-Mn-Ga-Cu in different structural states

A. Ivanova<sup>a\*</sup>, A. Karpenkov<sup>a</sup>, I. Musabirov<sup>b</sup>, E. Semenova<sup>a</sup>

<sup>a</sup> Tver State University, 170100, Zhelyabova, 33, Tver, Russia

<sup>b</sup> Institute for Metals Superplasticity Problems of Russian Academy of Sciences,  
450001, Stepana Khalturina, 39, Ufa, Russia

\*Ivanova.ai@tversu.ru

Heusler alloys are unique functional materials with shape memory effect and magnetocaloric effect, which are observed in alloys in the region of martensitic transformation [1,2].

For the study, an alloy of the composition  $\text{Ni}_{46.4}\text{Mn}_{17.4}\text{Ga}_{28.4}\text{Cu}_{7.8}$  was selected in two states: initial sample (IS), obtained by the argon-arc melting method and experimental sample (ES) after melting subjected to homogenization at 970°C for 24 hours, followed by slow cooling, extrusion at 700°C and vacuum annealing at 850°C for 2 hours.

The paper presents the results of studies of the microstructure, domain structure and magnetic properties of the samples.

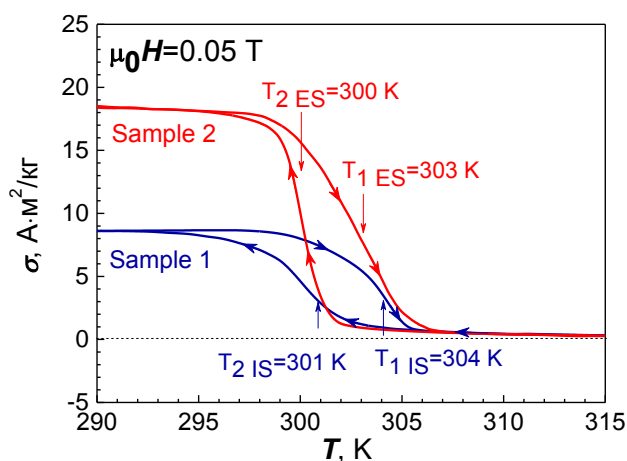


Figure 1. Temperature dependences of the specific magnetization of the initial and experimental samples

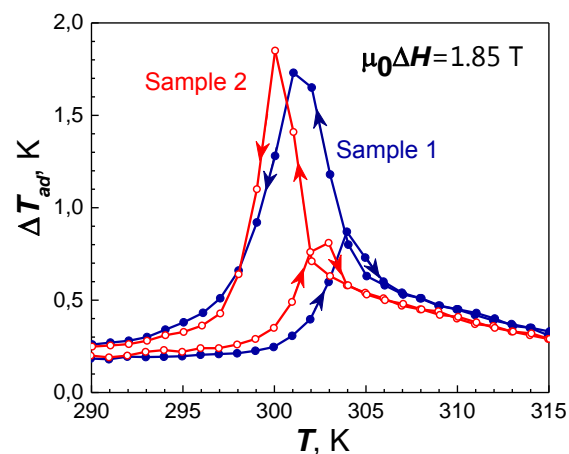


Figure 2. Temperature dependences of adiabatic change in temperature  $\Delta T_{ad}$  for the initial and experimental samples, measured in a magnetic field of 1.85 T

The data from vibration magnetometry and the method of measuring the adiabatic temperature change demonstrate a slight shift (1 K) of the phase transition temperature towards lower temperatures for the experimental deformed sample. Comparing the average temperature of direct martensitic transformation with the temperature of magnetic phase transition, it is possible to speak about merging of transitions into a single magnetostructural phase transition of the 1st kind from paramagnetic austenite to ferromagnetic martensite (magnetostructural PT) for both initial and experimental samples.

[1] I.I. Musabirov, R.M. Galeyev, I.M. Safarov. J.Magn. Magn. Mat. 514, 167160 (2020)

[2] A.I. Ivanova, I.I. Musabirov, E.M. Semenova et al. Physical and chemical aspects of the study of clusters, nanostructures and nanomaterials. 14, 132 (2022)



## Spin LED with intensity modulation

I. Kalentyeva\*, M. Ved, M. Dorokhin, A. Zdoroveyshchev, P. Demina

Lobachevsky State University of Nizhny Novgorod, 603022, Gagarin av. 23, Nizhny Novgorod, Russia

\*istery@rambler.ru

Combining discrete spintronic elements to working out their interactions and obtain new devices is a new stage in the development of this scientific field. This paper reports on the creation of a laboratory sample of a device emitting circularly polarized electroluminescence with the ability to control the intensity and circular polarization degree of the radiation independently by applying external magnetic fields.

The design of a spin LED consists of light-emitting and magnetoresistive parts-. The first part is based on a semiconductor heterostructure with an active region ( $\text{In}_{0.2}\text{Ga}_{0.8}\text{As}/\text{GaAs}$  quantum well) and a spin injector (multilayer ferromagnetic CoPt film [1]). The second part is a magnetoresistive element made in the form of a superlattice based on a structure with alternating layers of CoFeNi/Cu (thanks for the formation of the magnetoresistive element to D.Sc. M.A. Milyaev, IMP UB RAS).

When the device is introduced into an external magnetic field oriented in the plane of the layers, the resistance of the magnetoresistive element changes due to the giant magnetoresistance effect (fig.1). With a constant current through the structure, this leads to a redistribution of voltages on the magnetoresistive element and the light-emitting diode [2], as a result, modulation of the intensity of electroluminescence ( $I_{\text{EL}}$ ) of the LED is observed. The efficiency of this process is assessed by the relative change in radiation intensity depending on the magnetic field. It is worth noting that in the formed LEDs,  $I_{\text{EL}}$  modulation was observed at temperatures up to 300 K. The maximum change in the intensity of electroluminescence, when selecting the optimal value of the

electric current flowing through the structure, at room temperature was  $\sim 6\%$ .

When a magnetoresistive spin LED is introduced into an external magnetic field directed perpendicular to the surface of the layers, magnetization occurs until the CoPt ferromagnetic contact is saturated. As a result, when a direct electrical bias is applied, spin-polarized charge carriers are injected from the ferromagnetic CoPt contact into the active region of the light-emitting structure and recombine with the emission of partially circularly polarized radiation. By switching the polarity of the magnetic field, it is possible to remagnetize the CoPt ferromagnetic contact and change the sign of the circular polarization. Circularly polarized radiation was also observed at temperatures down to room temperature, the

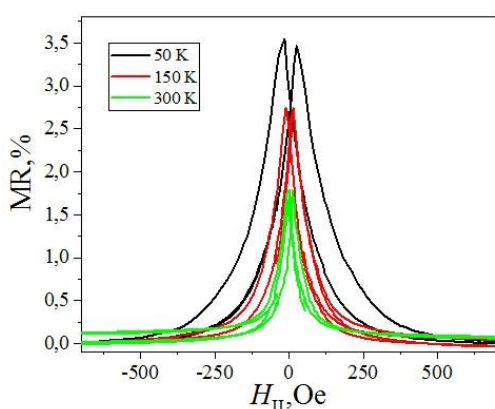


Figure.1. Dependence of the magnetoresistance value on the magnetic field.

maximum degree of circular polarization was  $\sim 0.4\%$ .

Thus, within the framework of this work, a combined device was formed that can be in four stable magnetic states (“high” – “low” radiation intensity, “positive” – “negative” circular polarization), which provides a twofold increase in information capacity without changing the area of the structure. From a practical point of view, the fundamental demonstration of a magnetoresistive spin light-emitting diode in four stable states can be used for wireless magnetometry, as well as for recording and transmitting information.

This work was supported by the Russian Scientific Foundation, project no. 25-29-00368.

[1] A.V. Zdoroveyshchev, Phys. of the Solid State 58, 2267 (2016)

[2] M.V. Ved, Appl. Phys. Lett. 118, 092402 (2021)

# Droplet Formation and Dynamics of Magnetic Fluid-Based Emulsions in a Microfluidic Chip in a Magnetic Field

P. Ryapolov, D. Kalyuzhnaya\*, E. Sokolov

Southwest State University, 305040, 50 Let Oktyabrya 94, Kursk, Russia

\*kalyuzhnaya.dariya@yandex.ru

One of the most popular methods for actively controlling droplets in microfluidics is manipulation via magnetic fields. Its advantages include cost-effectiveness, contactless control, and the absence of thermal and chemical effects [1]. Magnetic fluid (MF), which responds to the application of a magnetic field [2], can be utilised as a basis for the creation of magnetically sensitive emulsions, the properties of which can be altered by an external magnetic field.

The emulsion of magnetic fluid droplets was formed in a microfluidic chip with configured "flow focusing". Two samples of water-based magnetic fluid were used as the dispersed phase. MF1 has a density of  $\rho = 1120 \text{ kg/m}^3$ , a solid phase volume concentration of  $\phi = 3\%$ , a viscosity of  $\eta = 2.4 \text{ mPa}\cdot\text{s}$ , and a magnetisation  $M_S = 11.6 \text{ kA/m}$ . MF2 is characterised by the following properties:  $\rho = 1194 \text{ kg/m}^3$ ,  $\phi = 4.5\%$ ,  $\eta = 4.5 \text{ mPa}\cdot\text{s}$ , and  $M_S = 13.8 \text{ kA/m}$ . VDL 100 oil ( $\rho = 882 \text{ kg/m}^3$ ,  $\eta = 37 \text{ mPa}\cdot\text{s}$ ) with a mass fraction of hydrophobic surfactant Span 80 at 5% was used as the continuous phase. Both liquids were delivered to the microfluidic chip using a syringe pump. The flow rate of the dispersed phase (MF) remained constant at  $0.0054 \text{ }\mu\text{L/s}$ , while the oil flow rate varied from  $0.0054 \text{ }\mu\text{L/s}$  to  $0.027 \text{ }\mu\text{L/s}$ . A magnetic field was generated by two rectangular ferrite magnets measuring  $20\text{ mm} \times 10 \text{ mm} \times 5 \text{ mm}$  or two cubic neodymium magnets with a side length of 4 mm. These were positioned parallel to each other on either side of the microfluidic chip, separated by a distance of 17 mm, and could be shifted relative to the phase mixing zone either left or right. The magnetic field strength between the rectangular ferrite magnets was measured at  $15.5 \text{ kA/m}$ , while that between the cubic neodymium magnets was  $13.8 \text{ kA/m}$ . Results from numerical simulations of the magnetic field strength of the magnets corroborate the experimental data obtained using the TPU-01 milliteslameter.

Based on video recording of the generation of magnetic fluid droplets in the chip using the digital microscope MIKMED WiFi 2000X 5.0, and subsequent processing of the video sequence in the NI LabView software environment, graphs depicting the relationship between the diameter of the magnetic droplets, the oil flow rate, and the position of the magnets. These results demonstrated that an increase in the flow rate of the continuous phase leads to a reduction in the size of the magnetic droplets. Additionally, movement of the magnets resulted in changes in the diameters of the magnetic droplets at all magnet positions.

The findings indicate that the generation of droplets in the microfluidic chip can be regulated non-contact by an external magnetic field, without altering the configuration of the microchannel or the flow rates of the phases. The results of this study may serve as a foundation for the development of transport systems for drug delivery in microfluidic applications.

The work was supported by a grant from the Russian Science Foundation No 24-22-00309.

[1] J. Li, *Magnetochemistry*. 10, 4(2024)

[2] P. Ryapolov, *Nanomaterials*. 14, 2(2024)

## The composite systems based on ferromagnetic microwires for energy harvesting systems

V. Kolesnikova<sup>a\*</sup>, V. Salnikov<sup>a</sup>, V. Savin<sup>a</sup>, T. Ignatov<sup>b</sup>, A. Ignatov<sup>a</sup>, V. Rodionova<sup>a</sup>

<sup>a</sup> Immanuel Kant Baltic Federal University, 236004, Nevskogo 14, Kaliningrad, Russia

<sup>b</sup> MAOU secondary school No. 46, st. Letnyaya, 48, Kaliningrad, Russia

\*VGKolesnikova1@kantiana.ru

Multiferroic composites with nano- and micro-sized ferromagnetic active components possess perspectives in creation of technologies for energy harvesting and processing, as well as for biomedical applications [1-3]. That is why the study of internal magnetic interactions of the filler and its effect on changing the multiferroic properties of the composite is a topical issue.

The project is aimed to create a new type of multiferroic composite based on ferromagnetic Fe-based microwires and a piezoactive polymer for energy harvesting systems. The unique magnetic properties of Fe-based ferromagnetic microwires additionally with quick magnetostrictive respond at small values of the external magnetic field [4], lead to effectively induce mechanical stress in the piezoactive flexible matrix. Based on these properties, the flexible magnetoelectric composite, capable of converting free energy into a useful electrical signal, have been designed.

The pieces of  $\text{Fe}_{77.5}\text{B}_{15}\text{Si}_{7.5}$  and  $\text{Fe}_{74}\text{B}_{13}\text{Si}_{11}\text{C}_2$  microwires in the glass shell with metallic diameters from 10 up to 25  $\mu\text{m}$  have been used as the magnetic filler of the composites. Composites with ordered and disordered distribution of ferromagnetic microwires inside the polymer matrix have been produced. The magnetic properties of studied materials have been investigated with the vibration sample magnetometer. The dielectric and magnetoelectric properties of the produced composites have been investigated with the hand-made setups. The composites with disordered configuration of microwires inside the matrix shows the highest value of the magnetoelectric effect coefficient.

The conducted research of the project contributes to the understanding of the coupling mechanisms in two-phase magnetoelectric composites, ways to enhance the magnetoelectric effect through the use of a new composition with enhanced interface coupling, as well as the influence of anisotropic properties and high magnetic susceptibility on the formation of dielectric and magnetoelectric properties in flexible polymer composites.

- [1] L.N. Pereira, et. al., Designing Multifunctional Multiferroic Composites for Advanced Electronic Applications, (2024) 1–15
- [2] L.A. Makarova, et. al., Multiferroic Coupling of Ferromagnetic and Ferroelectric Particles through Elastic Polymers, Polymers (Basel). 14 (2022).<https://doi.org/10.3390/polym14010153>
- [3] K. Sobolev, et. al., Effect of Piezoelectric BaTiO<sub>3</sub> Filler on Mechanical and Magnetoelectric Properties of Zn<sub>0.25</sub>Co<sub>0.75</sub>Fe<sub>2</sub>O<sub>4</sub>/PVDF-TrFE Composites, Polymers (Basel). 14 (2022) <https://doi.org/10.3390/polym14224807>
- [4] V. Kolesnikova, et. al., The Interplay of Core Diameter and Diameter Ratio on the Magnetic Properties of Bistable Glass-Coated Microwires, Micromachines (2024) 1–9

# Template synthesis for the production of aligned arrays of Co nanowires as SERS-active platforms

E. Kozhina<sup>a,\*</sup>, S. Bedin<sup>a</sup>, I. Doludenko<sup>b</sup>, S. Kosolobov<sup>a</sup>, V. Drachev<sup>a</sup>

<sup>a</sup> Skolkovo Institute of Science and Technology, 121205, Territory of innovation center “Skolkovo”,  
Bolshoy blvd., 30, bld. 1, Moscow, Russia

<sup>b</sup> Shubnikov Institute of Crystallography, Kurchatov Complex of Crystallography and Photonics, National  
Research Centre “Kurchatov Institute,” 119333, Leninskiy Prospekt 59, Moscow, Russia

\*Elizaveta.kozhina@skoltech.ru

Template synthesis represents a highly promising approach for fabricating aligned nanowires or nanotubes with precise dimensions and tailored compositions. For instance, silver nanowires synthesized through this method have demonstrated strong SERS activity, making them effective for detecting organic compounds [1]. Moreover, the technique enables the creation of composite nanowires that combine magnetic and plasmonic metals, such as nickel and silver. This unique design allows for the fine-tuning of “hot spots”—nanoscale gaps between the tips of the nanowires—by applying an external magnetic field, which enhances the intensity of the SERS signal on about one order of magnitude [2]. It is worth noting that the combination with a magnetic metal such as cobalt can enhance the SERS signal in the UV range [3], which is promising for the study of biomolecules, such as nucleic acids and proteins, that exhibit absorption specifically in this spectral region. This opens up new possibilities for highly sensitive diagnostics of biologically significant analytes with high spatial resolution and reduced photoluminescence.

A critical limitation of cobalt when utilized as a SERS platform and in the investigation of its optical properties is its susceptibility to rapid oxidation, which is further exacerbated by localized heating induced by laser irradiation [4]. In the present study, to explore the interplay between the magnetic and optical properties of cobalt nanowires, the nanowires were synthesized within a polypropylene (PP) membrane characterized by low ultraviolet (UV) absorption. The nanowires embedded within the membrane exhibit a well-aligned orientation without any intersections. XRD analysis revealed that the acidity of the electrolyte significantly influences the crystallographic structure of the nanowires: pH 4 results in a hexagonal close-packed (hcp)  $\alpha$ -cobalt phase, while pH 2 leads to a face-centered cubic (fcc)  $\beta$ -cobalt phase. Hysteresis loops and absorption spectra were employed to assess the effect of an external magnetic field on the optical properties of the nanowires, enabling the identification of plasmonic resonance positions and the operational spectral range of such SERS platforms.

[1] E. Kozhina, Appl. Sci. 11, 1375 (2021)

[2] E. Kozhina, IEEE Magn. Lett. 13, 1 (2022)

[3] H. Bhatta, Sci. Rep. 9, 2019 (2019)

[4] E. Kozhina, Bull. Lebedev Phys. Inst. 51, S848 (2024)

# The Effect of Terbium and Hydrogen Addition on the Magnetic Properties of Medium-Entropy $\text{Gd}_{0.33}\text{Dy}_{0.33}\text{Y}_{0.33}\text{Ni}$ Alloy

A. Kurganskaya<sup>a,b,\*</sup>, Zh. Liu<sup>a</sup>, E. Kozlyakova<sup>a</sup>, I. Tereshina<sup>a</sup>, V. Verbetsky<sup>a</sup>, S. Mitrokhin<sup>a</sup>,  
A. Vasiliev<sup>a</sup>

<sup>a</sup> Lomonosov Moscow State University, 119991, Leninskie gory 1, Moscow, Russia

<sup>a</sup> Bauman Moscow State Technical University, 105005, Moscow, 2nd Baumanskaya str., 5, Moscow, Russia

\*kurganskaia.aa17@physics.msu.ru

Multicomponent alloys and compounds classified as medium- and high-entropy materials exhibit unique properties [1]. Hydrogenation of such materials can yield novel compositions exhibiting significantly altered physico-chemical properties, suitable for developing new advanced materials and designing on their basis efficient working bodies for industrial devices (refrigeration systems in particular) [2]. This work was aimed at studying how a combined addition of hydrogen and terbium to the multicomponent  $\text{Gd}_{0.33}\text{Dy}_{0.33}\text{Y}_{0.33}\text{Ni}$  compound affected its magnetic properties.

Magnetic characteristics of the two initial alloys ( $\text{Gd}_{0.33}\text{Dy}_{0.33}\text{Y}_{0.33}\text{Ni}$  and  $\text{Gd}_{0.25}\text{Tb}_{0.25}\text{Dy}_{0.25}\text{Y}_{0.25}\text{Ni}$ ) and their hydrides with maximum hydrogen amount per f.u. ( $\text{Gd}_{0.33}\text{Dy}_{0.33}\text{Y}_{0.33}\text{NiH}_3$  and  $\text{Gd}_{0.25}\text{Tb}_{0.25}\text{Dy}_{0.25}\text{Y}_{0.25}\text{NiH}_3$ ) were obtained with the use of a standard PPMS-9 setup. Curie temperatures were determined by the Belov-Arrot method. Magnetocaloric effect (MCE) was computed by an indirect method using Maxwell's equation [3]. The data obtained are placed in Table 1.

Table 1. Magnetic characteristics of the RNi-based multicomponent alloys and their hydrides

Sample	$M, \text{A} \cdot \text{m}^2 \cdot \text{kg}^{-1}$ ( $\mu_0 H = 7 \text{ T}$ , $T = 2 \text{ K}$ )	$T_C, \text{K}$ , Belov-Arrot method	$\Delta S_m, \text{J}/(\text{kg} \cdot \text{K}), (\mu_0 \Delta H = 7 \text{ T})$
$\text{Gd}_{0.33}\text{Dy}_{0.33}\text{Y}_{0.33}\text{Ni}$	136.33	60	10.9
$\text{Gd}_{0.33}\text{Dy}_{0.33}\text{Y}_{0.33}\text{NiH}_3$	122.12	6	16.5
$\text{Gd}_{0.25}\text{Tb}_{0.25}\text{Dy}_{0.25}\text{Y}_{0.25}\text{Ni}$	127.57	54	10.0
$\text{Gd}_{0.25}\text{Tb}_{0.25}\text{Dy}_{0.25}\text{Y}_{0.25}\text{NiH}_3$	113.94	3	15.2

It can be seen from the Table 1 that terbium addition slightly lowers  $M$ ,  $T_C$  and MCE values. Meanwhile hydrogenation also slightly decreases magnetization values, significantly lowers Curie temperatures, and increases MCE values by approximately 50%. The combination of Tb doping and adding maximum amount of hydrogen per f.u. yields the decrease of the Curie temperature down to 3 K. It opens up an opportunity for making a promising set of materials for helium liquefaction, transportation, and storage by varying the amount of hydrogen in the samples.

The study was conducted under the state assignment of Lomonosov Moscow State University.

Part of this study was conducted under the state assignrument of Lomonosov Moscow State University, project 122012400186-9.

[1] P. Kumari, A. K. Gupta, R. K. Mishra, M.S. Ahmad, R. R. Shahi, JMMM, 554 (2022).

[2] F. Marques, M. Balcerzak, F. Winkelmann, G. Zepon, M. Felderhoff, Energy Environ. Sci., 14 (2021).

[3] I.S. Tereshina, A.Yu. Karpenkov, A.A. Kurganskaya, V.B. Chzhan, S.A. Lushnikov, V.N. Verbetsky, E.S. Kozlyakova, A.N. Vasiliev, JMMM, 574 (2023).

# Magnetic properties of $\text{Cu}_2\text{MnBO}_5\text{:Cr}$ single crystals ludwigite

D. Popov, R. Eremina, R. Likero<sup>\*</sup>

Zavoisky Physical-Technical Institute, FRC Kazan Scientific Center of RAS, 420029, Sibirsky Trakt 10/7,  
Kazan, Russia

<sup>\*</sup>rodionlikerov@gmail.com

Ludwigite  $\text{Cu}_2\text{MnBO}_5$  is a compound with numerous possible magnetic structures due to the complex crystallographic structure of the ludwigite [1]. We studied  $\text{Cu}_2\text{MnBO}_5$  doped with Cr ions.

$\text{Cu}_2\text{MnBO}_5\text{:Cr}$  crystals were studied by X-ray fluorescence spectroscopy (XPS), electron paramagnetic resonance (EPR) in the temperature range from 50 to 120 K. Magnetization measurements were made in the temperature range from 5 to 315 K both FC and ZFC.

XPS revealed that Cr ions concentration is 0.08, Cu ions concentration is 2.05 and Mn ions concentration is 0.87. Temperature dependence of EPR spectrum showed that there are two critical points:  $T = 65$  K and  $T = 50$  K, where spectrum behavior changes significantly (Figure 1).

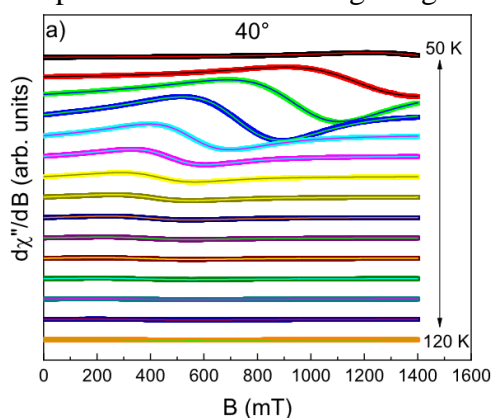
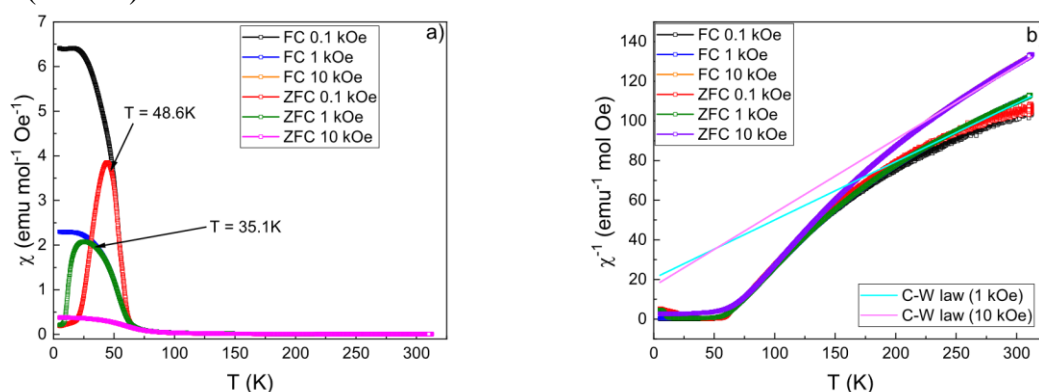


Figure 1. Temperature dependence of EPR spectrum of  $\text{Cu}_2\text{MnBO}_5\text{:Cr}$

Temperature dependence of magnetic susceptibility showed the existence of temperature shift of phase transition (Figure 2a) and temperature dependence of inverse magnetic susceptibility (Figure 2b) showed that for different magnetic field values (1 kOe and 10 kOe) the slope of approximation line changes suggesting the spin transition from high-spin  $\text{Mn}^{3+}$  ( $S = 5/2$ ) transition to low-spin  $\text{Mn}^{3+}$  ( $S = 1/2$ ).



Authors acknowledge the financial support for this research by the Russian Science Foundation (project no. 23-72-00047).

[1] A.A. Dubrovskiy, JETP Letters, , Vol. 106, No. 11, pp. 716–719. (2017)

# Development of the Ultra-sensitive Sensor of a Brain's Magnetic Field Based on the Magnetic Tunnel Junctions and Magnetic Concentrators

M. Lobkova<sup>a,\*</sup>, V. Kikteva<sup>a</sup>, P. Skirdkov<sup>a,b</sup>, K. Zvezdin<sup>a</sup>

<sup>a</sup> "New Spintronic Technologies" LLC, 121205, Innovation Centre Skolkovo, Bolshoi bulvar, 30/1, Moscow,  
Russia

<sup>b</sup> General Physics Institute of the Russian Academy of Sciences, 119991, st. Vavilova, 38, Moscow, Russia

\*m.shkanakina@nst.tech

Modern SQUID-based magnetoencephalography (MEG) systems have significant limitations, including the need for cryogenic cooling, bulky equipment, and limited spatial resolution [1-2]. In the same time, optically-pumped-magnetometers (OPM) [3] allow working in a wide frequency range and are less susceptible to electromagnetic interference due to optical measurements. It should be noted that long-term brain monitoring using OPM sensors leads to burns of the scalp at the site of electrode contact, in this regard, continuous brain research with OPM sensors is impossible without suspending monitoring for the cooling period. A promising solution is the development of minimally invasive sensors based on magnetic tunnel junctions (MTJs) [4] and innovative magnetic concentrators. The main requirements for the sensor's design are a small area ( $< 1 \text{ mm}^2$ ) and high sensitivity.

In order to achieve high sensitivity of MTJ, we conducted an analytical study of the electrical characteristics of MTJ with different properties of its magnetic layers. The paper presents a set of parameters affecting the MTJ sensitivity for each design, and as a result, the best design was selected. To reduce the impact of noise on the sensor operation, MTJs are connected using a Wheatstone bridge circuit. Also, to increase the sensitivity of the sensor, we used magnetic concentrators. We analyzed in detail the materials, size, and shape of magnetic concentrators in Ansys. Optimized parameters of MTJ and magnetic concentrators were used for the sensor design. It should be noted that the sensor size is limited by the area of the needle probe and is  $\sim 1 \text{ mm}^2$ . To simulate the sensor operation in Cadence, we developed a behavioral model of MTJ in the Verilog-A language. The model is based on the macrospin approach and takes into account the properties of magnetic layers in MTJ.

In our work the ultra-sensitive magnetic sensor of a brain's magnetic field was designed. Such a minimally invasive sensor will allow for the early detection of pathologies in the brain, including cancer and Alzheimer's disease.

This work was supported by Russian Science Foundation (grant № 25-12-00302).

- [1] Hari R., Neuroimage. 61, 2, 386-396 (2012)
- [2] Iivanainen J., NeuroImage. 147, 542-553 (2017)
- [3] Brookes M. J., Trends in Neurosciences. 45, №. 8, 621-634 (2022)
- [4] Yuasa S, Nature materials, 3, №. 12. 868–871 (2004)

# Spin-wave current in textured dielectric magnetic structures

I. Lyapilin<sup>\*</sup>, S. Novokshonov

M.N. Mikheev Institute of Metal Physics of UB RAS, Ekaterinburg, Russia

<sup>\*</sup>lyapilin@imp.uran.ru

Modern electronics and information technologies are mainly based on the use of electron charge. However, the field of spintronics is looking for efficient ways to utilise the spin properties of electrons and charge-neutral particles (magnons). From a practical point of view, effects based on spin momentum transfer (spintorque effect) and on topological properties of such structures (topological Hall effect), etc., are of interest.

In conducting magnetic structures, the electron spin current is due to conduction electrons and the external electric field. The situation is different in dielectric magnetic structures, in which the angular momentum transfer (spin-wave current) is associated with charge-neutral quasiparticles - magnons. Creation of spin-wave current in such systems (magnon flux) requires other external influences, for example, inhomogeneous temperature fields. Transferring spin moments less dissipatively than electrons, spin-wave current is considered promising for magnon spintronics. As in the case of conducting magnetic structures, the realization of magnon flux is accompanied by ‘emergenting’ spin-dependent electromagnetic fields, which have been discussed quite extensively in the literature [1-3]. ‘Emergeting’ fields -- real fields [4.5] that are measurable in transport studies [6]. These fields generate a spin-driven force, analogous to the Lorentz force, the manifestation of which is a universal phenomenon in magnetic metal. Unlike the spin electric field, which affects the dynamics of electrically charged particles, the spin magnetic field affects the dynamics of charge-neutral particles possessing spin. In conducting magnetic structures, the spin magnetic field deflects particles, depending on the spin orientation in opposite directions, thereby enhancing the spin current.

It is of interest to study the influence of the spin magnetic field realised in inhomogeneous dielectric magnetic structures in which spin-wave current (as well as energy transfer) is carried out by magnons (Bose-particles). A magnon is a charge-neutral quasiparticle possessing a magnetic moment (the spin of a magnon is equal to  $s=1$ ), which feels the influence of the spin magnetic field. In this work we investigate the influence of the spin magnetic field on the spin-wave current in nonuniform, dielectric magnetic structures realised by an inhomogeneous temperature field, when the Berry curvature leading to the fictitious magnetic field is due to the Dzyaloshinski-Moria exchange interaction [7].

This work was performed within the framework of the state assignment of the Ministry of Science and Technology of the Russian Federation (theme ‘Spin’ G. R. No. 122021000036-3)

- [1] S. E. Barnes, S. Maekawa. Phys. Rev. Lett. 98, 246601 (2007)
- [2] S. A. Yang, G.S. Beach, C. Knutson C, et.al. Phys. Rev. Lett. 102, 067201 (2009)
- [3] G. E. Volovik. J. Phys. C 20, L83 (1987)
- [4] Y. Yamane, S. Hematiyan. J. Ieda, et. al. Sci. 4, 6901 (2014)
- [5] S. Zhang and Z. Li. Phys. Rev. Lett. 93, 127204 (2004)
- [6] J. Ohe, Y. Shimada. Appl. Phys. Lett. 103, 242403 (2003)
- [7] I. Dzyaloshinsky. J. Phys. Chem. Solids 4, 241 (1958); T. Moriya, Phys. Rev. Lett. 4, 228 (1960)



# **New type of inductive compensation magnetization sensor for measurements in ultra-high magnetic fields: design and experimental results**

D. Maslov<sup>a,b</sup>, Yu. Kudasov<sup>a,b</sup>, E. Bychkova<sup>a</sup>, R. Kozabaranov<sup>a,b</sup>, V. Platonov<sup>a,b</sup>, I. Strelkov<sup>a</sup>,  
O. Surdin<sup>a,b</sup>, P. Katenkov<sup>a</sup>, A. Korshunov<sup>a</sup>, I. Makarov<sup>a</sup>, D. Botin<sup>a,b</sup>, A. Bykov<sup>a</sup>, A. Philippov<sup>a</sup>

<sup>a</sup> Russian Federal Nuclear Center - VNIIEF, 607188 Mira 57, Sarov, Russia

<sup>b</sup> SarFTI NRNU MEPhI, 607186 Dukhova 6, Sarov, Russia

\*maslov\_dem@mail.ru

A new type of induction compensation sensor for measuring magnetization of materials in ultra-high magnetic fields is proposed (Fig. 1). The sensor design determines its low sensitivity to both axial and radial inhomogeneities of the magnetic field. At the same time, the sensor has high electrical strength. Laboratory studies of the signal of the new sensor design in a non-uniform magnetic field were carried out, and a technique for determining the decompensation area was established. Magnetization measurements of various materials in the ultra-high magnetic field of the MK-1 generator were performed. A comparison of experimental data obtained using the new type of sensor and sensors of old designs is performed. The obtained magnetization curves are discussed.



Figure 1. Photograph of a new design compensation sensor.

The work was carried out within the framework of the scientific program of the National Center of Physics and Mathematics, direction No. 7 "Research in high and ultra-high magnetic fields".

# Temperature dynamics of magnetic and elastic oscillations in manganese-zinc spinel magnetic films of nonstoichiometric composition in the field of magnetic phase transition

L. Kotov, M. Mayburov\*

Syktyvkar State University, 167001, Oktyabrsky Ave., 55, Syktyvkar, Russia

\*mayburov@rambler.ru

Magnetoelastic dynamics of films and plates in the region of magnetic phase transitions (MPT) currently attracts much attention from researchers [1,2]. Modern studies of magnetic materials increasingly turn to nonlinear magnetoelastic dynamics, which is due to the large role of nonlinear effects in the creation of new devices, such as magnetic sensors and data storage devices, nonlinear frequency conversion devices, and ultra-sensitive magnetic field sensors [3]. Magnetic films based on manganese-zinc spinel (MZS) crystals are an attractive object for studying physical properties, since the magnetic crystallographic anisotropy constants  $K_1$  and  $K_2$  in these crystals can vary greatly depending on the sample temperature [4]. Moreover, for MZS crystals of nonstoichiometric composition, the first constant  $K_1$  at temperature  $T_S$  can become zero, called the temperature of the reorientation MPT. The strong change of the constants  $K_1$  and  $K_2$ , and the zero reversal of the first constant  $K_1$  at temperature  $T_S$ , allows us to reveal new magnetoelastic effects and find potential applications.

This work is devoted to the study of the temperature dynamics of magnetic and elastic oscillations in magnetic films made of the MZS crystal of non-stoichiometric composition  $Mn_{0.421}Zn_{0.44}Fe_{2.145}O_4$ , with different values of the anisotropy constants  $K_1$  and  $K_2$  corresponding to different temperatures of the crystal [4]. We calculated the time dependences of the amplitudes of magnetic and elastic oscillations of the MZS film at different constant magnetic fields based on the solution of a system of ordinary differential equations of magnetic and elastic dynamics [1,2]. It was assumed that the total sum of the energy densities of the crystalline film is equal to the sum of the densities of the magnetic, elastic and magnetoelastic energy. Based on the results of numerical calculations, the temperature dependences of the maximum amplitudes of the components of the magnetization vector  $m_{x,y}$ , and elastic displacement  $u_{x,y}$ , were constructed for the MZS layers in the region of the MPT at different values of the constant magnetic field strength. Thus, the work studied the nonlinear magnetoelastic dynamics of the MZS film in the temperature range including the reorientation MPT, where the first anisotropy constant  $K_1$  goes to zero. The obtained research results allow not only to expand theoretical knowledge in the field of magnetic phase transitions and nonlinear physics of oscillations, but also to offer practical recommendations for the development of new magnetic materials.

The research was supported by the grant of the Russian Science Foundation, project No. 25-72-20063

- [1] Kotov L.N., Bull. RUS: Physics 87, 3. (2023)
- [2] Kotov L.N., Physics of the Solid State 60, 1153 (2018)
- [3] Vlasov V.S., Acoustical Physics 68, 18 (2022)
- [4]. B.A. Goldin, L.N. Kotov, L.K. Zarembo, S.N. Karpachov, Spin-phonon interactions in crystals, Leningrad, Nauka (1991)

# Non-uniform magnetic structures in an FM / FeMn bilayer

A. Orlova<sup>a,\*</sup>, I. Fedotov<sup>a</sup>, N. Gusev<sup>a</sup>, S. Gusev<sup>a</sup>, E. Karashtin<sup>a,b</sup>, M. Sapozhnikov<sup>a,b</sup>, E. Skorokhodov<sup>a</sup>

<sup>a</sup>Institute for Physics of Microstructures RAS, Nizhny Novgorod, 603950, Russia

<sup>b</sup>Lobachevsky State University, Nizhny Novgorod, Russia, 603950

\*orlova.anastasia@ipmras.ru

Hybrid ferromagnet / antiferromagnet (FM / AFM) structures are of special interest due to their possible applications in magnetic memory devices, field sensors, and electromagnetic radiation generators. The main feature of such structures that is used in devices is the shift of the FM layer magnetization loop with respect to zero field due to the exchange coupling to the AFM layer called the exchange bias. The FM layer magnetization is usually called "pinned" on the AFM. This allows to create different non-uniform magnetic structures necessary for the field sensors or memory. An interesting opportunity is to control the frequency of a vortex spin-transfer nanoscillator via the exchange coupling of FM magnetization to the vortex state imprinted into AFM in micron-sized disks [1,2]. The main method used to create such non-uniform structures is thermal annealing at a temperature greater than the AFM blocking temperature in an applied magnetic field or in zero field.

In current work, we investigate the possibility to create non-uniform magnetic structures in an FM / AFM system where FeMn is used as AFM layer and Co or NiFe is used as FM. The structures were obtained by magnetron sputtering. We first obtain the shifted loops for both in-plane (Fig.1(a)) and perpendicular (Fig.1(b), black line) FM layer magnetization anisotropy by annealing at 160°C in an applied magnetic field of 1500Oe. After that, we anneal the sample with perpendicular anisotropy, starting at either magnetized (Fig.1(b), blue circle) or multidomain (Fig.1(b), red circle) state. We obtain magnetization hysteresis that is a sum of loops shifted to opposite sides (in different proportions) which is explained by a multidomain non-uniform state pinned into FeMn. Next, we create micron-sized disks from the film with in-plane FM magnetization anisotropy by electron lithography and ion etching. The imprinting of the vortex state from a ferromagnet into FeMn is realized by zero-field annealing at 160°C which is shown by MOKE and MFM measurements.

The work was supported by RSF Grant No. 25-72-20055.

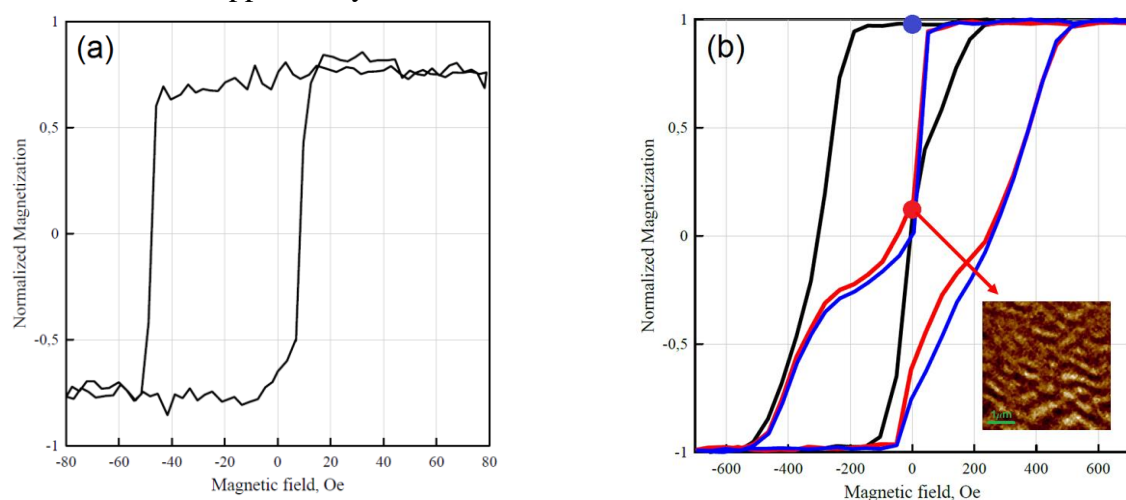


Figure. 1. Magnetization loop for (a) Ta(10)/Co(10)FeMn(20)/Ta(5) with in-plane FM magnetization and (b) Pt(10)/[Co(0.5)/Pt(1.5)]<sub>2</sub>/Co(0.5)/Pt(0.25)/FeMn(15)/Pt(5) as-grown (black line) and after annealing in zero field from a multidomain state (red circle; red line) or a magnetized state (blue circle; blue line) The inset shows MFM picture of a multidomain state. Thickness is in nm.

[1] J. Sort, K. S. Buchanan, V. Novosad, et al., PRL 97, 067201 (2006)

[2] K.S. Buchanan, A. Hoffmann, V. Novosad, S.D. Bader, J. Appl. Phys. 103, 07B102 (2008)

# Synthesis and Study of Structural, Magnetic and Magnetoelectric Properties of Sr-Substituted Bismuth Ferrite

D. Petrukhin<sup>\*</sup>, V. Salnikov, V. Belyaev, V. Rodionova

REC Smart Materials and Biomedical Applications, Immanuel Kant Baltic Federal University, 236004,  
Nevskogo 14, Kaliningrad, Russia

<sup>\*</sup>DAPetruhin@stud.kantiana.ru

Bismuth ferrite ( $\text{BiFeO}_3$ , BFO) is multiferroic material with combination of ferroelectric and magnetic orders at room temperature. However, its practical implementation is hindered by weak ferrimagnetism since antiferromagnetic order. Doping can be used to increase the magnetic moment in BFO, as well as to enhance its magnetoelectric properties due to spiral spin-modulated structure (SSMS) destruction. For this reason, the doping of BFO nanoparticles with the goal of enhancing their structural, magnetic, and electric properties is a promising area to obtain new functional materials. For instance, M.V. Shisode et al. [1] reported that strontium substitution in BFO leads to an increase in saturation magnetization  $M_S$ . Substitution with strontium provokes the destruction of SSMS. As a result, the mechanism of compensation of magnetic moments disappears, and an increase in spontaneous magnetization is observed — the magnetic moment becomes noticeable at the macroscopic level. At 30% of substitution an increase in residual magnetization  $M_R$  was observed [2].

In this work we successfully synthesized  $\text{Bi}_{1-x}\text{Sr}_x\text{FeO}_3$  ( $x = 0.20, 0.25, 0.30$ ) nanostructures by sol-gel technique and studied its structural, magnetic and magnetoelectric properties. Our results showed improvement of magnetic properties of  $\text{BiFeO}_3$  due to SSMS destruction. The study of magnetic properties by vibrating sample magnetometry has shown that an increase in the proportion of  $\text{Sr}^{2+}$  in the position of  $\text{Bi}^{3+}$  leads to a significant increase in saturation magnetization and change in coercivity, as well as lattice constant and nanoparticles size at room temperature. This combination of structural and magnetic properties lead to enhancement of magnetoelectric effect. These results are important for the manufacture of new BFO-based materials suitable for use in magneto-optics, spintronics, and energy storage devices.

This research was funded by the Russian Science Foundation under Project no. 25-72-30009 <https://rscf.ru/project/25-72-30009/>.

[1] M. Shisode, Appl Phys A Mater Sci Process 9, 124 (2018)

[2] T. Hussain, Prog Nat Sci Mater Int 5, 23 (2013)

# Design and synthesis of cobalt ferrite nanoparticles with different morphology: characterization of structural and magnetic properties

A. Prishchepa<sup>a,\*</sup>, A. Nikitin<sup>a,b</sup>, M. Abakumov<sup>a,b</sup>

<sup>a</sup> National University of Science and Technology «MISIS», 119049, Leninskiy Avenue 4, Moscow, Russia

<sup>b</sup> Pirogov Russian National Research Medical University, 117513, Ostrovityanova Street 1, Moscow, Russia

\*aprishcepa2000@yandex.ru

Cobalt ferrite magnetic nanoparticles (CF MNPs) have received considerable research because of the outstanding electromagnetic performance, chemical stability, mechanical hardness, high coercivity and saturation magnetization. Conventional techniques for preparation of nanoparticles including co-precipitation, sol-gel, hydrothermal, and aerosol-mediated techniques are simple and cost-effective, however these methods often lack control over the size, shape, size distribution, and crystallinity of nanoparticles. Also, nanoparticles synthesized by these methods tend to aggregate, which can significantly influence their magnetic properties and limit their practical applications. Thermal decomposition of metal acetylacetonate in a high boiling solvent is an alternative strategy for synthesizing monodisperse CF MNPs of a specific morphology and size.

In this work we synthesized a series of monodisperse CF MNPs with different morphology by thermal decomposition technique of metal–organic precursors. Cubic, spherical, clustered MNPs ranging in size from 5 to 99 nm were obtained by varying amount of surfactants (oleic acid, oleylamine) in the reaction mixture and incubation time. Characterization of morphology of MNPs was performed using transmission electron microscope. The hydrodynamic size of MNPs aqueous colloids was determined by dynamic light scattering technique. Phase composition of MNPs was studied by X-ray diffraction analysis. Magnetic properties of MNPs were analyzed by vibration magnetometry. Quantitative assessment of the content of iron and cobalt atoms in the composition of nanoparticles was carried out by the atomic emission spectroscopy method.

Varying the content of precursors and surfactants in the reaction mixture, changing the reaction duration, and using different synthesis methods we made it possible to obtain MNPs with different morphology. The results showed that an increase in the amount of oleic acid in the reaction mixture leads to the formation of nanoparticles with cubic morphology. To obtain clustered CF MNPs we reduced the amount of oleylamine in the reaction mixture. Synthesized CF MNPs show the cubic spinel structure  $\text{CoFe}_2\text{O}_4$ . CF MNPs samples are characterized by a high saturation magnetization and coercive force values, comparable to the value for massive cobalt ferrite. The synthesized CF MNPs with high coercivity and magnetization is potential to be utilized in biomedical applications. We showed that synthesized CF MNPs can be potentially used to convert magnetic field energy to heat and mechanical force for the use in magnetic hyperthermia and magneto-mechanical treatment.

The reported study was funded by Russian Science Foundation according to the research project №25-73-20132.

# Micromagnetic study of the domain structure of ThMn<sub>12</sub>-type compounds RFe<sub>11</sub>Ti

A. Guseva, A. Sinkevich, S. Smetannikova, E. Semenova\*, M. Lyakhova

Tver State University, 170100, Zhelyabova 33, Tver, Russia

\*semenova\_e\_m@mail.ru

Rare earth intermetallics based on RFe<sub>11</sub>Ti compounds are of particular interest as rare earth-lean materials with low rare earth content [1-3]. These compounds have a ThMn<sub>12</sub>-type crystal structure with I4/mmm space symmetry group and a body-centered tetragonal Bravais lattice. They are characterized by a wide compositional homogeneity range as well as relatively high values of Curie temperature, saturation magnetization and magnetocrystalline anisotropy constants [4, 5].

It has been shown in [4] that the Curie temperature for R(Fe,Ti)<sub>12</sub> compounds follows a similar patterns to other rare earth-iron intermetallic series, with a maximum at 607 K for R = Gd. Magnetic structures are ferrimagnetic for heavy rare earths and ferromagnetic for light rare earths with a wide variety of spin-reorientation transitions. At room temperature, these compounds have an “easy axis” and “easy plane” magnetocrystalline anisotropy type [5, 6].

The work presents the results of magnetic domain structure experimental study and micromagnetic parameters calculations of ThMn<sub>12</sub>-type intermetallic compounds RFe<sub>11</sub>Ti (R = Nd, Sm, Gd, Tb, Dy, Ho, Er).

Surface magnetic domain structure configuration of RFe<sub>11</sub>Ti single crystals has been investigated by magnetic force microscopy (MFM) using a SolverNext scanning probe microscope and commercially available low moment magnetic tips MFM-LM from TipsNano. The MFM images were obtained using the two-pass method and the phase mode.

The domain wall energy surface density  $\gamma$  was calculated based on the domain structure images and based on the theoretical approach. The final  $\gamma$  values range from 2.98 mJ/m<sup>2</sup> for the ErFe<sub>11</sub>Ti compound to 5.93 mJ/m<sup>2</sup> for the GdFe<sub>11</sub>Ti compound.

In some cases, the magnetic domain structure configuration on the sample surface depended on the surface preparation method. For samples with R = Tb and Dy, the domain patterns on the surface after polishing undergo significant changes with time due to the surface magnetic domain structure relaxation process.

This study was performed using the resources of the Laboratory of magnetic materials of the Center for Collective Use of Tver State University and was funded by the Ministry of Science and Higher Education of the Russian Federation in the framework of the State Program in the Field of the Research Activity (project No. 0817-2023-0006)

- [1] G. C. Hadjipanayis, Engineering. 6. 141-147 (2020)
- [2] Y. Hirayama, Scripta Materialia. 138. 62-65. (2017)
- [3] T. Ochirkhuyag, npj Comput. 8. 193. (2022)
- [4] B. P. Hu, J. Phys.: Condens. Matter. 1. 755-770. (1989)
- [5] K. Y. Guslienko, J. Magn. Magn. Mater. 150. 383-392 (1995)
- [6] I. S. Tereshina, J. Alloys Compd. 345. 16-19 (2002)

# Electronic and magnetic properties of cast and rapid melt quenched Cu-Co-Mn-Al Heusler alloys

Yu. Perevozchikova<sup>a</sup>, A. Semiannikova<sup>a,\*</sup>, V. Irkhin<sup>a</sup>, E. Chernov<sup>a</sup>, A. Lukoyanov<sup>a,b</sup>, A. Protasov<sup>a</sup>,

A. Korolev<sup>a</sup>, E. Marchenkova<sup>a</sup>, V. Marchenkov<sup>a,b</sup>

<sup>a</sup> M.N. Mikheev Institute of Metal Physics UB RAS, 620108, S. Kovalevskoy 18, Yekaterinburg, Russia

<sup>b</sup> Ural Federal University, 620062, Mira 19, Yekaterinburg, Russia

\*semiannikova@imp.uran.ru

New magnetic materials based on Cu-Co-Mn-Al Heusler alloys are promising for spintronics and microelectronics. The  $\text{Co}_2\text{MnAl}$  Heusler compound is half-metallic ferromagnet (HMF) with unusual electronic structure. A gap occurs at the Fermi energy level for one spin direction, while a gap is absent for spin-up charge carriers. This feature can lead to 100% spin polarization of charge carriers [1, 2].  $\text{Cu}_2\text{MnAl}$  is ferromagnetic (FM) with a relatively high Curie temperature (603 K) [3]. It is considered as a prototype for understanding electron correlations in Heusler intermetallics [4]. For practical application, a combination of certain electrical and magnetic properties is required. This can be achieved by changing the chemical composition of the material (the transition from  $\text{Co}_2\text{MnAl}$  to the  $\text{Cu}_2\text{MnAl}$ ) and/or its microstructure (for example, rapid melt quenching).

Therefore, the purpose of this work is to establish the relationship between the method of obtaining the alloy (cast and rapid melt quenched) with the structure, electronic, and magnetic properties of the  $(\text{Cu}_{1-x}\text{Co}_x)_2\text{MnAl}$  ( $0 \leq x \leq 1$ ) Heusler compounds during the transition from the HMF  $\text{Co}_2\text{MnAl}$  to FM  $\text{Cu}_2\text{MnAl}$ .

Cast  $\text{Cu}_2\text{MnAl}$ ,  $\text{Cu}_{1.5}\text{Co}_{0.5}\text{MnAl}$ ,  $\text{CuCoMnAl}$ ,  $\text{Co}_{1.5}\text{Cu}_{0.5}\text{MnAl}$ , and  $\text{Co}_2\text{MnAl}$  alloys were melted in an induction furnace. The prepared alloys were annealed at 1073 K in an argon atmosphere for 72 h, followed by cooling to room temperature. The resulting compounds were also subjected to rapid melt quenching at room temperature under a pressure of 0.28 atm in a purified argon atmosphere. The cooling rate was about  $10^4$ – $10^5$  deg/sec. The electrical resistivity was measured using the standard four-contact method from 78 K to room temperature. The magnetization was investigated at  $T = 4.2$  K and in magnetic fields up to 50 kOe. The electronic structure was calculated using DFT methods with different types of exchange-correlation potential.

The alloys studied are ferromagnetic. It was revealed that the electrical resistivity of all the alloys has a metallic type and decreases when replacing Co with Cu. Dependences of the residual resistivity  $\rho_0$  and spontaneous magnetization  $M_s$  on  $x$  correlate to a sufficient degree with each other. The results obtained are useful in selecting suitable materials for spintronics.

The research was supported by RSF (project No. 25-22-00481).

[1] R.A. de Groot et al., Phys. Rev. Lett. 50, 2024 (1983)

[2] V.Yu.Irkhin, M.I. Katsnelson, Phys. Usp. 37, 659 (1994)

[3] T. Graf et al., Progr. Solid State Chem. 39, 1 (2011)

[4] X. Liu et al., Phys. Rev. B 108, 094405 (2023)

## **Study of one-dimensional magnets in a ultra-high magnetic field**

I. Strelkov<sup>a,\*</sup>, A. Bykov<sup>a</sup>, A. Vasiliev<sup>c</sup>, S. Galanova<sup>a</sup>, Yu. Kudasov<sup>a,b</sup>, V. Platonov<sup>a,b</sup>, I. Makarov<sup>a</sup>,  
D. Maslov<sup>a,b</sup>, O. Surdin<sup>a,b</sup>, R. Kozabaranov<sup>a</sup>, P. Katenkov<sup>a</sup>, A. Korshunov<sup>a</sup>, P. Repin<sup>a</sup>, A. Filippov<sup>a</sup>

<sup>a</sup> Russian Federal Nuclear Center – VNIIEF, Sarov, Russia

<sup>b</sup> Sarov Institute of Physics and Technology, NRU MEPhI, Sarov, Russia

<sup>c</sup> Moscow State University named after. M.V. Lomonosov, Moscow, Russia

\*strelok64820@mail.ru

The magnetization of one-dimensional magnets was measured in magnetic fields up to 500 T. The study of  $\text{Gd}_2\text{BaNiO}_5$  and  $(\text{Y}_{1-x}\text{Nd}_x)\text{BaNiO}_5$  compounds containing Haldane spin chains of  $\text{Ni}^{2+}$  ( $S=1$ ) will be presented. Substitution of rare-earth ions allows changing the intensity of interchain interactions. The measurements were carried out at liquid helium temperature. The source of the superstrong magnetic field was the magnetocumulative generator MK-1 [1]. Magnetization curves of the compounds were obtained. The transition of the initially antiferromagnetic subsystem of gadolinium ions to the ferromagnetic state, as well as ferromagnetic ordering of nickel chains are observed.

Samples were provided by the Physics Department of Moscow State University and the Chemistry Department of the Higher School of Economics.

The work was carried out within the framework of the scientific program of the National Center of Physics and Mathematics, direction No. 7 "Research in high and ultra-high magnetic fields".

[1] Boriskov G.V. et al., Uspekhi Fizicheskikh Nauk 181 (4) 441 - 447 (2011).



# The Effect Of Cu Doping On The Phase, Structure And Magnetic Properties Of $\text{Mn}_{55-x}\text{Al}_{36}\text{Ga}_9\text{Cu}_x$ ( $x = 0, 1, 2, 3, 4, 5$ ) Alloys

N. Vazhinskii<sup>a,\*</sup>, K. Nechaev<sup>a</sup>, A. Fortuna<sup>a</sup>, M. Gorshenkov<sup>a</sup>, D. Karpenkov<sup>b</sup>

<sup>a</sup> National University of Science and Technology MISIS, 119049, Leninsky prospect 4-1, Moscow Russia

<sup>b</sup> Lomonosov Moscow State University, 119991, Leninskie gory 1, Moscow, Russia

\*nikita\_vazhinskiy@mail.ru

By combining the positive effects of Ga and Cu doping on the stability and flow stress [1] of the ferromagnetic  $\tau$ -phase, it is possible to improve the hysteresis magnetic properties of hard magnetic Mn-Al magnets. This work focuses on the determination of the structural state and magnetic properties, as well as their correlation with the Cu concentration due to the heat treatment on the Mn-Al-Ga alloys. Alloys with the nominal compositions  $\text{Mn}_{55-x}\text{Al}_{36}\text{Ga}_9\text{Cu}_x$  (where  $x = 0, 1, 2, 3, 4, 5$ ) were obtained using induction melting. A stable ferromagnetic phase content of approx. 98 vol.% was achieved for the as-cast  $\text{Mn}_{51}\text{Al}_{36}\text{Ga}_9\text{Cu}_4$  alloy. After homogenization annealing and quenching at the critical cooling rate the specimens contained the ferromagnetic  $\tau$ -phase and the  $\gamma_2$ -phase. Differential scanning calorimetry analysis showed shifting of the phase transition peaks toward lower temperatures with an increase in the Cu concentration. Annealing of the alloys with up to 3 at.% Cu produced a high volume of the  $\tau$ -phase (up to 93.9 vol.%) and the as-annealed alloys with 4 and 5 at.% Cu exhibited quite a slow  $\gamma_2$  to  $\tau(\gamma_2)$  transition due to the formation of chemical inhomogeneity in the  $\gamma_2$  phase. Analysis of the magnetic properties of the as-annealed  $\text{Mn}_{55-x}\text{Al}_{36}\text{Ga}_9\text{Cu}_x$  specimens ( $x = 1, 2, 3, 4, 5$ ) showed a high maximum magnetization (up to 369 kA/m for  $\text{Mn}_{52}\text{Al}_{36}\text{Ga}_9\text{Cu}_3$ ) which is comparable with that of the Mn-Al-Ga ternary alloys. Microstructural studies have confirmed the formation of a non-magnetic  $\gamma_2$  layer at the grain boundaries of the ferromagnetic phase with precipitates of the soft magnetic K-phase at Cu contents of 4 and 5 at.%. The Cu solubility limits in the  $\tau(\epsilon)$  and  $\tau(\gamma_2)$  ferromagnetic phases were determined to be 2.5 and 4.5 at.%, respectively.

[1] Jürries F. et al., Scientific Reports, 10 (2020) 1-10.

## Nuclear resonance methods for the study of nanowires containing iron and cobalt

K. Frolov<sup>a</sup>, A. Gippius<sup>b,c</sup>, D. Zagorskiy<sup>a\*</sup>, I. Doludenko<sup>a</sup>, S. Chuprakov<sup>d</sup>, I. Perunov<sup>a</sup>, A. Tkachev<sup>c</sup>,  
S. Zhurenko<sup>c</sup>, A. Muslimov<sup>a</sup>, I. Blinov<sup>d</sup>

<sup>a</sup> NRC "Kurchatov Institute", Moscow, Russia

<sup>b</sup> Lomonosov Moscow State University, Moscow, Russia

<sup>c</sup> Lebedev Physical Institute, Moscow, Russia

<sup>d</sup> M.N. Mikheev Institute of Metal Physics, Ural Branch of RAS, Yekaterinburg, Russia

\* dzagorskiy@gmail.com

Arrays of nanowires (NWs) of iron with different diameters and NWs containing cobalt and copper in different ratios were synthesized by the matrix method and studied by Mössbauer spectroscopy and NMR. For all samples, growth features were revealed and optimal synthesis modes were proposed. The obtained samples were studied by SEM and X-ray phase analysis.

A series of NW samples of pure iron with different diameters - from 30 to 600 nm - was obtained. Control samples of Layered iron and Bulk iron were also obtained. Using the X-ray method, it was determined that the structure of the nanoparticles is bcc (with a lattice parameter  $a = 2.872 \text{ \AA}$ ) and the size of the crystallites was estimated as 20-50 nm. For the first time, comparative studies were conducted for this type of objects using the Mössbauer spectroscopy method and the nuclear magnetic resonance method (NMR, in zero external magnetic field). The two methods independently determined the parameters of the hyperfine interaction, in particular, the values of the hyperfine magnetic fields on the iron nuclei were obtained. The values of the hyperfine magnetic field  $B_{hf}$  (corresponding to  $\alpha$ -Fe) in all samples of the NW and the control Layer are practically the same and are 0.1 T – 0.3 T less than the value of  $B_{hf} = 33 \text{ T}$  for the Bulk sample. The corresponding values of the isomer shift and quadrupole parameters are also practically independent of the NW diameter and are in the range characteristic of bulk  $\alpha$ -Fe. The field values obtained by the two methods differ slightly. The reason for this discrepancy may be that Mössbauer and NMR spectroscopy “feel” such a parameter as the hyperfine magnetic field on nuclei differently.

NMR peaks of all NWs array samples and the control Layered sample are significantly broadened compared to the peak of the control Bulk sample. The reason for this is a significant spread in the values of local magnetic fields on the iron nuclei, due to significant heterogeneity of the material - crystallite boundaries, etc. The values of relaxation times  $T_1$  and  $T_2$  indicate a significant acceleration of relaxation in NW relative to Bulk  $\alpha$ -Fe.

The orientation of the magnetization vector in NW (which spontaneously arose during their production) with respect to the direction of gamma quanta was determined - for NW this direction lies within the cone with an opening of 40 degrees, for the layered sample the misorientation is higher than -60-70 degrees, while the Bulk sample is magnetically isotropic. For cobalt-copper samples, it was shown that changing the selected growth modes (from potentiostatic to pulsed) allows one to switch from the synthesis of homogeneous NWs from the CoCu alloy to the synthesis of layered Co/Cu NWs.

Samples with different copper contents were obtained by changing component ratio in electrolyte.

The NMR spectra show a line at 218 MHz, corresponding to the fcc phase of cobalt. Additionally, the spectra show lines at 200, 182, and 164 MHz, which correspond to Co atoms in the coordination of which there are from one to three Cu atoms, respectively. In both cases, this allows one to estimate the number of Co atoms with different coordination. This serves to estimate the parameters of the solid solution or to characterize the boundaries between the layers and their length and “blurriness”.

Work was carried out within the state assignment of NRC “Kurchatov Institute”  
The Co NMR study was performed under the state assignment on “Function” No. 122021000035-6/

# Magnetic heterostructures $WTe_x$ /heavy metal/ferromagnet.

## Structure, magnetic and transport properties

S. Silina<sup>\*</sup>, N. Crernousov, Zh. Namsaraev, M. Bazrov and A. Kozlov

Laboratory of spin-orbitronic, Institute of High Technologies and Advanced Materials, Far Eastern Federal University, 690922, 320, 10 Ajax bay, Russkii Island Vladivostok, Russia

<sup>\*</sup>silina.sk@dvfu.ru

Modern research in spintronics is focused on finding new two-dimensional materials with strong spin-orbit coupling, acting as an interface modifier and capable of effectively controlling the magnetic properties of thin films [1]. In this paper, we investigate the effect of a two-dimensional topological material  $WTe_x$  on the characteristics of thin-film structures W/CoTb/W and Pd/Co/Pd and other heavy metal/ferromagnet structures.

A comprehensive experimental approach was used for the study. Thin film structures were grown by magnetron sputtering and molecular beam epitaxy under ultra-high vacuum conditions. Ultraviolet photolithography was used to create nanostructures using standard templates for Hall structures and subsequent ion-plasma etching.

Magnetic heterostructures were examined using scanning tunneling microscopy (STM) to analyze the surface morphology and calculate the surface roughness, high-energy electron diffraction (RHEED) to study the crystal structure, Kerr magneto-optical microscopy to study the dynamics of domain wall displacement, detect the SOT effect and determine the Dzyaloshinsky-Moriya interaction (DMI).

Our studies revealed several important effects that arise when introducing  $WTe_x$  into the studied structures. In the W/CoTb/W system, a significant increase in the efficiency of spin momentum transfer was observed, which is explained by the additional contribution of the spin-orbit interaction from  $WTe_x$ . In the study of the Pd/Co/Pd structure, an asymmetry in the nucleation/motion of domain walls was found, which is a key argument in favor of a strong DMI interaction at the interface with  $WTe_x$  [2]. Also, during the experiment, the unusual behavior of the Anomalous Hall Effect (AHE) was observed, which correlates well with the change in the domain structure observed on the Kerr microscope. This indicates a strong relationship between the transport and magnetic properties in the heterostructures studied.

The study demonstrates the high potential of  $WTe_x$  for controlling the magnetic and spin properties of thin-film structures. The results obtained are of great importance for the development of new directions in spintronics, namely: the development of energy-efficient magnetization switching devices using SOT, the development of new approaches to the design of spin logic devices.

Further research into the influence of the  $WTe_x$  thickness on magnetic properties, as well as the study of the possibilities of controlling these properties using an electric field, seems particularly promising.

This work was financially supported by Russian Scientific Foundation, under the grant № 23-42-00076

[1] Xie Q. et al. Giant enhancements of perpendicular magnetic anisotropy and spin-orbit torque by a MoS<sub>2</sub> layer //Advanced Materials. (2019) 31, **21**. 1900776.

[2] Pai C. F. et al. Determination of spin torque efficiencies in heterostructures with perpendicular magnetic anisotropy //Physical Review B. (2016) 93, **14**. 144409

## Diffusion of aqueous DMSO solutions of different concentrations in rat skin *ex vivo*

V. Genin<sup>a,\*</sup>, A. Petrov<sup>a</sup>, V. Tuchin<sup>a,b</sup>, E. Genina<sup>a</sup>

<sup>a</sup> Department of Optics and Biophotonics, Saratov State University, 410012, Astrakhanskaya 83, Saratov, Russia

<sup>b</sup> Institute of Precision Mechanics and Control Problems of the Russian Academy of Sciences, Federal Research Center "Saratov Scientific Center of the RAS", 410028, Rabochaya 24, Saratov, Russia

\*versetty2005@yandex.ru

DMSO is a biocompatible drug widely used in biomedicine to increase skin permeability [1]. It can also be used as a component of optical clearing agents [2]. However, the diffusion of DMSO solutions with various concentrations in the skin has not been sufficiently studied.

The diffusion study of aqueous DMSO solutions with volume concentrations of 50, 60, 70, 80, 90 and 100% was carried out in rat skin *ex vivo*. The refractive indices of the solutions were measured at room and physiological temperatures using an Abbe multiwave refractometer in the wavelength range of 480-1550 nm. The study material consisted of 52 samples. Thickness of the samples was measured using a micrometer before and after DMSO exposure.

The effective diffusion coefficient characterizes the average rate of agent flow into the tissue and interstitial fluid from the tissue. The effective diffusion coefficient of DMSO in rat skin was estimated from the measured collimated transmission spectra of the samples. Collimated transmittance was detected in the range of 600-900 nm for 0.5-4.5 hours (until the transmission value stabilized).

The diffusion coefficients were calculated in accordance with the mathematical model [3] and averaged over wavelengths of 600, 700, 800 and 900 nm. The algorithm is based on the minimization of the objective function, which includes theoretical and experimental data on the kinetics of changes in the collimated transmission of samples of the studied tissues during immersion of the agent in them, with the help of which the value of the diffusion coefficient of DMSO in biological tissues is restored [3]. The data obtained are presented in Table 1.

*Table 1. Diffusion coefficients of aqueous DMSO solutions of different concentrations in rat skin samples ex vivo*

Concentration of DMSO solution, %	Diffusion coefficients at different wavelengths, $10^{-7} \text{ cm}^2/\text{s}$				
	600 nm	700 nm	800 nm	900 nm	Average by concentration
50	$8.7 \pm 5.1$	$10.1 \pm 6.8$	$10.0 \pm 6.3$	$10.6 \pm 8.7$	$9.9 \pm 6.6$
60	$16.2 \pm 14.6$	$14.1 \pm 12.6$	$15.2 \pm 13.4$	$21.2 \pm 20.3$	$16.2 \pm 13.5$
70	$4.7 \pm 1.9$	$7.8 \pm 5.7$	$7.1 \pm 6.2$	$6.6 \pm 2.4$	$6.8 \pm 4.9$
80	$5.4 \pm 1.5$	$4.7 \pm 0.7$	$4.4 \pm 1.2$	$4.3 \pm 0.1$	$4.7 \pm 1.1$
90	$7.0 \pm 4.3$	$7.0 \pm 5.0$	$6.8 \pm 4.8$	$8.0 \pm 4.9$	$7.1 \pm 4.6$
100	$5.7 \pm 0.1$	$7.2 \pm 1.5$	$8.0 \pm 2.2$	$9.1 \pm 2.3$	$7.5 \pm 1.9$

These results correlate well with the results of other researchers [4].

The obtained data on DMSO diffusion in skin may help in developing effective protocols for optical clearing.

The study was supported by the Russian Science Foundation (Project No. 23-14-00287).

[1] J.-C. Xiang, The Applications of DMSO. Solvents as Reagents in Organic Synthesis, 315-353(2017).

[2] P. Karande, Biochim. Biophys. Acta 1788, 2362-73(2009)

[3] D.K. Tuchina, J. Biophotonics 8, 332-346(2015)

[4] P. Liu, J. Biomed. Opt. 18, 20507(2013)

# Study of Optical Clearing of Lung Tissue Using Inhalation Aerosols by Multi-wave Refractometry

E. Lazareva<sup>a,b,\*</sup>, A. Bucharskaya<sup>c,d</sup>, V. Tuchin<sup>a,b,d,e</sup>

<sup>a</sup> Institute of Physics, Saratov State University, 410012, 83 Astrakhanskaya st., Saratov, Russia

<sup>b</sup> Laser Molecular Imaging and Machine Learning Laboratory, Tomsk State University, 634050, 36 Lenin Ave., Tomsk, Russia

<sup>c</sup> Centre of Collective Use, Saratov State Medical University n.a. V.I. Razumovsky, 112 B. Kazach'ya, Saratov 410012, Russia

<sup>d</sup> Science Medical Center, Saratov State University, 410012, 83 Astrakhanskaya st., Saratov, Russia

<sup>e</sup> Institute of Precision Mechanics and Control, Federal Research Center «Saratov Scientific Center of the Russian Academy of Sciences», 410028, 24 Rabochaya st., Saratov, Russia

\*lazarevaen@list.ru

Optical clearing of lung tissue helps to reduce light scattering, which allows to significantly improve visualization of tissue structure and increase the probing depth of optical radiation [1]. This is of great importance for monitoring the impact of viral infection on alveolar tissue structure and oxygen transport [2, 3]. It should also be noted that air-filled lungs present significant challenges for optical imaging, including optical coherence tomography (OCT), confocal and two-photon microscopy, and Raman spectroscopy, due to the large refractive index mismatch between the alveolar walls and the enclosed air-filled region[4].

In this study, the effect of *in vivo* inhalation of a 50% polyethyleneglycol/50% glycerol mixture on rat lung tissue was investigated using multi-wavelength refractometry. The refractive indices of lung tissue from a control group of laboratory animals and from a group of animals after long-term inhalation exposure to the optical clearing agent mixture were compared. The study of the effect of a mixture of 50% polyethyleneglycol and 50% glycerol was performed on a multi-wave Abbe refractometer DR-M2/1550 (Atago, Japan).

The results showed that daily 25-minute inhalation of a mixture of polyethyleneglycol and glycerol after 28 days causes an increase in the refractive index of lung tissue by  $0.0083 \pm 0.0060$  in the spectral region of 480-1550 nm. The obtained results are in good agreement with the literature data of other scientific groups and further studies will allow a more detailed study of the *in vivo* effect of optical clearing agents on biological tissues, which is necessary for the development of the application of optical methods in medicine and biophotonics.

The work was supported by the Russian Science Foundation (project No. 23-14-00287, <https://rscf.ru/project/23-14-00287/>)

[1] A.N. Bashkatov et. al., J. Biomed. Opt. 23(9), 091416 (2018)

[2] C. Kumpitsch et. al., BMC Biol 17, 87, (2019)

[3] L. Knudsen, M. Ochs Histochem. Cell. Biol. 150(6), 661–676 (2018)

[4] A. Bucharskaya et. al, Biophys. Rev. 14, 1005–1022 (2022)

## Dumbbell-shaped nanoparticles induce cell death of human hepatocarcinoma cells during magneto-mechanical treatment

S. Pshenichnikov<sup>a\*</sup>, E. Korepanova<sup>a</sup>, A. Anikin<sup>a</sup>, D. Petrukhin<sup>a</sup>, V. Salnikov<sup>a</sup>, A. Motorzhina<sup>a</sup>,  
N. Chmelyuk<sup>b</sup>, V. Rodionova<sup>a</sup>, K. Levada<sup>a\*</sup>

<sup>a</sup>REC Smart Materials and Biomedical Applications, Immanuel Kant Baltic Federal University,  
Kaliningrad, Russia

<sup>b</sup>National University of Science and Technology MISIS, Moscow, Russia

\*SPshnikov@gmail.com

Nanomaterials offer prospective advancements in cancer therapy by enabling multifunctional particle designs that enhance treatment efficacy through multiple mechanisms. In current research  $\text{AuFe}_3\text{O}_4$  dumbbell-shaped nanoparticles were used as the instrument for magneto-mechanical (MM) treatment. Experiments were performed on human hepatocarcinoma Huh7 cell line. Magnets were used as sources of the pulsed magnetic field, which were switched on alternately, resulting in an overall magnetic field frequency of about 6 Hz across the sample. The magnetic field strength generated was 80-100 mT. Viability analysis of cells showed that MM treatment significantly decreased the percent of live cells (Fig. 1 A).

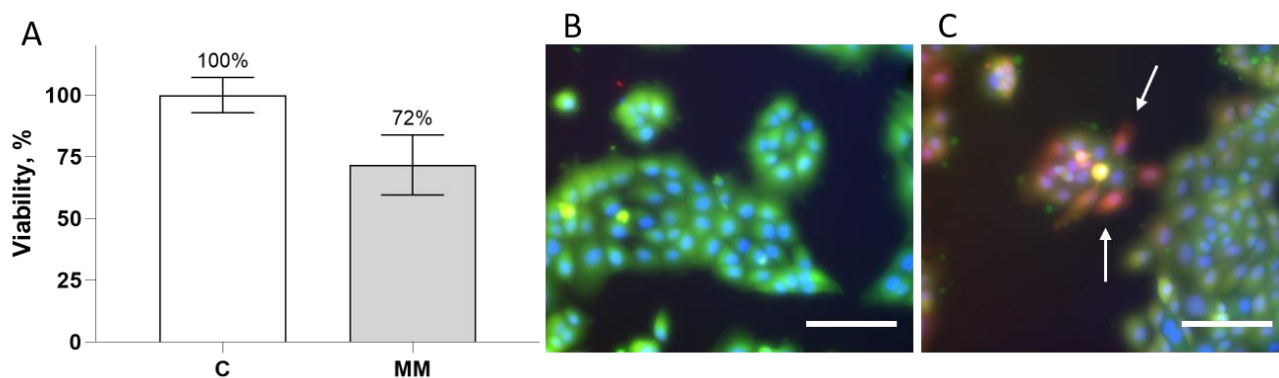


Figure 1. (A) NPs decreased Huh7 cell viability after MM treatment. Data obtained using WST-1 assay. Data values are normalized to control and represented as mean  $\pm$  SE. (B) and (C) – control and MM-treated cells, stained via Hoechst 33342 (blue, nuclei), calcein-AM (green, cytoplasm), propidium iodide (red, nuclei of dead cells). Images obtained using fluorescent microscopy. Scale bar – 100  $\mu\text{m}$ . White arrows show dead cells.

Further microscopy analysis (Fig. 1 B and C) demonstrated that morphology of treated cells was changed – the number dead cells were found (positive stained via propidium iodide). The obtained results complement existing knowledge on the potential applications of MM therapy for targeted elimination of tumor cells. The acquired data will be used for developing of biomedical applications based on magnetic nanoparticles and MM treatment.

## Study of the Effect of Hyaluronic Acid Solutions with Curcumin, Usnic Acid, and Mangiferin on Epithelial Cells

E. Vinogradova<sup>a\*</sup>, A. Motorzhina<sup>a</sup>, P. Snetkov<sup>b</sup>, S. Morozkina<sup>b</sup>, K. Levada<sup>a</sup>

<sup>a</sup> I. Kant Baltic Federal University, Kaliningrad, Russia

<sup>b</sup> ITMO University, Saint Petersburg, Russia

\*elenavinogradova887@gmail.com

Wound healing is often disrupted by increased inflammation, oxidative stress, and infection, which can lead to chronic wounds and excessive scarring [1]. Addressing these issues requires the development of multifunctional formulations that promote regeneration while controlling inflammation and microbial contamination. The use of formulations based on high molecular weight hyaluronic acid (HA) as a carrier in combination with curcumin (CUR), mangiferin (MNG), and usnic acid (USN) may be promising approach for this problem due to their anti-inflammatory, antioxidant, and antimicrobial properties [2–4].

In this study, the effect of 1.5 MDa and 2.0 MDa HA-based films containing CUR, CUR+USN, or CUR+MNG on a spontaneously immortalized adult human skin keratinocyte line (HaCaT) was investigated. For *in vitro* studies, films were dissolved in cell culture medium. Cell viability was assessed using the WST-1 reagent. Samples were tested at concentrations of 10, 50, and 100 µg/mL. Cell migration dynamics after incubation with samples solutions were assessed using a wound healing assay.

The study showed that HA-based films with CUR, USN, and MNG solutions significantly increased keratinocyte viability at a concentration of 50 µg/mL. Samples based on 2.0 MDa HA showed less impact on HaCaT viability. Therefore, cell migration was assessed on three compositions based on 1.5 MDa HA at 50 µg/mL concentration. None of them caused a statistically significant increase in the rate of wound closure compared to the control which was not treated with films solutions. Despite the published data showing that USN exhibits cytotoxicity, in this study, the HA-CUR+USN formulation did not reduce keratinocyte viability at 50 µg/mL concentration [3]. This combined effect may be promising in the development of wound treatment agents and will provide a synergistic healing effect due to increased keratinocyte viability and antibacterial effect.

Thus, combinations of HA with CUR, USN, and MNG show prospects for further study as therapeutic agents in cosmetology and medicine.

This work was supported by the Russian Science Foundation, grant № 21-72-20158-II.

[1] M. Robson, *Surg. Clin. North Am.* 77(1997)

[2] P. Snetkov, *Pharmaceutics* 14(2022)

[3] C. Pagano, *Colloids Surf. B Biointerfaces* 178(2019)

[4] S. Chae, *Biosci. Biotechnol. Biochem.* 75(2011)

## Effect of Curcumin Combined with Hyaluronic Acid on Human Melanoma

K. Zavkibekova<sup>a\*</sup>, A. Motorzhina<sup>a</sup>, P. Snetkov<sup>b</sup>, S. Morozkina<sup>b</sup>, K. Levada<sup>a</sup>

<sup>a</sup> Immanuel Kant Baltic Federal University, 236004, Nevskogo 14, Kaliningrad, Russia

<sup>b</sup> ITMO University, 197101, Kronverkskiy prospect 49, bldg. A, Saint Petersburg, Russia.

\*kseniazavkibekova230@gmail.com

Despite the advances during recent decades, the treatment of melanoma remains an extremely challenging problem. The tumor's external localization and the possibility of radical treatment at early stages provide grounds for therapeutic success. However, the high recurrence rate, unpredictable clinical course of the disease, and the lack of effective systemic therapy render the prognosis pessimistic in the cases of the disease progression [1]. This study explores the potential use of curcumin in melanoma therapy. Curcumin effectively modulates various intracellular signaling pathways, exerting anti-inflammatory and anticancer effects [2]. However, the therapeutic application of curcumin is limited by chemical instability and low oral bioavailability, underscoring the relevance of utilizing combination strategies to develop novel curcumin-based drug formulations [3].

The aim of this study was to investigate the effect of curcumin-loaded films based on hyaluronic acid (HA) as a potential therapeutic agent against human melanoma cells. Analyzed samples included HA with a molecular weight of 1.5 MDa or 2.0 MDa with curcumin at ratios of 1:5, 1:15, and 1:25 (w/w) have been dissolved in cell medium DMEM before the experiments. The proliferative activity of melanoma cells after 72 h incubation with films solutions was assessed using the WST-1 assay. Experiments were conducted on healthy control HaCaT line and two melanoma models – SK-MEL 28 and CVCL-7036. The experiment was performed at 10, 50, 100 µg/mL concentrations in six replicates. The results demonstrated that curcumin with HA at both molecular weights at a 1:5 ratio reduced proliferative activity at the concentration of 100 µg/mL on all cell lines (Fig. 1). However, curcumin with HA (2.0 MDa) shows significant decreasing of melanoma cells viability in addition to HaCaT viability rising. This combined effect may be promising in the development of melanoma treatment.

Funding: Polymer solutions and HA-based films with curcumin were elaborated and fabricated with financial support of the Russian Science Foundation (project number 24-23-00269).

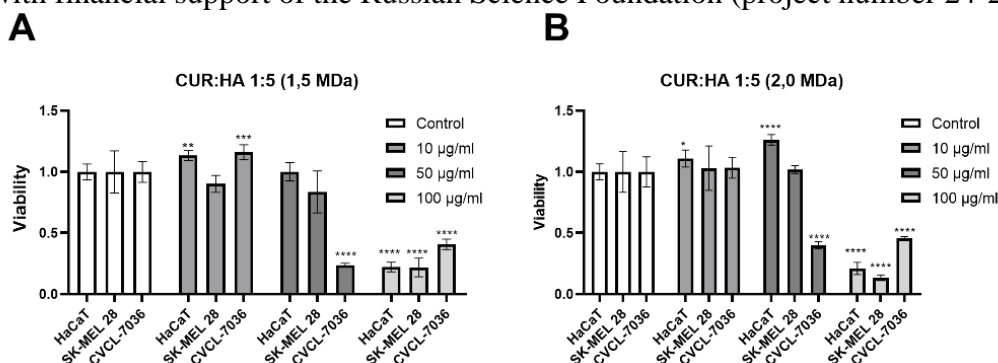


Figure.1 Viability of HaCaT, SK-MEL 28, and CVCL-7036 cell cultures with solutions based on curcumin-loaded HA films at concentrations 10, 50, 100 µg/mL. A – HA (1.5 MDa):CUR 5:1 (w/w). B – HA (2.0 MDa):CUR 5:1 (w/w)

[1] Mirzaei H. et al., *Int. J. Cancer*, 139(8), 1683–1695 (2016)

[2] Bush J.A. et al., *Exp. Cell Res.*, 271(2), 305–314 (2001)

[3] Dahmke I.N. et al., *PLoS ONE*, 8(12), e81122 (2013)



# Analysis of Electroencephalographic (EEG) Data Using Neural Network Approaches for the Classification of Functional Brain States

D. Koryakin<sup>a</sup>, A. Zaikina<sup>a</sup>, D. Kondratenko, K. Levada<sup>a,\*</sup>

<sup>a</sup> Immanuel Kant Baltic Federal University, 236004, Nevskogo 14, Kaliningrad, Russia

<sup>b</sup> Lomonosov Moscow State University, 119991, Leninskie gory 1, Moscow, Russia

**Introduction.** The automated classification of EEG patterns is of significant interest for neuroscience and the development of brain-computer interfaces (BCIs) [1]. However, EEG signals are characterized by their complex structure and high noise levels, which necessitates the application of sophisticated processing methods. This study aims to describe and validate a methodology for classifying functional brain states related to music perception using neural network approaches.

**Methods.** A comprehensive approach was employed, involving the preprocessing of multi-channel EEG data (filtering, artifact suppression via Independent Component Analysis (ICA) [2]) and the extraction of informative features: Power Spectral Density (PSD) and a set of statistical characteristics. For classification, a multi-stage methodology was adopted, which

included an initial screening of individual models (e.g., 1D CNN, GRU, MLP), the selection of 14 candidate models, and the subsequent creation of a weighted ensemble from the three best-performing, heterogeneous models. Feature importance for each model in the ensemble was assessed using the Permutation Importance method.

**Results and Discussion.** Evaluation on a hold-out test set demonstrated that individual models, such as a 1D Convolutional Neural Network (CNN) and a Gated Recurrent Unit (GRU) network, achieved accuracies of 0.7368 and 0.7105, respectively. The final weighted ensemble yielded the highest performance, with an accuracy of 0.7632, an F1-score of 0.7415, and a ROC AUC of 0.8123. The feature importance analysis revealed that the different model architectures focused on distinct EEG characteristics: the MLP primarily utilized inter-hemispheric asymmetries, the GRU captured dynamic changes in statistical moments, and the CNN leveraged power spectral density in high-frequency bands. The study demonstrated the effectiveness of ensembling heterogeneous neural network models for classifying EEG patterns [3]. The success of this approach is attributed to the reliance of different architectures on complementary features within the EEG signal. These findings highlight the potential of hybrid and ensemble methods to enhance the accuracy and robustness of automated systems for analyzing functional brain states.

[1] Y. Roy et al., J. Neural Eng. 16, 051001 (2019)

[2] A. Delorme, S. Makeig, J. Neurosci. Methods 134, 9 (2004)

[3] N. Al Otroshi et al., Neurocomputing 519, 239 (2023)

## The effect of magnetoelectric stimulation on the viability and proliferation activity of human mesenchymal stem cells

E. Vlasyuk, V. Frolova, V. Antipova\*, V. Salnikov, P. Vorontsov, K. Levada, V. Rodionova

Immanuel Kant Baltic Federal University, 236004, Nevskogo 14, Kaliningrad, Russia

\*valya.antipova24@gmail.com

The number of patients with bone damage resulting from trauma or diseases such as bone cancer and osteoporosis is increasing worldwide. Traditionally, autologous or allogeneic transplantation methods have been used to restore bone tissue; however, the risk of an immune response or infection with this treatment has led to the need to find new approaches to treatment. Tissue engineering proposes the use of bioinductive substrates capable of influencing cell activity, thereby promoting bone tissue regeneration. Such materials include polyvinylidene fluoride (PVDF)-based nanocomposites modified with  $\text{CoFe}_2\text{O}_4$  nanoparticles. These substrates have good mechanical and piezoelectric properties similar to bone tissue. This paper presents the results of a study of the effect of magnetic stimulation of PVDF-based nanocomposites on cell viability and proliferation activity.

Biological testing of nanocomposites was performed on a line of human mesenchymal stem cells (FetMSC). Cell stimulation was performed daily for 30 minutes. Proliferative activity was assessed using WST-1 analysis on days 7, 14, and 21 of stimulation, and cell viability was examined using live/dead cell staining.

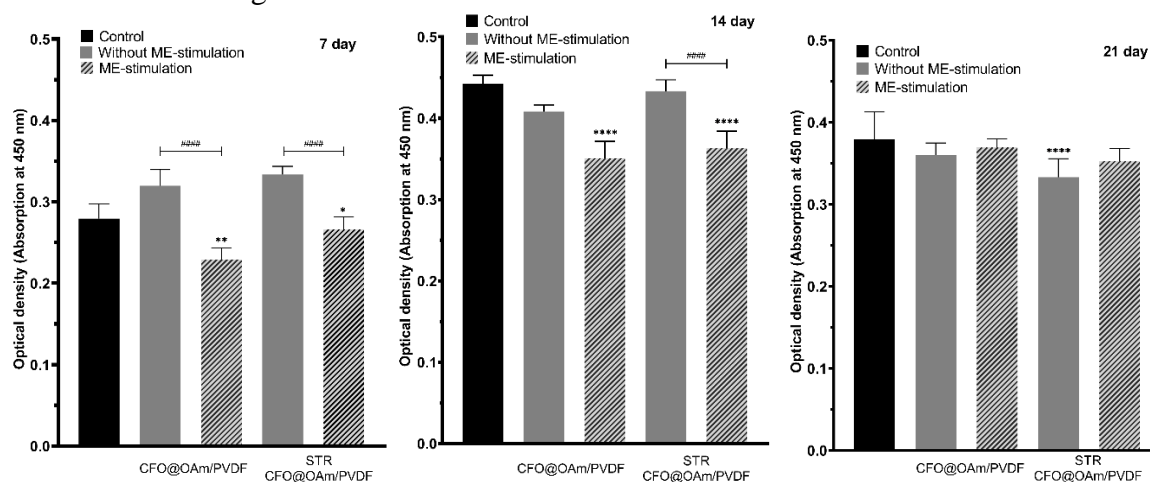


Figure Dependence of proliferation activity on culture conditions and duration of the experiment

The results showed that all groups exhibited a common pattern of proliferation activity changes: on day 14, cell proliferation activity increased relative to day 7 and decreased on day 21 of the experiment (Fig.1). At the same time, it was noted that the proliferation activity in the group of stimulated cells was lower than in the control group and the group of cells cultured on the surface of nanocomposites but not subjected to magnetic stimulation. The decrease in cell proliferation activity in the groups with magnetoelectric stimulation (ME stimulation) can be explained by the earlier onset of mesenchymal stem cell differentiation.

## Study of the influence of nanophotosensitizer based on upconversion particles on biological tissues

A. Fashchevsky<sup>a</sup>, E. Lazareva<sup>a</sup>, V. Kovalenko<sup>a</sup>, A. Mylnikov<sup>c</sup>, N. Navolokin<sup>c</sup>, I. Yanina<sup>a,b\*</sup>

<sup>a</sup> Saratov State University (National Research University), 410012, 83 Astrakhanskaya str., Saratov, Russia

<sup>b</sup> Tomsk State University (National Research University), 634050, 36 Lenin's av., Tomsk, Russia

<sup>c</sup> Saratov State Medical University, 410012, 112 B Kazachaya str., Saratov, Russia

\*irina-yanina@list.ru

Rare-earth-based upconversion nanotechnology has recently shown great promise for photodynamic therapy (PDT) [1, 2]. The use of upconversion nanoparticles (UCNPs) excited by an infrared light source and having emission in the visible part of the spectrum in combination with a photosensitizer, effectively excited at the emission wavelength of the particles, will expand the scope of application of the nanophotosensitizer by increasing the depth of penetration of light into biological tissues. Cyanine dyes, which are also actively used in PDT, effectively bind to proteins through a wide variety of functional groups, and therefore can be an even more effective pair for UCNPs during PDT [3, 4].

The aim of this work was to study the effect of a nanophotosensitizer based on upconversion particles on biological tissues such as tumors and blood.

We used the in-house synthesized UCNPs NaYF<sub>4</sub>: Yb<sup>3+</sup>, Er<sup>3+</sup> (fluoride matrix doped with ions of ytterbium and erbium). The UCNPs were synthesized by a hydrothermal method. UCNPs coated with shells of human serum albumin (HSA) and cyanine 3B NHS-ether (Cy3) were used. The UCNP concentration was 2 mg/mL.

The work was carried out on the group of 20 laboratory animals. For the group white laboratory rats of the Wistar breed weighing 300 ± 50 g, which were implanted subcutaneously in the area of the scapula, 0.5 ml of 25% tumor suspension in Hanks solution of the strain of alveolar liver cancer - PS-1. The rats were divided into 4 groups of 5 each. The comparison group was not any type of treatment. The experimental groups are: group 1 was injected with UCNPs-HSA+Cy3, group 2 – tumour was 980 nm laser irradiated and group 3 was injected with UCNPs-HSA+Cy3 and then tumour was 980 nm laser irradiated. We took blood daily for microscopic examination. The optical properties of the tumor tissue were examined after a month. Samples of organs and tumours were taken after a month of research. The test objects were 5 µm thick sections of paraffin blocks organs (heart, lung, liver, spleen, kidneys) and tumours in rats (blocks were used for histological analysis).

We have obtained a reliable reduction in tumor size when introducing a nanophotosensitizer based on UCNPs and irradiation. Analysis of blood morphometric parameters showed minor deviations from the norm. Based on the analysis of the obtained absorption spectra of scattering and dispersion dependence, changes associated with blood filling and changes in the degree of dehydration of pathological tissues are shown. Histological analysis showed the absence of a toxic effect on organs.

The study was supported by a grant Russian Science Foundation No. 25-22-00144, <https://rscf.ru/project/25-22-00144/>

[1] M. Chen, Q. Zhu, Z. Zhang, Q. Chen, & H. Yang, Chem. Asian J. 19(11), e202400268 (2024)

[2] J. Yan, B. Li, P. Yang, J. Lin, & Y. Dai, Adv. Funct. Mater. 31(42), 2104325 (2021)

[3] Y. Zhang, T. Lv, H. Zhang, X. Xie, Z. Li, H. Chen, Y. Gao, Biomacromolecules. 18 (7), 2146-2160 (2017)

[4] S. M. Usama, S. Thavornpradit, K. Burgess, ACS Appl. Bio Mater. 1 (4), 1195–1205 (2018)

# Critical behavior of the 3-state Potts model with quenched disorder on a square lattice

A. Babaev<sup>a,b\*</sup>, A. Murtazaev<sup>a,c</sup>, G. Ataeva<sup>a</sup>

<sup>a</sup> H. Amirkhanov Institute of Physics of the Daghestan Federal Research Centre of the Russian Academy of Sciences, 367010, Yaragskogo 94, Makhachkala, Russia

<sup>b</sup> Daghestan State Pedagogical Universities, 367003, Yaragskogo 57, Moscow, Russia

<sup>c</sup> Dagestan State University, 367025, Dzerzhinskogo, 12, Makhachkala, Russia

\*b\_albert78@mail.ru

The study of the influence of the quenched disorder on phase transitions and critical behaviour is one of the important problems in condensed matter physics. The Harris criterion [1] provides an answer to a principle question concerning a change of critical behavior when introducing the small amount of quenched impurities. According to this criterion a weak disorder effects on the critical behavior only when the specific heat of a corresponding pure system diverges in a critical point. This criterion is satisfied only by the systems whose effective Hamiltonian is isomorphs relative to the Ising model in the critical point. According to Harris' criterion [1] for the Potts model with  $q=3$ , impurities should affect the critical behavior, due to the fact that for this model the theory in the undiluted regime predicts a critical exponent for heat capacity  $\alpha>0$ ,  $\alpha=1/3$ . However, the question of the universality of the new critical exponents for the considered Potts model on a square lattice in the dilute regime remains open.

In this regard, the main objective of the present work is to investigate the critical behavior of the 3-state dilute Potts model on a square lattice.

The Hamiltonian for the system can be written as [2]

$$H = -\frac{1}{2}J \sum_{i,j} \rho_i \rho_j \delta(S_i, S_j), \quad S_i = P_1, P_2, P_3, \quad (1)$$

where  $J$  is the parameter of exchange ferromagnetic interaction ( $J>0$ ) between spins, summation in expression (1) is performed by the nearest-neighbors,  $P_q$  - number of different spin states,

$$\delta(S_i, S_j) = \begin{cases} 1, & \text{if } S_i = S_j, \\ 0, & \text{if } S_i \neq S_j. \end{cases} \quad \text{and} \quad \rho_i = \begin{cases} 1, & \text{if a site occupied by a magnetic atom} \\ 0, & \text{if a site occupied by a nonmagnetic impurity} \end{cases}.$$

Systems with linear dimensions  $L \times L = N$ ,  $L=10-160$  are investigated. For all analyzed systems in which a second-order transition occurs, we estimate the static critical exponents of the magnetization  $\beta$ , the susceptibility  $\gamma$ , and the heat capacity  $\alpha$  on the basis of the finite-size scaling theory [3]. The calculations are carried out for systems with periodic boundary conditions at spin concentrations  $p=1.0$ ,  $p=0.95$ ,  $0.90$ ,  $0.80$ . The data from our investigations indicate that the second-order phase transition takes place in the considered Potts model on a square lattice, in accordance with the predictions of analytical theories [4]. The inclusion of nonmagnetic impurities causes a change in the universality class of the critical behavior of the two-dimensional 3-state Potts model.

[1] A.B. Harris, J. Phys. C 7, 1671 (1974).

[2] F.Y. Wu, Rev. Mod. Phys. 54, 235 (1982).

[3] M.E. Fisher, M.N. Barber, Phys. Rev. Lett. 28, 1516 (1972).

[4] F.Y. Wu, Exactly Solved Models: A Journey in Statistical Mechanics. World Scientific, London, 2009.

# Electron dense plasma parameters for iron–based superconductors

N. Netesova \*

Lomonosov Moscow State University, 119991, Leninskie gory 1, Moscow, Russia

\*nbn@mig.phys.msu.ru

Within electron plasma model, a complex crystal of ABCD as a result of phase separation into four subsystems is considered. During the phase transition in the ABCD crystal, the valence bond breaking associated with the crystal lattice destruction. It is caused by the balance energies of the A-B-C-D and A-A, B-B, C-C, D-D bonds. The basic principle of the phase transition is caused by bonds being broken and dumbbell configurations of atoms are formed.

The pairing of electrons is guided by a plasma mechanism. Free electrons couple to lower system energy. When molecules are formed from individual atoms by dumbbell configuration, energy is released. The energy balance is caused by a change in the distances between atoms A-A, B-B, C-C, D-D, with decreasing temperature. It is necessary that in the phase transition region the total square plasma energy of the formed quasi-molecules is significantly greater than the square plasma energy of the original crystal. This is the condition for the superconducting phase transition in the crystal ABCD. During phase separation of a polyatomic crystal, a multigap energy system is formed. Experimental limitations make it difficult to determine all energy gaps.

$$2 \text{ ABCD} = \text{A}_2 + \text{B}_2 + \text{C}_2 + \text{D}_2.$$

$$q(\text{abcd}) = 4\beta \Phi^2(\text{abcd}) / (\Phi^2(a) + \Phi^2(b) + \Phi^2(c) + \Phi^2(d)) = 4\beta \Phi^2(\text{abcd}) / \sum(\text{abcd}),$$

where parameters are square  $\Phi^2(M, \rho, s)$ , square  $\Phi^2(\text{abcd})$ , square  $\Phi^2(a)$ , square  $\Phi^2(b)$ , square  $\Phi^2(c)$ , square  $\Phi^2(d)$ ,  $\sum(\text{abcd}) = (\Phi^2(a) + \Phi^2(b) + \Phi^2(c) + \Phi^2(d))$  are square electron energy in square eV<sup>2</sup> crystal abcd, a, b, c, d, respectively,  $T_c$  is the phase transition temperature,  $\rho$  is density,  $s$  is valence electron number,  $M$  is molecular (atomic) mass,  $q$  and  $\beta$  are interaction constants. The equations of the superconducting phase transition curve  $T_c(q)$  are derived within the known experimental data and our theoretical parameters. A method for finding the phase transition temperature of a crystal was proposed.

From the  $T_c(q)$  equation, the parameters of superconductors were determined. The electron dense plasma parameters in crystals LiFeAs, NaFeAs, LiFeP, LaFePO, LaFeAsO, LaFeAsO<sub>1-x</sub>F<sub>x</sub>, SmFeAsO, SmFeAsO<sub>0.9</sub>F<sub>0.1</sub> were calculated.

## Defining the structure of MFC images using the Python programming environment

L. Kotov, Z. Blinov\*, V. Ustyugov

Syktyvkar State University, 167001, Oktyabrsky Ave., 55, Syktyvkar, Russia

\*blinovzosim@gmail.com

Nanocomposite structures due to the abundance of applications in various fields of engineering continuously stimulate the interest of researchers to improve the methods of their creation, search for new chemical and structural compositions that solve numerous technical problems. Atomic force microscopy (AFM) is a key tool for analyzing the structure and surface topography of composite films, but the data obtained by this method must be reliably interpreted to further determine the parameters of the material under study. For example, the following types of structure can be observed on magnetic phase contrast (MPC) images: granular, granular-percolation and percolation [1-3]. Detection of domains on the obtained MFC is performed either manually or with the help of software, the parameters of which also need to be adapted to the peculiarities of a particular image. In the present work, the MFC of metal-dielectric films is analyzed using the PoreSpy library for the Python programming language [4]. Among the functions of this library are filtering and elimination of noise in images, the possibility of segmenting images, measuring the size of selected clusters, and statistical analysis of the obtained data.

The sputtering of the investigated films was performed on a lavsan sheet by ion bombardment of CoFeB metal alloy and SiO<sub>2</sub> dielectric targets. AFM images of the films for statistical analysis of the granular composition and magnetic structure were obtained on an atomic force microscope NT-MDT (Russia) at room temperature [2,3]. For analysis by the PoreSpy library functions, the obtained AFM images were loaded into the integrated development environment for scientific research, machine learning and data analysis Spyder.

In the course of the study, clusters of magnetic alloy CoFeB were identified on AFM images of composite film samples by an automated method, size distributions of the found particles were plotted, and structural parameters were estimated. The obtained results are used to build theoretical models of composite media and to study the relationship between their structural features and magnetic characteristics.

**The research was supported by the grant of the Russian Science Foundation, project No. 25-72-20063.**

- [1] S. Bedanta, A. Barman, W. Kleemann et al. Journal of Nanomaterials Vol. 2013. Article ID 952540. P.22. (2023)
- [2] L.N. Kotov, V.A. Ustyugov, V.S. Vlasov, A.A. Utkin, Bulletin RAS: Physics, 87(3), 385 (2023)
- [3] L.N. Kotov, M.P. Lasek, V.K. Turkov, D.M. Kholopov, V.S. Vlasov, Yu.E. Kalinin, A.V. Sitnikov, Bull. Russ. Acad. Sci. Phys. 84, 1065–1067 (2020)
- [4] J. T. Gostick et al. Journal of Open Source Software 4(37). P.1296 (2019)

## Simulation of spin wave propagation in a system of three laterally coupled microwaveguides

F. Garanin\*, V. Gubanov, A. Sadovnikov

Saratov State University named after N.G. Chernyshevsky, 410012, Astrakhanskaya 83, Saratov, Russia

\*garaninfedorwork@mail.ru

Currently, the development of magnonics ideas [1-2] aimed at studying the processes of transfer of the magnetic moment or electron spin instead of charge transfer opens up new possibilities for the application of spin waves (SW) for constructing the element base of devices for processing, transmitting and storing information. Irregular structures, for example, waveguides with a variable width, can be created as such devices. Yttrium iron garnet (YIG) films are used as a magnetic material used to form magnetic waveguide structures, demonstrating record low values of SW attenuation, including at nanometer YIG thicknesses. Technologies for producing YIG films include liquid-phase epitaxy, laser deposition and vacuum ion sputtering. The system under study is three parallel waveguides with a variable width and a fixed gap  $d$ .

The structure under study is a system of laterally coupled waveguide microwaves – three trapezoidal microwaves with variable width (see Fig. 1). These microwaves are YIG films with a thickness of  $t = 10 \mu\text{m}$ . The structure has the following parameters: the length of the microwaves  $L = 7000 \mu\text{m}$ , the width of the larger part of the microwave  $W_0 = 50 \mu\text{m}$ , the width of the smaller part  $W_1 = 200 \mu\text{m}$ , the gap width  $d = 40 \mu\text{m}$ .

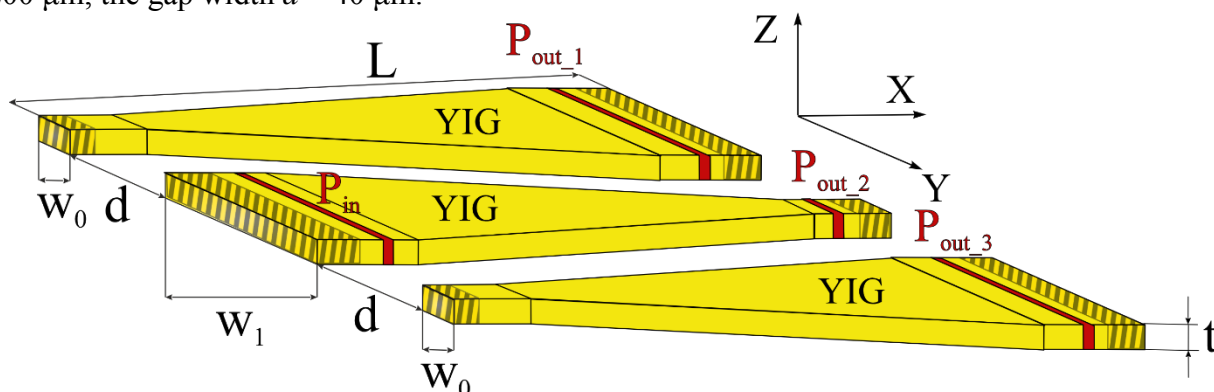


Figure 1. Schematic representation of a system of three microwave guides with varying width, located parallel with a gap  $d$

Micromagnetic modeling was performed in the MuMax<sup>3</sup> package [3], where the structure was divided into a grid, in the nodes of which the Landau-Lifshitz equation with Hilbert attenuation was numerically solved. In the micromagnetic modeling, conditions were created for the excitation of a surface magnetostatic wave (SMW), in which the external magnetic field  $H_0$  was applied along the positive direction  $Oy$ . The value of the external magnetic field parameter  $H_0$  was 1200 Oe.

Thus, using numerical modeling, a system of three laterally coupled microwave guides was investigated. This structure can be used as a directional branch of a microwave signal to create devices for processing information signals based on the principles of magnonics.

The work was supported by the Russian Science Foundation Grant No. 23-79-30027.

- [1] V.V. Kruglyak et al. J. Phys. D: Appl. Phys., 43, 264001, (2010)
- [2] D. Sander et al. J. Phys. D: Appl. Phys., 50, 363001, (2017)
- [3] A. Vansteenkiste et al. AIP Advances., 4, 107133, (2014)



# Micromagnetic modeling of spin wave propagation in YIG film with magnetite nanoparticles

F. Garanin\*, A. Sadovnikov, M. Lomova

Saratov State University named after N.G. Chernyshevsky, 410012, Astrakhanskaya 83, Saratov, Russia

\*garaninfedorwork@mail.ru

In recent years, magnonics, an innovative area of spintronics based on the use of iron garnets and spin waves (SW) for information transmission, has demonstrated rapid development [1]. Unlike traditional approaches, where the key role is played by the transport properties of spin-polarized electrons, magnonics offers a fundamentally new way of signal processing. This opens up broad opportunities for creating functional devices such as filters, modulators, and waveguides operating on the basis of spin waves [2].

In parallel with the development of magnonics, interest in the use of magnetic materials in biomedicine is growing. Particular attention is attracted by magnetic nanoparticles, which have unique properties, including high sorption capacity and the ability to be remotely controlled using external magnetic fields. These characteristics make them indispensable in areas such as diagnostics (for example, enhancing contrast in magnetic resonance imaging) and therapy (targeted drug delivery). One of the most promising materials for both magnonics and biomedicine is magnetite ( $\text{Fe}_3\text{O}_4$ ). Its exceptional magnetic properties allow magnetite nanoparticles to be effectively used in various applications.

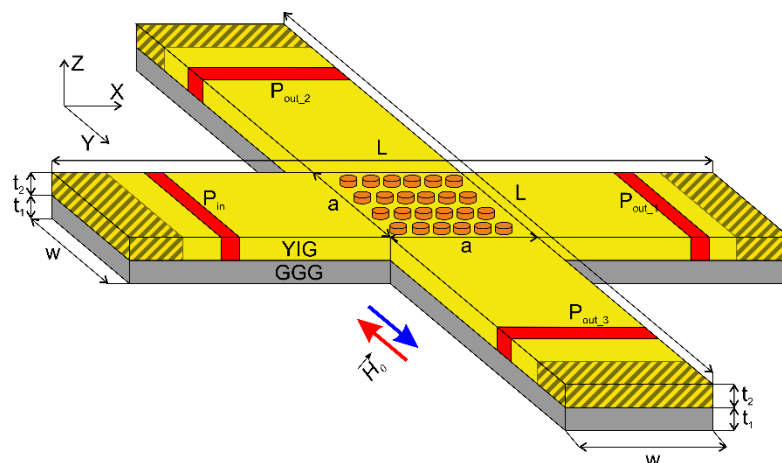


Figure. 1. Schematic representation of YIG film with magnetite nanoparticles

Micromagnetic modeling was performed in the MuMax<sup>3</sup> package [3], where the structure was divided into a grid, in the nodes of which the Landau-Lifshitz equation with Hilbert attenuation was numerically solved. In the micromagnetic modeling, conditions were created for the excitation of a surface magnetostatic wave (SMW), in which the external magnetic field  $H_0$  was applied along the positive/negative direction  $Oy$ . The value of the external magnetic field parameter  $H_0$  was 1200 Oe.

Thus, using numerical micromagnetic modeling, a cross-shaped structure with magnetite nanoparticles was investigated. This structure can be used as a microwave signal filter controlled by the orientation of the magnetic field.

The work was supported by the Russian Science Foundation Grant No. 23–13–00373.

[1] V.V. Kruglyak et al. J. Phys. D: Appl. Phys., 43, 264001, (2010)

[2] D. Sander et al. J. Phys. D: Appl. Phys., 50, 363001, (2017)

[3] A. Vansteenkiste et al. AIP Advances., 4, 107133, (2014)



# Superconducting concentrator in a sandwich-type combined magnetic field sensor

L. Ichkitidze<sup>a,b,\*</sup>, M. Belodedov<sup>c</sup>, D. Golub<sup>a</sup>, D. Telyshev<sup>a,b</sup>, S. Selishchev<sup>b</sup>

<sup>a</sup> I.M. Sechenov First Moscow State Medical University, Trubetskaya str., 8, building 2, 119991, Moscow, Russia

<sup>b</sup> National Research University Moscow Institute of Electronic Technology (MIET), Zelenograd, Shokina square, 1, 124498, Moscow, Russia

<sup>c</sup> Bauman Moscow State Technical University, 2th Baumanskaya St.5, Bldg. 1, 105005, Moscow, Russia

\*leo852@inbox.ru; ichkitidze\_1\_p@staff.sechenov.ru

Typically, combined magnetic field sensors (CMFS) consist of two main parts in the form of a superconducting magnetic field concentrator (MFC) and a magnetically sensitive element (MSE). A sketch of a typical sandwich-type CMFS is shown in Figure 1.

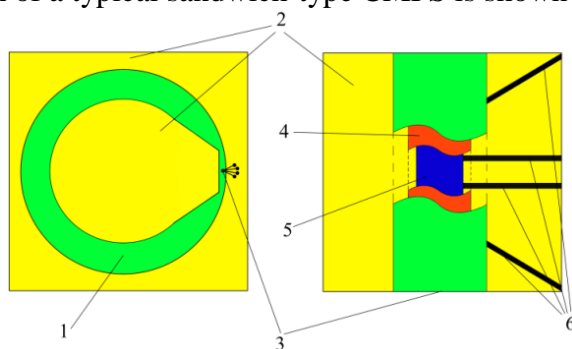


Figure 1. – Sketch of the sandwich-type CMFS:  
1 – ring of MFC, 2 – dielectric substrate, 3 – active strip (AS), 4 – insulating film, 5 – MSE, 6 – contact probes

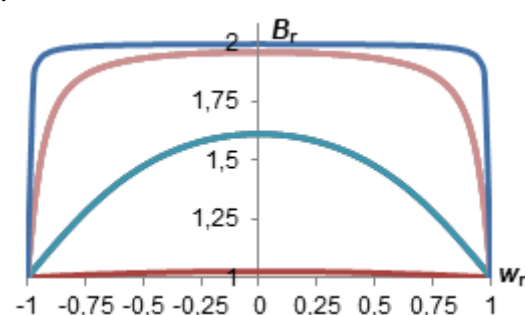


Figure 2. – Dependence  $B_r(w_r)$ ,  $B_r = B_{\max}/B_{\min}$ ,  $B_{\max}$  and  $B_{\min}$  are the maximum and minimum values of the magnetic fields in the MSE, respectively;  $w_r$  is the relative width of the AS

The antenna receives the measured magnetic flux, which is transferred to the MSE via the active strip (AS). Due to the fact that the screening current  $I_s$ , excited by the measured magnetic field, is distributed non-uniformly in the active band, the efficiency coefficient  $k_{\text{eff}}$  of the MFC decreases, which can be defined as the ratio of the average magnetic field in the MSE to the value of its non-uniformity, i.e.  $k_{\text{eff}} = |B_{\text{av}}/(B_{\max} - B_{\min})|$ . Here  $B_{\text{av}}$  is the average magnetic field in the MSE. Figure 2 shows the dependences of  $B_r(w_r)$  for different values of the relative width of the AS strip in the range of 0.35; 3.5; 35; and 350  $\mu\text{m}$  (from bottom to top), when  $I_s$  is uniformly distributed over the AS width.

It is evident that the  $B_r(w_r)$  dependence has a "bought-out" appearance. In the superconducting film,  $I_s$  is distributed non-uniformly and the  $B_r(w_r)$  dependence takes a "concave" appearance. It was found that with a width of 3.5  $\mu\text{m}$ , the AS and a magnetic field penetration depth of  $\sim 7 \mu\text{m}$ , the maximum  $k_{\text{eff}}$  value of  $\sim 6.3$  is reached. This value is 2.7 times greater than in the case of a uniform distribution of  $I_s$  in the AS. A high  $k_{\text{eff}}$  value will allow more efficient use of the capabilities of the MSE, and, in general, improve the magnetic sensitivity of existing CMFSs to the SQUID level, and use them to record magnetic fields (including biological ones) of the level of  $\leq 1$  pT.

The work was carried out within the framework of the state assignment of the Russian Ministry of Education and Science (Project FSMR-2024-0003).

# Study of the magnetic properties of NdSbSe in the GGA + U approximation

I. Iliushin\*, P. Mushtuk, L. Afremov, M. Tcuranova

Far Eastern Federal University, 690922, 10 Ajax Bay, Russky Island 14, Vladivostok, Russia

\*iliushin.ig@dvfu.ru

Research on ZrSiS-type compounds has revealed colossal magnetoresistance linked to their unique crystal symmetry, thus confirming their classification as nodal-line semimetals. In recent years, there has been a surge in research interest in such layered materials, with a view to controlling the interplay between topology and magnetism. The NdSbSe compound is noteworthy as the first example of a rare-earth material exhibiting frustrated magnetic interactions, characterised by spin-glass ordering. In the present study, we undertake the initial first-principles calculations of the magnetic properties of the NdSbSe system.

The simulations were performed using the Vienna Ab initio Simulation Package (VASP) [1]. Exchange-correlation effects were treated within the generalized gradient approximation (GGA) using the Perdew-Burke-Ernzerhof (PBE) functional [2]. To account for the strongly localized f-electrons of neodymium atoms, we employed the Hubbard correction (DFT+U) within the Dudarev formalism [3,4]. The effective Hubbard parameter  $U_{eff} = U - J$  was varied from 0 to 10 eV.

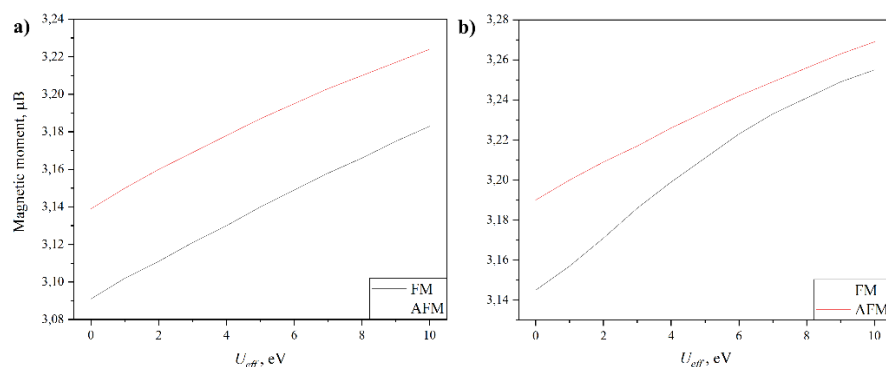


Figure 1. Dependence of the magnetic moment of the Nd atom on the  $U_{eff}$  (a) Calculations with the experimental value of the lattice constant NdSbSe. (b) Calculations with DFT-optimized value of a

Structural optimization of NdSbSe yielded lattice parameters of  $a = b = 4.228 \text{ \AA}$  and  $c = 9.044 \text{ \AA}$ , showing good agreement with experimental values ( $a = b = 4.185 \text{ \AA}$ ,  $c = 9.019 \text{ \AA}$  [5]). Figure 1 presents the dependence of the Nd magnetic moment in NdSbSe on the  $U_{eff}$  parameter, which accounts for on-site electron-electron repulsion. While the Nd magnetic moment increases with growing  $U_{eff}$ , it fails to reach the experimental value of  $3.75 \mu\text{B}$  [5] - this holds true for both calculations using the experimental lattice constants and those obtained from DFT-optimized ionic positions. In both cases, the antiferromagnetic ordering configuration exhibits higher magnetic moment values than the ferromagnetic one.

The research was supported by the Russian Science Foundation grant No. 24-71-10069, <https://rscf.ru/en/project/24-71-10069/>

[1] G. Kresse, J. Furthmuller, Phys. Rev. B 54, 11169(1996)

[2] P. Blöchl, Phys. Rev. B 50, 17953(1994)

[3] S. Dudarev, D. Nguyen Manh, A. Sutton, Philos. Mag. B 75, 613(1997)

[4] S. Dudarev et al., Phys. Rev. B 57, 1505(1998)

[5] P. K. Mishra et al., arXiv:2501.11038 (2025)

## Simulation of Polymer Magnetic Microrobots

M. Kalandiia\*, L. Makarova, N. Perov

Lomonosov Moscow State University, 119991, Leninskie gory 1, Moscow, Russia

\*mr.kalandiya@physics.msu.ru

Magnetorheological materials are composite systems consisting of magnetic particles dispersed within either an elastic or liquid matrix [1, 2]. Their tunable rheological properties under external magnetic field enable applications as biomedical microdevices for diagnostic purposes and targeted drug delivery. The locomotion dynamics of magnetoactive microrobots mimics bacterial movement in liquid media through flagellar propulsion mechanisms. Bio-compatible magnetoactive microrobots typically incorporate polymer matrices embedded with magnetic particles that serve as controllable actuation heads [3]. Research has demonstrated that magnetic field-driven microrobot motion proves particularly effective in low Reynolds number fluids such as blood, where viscous forces dominate over inertial effects.

This work presents numerical modeling of magnetorheological and magnetodeformation effects in composite magnetorheological materials. The study examines two cases: solid phase (polymer matrix) and liquid phase (liquid matrix). The ESPResSo software package was used to simulate interparticle interactions along with elastic and viscous effects. For magnetorheological elastomers, we obtained dependencies of deformation and elastic modulus for cubic models on magnetic particle size and the Young's modulus of the polymer matrix. For magnetorheological fluids, we demonstrated cluster formation in the absence of elastic constraints from the matrix under applied magnetic fields, and analyzed viscosity changes with increasing magnetic particle radius and matrix viscosity.

The numerical simulation results of these two-component systems were used to develop a three-component mathematical model describing the motion of microrobots, comprising magnetic particles with polymer flagella, in liquid media under both DC and AC magnetic fields. Creating such mathematical models for magnetoactive microrobot motion represents a fundamental multiparametric challenge, requiring simultaneous consideration of soft material mechanics, magnetic field effects, and fluid rheological properties. Integrating these physical factors enables optimization of microrobot design and material selection during development, while detailed analysis of external parameters improves control precision and behavior predictability in real-world conditions.

The study analyzed the mechanisms of magnetorheological effects in composite materials with different matrix types. We developed a 3D model of magnetoactive microrobot motion that demonstrated how the device's velocity and trajectory depend on both external conditions (magnetic field orientation/intensity, fluid viscosity/density) and intrinsic properties of the robot itself. Through modeling these complex interactions, we established relationships between motion parameters of a single biocompatible microrobot and the size/concentration of its magnetic components.

[1] E.Yu. Kramarenko, G.V. Stepanov, A.R. Khokhlov, *INEOS OPEN*, 2, 178 (2020)

[2] D. Isaev et al., *IJMS*, 20, 1457 (2019)

[3] Liang Lu et al., *Small Methods*, 2401558 (2025)

# **Transition-metal impurities on Ge(001): Adsorption, surface diffusion, and magnetic properties studied by density-functional theory**

A. Klavsyuk<sup>\*</sup>, A. Syromyatnikov, A. Saletsky

Lomonosov Moscow State University, 119991, Leninskie gory 1, Moscow, Russia

<sup>\*</sup>klavsyuk@physics.msu.ru

Ultrathin magnetic metal films on the surface of germanium are of interest as a possible material system for building spintronics devices with semiconductor technology [1],[2]. In order to achieve insight into epitaxial growth of such films on Ge(001), total-energy calculations are presented using density-functional theory. The density functional theory calculations reveal that it is energetically favorable for the deposited transition-metal impurities to exchange position with Ge atoms in the first layer. The energy barriers for surface diffusion, both along and perpendicular Ge dimer rows were determined. The electronic and magnetic properties of transition-metal impurities are investigated.

The density functional theory calculations were performed using the equipment of the shared research facilities of HPC computing resources at Lomonosov Moscow State University. Calculations of this study was financially supported by the Russian Science Foundation (Project No. 25-22-00051).

[1] Bocirnea, A. E., Costescu, R. M., Pasuk, I., Lungu, G. A., Teodorescu, C. M., Applied Surface Science 424, 337 (2017)

[2] Schlesag M., Stehling T.-J., Kubetschek N., Kurpick U., Matzdorf R., Phys. Rev. B 110, 195412 (2024)

# Effect of gold on stimulation of palladium magnetism by electric field in layered nanostructure Pd/BaO/Au

A. Korshunov<sup>a,\*</sup>, Yu. Kudasov<sup>a,b</sup>, V. Pavlov<sup>a</sup>

<sup>a</sup> Russian Federal Nuclear Center - VNIIEF, Mira ave., 37, Sarov, Nizhny Novgorod region, 607188, Russia

<sup>b</sup> Sarov Institute of Physics and Technology NRNU MEPhI, Dukhova str., 6, Sarov, Nizhny Novgorod region, 607186, Russia

\*korshunov@ntc.vniief.ru

Since palladium is a nearly ferromagnetic paramagnet, a strong electric field in a layered nanostructure of the metal/dielectric/metal type can convert it into a ferromagnetic state [1]. The possibility of such a transition was demonstrated experimentally [2], although a polar liquid nanolayer was used to enhance the efficiency of the electric field. It is assumed that one of the ways to create a "dry" nanostructure is to alternate layers of palladium and a more electronegative metal, such as gold, which can significantly reduce the magnitude of the applied external field required for the transition of Pd to the ferromagnetic state.

In this paper, full-electron calculations of the electronic structure of a solid-state Pd/BaO/Au nanostructure are performed with explicit inclusion of an external source of electric field in the form of a zigzag potential [3].

The calculations were performed using the full-electron linearized augmented plane wave (FPLAPW) method implemented in the Wien2k software package. The exchange-correlation potential was calculated in the GGA PBE approximation. The spin-orbit interaction was taken into account in the calculation only for palladium and gold atoms. Relaxation of the structure with optimization of the equilibrium positions of the atoms was carried out.

For the Pd/BaO/Pd and Pd/BaO/Au structures, a series of calculations were performed both without a field and in the presence of an external electric field in the form of a zig-zag potential [3] of different amplitudes. For the resulting supercell, the densities of state of pure palladium in the normal state and with a gold layer were calculated. It is evident that replacing palladium with a more electronegative material in itself forms a significant built-in electric field in the gap between the palladium layers, and in this case the threshold value of the electric field required to transfer the palladium layer to the ferromagnetic state turns out to be significantly lower than in the "pure" structure.

As a result of the simulation, a numerical estimate of the strong electric field required to stimulate the surface magnetism of palladium in a layered structure of the Pd/BaO/Au type was obtained. Direct calculations with a built-in electric field have proven a decrease in the threshold voltage of an external source due to the built-in electric field when replacing the palladium layer with gold.

The work was supported by the National Center for Physics and Mathematics (Direction No. 7 "Research in strong and superstrong magnetic fields").

[1] Yu.B. Kudasov, A.S. Korshunov, Surface ferromagnetism of palladium induced by strong electric field. *Physics Letters A* 364 (2007) 348–351

[2] A. Obinata et. al., Electric-field control of magnetic moment in Pd. *Scientific Reports* 5:14303; doi: 10.1038/srep14303, 2015

[3] J. Stahn, U. Pietsch, P. Blaha and K. Schwarz, Electric-field-induced charge-density variations in covalently bonded binary compounds *Phys. Rev. B* 63 (2001) 165205

# Comparative Study of $\text{XBi}_2\text{Te}_4$ Systems ( $\text{X} = \text{Sc, Ti, V, Mn, Fe, Co, Ni, Cu}$ )

R. Makeev\*, A. Eryzhenkov, A. Tarasov

Saint-Petersburg State University, 199034, Universitetskaya Embankment 7-9, Russia

\*radomir.makeev@sbpu.ru

Topological insulators (TIs) are materials that possess a nonzero bulk energy gap while hosting conductive topological surface states (TSS) [1]. The introduction of magnetic atoms into such systems can open a nonzero energy gap in the TSS as well [2]. The aim of this work is to conduct a comparative study of  $\text{XBi}_2\text{Te}_4$  systems (where  $\text{X} = \text{Sc, Ti, V, Mn, Fe, Co, Ni, Cu}$ ) and to investigate how the substitution of the magnetic atom affects the electronic and topological properties of the material. These materials are highly useful in realizing the quantum anomalous Hall effect [4]. They can also be employed in quantum computing to create stable qubits using Majorana fermions [2].

Calculations were performed within the framework of density functional theory (DFT) using the OpenMX software package [3]. The studied structures were derived from the  $\text{MnBi}_2\text{Te}_4$  unit cell by substituting the Mn atom with other 3d transition metals. All systems were modeled with antiferromagnetic ordering of magnetic moments.

As a result of the study, the electronic band structures were analyzed for each of the systems. The localization of TSS within the crystal was examined, and a correlation between the energy gap value and the magnetization of the TSS was established. The magnetization was quantified as:

$$\Delta w = \sum_{n=1}^{42} w_n M_n$$

where  $\Delta w$  is magnetization,  $w_n$  is the weight of the wavefunction for  $n^{\text{th}}$  atom and  $M_n$  is magnetic moment of  $n^{\text{th}}$  atom.

The analysis of band structures revealed that all systems, except for  $\text{CuBi}_2\text{Te}_4$ , exhibit the formation of TSS at the  $\Gamma$ -point within the bulk band gap. The largest energy gaps in TSS were observed for Mn, Fe, and Co-based structures. This is attributed to their high magnetic moments and significant localization of TSS on the magnetic atoms. The spatial localization analysis showed that the majority of the TSS is confined within the first septuple layer, with the peak of the wavefunction weight occurring on the sixth and seventh atomic layers. Furthermore, a linear relationship was found between the TSS energy gap and their magnetization. This indicates that the gap is exchange-driven and, therefore, physically tunable.

The authors acknowledge Saint-Petersburg State University for a research project 125022702939-2

[1] K.Mazumder, Journal of Alloys and Compounds, 888 (2021)

[2] M. M. Otrokov, Nature, 576.7787 (2019)

[3] T. Ozaki, Phys. Rev. B. **67**, 155108 (2003)

[4] Y. Deng, Science Volume 367, 6480 (2020)

# Magnetophotonic crystals with controlled hybrid state of Tamm plasmon-polariton and Fabry-Perot modes

T. Mikhailova<sup>a,\*</sup>, S. Lyashko<sup>a</sup>, A. Kudryashov<sup>a</sup>, S. Osmanov<sup>a</sup>, A. Karavainikov<sup>a</sup>, A. Shaposhnikov<sup>a</sup>,

N. Gusev<sup>b</sup>, S. Gusev<sup>b</sup>

<sup>a</sup> V.I. Vernadsky Crimean Federal University, 295007, Prospekt Vernadskogo 4, Simferopol, Russia

<sup>b</sup> Institute of Physics of Microstructures (IPM RAS), Russian Academy of Sciences, 603087, Academicheskaya Str., 7, Afonino, Nizhny Novgorod region, Kstovsky district, Kstovo region, Russia

\*taciamic@gmail.com

Photonic crystals with Tamm plasmon-polaritons (Tamm structures) arising at the boundary of a periodic structure with a plasmonic metal (Au, Ag, Cu) have found wide application in modern optoelectronic technologies [1]. Among all the diversity, one can highlight the structures of magnetophotonic crystals, which contain magneto-optically active layers [2]. Thanks to magneto-optical effects it is possible to create optical switches controlled by a magnetic field, magnetic sensors, and biosensors.

This work to explore new features of the hybrid state of Tamm plasmon-polariton (TPP) and Fabry-Perot (FP) modes. For this purpose, new Tamm structures were modeled and synthesized based on microcavity magnetophotonic crystals with different numbers of layer pairs in the Bragg mirrors and a magneto-optical double-layer iron garnet film of the nominal composition  $\text{Bi}_{1.0}\text{Lu}_{0.5}\text{Gd}_{1.5}\text{Fe}_{4.2}\text{Al}_{0.8}\text{O}_{12}/\text{Bi}_{2.8}\text{Y}_{0.2}\text{Fe}_5\text{O}_{12}$  (G1/G2) as a cavity layer:

$$GGG / (\text{TiO}_2/\text{SiO}_2)^2 / G1/G2 / (\text{SiO}_2/\text{TiO}_2)^6 / \text{SiO}_2/\text{Au}, \quad (1)$$

$$GGG / (\text{TiO}_2/\text{SiO}_2)^4 / G1/G2 / (\text{SiO}_2/\text{TiO}_2)^4 / \text{SiO}_2/\text{Au}, \quad (2)$$

$$GGG / (\text{TiO}_2/\text{SiO}_2)^6 / G1/G2 / (\text{SiO}_2/\text{TiO}_2)^2 / \text{SiO}_2/\text{Au}. \quad (3)$$

Here GGG is gadolinium gallium garnet substrate, and the top  $\text{SiO}_2$  layer is deposited with a gradient of the thickness  $h_b$  to control the spectral position of TPP. Optical and magneto-optical spectra of the structures at normal incidence demonstrated that the repulsion of the hybrid state of modes depends on the number of layer pairs in the Bragg mirrors of the structures (Figure 1). In this case, the degree of hybridization of modes will be higher for structure (3).

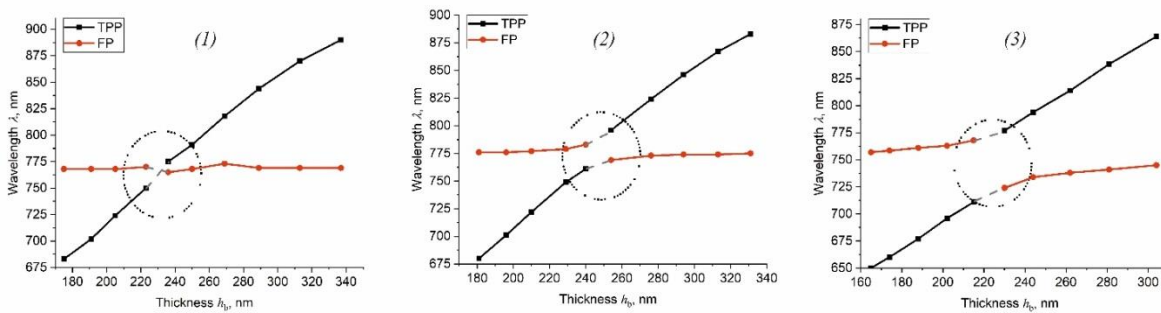


Figure 1. Dependences of the resonant wavelengths of the TPP and FP modes on  $h_b$  for Tamm structures (1), (2) and (3). The region of formation of the hybrid state with the highest degree of mode hybridization is marked by a dotted line.

Structure development was carried out using the equipment of Common Research Center «Physics and technology of micro- and nanostructures» of the IPM RAS.

The work was supported by the Russian Science Foundation (project №19-72-20154, <https://rscf.ru/project/19-72-20154/>)

[1] C. Kar, Sh. Jena, D. V. Udupa, K. D. Rao, Optics & Laser Technology 159, 108928 (2023)

[2] T. Mikhailova, S. Tomilin, S. Lyashko et al. Opt. Mater. Express 12(2), 685 (2022)

# Effect of mechanical stress on core/shell nanoparticle blocking temperature.

P. Mushtuk\*, L. Afremov, I. Iliushin, A. Tyurenkov

Far Eastern Federal University, 690922, 10 Ajax Bay, Russky Island 14, Vladivostok, Russia

\*mushtuk\_ps@dvfu.ru

The interest in core/shell particles is related to their application in many areas such as: development of magnetic materials and memory devices, electronics, medical biotechnology (radiation therapy, targeted drug delivery), geophysics (rock magnetism). In the present work we investigated the temperature dependences of core/shell particles due to their application in many areas such as: development of magnetic materials and memory devices, electronics, medical biotechnology.

This paper presents an analytical model of a nanoparticle with core/shell structure ( $\text{Fe}_3\text{O}_4/\text{Fe}_{2.44}\text{Ti}_{0.56}\text{O}_4$ ) discussed in detail in [1]. A homogeneously magnetised particle (phase (1)) with volume  $V$ , having the shape of an ellipsoid of rotation with elongation  $Q$  and small semi-axis  $B$ , contains a homogeneously magnetised ellipsoidal core (phase (2)) with volume  $v=\varepsilon V$  and elongation  $Q$  and small semi-axis  $B$ , the long axis of which coincides with the length axis of the nanoparticle oriented along the  $Oz$  axis. The crystallographic anisotropy axes of ferromagnetics are parallel to the long axes of the nanoparticle and the nucleus, respectively. The spontaneous magnetisation vectors of the  $M^{s1}$  and  $M^{s2}$  phases (as well as the long axes of the magnetic phases) are in the  $yOz$  plane and make angles  $\theta_{(1)}$  and  $\theta_{(2)}$  with the  $Oz$  axis, respectively. The external magnetic field  $H$  is applied along the  $Oz$  axis. Minimising the total energy of the nanoparticle, it can be shown that the equilibrium states of the nanoparticle are the states with parallel and antiparallel orientation of the magnetic moments of the core and shell. In this paper, we investigate the dependence of the blocking temperature on mechanical stresses for particles of three different sizes. This paper presents an analytical model of a nanoparticle with core/shell structure ( $\text{Fe}_3\text{O}_4/\text{Fe}_{2.44}\text{Ti}_{0.56}\text{O}_4$ ) discussed in detail in [1].

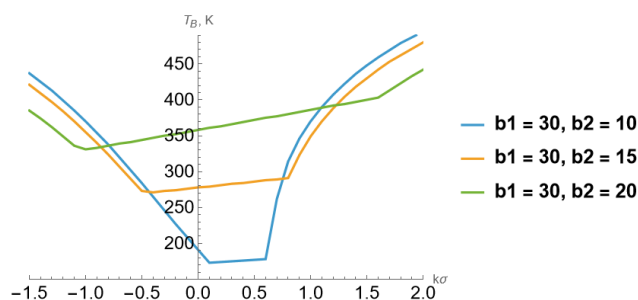


Figure 1. Dependence of blocking temperature  $T_B$  on stresses  $\sigma$

Fig.1 shows the dependences of blocking temperature  $T_B$  on mechanical stress  $\sigma$  for particles of three different sizes. The blocking temperature of nanoparticles strongly depends on the applied mechanical stress, the effect is not symmetric. An increase in  $|\sigma|$  leads to an increase in  $T_B$ , an increase in the radius of the nanoparticle nucleus also leads to an increase in the blocking temperature and a decrease in the influence of stress on  $T_B$ .

The work was supported by the state assignment of the Ministry of Science and Higher Education of the Russian Federation (Project No. FZNS-2023-0012)

[1] Afremov L. L., Anisimov S. V., Iliushin I. G. Chinese Journal of Physics. 70. 324. (2021)



# Dynamics of Composite Objects Based on Magnetic Fluids in a Vertical Channel Under the Influence of a Magnetic Field

P. Ryapolov<sup>a,\*</sup>, D. Kalyuzhnaya<sup>a</sup>, E. Sokolov<sup>a</sup>

<sup>a</sup> Southwest State University, 305040, 50 Let Oktyabrya 94, Kursk, Russia

\*r-piter@yandex.ru

External magnetic fields provide effective control over magnetic fluid droplet and emulsion dynamics. The incorporation of magnetically susceptible materials like magnetic fluids (MF) permits system manipulation via magnetic field application [1]. Current literature contains numerous studies examining both MF droplets in non-magnetic liquids (NML) [2] and non-magnetic droplets in MF [3].

This study presents key findings on the dynamics of magnetic emulsions based on magnetic fluids. The emulsification process was conducted in a planar microchannel under an applied magnetic field. Numerical simulations using FEMM 4.2 and MATLAB software packages were performed to calculate the forces acting on: non-magnetic inclusions in MF, and MF droplets suspended in non-magnetic liquids under magnetic field exposure. Both experimental and computational results demonstrated the effective control of non-magnetic inclusions within the magnetic medium and MF droplets in NML through external magnetic field manipulation.

An example of modeling systems in FEMM is shown in Figure 1.

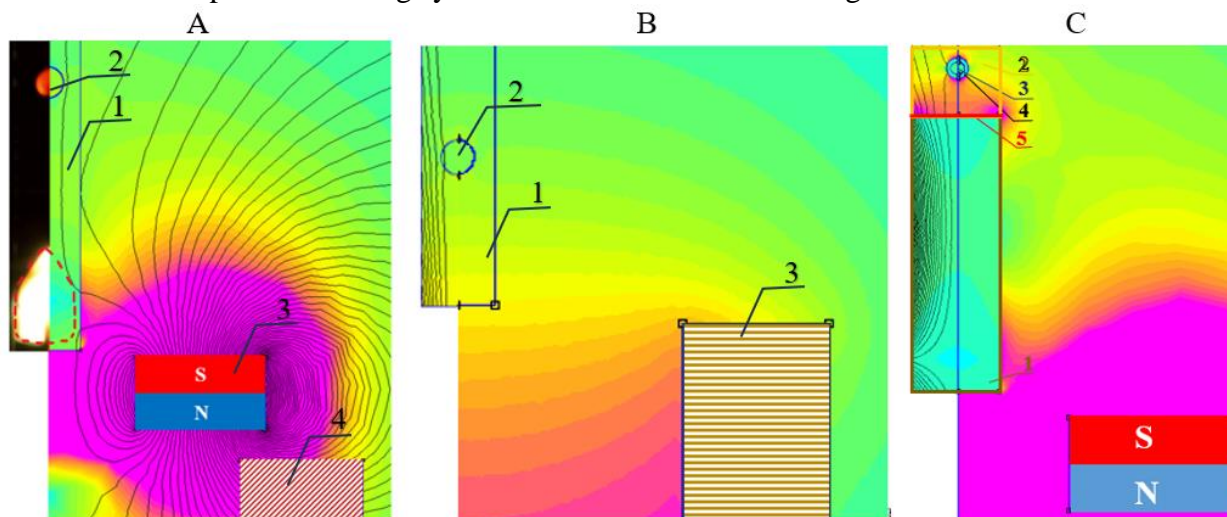


Figure 1. FEMM modeling results: (A) Water droplet in MF (1 - Flat channel filled with MF sample, 2 - Water droplet, 3 - Ring-shaped magnet, 4 – Solenoid); (B) MF droplet in NML (1 – Channel with NML, 2 - MF droplet, 3 – Solenoid); (C) Composite bubble with MF shell (1 – MF, 2 - Oil layer, 3 – Air, 4 - MF shell of the bubble, 5 - MF-oil interface boundary)

[1] G. P. Zhu, Biosensors. 12, 3(2022)

[2] D. Bhattacharjee, Physics of Fluids. 36, 9(2024)

[3] Z. Q. Dong, JMMM. 589 (2024)

The article was prepared within the framework of the state assignment for 2025 No. 075-03-2025-526.

# Coarse-grained Molecular Dynamics Simulation of Core-Shell Magnetic Microgels

A. Ryzhkov \*

Institute of Continuous Media Mechanics of the Ural Branch of Russian Academy of Science, 614068,  
Akademika Koroleva 1, Perm, Russia

\*ryzhkov.a@icmm.ru

Magnetic microgels (microferrogels) are promising submicron particles for remote intracellular drug delivery or pathogen substance collection. Microferrogels are based on a mesh hydrogel matrix with magnetic nanoparticles physically or chemically embedded into it. Active experimental studies encourage the development of adequate model concepts of the processes in microgels caused by structure formation under the influence of an external magnetic field. In addition to microgels with uniformly distributed magnetic nanoparticles, two types of core-shell geometries are also common: “magnetic core + polymeric shell” and vice versa (Figure 1). It is proposed to study the response features of such systems using numerical simulation by the coarse-grained molecular dynamics method [1].

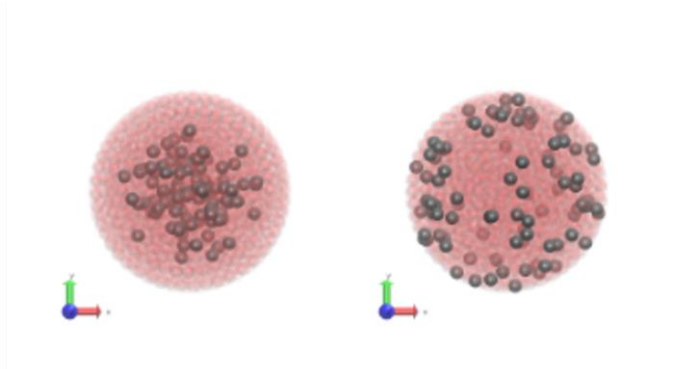


Figure 5. Two types of templates for core-shell magnetic microgels simulation: “magnetic core + polymeric shell” (left) and “polymeric core + magnetic shell” (right). Polymer particles are shown in red translucent, magnetic nanoparticles in gray. In these eight-layer templates examples 75% of internal layers are considered as the core.

The model is based on the preliminary generation of spherical templates with a specified layer-by-layer number of polymeric particles and magnetic nanoparticles (MNPs). The developed procedure allows filling by MNPs a specified proportion of internal or external layers to obtain a flexibly adjustable core-shell structure. Then the particles in the templates with different proportions of MNPs are connected by elastic bonds according to the developed algorithm. The resulting cross-linked magnetopolymeric assemblies are then considered in a computational experiment with different magnetic interaction parameters during magnetization in a uniform magnetic field. The joint magnetic, structural and mechanical response of the microgels is analyzed regarding the features of geometry and the method of cross-linking.

The research was supported by the grant of the Russian Science Foundation No. 24-71-00055, <https://rscf.ru/en/project/24-71-00055/>.

[1] F. Weik et.al., Eur. Phys. J.: Spec. Top. 227, 1789-1816 (2019)

# Magnetic characteristics and critical temperature of spin systems: approaches based on the method of Green's functions

A. Samigullina\*, I. Sharafullin

Ufa University of Science and Technology, 450076, Zaki Walidi 32, Ufa, Russia

\*angelasamig2002@gmail.com

The problem of studying competing interactions in spin systems is one of the central tasks of modern condensed matter physics. The competition of exchange interactions can lead to frustration, which significantly affects the properties of the model [1]. Spin systems with frustrations exhibit behavior that is qualitatively different from the properties of their non-frustrated counterparts, which makes their study especially important for understanding complex magnetic phenomena.

The Heisenberg model, in which frustration arises from competing exchange interactions, remains insufficiently investigated. In particular, taking into account the antiferromagnetic interaction between the second nearest neighbors in classical models leads to degeneration of the ground state, which significantly complicates the analysis of the system. This degeneracy contributes to the formation of various magnetic structures. To further study such systems, it is necessary to use theoretical approaches, including numerical modeling methods and analytical techniques such as perturbation theory and the theory of two-time Green's functions.

In this paper, the method of Green's functions is used to calculate the energy spectrum of the lattice of magnetic skyrmions and analyze the magnetic characteristics.

A bilayer model consisting of a ferroelectric film serving as a substrate and a magnetic film with a crystal structure of a simple cubic lattice is considered. The Heisenberg spins with a quantum number  $S = 1/2$  are located in the nodes of the magnetic film. The complete Hamiltonian of this model has the following form:

$$H = -J_1 \sum_{i,j} \vec{S}_i \vec{S}_j - J_2 \sum_{i,i'} \vec{S}_i \vec{S}_{i'} - \sum_{i,j} I_{i,j} \vec{S}_i^z \vec{S}_j^z - g\mu_B h \sum_i \vec{S}_i^z - J_{mf} \sum_{i,j} (\vec{S}_i \cdot \vec{S}_j)^z \vec{P}^z - J_f \sum_{i,j} \vec{P}_i \vec{P}_j - \sum_i E^Z P_i^z \quad \#(1)$$

The first term describes the ferromagnetic interaction between the nearest neighboring spins, the second term describes the antiferromagnetic interaction between the next nearest neighbors along the y axis. The third term corresponds to the anisotropic interaction, the fourth to the interaction with an external magnetic field, and the fifth to the magnetoelectric interaction between magnetic and ferroelectric films. The sixth and seventh terms describe the Hamiltonian of the ferroelectric system.

An increase in the magnetic field strength in the models leads to a change in the energy landscape, which contributes to the formation of more ordered magnetic states due to increased magnetic interactions within the layer. In the absence of an external magnetic field, a symmetrical energy distribution is observed relative to the wave vector  $k$ . When a magnetic field ( $h > 0$ ) is applied, energy levels shift, indicating its effect on the spin configuration and energy states of the system. The periodicity of the spiral structure, determined by the wave vector  $k$ , leads to the formation of energy zones separated by slits.

Using the method of Green's functions, the critical temperature of the system was determined at the specified parameters, and a phase transition was revealed.

The work was performed within the framework of the state assignment agreement No. 075-03-2024-123/1 dated 02/15/2024 topic No. 324-21.

[1] S.E. Hog, I.F. Sharafullin, H.T. Diep, H. Garbouj, M. Debbichi, M. Said, J. of Magnetism and Magnetic Materials 563, 169920 (2022)

# Influence of Dzyaloshinskii-Moriya Interaction on the Magnetic Structure of Square-Kagome Compounds

L. Taran<sup>a,\*</sup>, F. Temnikov<sup>a</sup>, S. Streltsov<sup>a,b</sup>

<sup>a</sup> M. N. Mikheev Institute of Metal Physics, Ural Branch of Russian Academy of Sciences, 620137, st. S. Kovalevskaya, 18, Yekaterinburg, Russia

<sup>b</sup> Institute of Physics and Technology, Ural Federal University, 620002 Yekaterinburg, Russia

\*leonidtaran97@gmail.com

In recent years, frustrated magnets with a kagome lattice structure have attracted significant attention [1-2]. In such systems, competition between different spin interactions often leads to frustration, as the system cannot simultaneously minimize the energy of all exchange bonds. The kagome lattice, with its triangular motifs, naturally promotes magnetic frustration. Spin systems with triangular geometry, described by the Heisenberg model with antiferromagnetic nearest-neighbor interactions, have been extensively studied, frequently yielding quantum spin liquid states characterized by the absence of long-range magnetic order [3-4]. Identifying real materials hosting such states and studying their physical properties remains a key challenge in modern magnetism.

Recently, compounds with a novel square-kagome geometry, comprising  $\text{Cu}^{2+}$  ions, have been discovered [5-6]. These systems exhibit strong exchange frustration, potentially stabilizing a quantum spin liquid state. In  $\text{Cu}^{2+}$ -based compounds lacking inversion symmetry between magnetic ions, the Dzyaloshinskii-Moriya (DM) interaction plays a crucial role [7]. This interaction can determine magnetic ordering [8] and induce spontaneous electric polarization via the Katsura-Nagaosa-Balatsky mechanism [9].

In this work, we employ first-principles density functional theory calculations to evaluate the impact of the DM interaction on the magnetic structure of recently discovered square-kagome compounds  $\text{KCu}_6\text{AlBiO}_4(\text{SO}_4)_5\text{Cl}$  [5] and  $\text{Na}_6\text{Cu}_7\text{BiO}_4(\text{PO}_4)_4[\text{Cl}(\text{OH})]_3$  [6].

The work was carried out within the framework of the state assignment of the Ministry of Science and Higher Education of the Russian Federation for the IMP UB RAS and IMP UB RAS youth scientific project No. m 12-24.

- [1] X. Teng et al., *Nature* **609**, 490 (2022)
- [2] H. Li et al., *Phys. Rev. X* **11**, 031050 (2021)
- [3] T.-H. Han et al., *Nature* **492**, 406 (2012)
- [4] S. Depenbrok et al., *Phys. Rev. Lett.* **109**, 067201 (2012)
- [5] M. Fujihala et al., *Nat. Commun.* **11**, 3429 (2020)
- [6] O. V. Yakubovich et al., *Inorg. Chem.* **60**, 11450 (2021)
- [7] Smirnov et al., *Phys. Rev. B* **92**, 134417 (2015)
- [8] Y. Q. Guo et al., *JMMM* **572**, 170594 (2023)
- [9] Katsura et al., *Phys. Rev. Lett.* **95**, 057205 (2005)

# DFT Study of Hyperfine Interaction Parameters and Magnetic State in Ternary Fe-Al-B Alloys

A. Abdullin, E. Voronina\*

Kazan Federal University, 420008, Kremlyovskaya str. 18, Kazan, Russia

\*Elena.Voronina@kpfu.ru

Multicomponent compounds based on the Fe-Al system remain of significant interest both for developing practical applications and as model systems for studying magnetic phenomena in strongly correlated electronic systems. In particular, Fe-Al-based materials with boron additives are important for technical applications due to their magnetoelastic properties [1] and show promise as materials for sensors and transducers. Moreover, ordered Fe-Al alloys with aluminum contents exceeding 30 at.% have proven to be convenient model objects for investigating the emergence and stabilization of nanoscale magnetic inhomogeneities in structurally homogeneous magnets, especially within incommensurate spin structures [2].

In this work, we present the results of quantum-mechanical calculations of the electronic structure, magnetic moments, hyperfine interaction parameters, and magnetic state of both binary Fe-Al and ternary Fe-Al-B systems. The local magnetic characteristics – namely, the Fe magnetic moment ( $m_{\text{Fe}}$ ) and the  $^{57}\text{Fe}$  hyperfine magnetic field (HMF) – were calculated within the density functional theory using WIEN2k, while the magnetic structure was analyzed with the WIENncm program [3,4].

For the quantum-mechanical calculations, 16-atom unit cells with varying compositions of Fe, Al, and B were employed. An analysis of local HMF values, isomer shifts, and magnetic moments was conducted as a function of both the type and position of the atoms within the cell. It was observed that the calculated local HMF decreases on average by approximately 2.7 T per atom for each additional B or Al atom introduced into the first coordination sphere of an Fe atom. The results indicate that the HMF values, as well as the isomer shifts and  $m_{\text{Fe}}$ , strongly depend on both the number of substituting Al and B atoms in the second, third, and fourth coordination spheres and on their specific positions within the cell. Calculations for structures with interstitial boron positions showed that, on average, the addition of one boron atom leads to an approximate 10% decrease in the calculated HMF. However, it would be erroneous to generalize this trend, since occupation of certain interstices by boron results in an increase of the local HMF. These increases are associated with a local expansion of the interatomic distances between Fe atoms.

Theoretical investigations of the magnetic ordering in the binary  $\text{Fe}_9\text{Al}_7$  and ternary  $\text{Fe}_9\text{Al}_6\text{B}$  systems revealed that the ferromagnetic state is energetically unfavorable, with the spin spiral state being realized in most cases. The position and type of *sp*-elements (Al, B) within the unit cell influence the energy difference between the spin spiral and ferromagnetic states, and whether either state represents an equilibrium configuration depends on both the atomic positions and the specific substituting element. Calculations showed that in the ternary  $\text{Fe}_9\text{Al}_6\text{B}$  systems the ground state is characterized by a spin spiral with a *q*-vector oriented along [111]. For all systems considered, the spin spiral state remains energetically most favorable at a lattice parameter for which the average magnetic moment attains 1  $\mu_{\text{B}}$  per Fe atom, regardless of the specific positions occupied by the boron atoms.

[1] C. Bormio-Nunes, O. Hubert, JMMM 393, 404(2015)

[2] D. R. Noakes *et al*, PRL 91, 217201(2003)

[3] P. Blaha *et al*, J. Chem. Phys. 152, 074101(2020)

[4] R. Laskowski, G. K. H. Madsen, P. Blaha, K. Schwarz, PRB 69, 140408 (2004)

# Bright Envelope Solitons in the Antiferromagnetic Metals/Semiconductors for Terahertz Frequency Range

A. Zhabova<sup>a,\*</sup>, S. Grishin<sup>a</sup>, S. Nikitov<sup>b</sup>

<sup>a</sup> Saratov State University, 410012, Astrakhanskaya 83, Saratov, Russia

<sup>b</sup> Kotelnikov Institute of Radioengineering and Electronics of Russian Academy of Sciences, 125009, Mokhovaya 11 str.7, Moscow, Russia

\*aleksis.bogomolova@yandex.ru

Nowadays, one of the important problems of modern radiophysics and electronics is the creation of sources of short and ultrashort microwave (MW) pulses [1]. In the MW range, a convenient medium for the short MW pulse formation is an insulator ferrimagnetic (yttrium iron garnet - YIG) film. It supports the propagation of the magnetostatic spin waves (MSWs) [2] that possess the various types of dispersions and take part in the nonlinear processes [3]. In the YIG films, the competition between dispersion and nonlinearity leads to the formation of bright envelope solitons of MSW with a duration of about tens of nanoseconds [4].

To control a soliton-like pulse duration, the bigyrotropic media possessing both the ferromagnetic and plasma properties are more attractive [5]. So, the effect of free charge carriers (electrons) on magnetization of the bigyrotropic medium with the antiferromagnetic metal/semiconductor (AFMM/AFMSC) properties leads to that the effective permittivity and permeability become simultaneously negative in a certain frequency range. In this range, the backward electromagnetic waves (BEMWs) exist. The BEMW bandwidth depends on an electron concentration that determine the BEMW bright envelope soliton duration (see Fig.).

The paper presents the results of a theoretical study of bright envelope soliton formation in a double negative medium based on a transversely magnetized AFMM/AFMSC. The nonlinear Schrodinger equation with periodic boundary conditions is used for numerical simulation of soliton modes. It is shown that the duration of BEMW bright envelope solitons is decreased with an increase in the concentration of free charge carriers (electrons) in the AFMM/AFMSC.

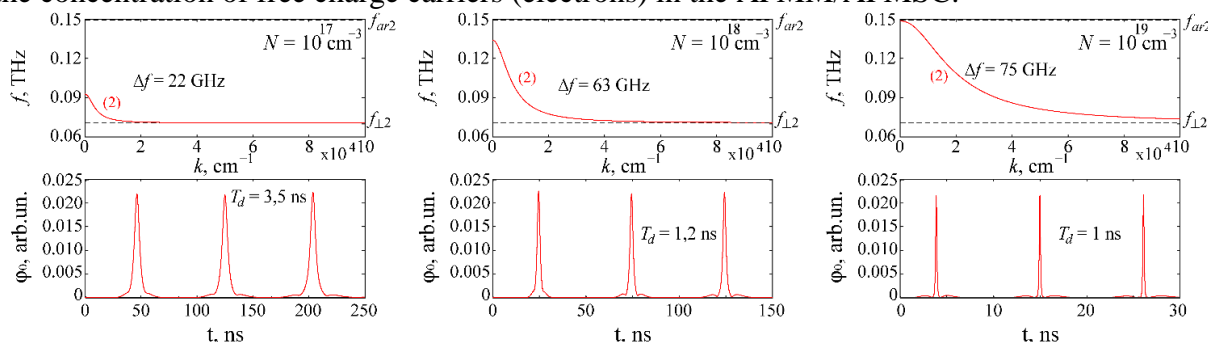


Figure. Periodic sequences of BEMW bright envelope solitons.

The obtained results may be of interest in developing short pulse sources for magnonic logic systems and neuromorphic computing.

The study was supported by the Russian Science Foundation (project No 23-79-30027).

- [1] N. Ginzburg, et al., Phys. Rev. Appl., 13 (4), 044033 (2020)
- [2] A. Vashkovsky, et al., (Izd-vo SGU, Saratov, 1993). (in Russian)
- [3] A. Kondrashov, et al., J. Appl. Phys., 132 (17), 173907 (2022)
- [4] M. Wu, Solid State Phys., 62, 163 (2010)
- [5] A. Gurevich, et al., (Fizmatlit, M., 1994). (in Russian)

# Micromagnetic modeling of spin wave propagation in YIG film with magnetite nanoparticles

F. Garanin\*, A. Sadovnikov, M. Lomova

Saratov State University named after N.G. Chernyshevsky, 410012, Astrakhanskaya 83, Saratov, Russia

\*garaninfedorwork@mail.ru

In recent years, magnonics, an innovative area of spintronics based on the use of iron garnets and spin waves (SW) for information transmission, has demonstrated rapid development [1]. Unlike traditional approaches, where the key role is played by the transport properties of spin-polarized electrons, magnonics offers a fundamentally new way of signal processing. This opens up broad opportunities for creating functional devices such as filters, modulators, and waveguides operating on the basis of spin waves [2].

In parallel with the development of magnonics, interest in the use of magnetic materials in biomedicine is growing. Particular attention is attracted by magnetic nanoparticles, which have unique properties, including high sorption capacity and the ability to be remotely controlled using external magnetic fields. These characteristics make them indispensable in areas such as diagnostics (for example, enhancing contrast in magnetic resonance imaging) and therapy (targeted drug delivery). One of the most promising materials for both magnonics and biomedicine is magnetite ( $\text{Fe}_3\text{O}_4$ ). Its exceptional magnetic properties allow magnetite nanoparticles to be effectively used in various applications.

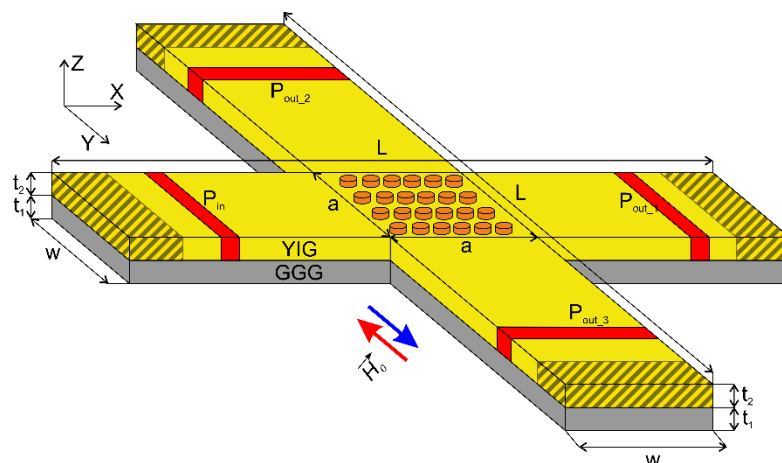


Figure. 1. Schematic representation of YIG film with magnetite nanoparticles

Micromagnetic modeling was performed in the MuMax<sup>3</sup> package [3], where the structure was divided into a grid, in the nodes of which the Landau-Lifshitz equation with Hilbert attenuation was numerically solved. In the micromagnetic modeling, conditions were created for the excitation of a surface magnetostatic wave (SMW), in which the external magnetic field  $H_0$  was applied along the positive/negative direction  $Oy$ . The value of the external magnetic field parameter  $H_0$  was 1200 Oe.

Thus, using numerical micromagnetic modeling, a cross-shaped structure with magnetite nanoparticles was investigated. This structure can be used as a microwave signal filter controlled by the orientation of the magnetic field.

The work was supported by the Russian Science Foundation Grant No. 23–13–00373.

[1] V.V. Kruglyak et al. J. Phys. D: Appl. Phys., 43, 264001, (2010)

[2] D. Sander et al. J. Phys. D: Appl. Phys., 50, 363001, (2017)

[3] A. Vansteenkiste et al. AIP Advances., 4, 107133, (2014)



# Optical methods for measuring the electrical conductivity of magnetic colloids based on liquid dielectrics

I. Es'kova\*, C. Yerin

North Caucasus Federal University, 1 Pushkin st., 355017 Stavropol, Russia,

\*i.tatova@inbox.ru

In magnetic fluids, when exposed to an electric field, particle aggregation occurs, a volume charge is formed, which generally leads to changes in the macroscopic properties of the magnetic colloid. One of the key electrophysical parameters is electrical conductivity. Traditionally, electrical conductivity is measured using the volt-ampere characteristic.

We propose a new method for measuring the conductivity of a magnetic fluid based on liquid dielectrics by measuring the characteristic times of Maxwell-Wagner relaxation in a cell with an electrode covered with a solid insulating film. The presence of a polypropylene film with a thickness of 40-250  $\mu\text{m}$  on at least one of the electrodes made it possible to exclude free charge exchange, which prevents the external field from being compensated by the internal field of an unevenly distributed volume charge. To determine the relaxation time of the electric field, the electro-optical effect of double refraction in a field of rectangular pulses lasting several seconds was used.

We propose a new method for measuring the conductivity of a magnetic fluid based on liquid dielectrics by measuring the characteristic Maxwell-Wagner relaxation times in a cell with an electrode coated with a solid insulating film. The presence of a polypropylene film with a thickness of 40-250  $\mu\text{m}$  on at least one of the electrodes made it possible to exclude the free exchange of charges, which prevents the external field from being compensated by the internal field of an unevenly distributed volumetric charge. To determine the relaxation time of the electric field, the electro-optical effect of double refraction in the field of rectangular pulses lasting several seconds was used.

Figure 1 shows the characteristic shape of an electro-optical signal in a magnetic kerosene-based liquid with a concentration of 0.01% when exposed to rectangular high-voltage (9 kV) pulses with a duration of 5 s. The characteristic signal decay after switching the field on and off has an exponential shape with a characteristic time determined by the thickness, dielectric constant of the layer, and the conductivity of the colloid. Conducting such experiments for insulating films of various thicknesses makes it possible to calculate the specific conductivity of a magnetic colloid. To do this, it is necessary to determine the tangent of the angle of inclination of the relaxation time dependence on the ratio of the thicknesses of the dielectric film on the surface of the electrode  $d_1$  and the magnetic colloid  $d_2$  (Figure 2). The low-frequency electrical conductivity determined in this way is in good agreement with the measurement data of the volt-ampere characteristic.

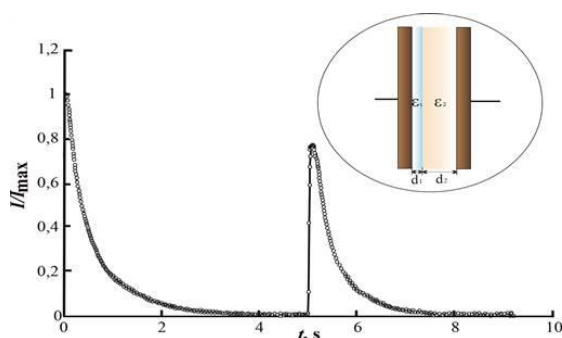


Figure 1.

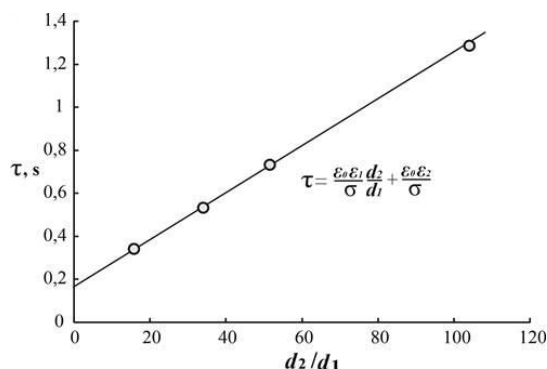


Figure 2.



# Development of reconfigurable optical microdevices based on the photopolymer with magnetic nanoparticles

A. Buldakova\*, M. Sharipova, V. Tolmacheva, A. Frolov, A. Fedyanin

Lomonosov Moscow State University, 119991, Leninskie gory 1, Moscow, Russia

\*makarovaav@my.msu.ru

Microstructures with diverse functionalities, fabricated from polymer materials using two-photon polymerization (TPP) technology, hold significant promise for applications in micromechanical and micro-optical systems [1]. However, structures fabricated by this technique are often limited by their passive response to external stimuli. The integration of magnetic nanoparticles provides a pathway to develop microdevices that can be actively reconfigured through the application of an external magnetic field.

In this study, we report the design, fabrication, and characterization of a magnetoactive optical modulator in the form of a diffraction grating, produced by two-photon polymerization in a magnetic photopolymer composite.

Several compositions of magnetic photopolymer composites were developed, comprising of SU-8, SZ-2080, andOrmocomp photopolymers mixed with superparamagnetic  $\text{Fe}_3\text{O}_4$  nanoparticles with an average diameter of 16 nm. To prevent nanoparticle agglomeration, surfactants such as oleic acid and polyvinylpyrrolidone were used, and toluene and ethanol were used as solvents for homogeneous dispersion of the nanoparticles within the photopolymer matrix. Three-dimensional models of the diffraction gratings were designed for fabrication (Fig. 1a). The first model consists of zigzag-shaped strips with a length of 43  $\mu\text{m}$ , a thickness of 1.5–2  $\mu\text{m}$ , and a period of 3  $\mu\text{m}$ . The second model features a similar zigzag geometry, with connected strips at both edges, with a total length of 78  $\mu\text{m}$ , a thickness of 0.75–1  $\mu\text{m}$ , and the same periodicity.

The optimized magnetic photopolymer composite, ensuring uniform nanoparticle distribution, sensitivity to the magnetic field, and structural flexibility was formulated using SZ-2080 photopolymer,  $\text{Fe}_3\text{O}_4$  nanoparticles, toluene, and oleic acid.

Diffraction gratings fabricated with  $\text{Fe}_3\text{O}_4$  nanoparticle concentration ranging from 0.5 wt% to 5 wt% (Fig. 1b, c) exhibited diffraction orders at angles of 20° and 45° that are in good agreement with a theoretical prediction.

Gratings containing 3–5 wt%  $\text{Fe}_3\text{O}_4$  nanoparticles demonstrated actuation in response to an external magnetic field. These structures showed reversible stretching toward the magnetic field (Fig. 1d).

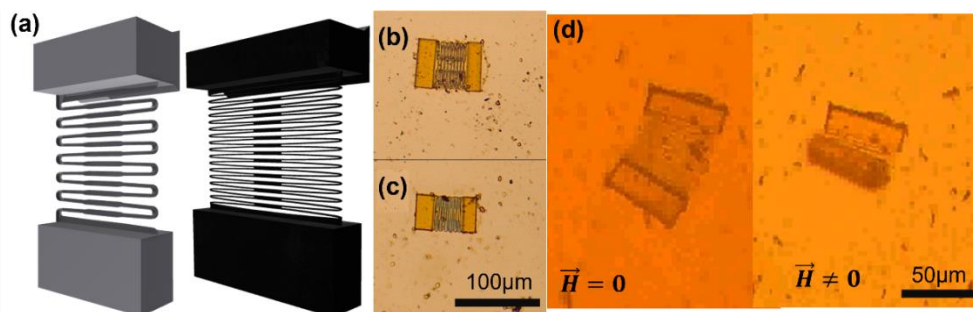


Figure 1. (a) Three-dimensional models of the fabricated gratings. Optical microscope images of the fabricated gratings corresponding to the first model (b), the second model (c,d) and bending of structures under the application of an external magnetic field (d).

# Transformation of optical Kerr effect of ferromagnetic transition metal by additional nanolayers of normal metals

V. Skidanov \*

NRC «Kurchatov institute», 123182, Kurchatov square 1, Moscow, Russia

\*skidanov@ippm.ru

Phenomena at the interface between magnetic and nonmagnetic media attract growing attention during last decade [1]. Besides application of Kerr effect of ferromagnetic metallic layers is considered as a promising way to enhance sensitivity of biochips based on plasmonic properties of metal films in recent years [2].

The present report is devoted to the unexpected results of experimental investigation of possibility to modify magneto-optical signal by additional nonmagnetic metal layers with thickness significantly exceeding the depth of light penetration atop and/or under ferromagnetic film.

Objects for investigation were fabricated by magnetron sputtering of metallic targets on glass substrates. The transverse Kerr signal related to the magnitude of whole hysteresis loop for every object was measured. All measurements made at the same intensity level of reflected light.

It was found that the magnitude of magneto-optical signal from permalloy (Py) film can be enhanced by additional nonmagnetic transition layer with thickness  $\sim 20$  nm on top of the Py if outer  $d$ -band of nonmagnetic metal is partially filled (Ti, Ta). From the other hand additional layer of transition metal with empty or filled  $d$ -band (Al, Cu, Au) under Py layer enables to double Kerr signal as well (Figure 1). Considering this it is interesting to multiply both effects to enhance magneto-optical reply to external magnetic field.

The experimental results of investigation of three-layered structures Ta/Py/Al and their comparison with two-layered structures Ta/Py are shown in Figure 1. It is clear that the mutual effect of both nonmagnetic metals seems additive instead of multiplying so that influences of Ta and Al compensate each other due to different signs of Ta and Al effects on Kerr signal. Few experiments were made with various two- and three-layered structures to clarify this unexpected results and interpretation was proposed in terms of deep spin diffusion of unexcited electrons in metals [3].

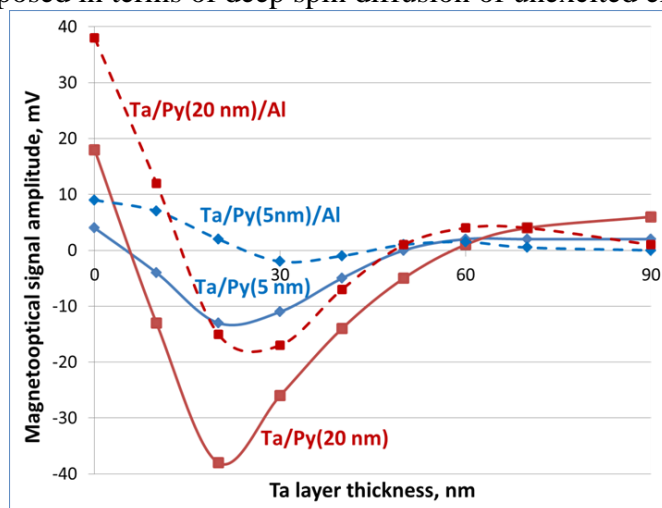


Figure 1. Dependences of magneto-optical Kerr signal of two- (Ta/Py) and three-layered (Ta/Py/Al) structures on Ta layers thickness with (dashed lines) and without (solid lines) Al layer under Py films.

[1] F. Hellman et al., Rev. Mod. Phys. 89 (2), (2017)

[2] G. Armelles et al. Adv. Opt. Mat. 1 (1), 10-35 (2013)

[3] V. P. Zhukov and E.V. Chulkov, Physics - Uspekhi 52(2), 105 (2009)

## Investigation of magnetic properties of filamented HTS tapes

S. Veselova\*, M. Osipov, D. Abin, S. Pokrovskii

National Research Nuclear University MEPhI, 115409, Kashirskoe shosse, 31, Moscow, Russia

\*i@svveselova.ru

In non-filamented high-temperature superconducting (HTS) tapes operating under alternating magnetic fields, the motion of Abrikosov's whirlwinds leads to energy dissipation. Laser or mechanical segmentation into parallel isolated conductors reduces hysteresis losses during remagnetization by restricting lateral whirlwinds movement through the creation of physical barriers [1-2]. Additionally, filamentation localizes heat generation during quench events. Each filament is encapsulated by a copper coating, which enhances heat dissipation and prevents overheating of the entire tape.

This study focused on optimizing laser-cutting parameters for second-generation HTS tapes to establish conditions for reproducible filamentary structures. Samples with varying numbers of filaments were fabricated. Surface morphology was analyzed via longitudinal profilometer scanning, enabling quantitative evaluation of average roughness ( $R_a$ ) and average depth ( $R_z$ ). Samples with an optimal laser ablation depth of  $19 \pm 1 \mu\text{m}$ , achieved through 10 laser processing iterations, were selected for reproducible filamentation. Magneto-optical imaging confirmed spatial isolation of the superconducting layer into discrete filaments.

Magnetic characterization was performed using an MPMS-5 system within a temperature range of 4.2–77.4 K under a cyclic magnetic field of  $\pm 5$  T. Magnetization hysteresis curves revealed the dependence of remagnetization losses on the degree of filamentation. At 4.2 K, a significant reduction in hysteresis losses was observed. As the temperature increased to 40 K, the effect diminished, with further degradation occurring at 77.4 K. These results demonstrate the temperature-dependent efficacy of filamentation in mitigating energy dissipation in HTS tapes.

The work was carried out under the State Assignment (project FSWU-2025-0008) with the support of the Ministry of Science and Higher Education of the Russian Federation

[1] Lan, Tian, *IEEE* y 33.6, 2023

[2] Skov-Hansen, *IEEE*, 2617, 1999

# Magneto-optical and magnetic resonance studies of two-layer films FeNi-V<sub>2</sub>O<sub>3</sub> system

G. Patrin<sup>a,b,\*</sup>, I. Anisimov<sup>a</sup>, A. Kobayakov<sup>a,b</sup>, V. Yushkov<sup>a,b</sup>, Ya. Shiyan<sup>a,b</sup>, S. Semenov<sup>a,b</sup>

<sup>a</sup> Siberian Federal University, Svobodny pr., 79, Krasnoyarsk, 660041, Russia

<sup>b</sup> L.V. Kirensky Institute of Physics, Federal Research Center KSC SB RAS, Akademgorodok, 50/38, Krasnoyarsk, 660036, Russia

\*patrin@iph.krasn.ru

For film structures, many properties are determined by interactions at the interface of different materials. Interfaces not only change the bulk magnetic properties, but can also induce magnetism in non-magnetic layers, changing the nature of the magnetic state. At the interfaces in heterostructures, noncollinearity, interface anisotropy, interface-induced spin textures, etc. arise. The best known effects are exchange bias, magnetic springs, the spin Hall effect, and topological insulators. In general, the magnetic properties of a material ( $M_s$ ,  $T_C$ , etc.) change whenever its dimensions become comparable to the corresponding magnetic correlation length.

We attempted to study two-layer structures with a vanadium oxide layer, which exhibits a metal-insulator transition (MIT). The films were deposited on a glass substrate using an Omicron ultrahigh-vacuum magnetron sputtering system (with a film thickness control system during growth) at a base pressure of  $10^{-10}$  Torr. A V<sub>2</sub>O<sub>3</sub> target was used to deposit the vanadium oxide layer, and a Fe<sub>14</sub>Ni<sub>86</sub> alloy target was used to deposit the ferromagnetic layer. Electron microscopic studies of the cross section were performed on a JEOL JEM-2100 electron microscope. To measure the resonance properties, we used a Bruker E 500 CW EPR spectrometer operating at a frequency  $f_{\text{MWF}} = 9.49$  GHz, and magneto-optical data were obtained on a NanoMOKE-2 magneto-optical Kerr effect setup.

The behavior of the temperature of the transition metal transition of single-layer films of the V<sub>2</sub>O<sub>3</sub> compound depending on the thickness was studied [1]. It was found that at vanadium oxide layer thicknesses of more than 100 nm, the transition temperature practically approaches the transition temperature for the bulk crystal. A sharp increase in the transition temperature is observed when the film thickness decreases to 50 nm. The study of the dependences of magnetization and the Kerr effect, taken at different temperatures, shows that the shape of the hysteresis loop depends on the sequence of deposition of layers, while the effect of exchange bias takes place. The coercive force of the structure is approximately an order of magnitude greater than that of the nominal permalloy layer. The temperature dependences of the resonance field ( $H_r$ ) for FeNi/V<sub>2</sub>O<sub>3</sub> and V<sub>2</sub>O<sub>3</sub>/FeNi films are qualitatively similar, but differ in the value of  $H_r$ . A feature typical of the single-ion relaxation mechanism is observed in the temperature dependences of the line width [2].

The research was conducted according to the state assignment of the Ministry of Science and Higher Education of the Russian Federation and the Federal State Autonomous Educational Institution of Higher Education Siberian Federal University (No. FSRZ-2023-0008).

[1] G.S. Patrin, A.V. Kobayakov, V.I. Yushkov, et al. Processes. 11(7), 2084 (2023)

[2] B. Brown, EPJ 33, 255 (2011)

# Magneto-optical Kerr Visualization of Amorphous Ribbons

## Magnetic Microstructure

S. Samchenko<sup>a,\*</sup>, M. Simdyanova<sup>a</sup>, N. Perova<sup>a</sup>, R. Radjabov<sup>b</sup>, N. Perov<sup>a</sup>, E. Gan'shina<sup>a</sup>,  
A. Granovsky<sup>a,b,c</sup>

<sup>a</sup> Lomonosov Moscow State University, 119991, Leninskie gory 1, Moscow, Russia

<sup>b</sup> Samarkand State University, 140104, University blv. 15, Samarkand, Uzbekistan

<sup>c</sup> Institute for Theoretical and Applied Electrodynamics of Russian Academy of Sciences, 125412,  
Izhorskaya 13, Moscow, Russia

\*samchenkosv@my.msu.ru

We present results of structural, bulk and surface magnetic properties, magneto-optical (MO) spectra of series amorphous iron- and cobalt-based ribbons with varying elemental composition focusing on their magnetic microstructure near surface. The following compositions were studied:  $\text{Fe}_{83,9}\text{Co}_{2,3}\text{Ni}_{6,7}\text{Si}_{7,1}$ ,  $\text{Fe}_{5,1}\text{Co}_{91,3}\text{Si}_{3,6}$ ,  $\text{Fe}_{68,5}\text{Ni}_{19,1}\text{Si}_{4,9}\text{C}_{7,5}$ ,  $\text{Fe}_{81,7}\text{Ni}_{10,6}\text{Si}_{7,7}$ ,  $\text{Fe}_{86,6}\text{Ni}_{9,6}\text{Si}_{3,8}$ ,  $\text{Fe}_{67,3}\text{Ni}_{18,2}\text{Si}_{5,1}\text{C}_{9,4}$ ,  $\text{Fe}_{71,6}\text{Ni}_{18,7}\text{Si}_{5,4}\text{C}_{4,7}$ , and  $\text{Fe}_{70,5}\text{Ni}_{18,3}\text{Si}_{5,6}\text{C}_{6,2}$ . The samples were fabricated by the rapid quenching. Magnetic hysteresis loops were obtained using a vibrating sample magnetometer (VSM) in fields up to  $\pm 1.5$  kOe. Three types of MO investigations were carried out: measurements of magnetic field dependencies and MO spectra in the transverse Kerr effect geometry; visualization of magnetic microstructure and magnetic reversal using Kerr microscope in the longitudinal geometry (Evicomagnetics GmbH, Germany).

High sensitivity of bulk magnetic properties to alloy composition was observed with large contrast between Fe-based and Co-based alloys. The samples with a higher Co content exhibit lower saturation magnetization and coercivity compared to Fe-rich compositions. The obtained MO spectral Kerr curves confirmed the amorphous nature of the ribbons and provided also a clearer contrast between Fe-based and Co-based compositions.

Due to surface defects and roughness, stable domain patterns were observed only on the free side of the ribbons. Fe-rich compositions exhibited labyrinthine domain textures, while such structure was not observed for the sample with predominant Co content. Furthermore, spatially resolved by Kerr microscope hysteresis loops, obtained from different small areas of surface along the length and width of the ribbons, revealed strong variations in coercivity, MO signal intensity and even the MO sign, indicating inhomogeneous magnetization behavior.

These findings highlight the necessity of combining integral magnetic characterization with spatially and spectrally resolved magneto-optical techniques to understand the complex magnetic behavior of amorphous materials.

## Magnetic resonance investigations of interlayer coupling in CoNi/Si/FeNi films

G. Patrin<sup>a,b,\*</sup>, Ya. Vakhitova<sup>b</sup>, Ya. Shiyan<sup>a,b</sup>, A. Kobayakov<sup>a,b</sup>, V. Yushkov<sup>a,b</sup>

<sup>a</sup> Siberian Federal University, Svobodny pr., 79, Krasnoyarsk, 660041, Russia

<sup>b</sup> L.V. Kirensky Institute of Physics, Federal Research Center KSC SB RAS, Akademgorodok, 50/38,  
Krasnoyarsk, 660036, Russia

\*patrin@iph.krasn.ru

Due to the specific nature of their structure, nanomagnetic materials have a set of unusual properties, which arouses interest in them, both in terms of fundamental research and in terms of possible practical applications. To control the interlayer interaction, as a determining parameter when creating structures such as a magnetic spring with given characteristics, attempts are being made to introduce additional layers, for example, from a semiconductor material, between the magnetic layers.

The films were sputtered onto a glass substrate using an ultrahigh vacuum magnetron sputtering system from Omicron NanoTechnology (Taunusstein, Germany) with Pfeiffer Vacuum turbomolecular pumps. The deposition was carried out at a base pressure of  $10^{-10}$  Torr in an argon atmosphere. The nickel content in the CoNi layer (magwas 19.5 at. %, and in the FeNi layer there was 83 at. %. The thickness of the CoNi layer was  $t_h = 53$  nm and was chosen so that it would exhibit the properties of a magnetically hard layer when measured in available magnetic fields. The thickness of the soft magnetic FeNi layer was  $t_s = 72$  nm. The thickness of the non-magnetic semiconductor layer was variable and varied in the range  $t_{Si} = 0 - 23$  nm. Magnetization measurements were carried out using an MPMS-XL setup in the temperature range from helium temperature to room temperature. Electron microscopic studies of the cross section were performed on a JEOL JEM-2100 electron microscope. To measure the resonance properties, we used a Bruker E 500 CW EPR spectrometer operating at a frequency  $f_{MWF} = 9.49$  GHz.

Earlier, it was found that, depending on the thickness of the silicon layer, the trilayer structure, along with the properties inherent in magnetic springs, exhibits the effect of positive exchange bias [1], depending on the thickness of silicon. An unusual behavior of the angular dependences of the resonant field of the magnetic resonance lines was also found, which is associated with the existence of a biquadratic interlayer interaction [2]. Particular attention is paid to the influence of the interface on the formation of the magnetic state of the multilayer structure. It was found that perpendicular anisotropy is induced at the CoNi-Si interface. Magnetostatic data give grounds to assert that the magnetizations of the soft and hard magnetic layers in the ground state are oriented perpendicular to each other. More complete information on the mutual orientation of the film layers with different silicon thicknesses was obtained by the electron magnetic resonance method. A theoretical analysis of the magnetic resonance data was carried out. For different thicknesses of silicon, data on the relative magnitude of bilinear and biquadratic interactions were obtained.

The research was conducted according to the state assignment of the Ministry of Science and Higher Education of the Russian Federation and the Federal State Autonomous Educational Institution of Higher Education Siberian Federal University (No. FSRZ-2023-0008).

[1] G.S. Patrin, I.A. Turpanov, V.I. Yushkov, et al. JETP Lett. 109, 320 (2019)

[2] G.S. Patrin, Ya.A. Vakhitova, Ya.G. Shiyan, et al. Techn.Phys.Lett. 51(4) 46 (2025) (in Russian)



## Effect of Barium Titanate Coating on SAR in Magnetic Hyperthermia of $\text{CoFe}_2\text{O}_4$ Nanoparticles

I. Shamanov, V. Salnikov, D. Petrukhin, V. Belyaev, V. Rodionova, A. Anikin

Immanuel Kant Baltic Federal University, 236004, Nevskogo 14, Kaliningrad, Russia

\*israfilshamanov3@gmail.com

Magnetic hyperthermia is a method of localized living tissue heating using magnetic nanoparticles exposed to a high-frequency alternating magnetic field [1]. It is applied in cancer therapy for the selective destruction of tumor cells. Fields with an amplitude of 1–50 kA/m and frequency of 100–1000 kHz are typically used, allowing for effective heating without damaging healthy tissue.

One promising direction in magnetic hyperthermia is the use of nanoparticles based on magnetite ( $\text{Fe}_3\text{O}_4$ ) and cobalt ferrite ( $\text{CoFe}_2\text{O}_4$ ). To stabilize them in aqueous solutions with pH close to physiological values and to improve biocompatibility, the particles are coated with various organic and inorganic shells. These coatings reduce aggregation and influence the relaxation mechanisms of the nanoparticles in a magnetic field.

In this study, spheroidal  $\text{CoFe}_2\text{O}_4$  (CFO) nanoparticles with diameters of 10, 20, and 30 nm were synthesized, both uncoated and coated with barium titanate ( $\text{BaTiO}_3$ ) in mass ratios of 1/4 and 1/6 (CFO@BTO). Magnetic and structural characterizations of the samples were performed. For all samples, solution concentrations were determined, and heating kinetics in an alternating magnetic field were measured. The measurements were carried out at a field frequency of 730 kHz and an amplitude of 2 mT. Based on the experimental data, the specific absorption rate (SAR) and intrinsic loss power (ILP) were calculated. A comparative analysis of the obtained values for different types and sizes of particles revealed the influence of composition and morphology on heat generation.

The study was supported by the Russian Federal Academic Leadership Program “Priority 2030” at the Immanuel Kant Baltic Federal University, project № 123101900024-9.

[1] X. Liu, Y. Zhang, Y. Wang et al., *Theranostics* 2020; 10(8):3793–3815 (2020).



# Magnetic and magneto-optical properties of one-dimensional magnetoplasmonic crystals with broken mirror symmetry

Z. Grigoreva\*, D. Murzin, V. Rodionova, V. Belyaev

Immanuel Kant Baltic Federal University, 236004, Nevskogo 14, Kaliningrad, Russia

\*grigoreva-zoja@rambler.ru

The use of nanomaterials is increasingly relevant and in high demand across various fields of science and technology. One specific type of nanomaterials is magnetoplasmonic crystals (MPICs), which are nanostructures composed of metallic films deposited on diffraction gratings. In MPICs, an enhancement of the Transversal Kerr effect (TKE) is observed due to the excitation of surface plasmon-polaritons (SPPs) [1]. These structures can be effectively utilized as concentration or magnetic field sensors [2, 3].

In this work, the samples were fabricated using oblique angle deposition magnetron sputtering using the ORION system, manufactured by AJA International. During the experiment, a 150 nm layer of permalloy ( $\text{Ni}_{80}\text{Fe}_{20}$ ) was deposited at angles  $55^\circ$ ,  $60^\circ$ ,  $65^\circ$  and  $70^\circ$  onto silicon wafer substrates and polymer diffraction gratings (DVD substrates) with period of 740 nm and stripe's height of 100 nm. In this work, the samples were fabricated using oblique angle deposition magnetron sputtering with the ORION system, manufactured by AJA International.

The magnetic properties were analyzed with a LakeShore VSM7400 vibrating sample magnetometer. Optical and magneto-optical properties were studied using the handmade spectroscopy setup made of a halogen lamp, two GT-10 polarizers by Thorlabs, a pair of electromagnets, an OCV-6300 optomechanical modulator from Avesta, an MS-6400i monochromator by Sol Instruments, and a Thorlabs PMM01 photomultiplier tube with a SR830 Lock-In amplifier by Stanford Research Systems as a detecting system. Optical measurements were conducted in p-polarized light in a wavelength range from 600 to 900 nm at an incidence angle of  $60^\circ$ , in order to satisfy the SPPs excitation conditions at the -2 diffraction order. The experiment showed that the spectral dependencies of the reflectivity demonstrate a pronounced dip at wavelengths of  $\lambda = 730 \pm 2$  nm and  $\lambda = 736 \pm 2$  nm for the MPICs based on DVD substrates. The difference in the dip positions for the samples is related to different oblique deposition angles, which cause non-uniform coverage of the grating tracks with the permalloy layer.

Comparison with literature data for smooth permalloy films of similar parameters shows an enhancement of the Transversal Kerr effect (TKE) for samples with broken mirror symmetry [4]. For the MPIC deposited at  $65^\circ$ , the enhancement is observed in the wavelength range of the reflectivity dip, with a maximum TKE value of -1.2%.

For comparison, the TKE spectrum was obtained for a symmetric multilayer structure DVD//Au//Ni//SiN. Its maximum TKE value was 2.6% with enhancement in the 700–810 nm range. The multilayer structure shows a higher TKE amplitude, while the MPIC with broken mirror symmetry demonstrates broadband spectral sensitivity.

[1] V. K. Belyaev et al., "Magnetic field sensor based on magnetoplasmonic crystal", Scientific Reports 10, 7133 (2020)

[2] Z. Li et al., "Tailored Fano resonance and localized electromagnetic field enhancement in Ag gratings", Scientific Reports 7, 44335 (2017)

[3] H. Kwon et al., "Three-dimensional metal-oxide nanohelix arrays fabricated by oblique angle deposition: fabrication, properties, and applications", Nanoscale Research Letters 10, 1-12 (2015)

[4] Belyaev V. K. et al. Permalloy-based magnetoplasmonic crystals for sensor applications //Journal of Magnetism and Magnetic Materials. – 2019. – T. 482. – C. 292-295

# Bending of Magnetic Elastomer under the Influence of an External Magnetic Field

D. Chirikov<sup>a,\*</sup>, A. Zubarev<sup>a</sup>, G. Stepanov<sup>b</sup>

<sup>a</sup> Ural Federal University, named after the first President of Russia, Boris Yeltsin, 620002, Mira 19,  
Yekaterinburg, Russia

<sup>b</sup> State Research Institute of Chemistry and Technology of Organoelement Compounds, 105118, Entuziastov  
Highway 38, building 25, Moscow, Russia

\*d.n.chirikov@urfu.ru

The report is devoted to experimental and theoretical studies of bending deformations of magnetic elastomers under the influence of an external magnetic field. Two types of silicone elastomer-based samples, containing micron-sized carbonyl iron particles (average diameter 5  $\mu\text{m}$ ) with a volume concentration of 30%, have been prepared. The Young's moduli of the elastomers were 0.5 MPa and 1.4 MPa. Cylindrical samples with a diameter of 4.5 mm and a length of 36 mm were placed on a horizontal substrate. One end of the sample was fixed, the other one was free. The samples were placed between coaxial cylindrical electromagnets (above and below the samples), creating a vertically directed magnetic field. Diameter of the magnet poles was 100 mm, the distance between them – 50 mm. Experiments have shown that if the field near the substrate is less than a certain critical value (equal to 187 and 212 mT for elastomers with elastic moduli of 0.5 MPa and 1.4 MPa, respectively), then the samples on the substrate remained undeformed. If the field exceeded these threshold values, the samples abruptly bent upward to almost the maximum possible bending degree. As the field was reduced, a gradual decrease of the bending was observed and the samples assumed a horizontal shape at 32 and 50 mT, respectively. Thus, a threshold nature of deformation and a wide hysteresis of the dependence of the sample bending on the magnetic field have been detected.

To explain these results, a theoretical model is proposed based on recording the free energy of a long magnetizable cylinder as a functional of its vertical deformation as a function of the horizontal coordinate. The real deformation corresponds to the minimum of the free energy functional. Minimization of the energy leads to a nonlinear differential equation of the fourth degree with respect to the deformation and the boundary conditions at the free end of the cylinder. This equation was solved numerically.

The analysis showed that in a completely uniform field, gravity prevents spontaneous bending of the sample. This bending can only occur if the field increases in the upward direction and the ponderomotive forces acting on the elements of the sample exceed the gravitational forces. As a result, the bent state corresponds to the minimum of a certain potential pit. As the field decreases, the energy of the "bottom" of this pit increases, but the system cannot leave it until the fields at which the pit disappears. At these fields, the deformation of the elastomer disappears.

This study examines the possibility of modeling the deformation behavior of an elastomeric material using a fourth-order polynomial dependence. Such a model allows for a more accurate consideration of the nonlinear deformation characteristics appropriate in elastomers, especially at high stretches. The implementation of the dependence as a fourth-order polynomial provides sufficient flexibility to describe the complex mechanics of the material, while remaining computationally efficient for practical application in engineering calculations and numerical modeling.

This work was carried out under the financial support of the Ministry of Science and Education of the Russian Federation, program FEUZ 2023-0020.

# Magnetically Actuated Microrobots with Contactless Control

A. Malchikov<sup>\*</sup>, S. Jatsun, P. Ryapolov

Southwest State University, 305040, 50 let Oktyabrya str. 94, Kursk, Russia

<sup>\*</sup>zveroknnp@gmail.com

Magnetically Actuated Microrobots with Contactless Control represent a promising direction for advancing minimally invasive microsurgery, biopsy, and targeted drug delivery. The key challenge in creating safe and high precision magnetically controlled microrobots lies in developing a contactless control system. The design, debugging, and calibration of such a system require accounting for multiple specific factors, such as: magnetic field inhomogeneity, environmental uncertainty, external disturbances, and stringent medical constraints [1-3].

The objective of this work is to develop an adaptive automatic control system for magnetically actuated biocompatible microrobots, incorporating a mathematical model that evaluates input parameters and generates control signals for the electromechanical subsystem. A key feature of the proposed algorithms is their ability to implement different motion modes (sliding, rolling, and rolling with slippage) for spherical deformable magnetically active objects (MAOs). These motion modes, determined by environmental properties, MAO characteristics, and control inputs, enable navigation through obstacles and bifurcations in channels, as well as precise operational interventions in confined spaces.

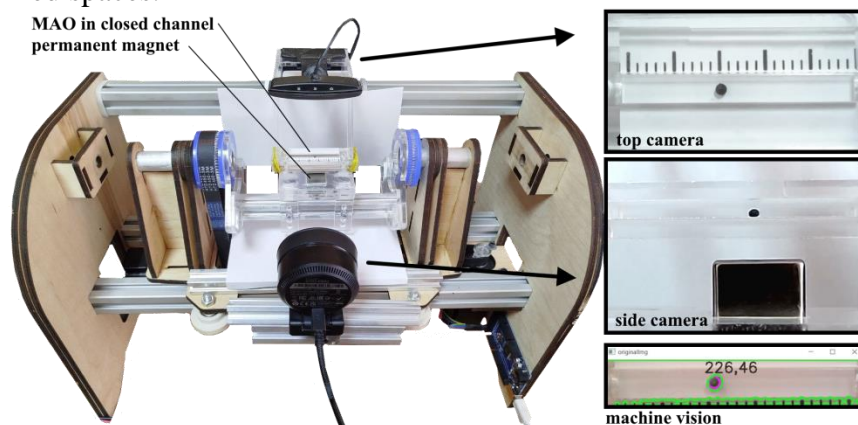


Figure 1. An experimental stand for studying MAO movements

Experimental validation (fig. 1) of the mathematical modeling results demonstrates distinct patterns of MAO motion. Under significant deformation, slippage dominates, with motion occurring via smooth, short bursts due to insufficient rolling torque. In high-friction contact, rolling is energetically favorable, and overcoming rolling friction results in more intense motion with a higher amplitude. In practice, there is almost always a combination of these two modes due to the heterogeneity of medium properties and MAO. The study focuses on MAOs fabricated from iron-doped biocompatible polymers ( $\leq 40\%$  ferromagnetic particle concentration), which exhibit paramagnetic properties and interact with the field via induced magnetic moments. The developed mathematical model calculates the optimal magnetic field source position to achieve the desired energy landscape for controlled microrobot motion.

In summary, developed adaptive control system improves microrobot performance in heterogeneous environments, as experimentally validated for biocompatible materials.

*The work was supported by RSF, research project No.24-29-00653*

[1] Malchikov A., et al. RusAutoCon. (2024)

[2] Malchikov A., et al. Robotics and technical cybernetics. 12(4). (2024)

[3] Malchikov A., et al. ElCon (2025)

## Influence of an external bias magnetic field on the magnetoelectric effect in layered composites

M. Musaev\*, R. Makarin, L. Makarova, N. Perov

Lomonosov Moscow State University, 119991, Leninskie gory 1, Moscow, Russia

\*musaev.mt21@physics.msu.ru

Multiferroic materials belong to a class of multifunctional materials and reveal magnetoelectric effect (if the material exhibits both ferromagnetic and ferroelectric properties). The magnetoelectric effect (MEE) consists in inducing electric polarization in a material in an external magnetic field. Layered multiferroic heterostructures are composites consisting of piezoelectric and magnetostrictive layers. They are among the leaders in terms of magnetoelectric coefficient. Multiferroic composites potentially have many applications: biomedicine, sensorics, transmission and reception of electromagnetic waves, and power generation.

The two-layer piezopolymer-magnetic elastomer (PEP-MAE) structures are investigated in AC gradient magnetic field. The application of an external permanent magnetic field (bias field) to the sample can significantly change the MEE values [1]. This allows to expand the possibilities of their application. The purpose of this work is to investigate the effect of a bias magnetic field on the magnitude of the effect and on its resonant frequency.

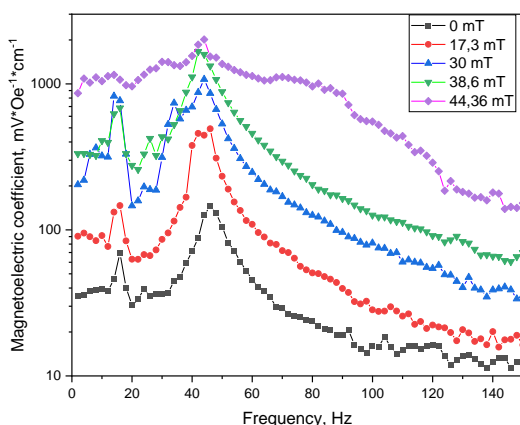


Figure 6. Dependence of the ME coefficient on the frequency with elastomer Fe

145 mV\*Oe<sup>-1</sup>\*cm<sup>-1</sup>. When the 44 mT field was applied, the value increased to 2022 mV\*Oe<sup>-1</sup>\*cm<sup>-1</sup>. It was also found that the application of an external field does not affect the resonance frequency in any of the experiments

*The work was supported by the Russian Science Foundation (Project No. 22-72-10137)*

[1] Makarova L.A., Polymers 15, 2262 (2023)

Two-layer structures were used as the studied samples: the first layer was a piezoelectric substrate made of PVDF film, the second was magnetic elastomers with a silicone matrix and ferromagnetic particles (iron microparticles 75 mass%, Zn-substituted cobalt ferrite nanoparticles 16 mass%). The bias field was created by the system of ferrite permanent magnets and varied from 0 to 44.4 mT. It was expected that the application of a DC magnetic field would lead to an increase in the magnitude of the effect due to the preliminary orientation of the magnetic moments of the particles in the elastomer.

As a result of the study, it was found that the MEE increases with increasing induction of a constant field. When using an elastomer with iron particles, the maximum magnitude of the effect without field was

# Magnetic Polymer Composites Based on Polysiloxane–Urea Copolymers for Additive Manufacturing

E. Olenich<sup>a,\*</sup>, V. Gorodov<sup>a</sup>, S. Kostrov<sup>a,b</sup>, S. Milenin<sup>a,c</sup>, A. Muzafarov<sup>a,b</sup>, Jun Zou<sup>e,d</sup>,

E. Kramarenko<sup>a,b,f</sup>

<sup>a</sup> Institute of Synthetic Polymer Materials named after N.S. Enikolopov, Moscow, Profsoyuznaya st.,70, Russia

<sup>b</sup> A.N. Nesmeyanov Institute of Organoelement Compounds of the Russian Academy of Sciences, Moscow, Vavilov St., 28., Russia

<sup>c</sup> Tula State Pedagogical University named after. L. N. Tolstoy, Tula, Lenin Ave., 125

<sup>d</sup> State Key Laboratory of Fluid Power and Mechatronic Systems, Zhejiang University, China

<sup>e</sup> School of Mechanical Engineering, Zhejiang University, China

<sup>f</sup> Lomonosov Moscow State University, 119991, Leninskie gory 1, Moscow, Russia

\*ekaterina.olenich@ispm.ru

The active development of 3D printing with soft materials is allowing valuable products to be created based on their digital models. The development of soft robots is one of the promising directions of 3D printing soft materials. Soft robots, compared to traditional ones, have a number of unique properties, such as variable rigidity, ability to deform for certain tasks, adaptation to external conditions, etc. [1] Such systems, along with traditional ones, already demonstrate huge potential. In addition, soft robotics is actively developing in the field of biomedical applications including endoscopy, minimally invasive surgery and drug delivery [2].

In this work, polydimethylsiloxane-based copolymers containing urea fragments were synthesized and used as matrices for magnetic composites (fig.1). Soft iron particles were introduced as a magnetic filler in varying concentrations to enable remote actuation under external magnetic fields.

Filaments based on these composites were produced and successfully used in additive technology to fabricate complex geometries with potential applications in soft robotics. The effect of filler concentration on the rheological, mechanical, and magnetic properties was also investigated.

The composites demonstrated a controlled response to external magnetic fields, with actuation behavior depending on the filler content. The results highlight the potential of these materials for additive manufacturing of magnetically responsive soft structures.

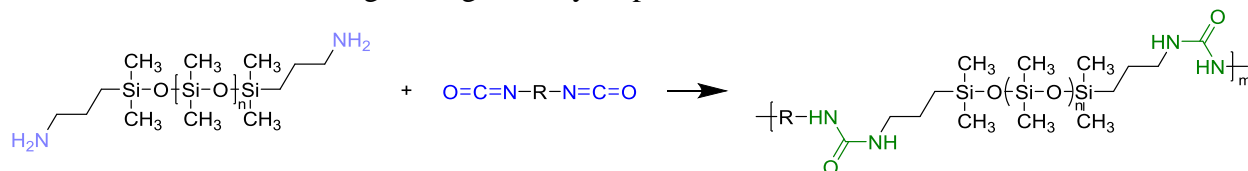


Figure 1. A method for producing TPU siloxane

The work was carried out with the financial support of the Russian Science Foundation, project No. 23-43-00057.

[1] K. E. Sachyani et al., Adv. Mater. 33, 2003387 (2021)

[2] M. Cianchetti et al., Nat. Rev. Mater. 3, 143 (2018)

## Morphostructural properities of PVDF/CFO@OAm magnetoelectric composites

V. Savin\*, V. Salnikov, D. Petrukhin, P. Vorontsov, A. Omelyanchik, V. Kolesnikova, V. Rodionova

Immanuel Kant Baltic Federal University, 236004, Nevskogo 14, Kaliningrad, Russia

\*savin\_vv@bk.ru

Recently, magnetoelectric (ME) composites have found wide application in the various fields such as sensor, actuators and energy harvesting devices [1-2]. The ME effect (the electric polarization induced by applied magnetic field or vice versa as the magnetization induced by applied electric field) in polyvinylidene fluoride with  $\text{CoFe}_2\text{O}_4$  (PVDF/CFO) composites is weaker compared to ceramic or layered structures, but flexibility, ease of fabrication and biosafety make them promising candidates for developing inks, wearable electronics, scaffolds controlled by external magnetic fields [3-4].

In this work we studied the changes in the phase composition, the mechanical properties and the magnitude of ME coefficient of PVDF/CFO composites as a result of coating of nanoparticles with an oleylamine (OAm) and composite stretching. It was shown that this could drastically change phase composition and magnitude of ME coefficient from 17 mV/cm·Oe to 38 mV/cm·Oe. Although, coating of nanoparticles leads to an increase the ultimate tensile stress from 13.1 MPa to 15.6 MPa of PVDF/CFO composites.

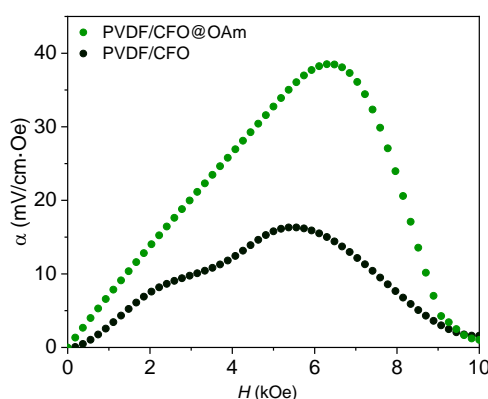


Figure 1. Field dependencies of the ME voltage coefficient on DC bias magnetic field.

It has been established that surface coating plays a crucial role in improving the coupling between the filler and the polymer matrix, which in turn enhances magnetoelectric response of composite.

- [1] Bichurin M. et al. Magnetoelectric magnetic field sensors: A review //Sensors. – 2021. – T. 21. – №. 18. – C. 6232
- [2] Narita F., Fox M. A review on piezoelectric, magnetostrictive, and magnetoelectric materials and device technologies for energy harvesting applications //Advanced Engineering Materials. – 2018. – T. 20. – №. 5. – C. 1700743
- [3] Chen X., Han X., Shen Q. D. PVDF-based ferroelectric polymers in modern flexible electronics //Advanced Electronic Materials. – 2017. – T. 3. – №. 5. – C. 1600460
- [4] Antipova V. et al. Effect of Surface Properties of PVDF-Based Nanocomposites on the Viability of Mesenchymal Stem Cells //Journal of Surface Investigation: X-ray, Synchrotron and Neutron Techniques. – 2024. – T. 18. – №. Suppl 1. – C. S166-S173

# First Experimental Observation of Magnetization Dynamics in a Magnetic MAX Phase

A. Gorshkov<sup>a\*</sup>, Ia. Mogunov<sup>a</sup>, S. Lyaschenko<sup>b</sup>, T. Andryushchenko<sup>b</sup>, A. Kalashnikova<sup>a</sup>

<sup>a</sup> Ioffe Institute, 194021 St. Petersburg, Russia

<sup>b</sup> Kirensky Institute of Physics of SB RAS, 660036 Krasnoyarsk, Russia

\*artem.gorshkov@mail.ioffe.ru

Spintronics and magnetoacoustics are advancing magnetic computing technologies by enabling the control of spin states in magnetically ordered materials by electrical, magnetic and elastic stimuli. Recently, these fields have focused their research on layered magnetic materials, such as van der Waals magnets [1] and graphene-based heterostructures [2], due to their unique structural properties leading to competition between inter- and intra-layer magnetic interactions. However, in materials with a similar structure - magnetic MAX phases - dynamic magnetic properties have not yet been observed, despite extensive research on their static magnetism. Magnetic MAX phases represent a family of layered metallic magnetically ordered ceramics with interlayer lattice constants greater than 1 nm. The competition between ferromagnetic and antiferromagnetic interactions results in the formation of nontrivial magnetic configurations, including helical [3] and non-collinear [4]. This work presents the first experimental demonstration of the magnetization dynamics in magnetic MAX phases.

To study the magnetization dynamics in MAX phases, we chose  $(\text{Cr}_{0.5}\text{Mn}_{0.5})_2\text{GaC}$ . This compound exhibits the highest saturation magnetization among known magnetic MAX phases [4], magnetically orders below  $T_c = 220$  K [5] and exhibits a ferromagnetic component in static measurements [5]. The sample was a 40 nm thick  $(\text{Cr}_{0.5}\text{Mn}_{0.5})_2\text{GaC}$  film grown by magnetron sputtering on a MgO (111) substrate (see details in [4]) with layers stacked along the surface normal. The magnetization dynamics was observed by femtosecond pump-probe method with magneto-optical Kerr detection, the probe beam was incident on the sample at  $45^\circ$ . In the experiment, the temperature was varied in range 66 - 294 K and an external in-plane magnetic field was up to 300 mT.

We analyzed the even and odd contributions with respect to the magnetic field separately. The even part showed damped magnetization precession with a frequency 5-16 GHz superimposed on exponential thermal relaxation, while the odd part showed ultrafast demagnetization with a characteristic timescale of  $\sim 80$  ps, comparable to values ( $\sim 20$  ps) reported for other layered metallic systems such as van der Waals magnets [1]. Both precession and demagnetization were independent on the magnetic field, within the experimental uncertainty, and disappeared above  $T_c = 220$  K. The precession frequency versus temperature, in contrast to static FMR studies [5], showed a maximum of 16 GHz at 130 K, which may indicate another metamagnetic phase transition. Our results provide the first experimental demonstration of laser-induced magnetization dynamics in the magnetic MAX phase  $(\text{Cr}_{0.5}\text{Mn}_{0.5})_2\text{GaC}$ , suggesting the potential of MAX phases in spintronics and magnetoacoustics.

This work was supported by the Russian Science Foundation grant (Project No. 24-72-00111).

- [1] T. Lichtenberg et al., 2D Mater. 10, 015008 (2023)
- [2] C. Gong et al., Science 363, 706 (2019)
- [3] I.P. Novoselova et al., Sci. Rep. 8, 2196 (2018)
- [4] A. Petruhins et al., J. Mater. Sci. 50, 4495 (2015)
- [5] R. Salikhov et al., Mater. Res. Lett. 3, 156 (2015)



## Features of the structural state and magnetic structure of thin films of the Gd-Co system

E. Kudyukov<sup>a,\*</sup>, A. Nizaev<sup>a</sup>, A. Gorkovenko, A. Ushkov, V. Lepalovskij, V. Vas'kovskiy<sup>a,b</sup>

<sup>a</sup> Ural Federal University, 620002, Mira 14, Yekaterinburg, Russia

<sup>b</sup> Institute of Metal Physics, Ural Branch of the Russian Academy of Sciences, 620108, S. Kovalevskaya 18, Yekaterinburg, Russia

\*e.v.kudyukov@urfu.ru

Magnetic structures with non-uniform distribution of magnetization are increasingly attracting the attention of researchers due to their great potential for application in various spintronics and magnetic memory devices [1,2]. Natural sources of magnetic inhomogeneities are rare earth metals, in which various exchange interactions lead to the emergence of helical structures, asperomagnetism, and speromagnetism. However, in the thin-film state, which is most interesting from the point of view of practical application, the features of the structural state can significantly affect the magnetic properties. For example, in the work [3] we showed that in nanocrystalline films of pure Gd a highly inhomogeneous magnetic structure is realized, which has signs of an asperomagnetic state. When adding a 3d transition metal to such a system, for example Co, a sharp amorphization of the structure occurs, which in turn also leads to a change in the magnetic structure. The aim of this work is to establish the patterns of formation of magnetic properties and structure during amorphization with a smooth increase in the Co content in the Gd-Co system.

Thin films of the Gd-Co system were obtained on the AJA Orion-8 installation by magnetron sputtering in an argon atmosphere on glass substrates from Corning. The composition of the films was controlled by selecting the power on the Gd and Co targets and lay within the range from 0 to 25 at.% Co. Quantum Design MPMS-7 and DynaCool 9T measuring complexes were used to measure magnetic properties. The measurements were carried out in magnetic fields  $H$  with a strength of up to 70 kOe and varying the temperature  $T$  in the range of 5-350 K. X-ray diffraction analysis was performed on a PANalytical Empyrean Series 2 diffractometer using  $\text{CoK}\alpha$  radiation and Bragg-Brentano geometry ( $\theta$ - $2\theta$ ).

In this work, the regularities of the change in the structural state of Gd-Co films during their gradual amorphization with an increase in the Co content from 0 to 25 at.% are established. Also in the work, the concentration dependences of the magnetic characteristics of these films such as the coercive field, Curie temperature, and effective magnetic moment are obtained and analyzed. At the same time, the relationship between the structural state and magnetic properties is established for both pure Gd films and Gd-Co films. It is found that in pure Gd films, the asperomagnetic state is realized due to a highly defective nanocrystalline structure in which both hcp and fcc Gd are present. Such a highly defective structure leads to a strong frustration of the exchange interaction, which in turn leads to the implementation of a highly inhomogeneous asperomagnetic state.

This work was carried out with financial support from the Russian Science Foundation, grant No. 24-22-00173

[1] S. Gosh et al., Solid State Physics, 71, 1-38 (2020)

[2] B. Pal et al., Sci. Adv. 8, 5930 (2022)

[3] V. Vas'kovskiy, E. Kudyukov et al., JMMM, 565, 170254 (2023)



# Pulsed Laser Ablation of Co Nanofilms in Water for Magnetic Nanoparticles Production

V. Nesterov<sup>a,\*</sup>, Ya. Mineev<sup>a</sup>, I. Dzhun<sup>a,b</sup>, D. Shuleiko<sup>a</sup>, D. Presnov<sup>a</sup>, N. Chechenin<sup>a,b</sup>, S. Zabotnov<sup>a</sup>

<sup>a</sup> Faculty of Physics, Lomonosov Moscow State University, 119991, 1/2 Leninskie Gory, Moscow, Russia

<sup>b</sup> Skobeltsyn Institute of Nuclear Physics, Lomonosov Moscow State University, 119991, 1/2 Leninskie Gory, Moscow, Russia

\* nesterovvy@my.msu.ru

Nowadays, magnetic biosensors are being actively developed to detect and count required analytes in labs-on-a-chip – miniature devices that perform the functions of a diagnostic laboratory in vitro [1]. Magnetic biosensors detect changes in the magnetic field created by magnetic nanoparticles (MNPs) conjugated to biomolecules or penetrated into cells. For that reason, universal technologies for synthesizing MNPs without chemical impurities, with a given size distribution and desired properties are required.

Pulsed laser ablation in liquid (PLAL) is a promising single-stage technology to produce MNPs. The advantages of PLAL are the ability to synthesize chemically pure nanoparticles and control their size and composition by varying laser parameters and choosing an appropriate buffer liquid [2].

In our work, to fabricate MNP suspensions, we irradiated magnetron-sputtered Co nanofilms with a thickness varying in the range from 5 to 500 nm in distilled water with picosecond laser pulses (1064 nm, 34 ps, 5 mJ, 10 Hz) for 60 minutes. The use of such targets in PLAL instead of bulk materials can add opportunities to control a size distribution [3], morphology and composition of laser-ablated MNPs.

Scanning and transmission electron microscopy images showed that the morphology of the formed MNPs is determined by the thickness of the ablated nanofilm: at thicknesses greater than 35 nm, the obtained MNPs are predominantly spherical; in the case of smaller thicknesses, flakes and coagulants of various shapes are additionally formed. According to dynamic light scattering and scanning electron microscopy data, the average MNPs size ranges from 70 to 1000 nm and depends non-monotonically on the Co film thickness with a sharp increase at 35 nm Co film. The standard deviation of the MNP sizes reaches the minimum value ~20% at film thicknesses of less than 35 nm (i.e. the skin-layer depth). Such behavior of the MNPs size distribution relates to peculiarities of PLAL of the small-thickness Co films when PLAL in the mode of phase explosion is implemented.

A detailed analysis of the transmission electron microscopy results revealed that the MNPs contain predominately Co oxide with unoxidized Co inclusions. Raman and electron paramagnetic resonance spectra for the formed nanoparticles confirmed the content of Co oxide, in particular Co<sub>3</sub>O<sub>4</sub>, in their composition. All nanoparticles obtained exhibit magnetic response at applying an external magnetic field. In addition, they are characterized by a ferromagnetic hysteresis loop at room temperature. Since Co<sub>3</sub>O<sub>4</sub> is paramagnetic at room temperature such behavior may be caused by the presence of inclusions of unoxidized Co in the nanoparticles.

Therefore, PLAL of Co nanofilms allows the production MNPs with a variable average size and a relatively narrow size distribution that are promising as magnetic labels in biosensorics.

This investigation was supported by the Russian Science Foundation grant # 25-29-00176, <https://rscf.ru/en/project/25-29-00176/>.

[1] H. Huang, et al., SPIN 9, 1940002 (2018)

[2] E. Ghaem, et al., Opt. Quant. Electron. 53, 36 (2021)

[3] I. Dzhun, et al., Bull. RAS: Phys. 88(4), 540 (2024)

## Spin crossover in ludwigite $\text{Co}_2\text{FeBO}_5$ under pressure

V. Zhandun\*, N. Kazak

<sup>a</sup> Kirensky Institute of Physics, Federal Research Center KSC SB RAS, 660036 Krasnoyarsk, Russia

\*jvc@iph.krasn.ru

The borate oxides belong to a large class of strongly correlated systems with the exciting interrelationship between spin, charge, lattice, and orbital degrees of freedom.  $\text{Co}_2\text{FeBO}_5$  oxyborate is of particular interest because of its intriguing magnetic and electronic behavior. Orthorhombic  $\text{Co}_2\text{FeBO}_5$  crystallize in ludwigite structure (space group  $\text{Pbam}$ ), where the cations occupy four nonequivalent metal sites 2a, 2b, 4g, and 4h, which are usually numbered as M1, M2, M3, and M4, correspondingly (Fig. 1a). The first three are occupied by divalent metal ions, whereas the latter site is occupied by the trivalent cations. The possibility of the control and tuning of the magnetic properties by pressure is attractive for possible application in the electronic and electronic devices. Therefore, we have studied the effect of the pressure on the magnetic and electronic properties of the  $\text{Co}_2\text{FeBO}_5$  ludwigite by means of the DFT+GGA calculations. Analysis of the high pressure magnetic structure suggests pressure induced site- selective spin crossover for Co and Fe ions. It was found that Me4 ion undergo first spin-state transition at the lowest pressure, the second spin crossover arises at Me2 ion in triad 4-2-4 (Fig.1b). In turn, Me1 and Me3 ion in triad 3-1-3 has the weak pressure dependence in the studied pressure range. The mechanism of spin-crossover is discussed in terms of redistribution of d-electrons under pressure. The spin-crossover is accompanied by metal-insulator electronic transition at the critical pressure.

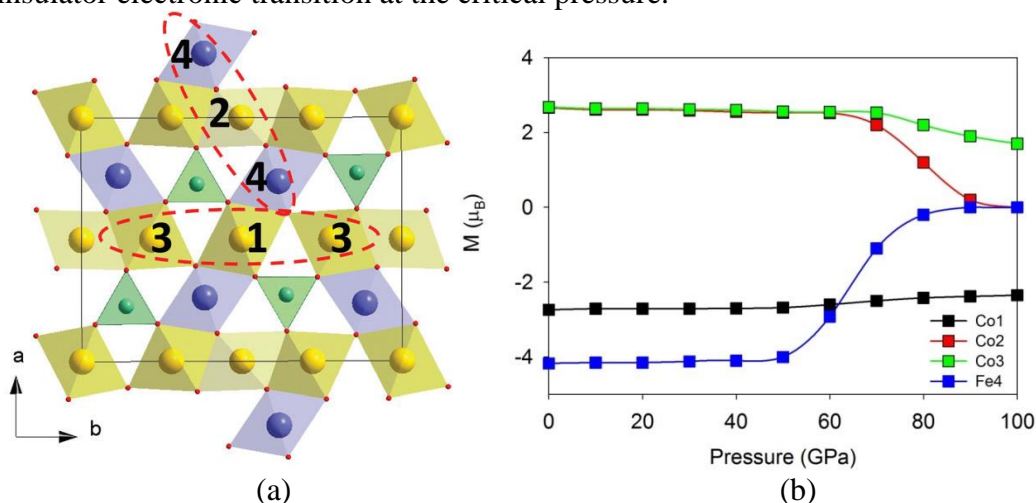


Figure 1. (a) Crystal structure of  $\text{Co}_2\text{FeBO}_5$  presenting the  $ab$  plane. Four symmetry different metal sites 2a, 2b, 4g, and 4h are numbered as M1, M2, M3, and M4, respectively. The Co and Fe ions are shown as yellow and blue spheres, respectively. The planar triangular  $\text{BO}_3$  groups are shown in green. The triads M3–M1–M3 and M4–M2–M4 are depicted by red dotted lines. (b) Calculated pressure dependencies of magnetic moments at metal sites

This research was supported by the Russian Science Foundation and Krasnoyarsk Regional Fund of Science and Technology Support, Grant No.24-12-20012, <https://rscf.ru/project/24-12-20012/>.

# Synthesis and characterization of a new type of MXenes (Ti,Ta)3C2Tx and (Ti,Nb)3C2Tx for energy applications

V. Porokh<sup>a\*</sup>, N. Shilov<sup>a</sup>, K. Sobolev<sup>b</sup>, K. Magomedov<sup>a</sup>, V. Rodionova<sup>a</sup>

<sup>a</sup> Immanuel Kant Baltic Federal University, 236004, Nevskogo 14, Kaliningrad, Russia

<sup>b</sup> Ben-Gurion University, Be'er Sheva, Israel

\*vap\_789@mail.ru

The increasing prevalence of electrical appliances in households is driving expansion in the electricity generation industry. This necessitates the development of enhanced energy storage solutions, either through increased storage capacity or improved storage efficiency. Advancements in battery technology are intrinsically linked to the materials employed in their construction. The discovery and refinement of novel materials hold the potential to revolutionize battery design and performance. MXenes, a class of two-dimensional materials, have emerged as promising candidates for enhancing the performance characteristics of energy storage devices. Various MXene-based materials have already been successfully synthesized [1-3].

Novel MXene compositions, specifically (Ti,Ta)3C2Tx and (Ti,Nb)3C2Tx, were synthesized using a top-down etching method.

The synthesis protocol involves the following steps: Reagents were selected in the following proportions per 1g of MAX-phase: 1.5g LiF; 15ml HCl (37%); 5ml of deionized water. The resulting solution was maintained at a constant temperature of 37°C under gentle agitation for 24 hours. This process facilitated the selective etching of aluminum from the MAX phase structure and the introduction of surface functional groups. Subsequently, the solution underwent sonication in an ultrasonic for 30 minutes to exfoliate the MXene layers. Finally, the resulting dispersion was repeatedly washed with deionized water and dried in a drying oven at 45°C until complete solvent evaporation.

Characterization of the synthesized materials using various analytical techniques confirms the successful synthesis of the targeted novel MXene compositions.

The synthesized novel MXene materials are proposed for utilization in the development of diverse energy-related applications, with a specific focus on battery technology [4]. Future work entails the fabrication of at least two distinct battery prototypes to optimize either the energy storage capacity or other performance parameters.

[1] Chy, M.N.U.; Rahman, M.A.; Kim, J.-H.; Barua, N.; Dujana, W.A. MXene as Promising Anode Material for High-Performance Lithium-Ion Batteries: A Comprehensive Review. *Nanomaterials* 2024, 14, 616. <https://doi.org/10.3390/nano14070616>

[2] Tang, Q., Zhou, Z., & Shen, P. (2012). Are MXenes Promising Anode Materials for Li Ion Batteries Computational Studies on Electronic Properties and Li Storage Capability of Ti3C2 and Ti3C2X2 (X = F, OH) Monolayer. *Journal of the American Chemical Society*, 134(40), 16909–16916. doi:10.1021/ja308463r

[3] Jiang, X., Tang, C., Zhou, X., Hou, J., Jiang, S., Meng, L., & Zhang, Y. (2024). Recent progress in Si/Ti3C2Tx MXene anode materials for lithium-ion batteries. *iScience*, 27(11). doi:10.1016/j.isci.2024.111217

[4] Papadopoulou, Konstantina & Chroneos, Alexander & Christopoulos, Stavros-Richard G.. (2023). Latest advances and comparative analysis of MXenes as anode and cathode electrodes in secondary batteries. *Journal of Applied Physics*. 133. 030901. 10.1063/5.0136840

## Smart design of $\text{Ti}_3\text{C}_2\text{T}_x/\text{Fe}_3\text{O}_4@\text{PAA}$ nanocomposites for adsorption of methylene blue (MB) from water

S. Drach<sup>a</sup>, E. Tarasova<sup>a</sup>, N. Shilov<sup>a</sup>, S. Aga-Tagieva<sup>b</sup>, V. Ni<sup>a</sup>, K. Magomedov<sup>a</sup>, K. Sobolev<sup>c</sup>,

V. Rodionova<sup>a</sup>

<sup>a</sup> Immanuel Kant Baltic Federal University, 236004, Nevskogo 14, Kaliningrad, Russia

<sup>b</sup> SCAMT Laboratory, ITMO University, Saint Petersburg, Russia.

<sup>c</sup> Ben-Gurion University, Be'er Sheva, Israel

\*sof\_anarci@mail.ru

Water contamination is one of the most unfavorable environmental problems in the world. Thus, the removal of dyes from effluents are of the urgent importance [1, 2].

MXenes are a new class of two-dimensional materials. They have attracted the attention of scientists due to their exceptional properties (hydrophilicity, metallic conductivity, large specific surface area, negatively charged surface, etc.), in particular, they can be used for sorption of heavy metals, radionuclides, dyes and antibiotics due to their negatively charged surface. The negatively charged active surface of MXenes also makes it easy to functionalize them with various molecules or nanostructures, thereby, for example, improving sorption properties or creating new ones.

In this work we functionalize the surface of  $\text{Ti}_3\text{C}_2\text{T}_x$  MXene with  $\text{Fe}_3\text{O}_4$  magnetic nanoparticles, which allows the sorbent to be easily removed from the purified water. To increase the adsorption capacity, the surface of such obtained nanocomposite was additionally functionalized with polyacrylic acid (PAA). Then, an adsorption experiment on the extraction of methylene blue (MB) was carried out to confirm our theory.

As a result of the experiment, it was found that the percentage of MB adsorption for  $\text{Ti}_3\text{C}_2\text{T}_x/\text{Fe}_3\text{O}_4@\text{PAA}$  increases with an increase in pH from 2 to 8 (Figure 1). As shown in Figure 2, the adsorption capacity of  $\text{Ti}_3\text{C}_2\text{T}_x/\text{Fe}_3\text{O}_4@\text{PAA}$  nanoadsorbent decreased with increasing the mass of added nanocomposite as the number of adsorption centers per unit mass decreased. The developed  $\text{Ti}_3\text{C}_2\text{T}_x/\text{Fe}_3\text{O}_4@\text{PAA}$  nanocomposite demonstrated exceptional adsorption performance, achieving record-high adsorption capacity for methylene blue removal. These results highlight the potential of functionalized MXene-based materials as highly efficient adsorbents for water purification applications.

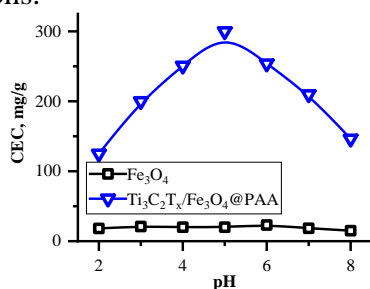


Figure 1. Dependence of the adsorption capacity of  $\text{Ti}_3\text{C}_2\text{T}_x/\text{Fe}_3\text{O}_4@\text{PAA}$  nanocomposite on the acidity (pH) of the medium.

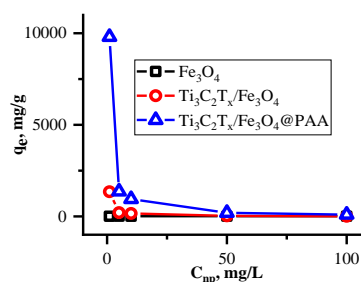


Figure 2. Dependence of sorption capacity of sorbent on methylene blue on sorbent concentration.

[1] F. Deniz, A. Yasubuga, "The effects of synthetic dye pollution on the aquatic environment and human health," Conference: III. International Siirt Scientific Research Congress At: Siirt, Turkey, Nov. 2022

[2] K. S. Bharathi, S. T. Ramesh, "Removal of dyes using agricultural waste as low-cost adsorbents: a review," Applied Water Science, vol. 3, pp. 773–790, Jul. 2013, doi: 10.1007/s13201-013-0117-y

# Sonophotocatalytic Degradation of Methylene Blue Using Magnetic $\text{Ti}_3\text{C}_2\text{T}_x$ MXene/ $\text{Fe}_3\text{O}_4$ Nanocomposites: Catalysis and Chemometric Quantification

E. Tarasova\*, S. Drach, N. Shilov, K. Magomedov, V. Rodionova

Immanuel Kant Baltic Federal University, 236004, Nevskogo 14, Kaliningrad, Russia

\*ejtarasova@stud.kantiana.ru

Magnetically assisted advanced oxidation processes represent a promising direction for environmental remediation. In this study, we demonstrate the application of a novel sonophotocatalytic system based on magnetic nanocomposites of  $\text{Ti}_3\text{C}_2\text{T}_x$  MXene and  $\text{Fe}_3\text{O}_4$  nanoparticles, specifically designed for the degradation of synthetic dyes in aqueous solutions. The 2D MXene provides a high-surface-area conductive platform, while  $\text{Fe}_3\text{O}_4$  imparts both magnetic separability and redox activity via Fenton-like reactions.

The system was evaluated for the degradation of methylene blue under simultaneous ultrasound and UV-visible light irradiation. The synergistic interplay of acoustic cavitation and photocatalytic charge separation was found to significantly enhance the generation of reactive oxygen species ( $\bullet\text{OH}$ ,  $\text{O}_2\bullet^-$ ), resulting in improved degradation performance.

## Synthesis Strategy:

- $\text{Ti}_3\text{C}_2\text{T}_x$  MXene was synthesized via selective etching of the aluminum layer from  $\text{Ti}_3\text{AlC}_2$  using a mixture of HCl and HF.
- $\text{Fe}_3\text{O}_4$  nanoparticles were introduced through sonochemical co-precipitation.

## Catalytic Testing and Chemometric Analysis:

The degradation kinetics of methylene blue were monitored spectrophotometrically. To improve data robustness and quantitative accuracy, a **chemometric approach** based on full UV-vis spectra was implemented. Models based on partial least squares regression (**PLS**), principal component regression (**PCR**), and artificial neural networks (**ANNs**) were successfully applied for precise concentration prediction, even under spectral interference.

The synergistic effect of sonophotocatalysis was quantified using a comparative kinetic model:

$$\text{Synergism (\%)} = \frac{k_{\text{sonophotocatalysis}} - (k_{\text{photocatalysis}} + k_{\text{sonocatalysis}})}{k_{\text{sonophotocatalysis}}} \times 100, \quad (1)$$

This work presents, for the first time, a kinetic evaluation of sonophotocatalysis employing magnetic MXene/ $\text{Fe}_3\text{O}_4$  nanocomposites, offering a magnetically recoverable and scalable catalytic system for environmental applications.

[1] A.O. Shuaibov, M.G. Abdurakhmanov, A.G. Magomedova, A. Omelyanchik, V. Salnikov, S.A. Tagieva, V. Rodionova, M.Kh. Rabadanov, F.F. Orudzhev, Sonophotocatalytic degradation of methylene blue with magnetically separable Zn-doped  $\text{CoFe}_2\text{O}_4/\alpha\text{-Fe}_2\text{O}_3$  heterostructures, J. Environ. Chem. Eng. 12 (2024) 109874.

# Author index

## A

Abakumov M. ....	141
Abdullin A. ....	173
Abin D. ....	179
Acuna A. ....	88, 127
Afremov L. ....	120, 162, 168
Aga-Tagieva S. ....	196
Albino M. ....	55
Aliev A. ....	89
Amirov A. ....	45, 93
Amosov A. ....	117
Andryushchenko T. ....	191
Anferova V. ....	56
Anikin A. ....	10, 55, 86, 106, 150, 184
Anisimov I. ....	180
Antipova V. ....	57, 154
Antipova V. ....	107
Antonov V. ....	39
Ataeva G. ....	156
Averkiev N. ....	75
Azarevich A. ....	58

## B

Babaev A. ....	156
Balaeva V. ....	64, 123
Bandarenka H. ....	29
Baranov N. ....	74
Baryshev A. ....	6
Baydikova A. ....	124
Baykaziev A. ....	16
Bazrov M. ....	120, 147
Bedin S. ....	132
Belodedov M. ....	126, 161
Belotelov V. ....	9, 13
Belyaev V. ....	10, 98, 106, 110, 140, 184, 185
Berdonosod P. ....	61
Bichurin M. ....	95
Blinov I. ....	146
Blinov Z. ....	158
Bobrinetskiy I. ....	113
Bogach A. ....	58
Bolotina E. ....	17
Botin D. ....	137
Bouravleuv A. ....	100
Bucharskaya A. ....	84, 115, 149
Buchelnikov V. ....	41
Buldakova A. ....	109, 177
Burko A. ....	29
Buryakov A. ....	18, 50
Bychkova E. ....	137
Bykov A. ....	137, 144

Bykov I. ....	42
---------------	----

## C

Chechenin N. ....	193
Chernousov N. ....	120
Chernov E. ....	143
Chernozem P. ....	11, 53
Chernozem R. ....	11, 53
Chirikov D. ....	186
Chirkina M. ....	28
Chmelyuk N. ....	150
Chuprakov S. ....	146
Crernousov N. ....	147

## D

Dadagishiev D. ....	71
Davydenko A. ....	120
Davydenko L. ....	120
Demicheva O. ....	126
Demin G. ....	70, 76
Demina P. ....	66, 129
Demishev S. ....	85
Djuzhev N. ....	70, 76
Dmitrieva M. ....	44
Dokukin M. ....	6
Dolgova T. ....	25
Doludenko I. ....	26, 83, 132, 146
Dorofeenko A. ....	42
Dorokhin M. ....	66, 129
Drach S. ....	69, 196, 197
Drachev V. ....	132
Draganyuk O. ....	23
Drovoisekov A. ....	44
Dubitskiy N. ....	124
Dzhun I. ....	193

## E

Edelman I. ....	33
Elfimova E. ....	21
Elkina Yu. ....	97
Emelyanova S. ....	91
Eremina R. ....	85, 134
Ershov P. ....	29, 45, 90, 105
Eryzhenkov A. ....	102, 166
Es'kova I. ....	176

## F

Fashchevsky A. ....	155
Fazlizhanov I. ....	85

Fedorova A. ....	117
Fedotov I. ....	68, 139
Fedyanin A. ....	25, 36, 78, 80, 109, 177
Feng Y. ....	67, 120
Fetisova A. ....	11, 94
Filippov A. ....	118, 144
Firoz A. ....	94
Flachbart K. ....	58
Fominykh B. ....	52
Fortuna A. ....	114, 116, 145
Frolov A. ....	54, 78, 109, 177
Frolov K. ....	146
Frolova V. ....	57, 154

## G

Gabani S. ....	58
Galanova S. ....	144
Gan'shina E. ....	181
Ganshina E. ....	42
Garanin F. ....	159, 160, 175
Gareev T. ....	82
Gaviko V. ....	111
Gavrilkina S. ....	58
Gavrilyuk S. ....	125
Gavryushina M. ....	80
Genin V. ....	84, 148
Genina E. ....	84, 148
Gerasimenko A. ....	34, 126
Gerasimov E. ....	111
German S. ....	27
Gippius A. ....	146
Gladyshev I. ....	38
Glazkov V. ....	61
Golub D. ....	161
Gorin D. ....	27
Gorkovenko A. ....	192
Gorodov V. ....	189
Gorshenkov M. ....	114, 116, 145
Gorshkov A. ....	191
Granovsky A. ....	5, 42, 103, 181
Grigoreva Z. ....	98, 185
Grishin S. ....	174
Gritsenko Ch. ....	63, 98
Grokhotoeva E. ....	21
Gubanov V. ....	159
Gudkov V. ....	75
Gulyaev I. ....	28
Gusev N. ....	72, 108, 139, 167
Gusev S. ....	139, 167
Guseva A. ....	142
Gushchina N. ....	52

## H

Hesuan Y. ....	19
----------------	----

## I

Ibraeva A. ....	53
Ibragimova E. ....	103
Ichkitidze L. ....	126, 161
Ignatov A. ....	45, 107, 127, 131
Ignatov T. ....	131
Iliushin I. ....	120, 162, 168
Inoue M. ....	25
Irkhin V. ....	143
Ivanov A. ....	21
Ivanova A. ....	128
Ivanova O. ....	33
Ivantsov R. ....	33

## J

Jatsun S. ....	187
----------------	-----

## K

Kalandiia M. ....	163
Kalashnikova A. ....	191
Kaldko D. ....	43
Kalentyeva I. ....	66, 129
Kalinin Yu. ....	49
Kalyuzhnaya D. ....	130, 169
Kamaeva O. ....	28
Kamzin A. ....	46
Kanevskiy V. ....	26
Kanurin D. ....	93
Kapranova K. ....	43
Karashin E. ....	68, 108, 139
Karavainikov A. ....	167
Karpenkov A. ....	112, 128
Karpenkov D. ....	32, 112, 116, 145
Katenkov P. ....	118, 137, 144
Kaver K. ....	109
Kazak N. ....	194
Khairtdinova D. ....	26, 83
Khanadeev V. ....	106
Kharlamova A. ....	47
Khashirov A. ....	90
Khashirova S. ....	16, 90
Khizriev K. ....	39
Khlebtsov B. ....	84
Khokhlov N. ....	82
Khusainova E. ....	114
Kichin G. ....	7
Kikteva V. ....	135
Kimel A. ....	82



Kirgizov S.....	47
Kirillin M.....	84
Kiryanov M. ....	25
Kislyuk A.....	17
Klavsyuk A.....	164
Klimenko M.....	28
Kobyakov A.....	180, 182
Kolesnikova V.....	45, 77, 85, 107, 131, 190
Komlev A.....	93
Kondratenko D. ....	153
Kononenko D.....	48
Korepanova E. ....	59, 150
Korolev A.....	143
Korostelin Yu. ....	75
Korshunov A. ....	118, 137, 144, 165
Koryakin D. ....	153
Kosolobov S. ....	132
Kosova A.....	121
Kostrov S.....	189
Kotov L.....	49, 125, 138, 158
Kovalenko V.....	155
Kozabaranov R. ....	118, 137, 144
Kozhina E.....	132
Kozlov A. ....	67, 120, 147
Kozlyakova E. ....	133
Kramarenko E.....	189
Krasikov K.....	58
Kriukov R.....	66
Kubasov I.....	17
Kudasov Yu.....	118, 137, 144, 165
Kudriavtseva A.....	113
Kudrin A.....	66
Kudryashov A.....	167
Kudyukov E.....	192
Kulikova D. ....	6
Kurakina D. ....	84
Kurbanova D. ....	65
Kurdanova Zh.....	16
Kurganskaya A. ....	133
Kuritsyn D. ....	108
Kuts V.....	17
Kuzmichev A.....	9
Kuznetsov A. ....	41, 62
Kuznetsova M.....	67, 120
Kvashnin D.....	24

## L

Lazareva E.....	149, 155
Lepalovskij V. ....	192
Levada K. ....	10, 57, 59, 86, 117, 150, 151, 152, 153, 154
Likerov R.....	134
Likhoida L.....	120
Lipengolts A. ....	27
Liu Zh.....	133

Lobanov N. ....	123
Lobkova M.....	135
Lobov I.....	38
Lomova M. ....	160, 175
Lukoyanov A. ....	143
Lyakhova M.....	112, 142
Lyapilin I. ....	136
Lyaschenko S.....	191
Lyashko S. ....	167
Lysenko E. ....	97

## M

Magomedov K. ....	63, 69, 107, 117, 195, 196, 197
Magomedov M.....	65
Makarin R. ....	47, 103, 112, 188
Makarov I.....	118, 137, 144
Makarova L.....	32, 47, 163, 188
Makarova M.....	38
Makeev R.....	166
Malchikov A. ....	187
Malinkovich M. ....	17
Malkеров J. ....	113
Mallphanov I.....	63
Marchenkov V. ....	52, 91, 143
Marchenkova E.....	52, 143
Markina M. ....	61
Markov I. ....	95
Maslov D. ....	118, 137, 144
Matyunina M.....	41
Mayburov M. ....	138
Meng F.....	67, 120
Mikhailova T.....	167
Milenin S. ....	189
Mineev Ya. ....	193
Mishina E.....	18, 50
Mitrokhin S.....	133
Mogunov Ia.....	191
Moiseeva E. ....	27
Mollaeva M.....	28
Morozkina S.....	119, 121, 151, 152
Morozova M. ....	64, 123
Morozova T. ....	114
Moskal I. ....	124
Motorzhina A.....	10, 55, 59, 86, 150, 151, 152
Mukhortova Y.....	94
Mukhuchev A. ....	89
Murtazaev A. ....	65, 156
Murtazoev A. ....	61
Murzin D.....	110, 185
Musabirov I.....	128
Musaev M. ....	47, 188
Mushnikov N. ....	111
Mushtuk P.....	120, 162, 168
Muslimov A. ....	146

# IBCM-2025

Musorin A. ....	80
Musov I. ....	16, 45
Muzafarov A. ....	189
Mylnikov A. ....	115, 155

## N

Namsaraev Zh. ....	120, 147
Naumov S. ....	52
Naumova L. ....	108
Navolokin N. ....	84, 115, 155
Nechaev K. ....	116, 145
Nerovnaya A. ....	78
Nesterov V. ....	193
Netesova N. ....	157
Ni V. ....	196
Nikitin A. ....	77, 141
Nikitin P. ....	113
Nikitov S. ....	174
Nikolaev A. ....	42
Nikolaev S. ....	44
Nikolaeva E. ....	40
Nikolskaya E. ....	28
Nizaev A. ....	192
Nosova N. ....	74
Novakova A. ....	101
Novikov I. ....	25
Novokshonov S. ....	136

## O

Ognev A. ....	120
Olenich E. ....	189
Omelyanchik A. ....	10, 45, 77, 99, 101, 190
Orlov A. ....	113
Orlova A. ....	139
Orudzev F. ....	71
Osidak E. ....	20
Osipov M. ....	179
Osmanov S. ....	167
Ostanin G. ....	25
Ostras M. ....	9
Ovchinnikov V. ....	52
Ovsyannikov G. ....	124

## P

Panfilov S. ....	101
Panina L. ....	10, 26, 45, 77, 83, 86, 87, 88, 127
Park J. ....	38
Parkhomenko Yu. ....	17, 93
Pashenkin I. ....	68, 72
Pashnina A. ....	87
Patrin G. ....	180, 182
Pavlov V. ....	31, 165

Pavluk E. ....	9
Peddis D. ....	99
Perevalova A. ....	52
Perevozchikova Yu. ....	143
Perov N. ....	32, 103, 163, 181, 188
Perova N. ....	181
Perunov I. ....	146
Petrov A. ....	148
Petrov D. ....	33
Petrovskaya G. ....	101
Petrukhin D. ....	106, 107, 140, 150, 184, 190
Petrzhik A. ....	124
Philippov A. ....	137
Platonov V. ....	118, 137, 144
Pokrovskii S. ....	179
Popov D. ....	134
Porokh V. ....	195
Preobrazhensky V. ....	18, 50
Presnov D. ....	193
Prikhodchenko A. ....	67, 120
Pripechenkov I. ....	42
Prishchepa A. ....	141
Protasov A. ....	143
Pshenichnikov S. ....	10, 55, 59, 86, 150
Ptashenko A. ....	37
Punda A. ....	103
Pyatakov A. ....	40

## R

Radjabov R. ....	181
Raikher Yu. ....	8
Ramazanov M. ....	65
Ramazanov Sh. ....	71
Razlivina J. ....	43
Rebrov Ya. ....	61
Repin P. ....	118, 144
Rodionova V. ....	45, 55, 57, 59, 63, 69, 77, 85, 98, 101, 105, 106, 110, 127, 131, 140, 150, 184, 185, 190, 195, 196, 197
Rodionova V. ....	154
Romanenko D. ....	64
Romashchenko A. ....	53
Ryapolov P. ....	130, 169, 187
Ryazanov V. ....	51
Rybakov V. ....	94
Rylkov V. ....	42, 44
Ryzhkov A. ....	170

## S

Sadovnikov A. ....	37, 159, 160, 175
Safiullin D. ....	25
Salakhitdinova M. ....	103
Saletsky A. ....	164

# IBCM-2025

Salnikov V. ....	10, 45, 57, 77, 90, 101, 105, 106, 107, 131, 140, 150, 154, 184, 190
Samchenko S. ....	181
Samigullina A. ....	171
Sangregorio C. ....	55
Sapozhnikov M. ....	18, 50, 68, 72, 139
Sarychev M. ....	75
Savin V. ....	45, 105, 131, 190
Selezneva N. ....	74
Selishchev S. ....	126, 161
Semenov S. ....	180
Semenova E. ....	112, 128, 142
Semiannikova A. ....	143
Serbun P. ....	119, 121
Serebryakova I. ....	84
Sergeev E. ....	45
Sgibnev E. ....	6
Shadrin A. ....	124
Shaikenov R. ....	119, 121
Shakhmurzova K. ....	16
Shalomov K. ....	52
Shamanov I. ....	86, 184
Shaposhnikov A. ....	167
Sharafullin I. ....	171
Sharipova M. ....	109, 177
Shelaev A. ....	6
Shestakov A. ....	85
Shestopalov R. ....	120
Shikin A. ....	56, 102
Shilov N. ....	59, 63, 69, 117, 195, 196, 197
Shipkova E. ....	103
Shirokiy N. ....	43
Shishelov A. ....	120
Shiyan Ya. ....	180, 182
Shlapakova L. ....	11, 92, 94
Shuleiko D. ....	193
Shushunova N. ....	84, 115
Shvets P. ....	63
Sigov A. ....	18
Silina S. ....	147
Simdyanova M. ....	38, 42, 181
Simonov-Yemelyanov I. ....	90
Sinkevich A. ....	112, 142
Sitnikov A. ....	42, 44, 49
Siurakshina L. ....	81
Skidanov V. ....	178
Skirda A. ....	113
Skirdkov P. ....	7, 135
Skorokhodov E. ....	68, 139
Skribitsky V. ....	27
Slonov A. ....	16
Sluchanko N. ....	58
Smetannikova S. ....	142
Snetkov P. ....	119, 121, 151, 152
Sobko A. ....	127

Sobola D. ....	71
Sobolev K. ....	63, 69, 195, 196
Sokol M. ....	28
Sokolov A. ....	33
Sokolov E. ....	130, 169
Sokolov O. ....	95
Sokolovskiy V. ....	41
Solovyova A. ....	21
Stadnichuk V. ....	25
Stepanov G. ....	186
Stolbov O. ....	8
Strelkov I. ....	118, 137, 144
Streltsov S. ....	172
Surdin O. ....	118, 137, 144
Surkov Yu. ....	84
Surmenev R. ....	11, 53, 92, 94
Surmeneva M. ....	11, 53, 92, 94
Syromyatnikov A. ....	164
Sysoev V. ....	22
Syurakshin A. ....	73

## T

Taaev T. ....	39
Tabachkova N. ....	93
Tananaev P. ....	6
Taran L. ....	172
Tarasov A. ....	54, 56, 102, 166
Tarasova E. ....	69, 196, 197
Tashkinov M. ....	45
Tatarskiy D. ....	66
Tcuranova M. ....	162
Telyshev D. ....	126, 161
Temirov A. ....	17
Temnikov F. ....	172
Terentev P. ....	111
Tereshina I. ....	133
Tikhonov R. ....	76
Tishin A. ....	4, 93
Tkachev A. ....	146
Tolmacheva V. ....	109, 177
Tomberg E. ....	96
Tsiurko D. ....	27
Tsvetkov A. ....	58
Tuchin V. ....	84, 115, 148, 149
Tuchina D. ....	115
Turutin A. ....	17, 93
Tyurenkov A. ....	168

## U

Ulybyshev D. ....	83
Urakova A. ....	53
Usachov D. ....	54
Ushkov A. ....	192

# IBCM-2025

Usov N. ....	15
Ustyugov V. ....	158
Utkin A. ....	49

## V

Vagapov V. ....	126
Vakhitova Ya. ....	182
Vas'kovskiy V. ....	192
Vasiliev A. ....	61, 133, 144
Vazhinskiy N. ....	116, 145
Ved M. ....	66, 129
Verbetsky V. ....	133
Veselova S. ....	179
Vetoshko P. ....	9
Vindizheva A. ....	90
Vindokurov I. ....	45
Vinnik D. ....	103
Vinogradova E. ....	151
Vivchar V. ....	104
Vlasov V. ....	97
Vlasyuk E. ....	57, 154
Volchikov I. ....	83
Volkova D. ....	40
Voronina E. ....	173
Voronina S. ....	96
Vorontsov P. ....	45, 57, 105, 154, 190
Vorontsov S. ....	45

## W

Wang Y. ....	67, 120
--------------	---------

## Y

Yabbarov N. ....	28
------------------	----

Yanina I. ....	115, 155
Yashin M. ....	38
Yerin C. ....	104, 176
Yudanov N. ....	87, 88, 127
Yudin S. ....	114
Yurasov A. ....	38, 42
Yurlov V. ....	7
Yushankhai V. ....	73
Yushkov V. ....	180, 182

## Z

Zabotnov S. ....	193
Zagorskiy D. ....	26, 146
Zagrebin M. ....	41
Zaikina A. ....	153
Zakinyan A. ....	14, 48
Zamkova N. ....	23
Zavkibekova K. ....	152
Zdoroveishchev D. ....	72
Zdoroveyshchev A. ....	66, 129
Zdoroveyshchev D. ....	66
Zhabova A. ....	174
Zhandun V. ....	23, 194
Zhansitov A. ....	16, 45
Zherlitsyn S. ....	75
Zhevstovskikh I. ....	75
Zhivulin V. ....	103
Zhurenko S. ....	146
Zinnyatulina D. ....	86
Zou J. ....	189
Zubarev A. ....	60, 186
Zubkov S. ....	66
Zverev V. ....	62
Zvezdin K. ....	7, 135